Project Report on

Energy Dissipation on Block Ramps

Submitted to

Indian National Committees
on Surface Water
Ministry of Water Resources
(MoWR), R K Puram,
New Delhi

Investigating Team

Dr. Z. Ahmad, Professor (PI)
Dr. Nayan Sharma, Professor
Dr. N. R. Singh, Former
Research Scholar
Mr. D. G. Khan, Former SRF
Mr. S. Ahmad, Former SRF

DEPARTMENT OF CIVIL ENGINEERING

INDIAN INSTITUTE OF TECHNOLOGY ROORKEE

ROORKEE – 247 667, Uttarakhand, India

December 2015

ABSTRACT

Hydraulic imbalance and instability of the flow in steep channels due to natural and anthropogenic causes has often been resulting in the degradation of rivers. Practicing engineers and planners have been confronted with the task of finding a feasible and cost–effective solution for restoring such rivers. Various stream restoration structures have been established upon as a solution to this manifested problem. Block ramps have recently been indicated to be viable stream restoration structures with respect to its energy dissipation characteristics and efficient composition. Block ramps can be defined as grade–control structures applied to maintain the morphological continuity of the stream especially in mountainous reaches of rivers and are created by superimposing one or more rock layers on the original river bed. These structures are generally adopted where there is an appreciable fall in the river grade and are made of natural boulders whose mean diameter varies between 0.3 m and 1.5 m. The deployment of block ramps induces a considerable dissipation of energy with the creation of high turbulence zones within the macroroughness boulder elements.

Chiavacinni (2004) pointed out that the energy dissipation on block ramps generally increases with the decline of the bed slope, and the differences tend to diminish with decreasing discharges. However the same authors (2006a) indicated that for the same discharge values, the dissipation is directly proportional to the height of the ramp and, for the same slope, to its length. Further when the same authors (2006b) adopted macroroughness boulders on block ramps in their study, they found that the slope seems not to influence the increase in energy dissipation. The authors also stated that the effect of Reynolds number is negligible, because Re was greater than 10^4 in their test conditions, as also stipulated by other investigators (Lawrence 1997; Ferro 1999). Further the authors concluded that as the boulder concentration increases, the dissipation increases, with a maximum of 10 – 12 % for a concentration of 30 –35 % for boulders in row and random arrangements. It has been suggested that the Reynolds number is an important parameter of highly turbulent flows (Nezu and Nakagawa, 1993; Jimenez, 2004). The effect of boulder spacing and distribution on the energy dissipation process for block ramps with boulders has not been examined in detail so far. Also the ranges of boulder concentration to achieve optimum

energy dissipation needs to be ascertained for other boulder arrangements as the staggered configuration, and variant boulder sizes. The correlation of flow resistance with the energy dissipation on block ramps has not been directly examined, though several studies in close relation to block ramp have been done. Canovaro and Solari (2007) investigated flow resistance developed by macroroughness pebbles positioned on a granular layer according to a regularly spaced stripe pattern on steep bed slopes. Pagliara and Chiavacinni (2006c) proposed a combined friction factor for the boulder block ramps and have concluded that boulders on the block ramp increases the flow resistance; the increase in flow resistance depend on the ramp slope, on the boulder concentration and disposition, and on the boulder roughness. These facets are further examined and addressed in the present experimental study. The objective of the study was to comprehend the energy dissipation characteristics on boulder block ramps with focus on the staggered configuration of boulders, and find out the boulder spacing and distribution which can generate efficient energy dissipation, and to ascertain its practical application.

Experiments were conducted to investigate the manifold parameters characterizing energy dissipation on block ramps for different configurations such as smooth condition, ramp with base material and ramp with protruding boulders over the base material. The experiments were carried out at the Hydraulics Laboratory of the Department of Civil Engineering, Indian Institute of Technology Roorkee, India, and were performed on a concrete flume having a rectangular ramp of width 0.30 m, horizontal length 4.0 m with side walls of height 0.45 m. Three ramp slopes (S) 1V:5H, 1V:7H and 1V:9H were investigated. The flow discharge used in the experiments varied from 0.007 to 0.039 m^3/s. The ramp was tested in the smooth condition followed by the block ramp with base material using angular stone aggregate with size distribution for d_{10} = 16 mm and d_{84} = 25 mm. To test the effect of angularity of the base material on the energy dissipation, round river bed aggregate with d_{50} = 20 mm were also used. Then boulders using semi-hemispherical blocks of various sizes (0.042 m $\leq D_B \leq$ 0.10 m) were used to examine the effects of the primary variables as boulder concentration, size, spacing and distribution along with the flow parameters on the energy dissipation process for boulder concentration (Γ) in the range of 8 to 32 %. The staggered configuration formed the main criteria of the experimental study within which two boulder distributions were tested: (i) uniform distribution with a regular S_x/D_B (S_x=longitudinal spacing), and (ii) non–uniform distribution with a differential S_x/D_B, on the block ramp.

Experimental data observed for block ramps in various configurations were analyzed to examine the effects of the various parameters related to the relative energy dissipation for the case of smooth ramps, block ramps with base material and block ramps with boulders under various permutations and combinations of test conditions. The smooth ramp condition was analyzed to check its consistency in dissipating energy and serve as a benchmark for comparing the magnitude of energy dissipation for other block ramp conditions. It was found that the smooth ramp yielded a maximum relative energy dissipation of 56% on the steepest slope tested 1V:5H. Block ramps with base material were investigated in the next case, and it was found that this ramp condition produced a maximum relative energy dissipation of 82%, on the slope 1V:5H. The angularity of the base material was analyzed using angular and round stone aggregates, and no significant variation was being found in their energy dissipation characteristics. The slope showed a dominant role and it was observed that maximum energy dissipation was realized in the steepest slope tested. It was also found that the relative energy dissipation ΔE_r computed using the Pagliara and Chiavacinni (2006a) equation overestimated the values by more than 5% when compared with the observed values for the range $0.07 \leq h_c/H \leq 0.26$ (h_c = critical depth; H = ramp height).

For the block ramps with boulders, which formed the main component of the study, the variation of relative energy dissipation with respect to the primary energy dissipation variables were exhaustively analyzed for each tested slope under various boulder concentration and configuration in the flow parameter range of 0.05 to 0.26. The Reynolds number was found to range from 2.55×10^4 to 10.68×10^4 with a distinct correlation for each tested slope with respect to the flow parameter in the tested conditions for boulder block ramps. The flow resistance associated with the macroroughness boulders on the block ramp were analysed in terms of the resistance function. A comparative assay of boulders in rows and staggered configuration showed that the staggered configuration generated higher relative energy dissipation when tested with boulders of the same size at the spacing under. The two roughness parameters E and F (functions of arrangement and roughness of boulders) which were postulated by Pagliara and Chiavacinni (2006b) were re–examined and reinstated to be 0.23 and 11.6 respectively, for boulders bigger than 0.042 m diameter for rows configuration and rounded (smooth) condition. Within the staggered configuration, a subjective analysis was conducted for the boulder distribution in the form of uniform and non–uniform configurations. The differential and integral

effects of the boulder concentration, spacing, distribution and size were investigated for each individual slope as the relative energy dissipation due to boulders only i.e. $\Delta E_{rB}/\Delta E_r$, showed an apparently unvaried effect with the slope.

On the 1V:5H sloped–boulder block ramp, the relative energy dissipation observed was between 73 – 92 % for the range of boulder concentration 8 to 32 %. On this slope, closer spacing with $S_x/D_B \leq 1.5$ and certain non-uniform configurations exhibited higher dissipation of energy than the other configurations. On the 1V:7H sloped–boulder block ramp, the relative energy dissipation observed was between 74 – 83 % for the range of boulder concentration 14 to 29 %. On the 1V:9H sloped–boulder block ramp, the relative energy dissipation observed was in the range of 67 to 77 % and ΔE_{rB} was found to decrease considerably as the flow parameter increases, for the range of boulder concentration 19 to 29 %. At this slope, a particular non–uniform configuration (NU–4) exhibited higher dissipation of energy than the other tested configurations in the case of boulders bigger than 0.065 m diameter. It was found that the behaviour of the uniform and non–uniform boulder distributions had varied asymptotes and dependent on the boulder size and concentration at each tested slope.

From the sequence of analyses, a threshold boulder concentration beyond which there is negligible or diminishing effect on the relative energy dissipation could be earmarked. This threshold boulder concentration was found to be in the range 22 – 25 % for the tested boulder configurations and sizes for all the three slopes tested. Certain deductions were also made as the ratio of channel width to boulder size which characterized the energy dissipation trend along with the boulder configuration for particular slopes. Specific examinations were done to examine the variance of the major energy dissipation parameters and it was generally found that along with the flow parameter, the boulder concentration, spacing and size were primary parameters in describing the energy dissipation trend.

Relations are proposed for computing the relative energy dissipation for block ramps with boulders in staggered and non-uniform arrangements using $3/4^{th}$ of the optimal dataset with boulder concentration 10 to 30 % and the same is validated using the remaining $1/4^{th}$ of the dataset. The equation can be used satisfactorily within ± 5% error margins in the similitude range of the tested conditions. Conclusively the relations proposed for the estimation of energy

dissipation on boulder block ramps with boulders in staggered configuration were validated along with existing relations, and thereby projected as the main outcome of the study.

The derivations made from the analysis of the observed data were used to formulate design guidelines and plots that can aid in practical applications of boulder block ramps. The design methodologies have been formulated by also taking into consideration the philosophy of relevant studies and findings reported for block ramps structures. The element of block ramp application in the field was demonstrated using a case study highlighting the riparian river conditions and the effectiveness of the design approach in applying boulder block ramps for actual site conditions.

The present study was also aimed at to estimate the critical discharge over block ramp at local failure. Tests were conducted on chutes with three bed slopes 1V:6H, 1V:4.87H and 1V:2.88 H and with bed materials of different sizes. It is found that the critical discharge increases with non-dimensional parameter d^*_{50} while decreases with chute slope. The critical discharge also increases exponentially with the increase in uniformity coefficient of the boulders. The available data have been used to develop a relationship for critical discharge estimation at local failure. The proposed relationship satisfactorily estimates the critical discharge at local failure with $\pm 30\%$ error.

CONTENTS

List of Figures

List of Tables

Notations

The following notations / symbols are used in this thesis:

A,B,C = parameters that ascribe scale roughness conditions of base material block ramp ;

A_f = cross sectional area of the flow;

E,F = parameters that ascribe roughness and arrangement on reinforced block ramp ;

C = Chezy's coefficient;

C_D = drag coefficient;

C_m = non-dimensional mean air concentration

d_{xx} = base material size for which (xx)% of material is finer ;

D_B = diameter of the boulders (diameter of hemispheres ≈ ½ D_B);

D_l = long–axis diameter of boulders (ellipsoids);

D_m = median–axis diameter of boulders (ellipsoids);

D_s = short–axis diameter of boulders (ellipsoids);

E_o = total energy upstream ;

E_t = total energy downstream at toe ;

a_1 = A constant depends upon boulder disposition;

b_0 = constant associated with general flow resistance equation;

b_1 / b_2 = a constant depends upon boulder disposition;

f = Darcy-Weisbach friction factor;

f_{tot} = Darcy-Weisbach friction factor for large scale roughness combined with boulders;

F_d = Densimetric Froude number of boulders;

F_{dc} = Critical densimetric Froude number of boulders;

Fr = Froude number ;

g = acceleration due to gravity ;

h = flow depth ;

h_b = depth of flow in effective lower layer (in case of beds with large roughness);

h_c = critical flow depth;

h_i = flow depth at upstream inlet section (u/s of crest);

h_0 = flow depth at upstream crest section;

h_{mean} = mean or averaged flow depth ;

H = ramp height;

k / k_s = size of representative roughness elements;

L = horizontal distance at beginning of jump from toe of ramp;

L_R = ramp length ;

L_T = horizontal length of block ramp;

N = non-uniformity of the channel in both profile and plan;

N_B = number of boulders ;

n = Manning coefficient;

n_r = roughness coefficient associated with skin friction only ;

n_{tot} = Manning coefficient for rock chute / block ramp with protruding boulders;

Q = water discharge;

q = specific discharge or water discharge per unit width;

q_c = failure unit discharge

q_{cb} = critical failure discharge for reinforced chute;

R = hydraulic radius;

Re = Reynolds number ;

S_x = Longitudinal spacing between boulders or blocks ;

S_x = transverse spacing between boulders or blocks ;

S = slope of the ramp ;

U = Mean flow velocity;

v = velocity of flow ;

v_t = velocity of flow at the toe of the ramp ;

v_b = velocity of flow in effective lower layer (in case of beds with large roughness);

W = ramp width ;

GREEK SYMBOLS

α = kinetic energy correction coefficient (Coriolis coefficient);

β = momentum correction coefficient (Boussinesq coefficient);

γ = texture factor related to Nikuradse standard;

γ_s = rock specific weight;

γ_w = Water specific weight;

ϕ = representing a function

η = cross sectional geometric shape

ε = rate of dissipation of turbulent kinetic energy;

δ = boundary layer thickness;

κ = Von Karman's constant (κ = 0.4),

τ_0 = shear force per unit area in the plane of the bed of the channel;

ΔE = energy loss (generally between upstream and downstream channel sections);

ΔE_r = relative energy dissipation ;

ΔE_{rB} = relative energy dissipation due to protruding boulders ;

Δz = drop crest elevation in downstream toe (for dropshafts);

λ = centre to centre spacing;

Λ = inundation ratio;

Γ = boulder concentration ;

Ω = functional symbol in Eqs.(4.3) and (4.4);

θ = ramp slope w.r.t. horizontal (in degrees);

υ = kinematic viscosity;

ψ = reduction coefficient (< 1);

ABBREBIATIONS

c/c = centre to centre spacing (equiv. to λ);

LC = load cells (used to measure drag forces);

LF = local failure;

GVF = Gradually varied flow;

RVF = Rapidly varied flow;

NU-1 = Boulder arrangement and spacing under Non-uniform-1 configuration;

NU-2 = Boulder arrangement and spacing under Non-uniform-2 configuration;

NU-3 = Boulder arrangement and spacing under Non-uniform-3 configuration;

NU-4 = Boulder arrangement and spacing under Non-uniform-4 configuration;

PVC = Poly Vinyl Chloride;

USBR = United States Bureau of Reclamation.

1 INTRODUCTION

1.1 MOTIVATION

Hydrodynamic imbalance and instability in river systems due to natural and anthropogenic causes has become a subject of concern. One of the most challenging problems faced by river engineers today is the stabilization of degrading rivers and streams. Various stream restoration techniques have been delved upon as a solution to this manifested problem. Amongst the potential solutions, block ramps have been pointed out to be viable stream restoration engineering structures with respect to its energy dissipation characteristics. The ability to accurately predict the flow and energy dissipation rate in block ramps, which are characterized as steep open–channel flow with large scale roughness, using only the free surface characteristics is currently limited by the capabilities of the measurement instruments and lack of adequate mathematical models to describe the process for a variety of situations encountered in both laboratory and field conditions. The present study is motivated to quantify the energy dissipation at various scales and distribution of large scale roughness on block ramps.

In general, evaluation of energy of flow is based on precise discharge estimation, which requires information on critical parameters such as flow depth, velocity over the sectional depths, channel profiles and bed roughness. These facts are addressed through an experimental study to comprehend objective use of relations and putting them in practice.

1.2 OVERVIEW

Channel degradation leads to damage of both riparian infrastructure, as well as the environment. Urbanization had led to an acute decline in the quality of numerous watercourses and riverine ecosystems. Different form of degradation has occurred in water course not only because of impacts of urbanization on the hydrologic and hydraulic conditions, but also because of the presence of in–channel works. The most common method of establishing grade control is the construction of in–channel grade control structures. A wide variety of grade control structures are used in channel systems. These treatments range

from simple loose rock structures to reinforced concrete weirs and vary in scale from small streams to large rivers.

Stream restoration has been a subject of interest to the scientific community to advance upon environmental–friendly river training techniques which balances the stream ecosystems characteristics and morphological functions. Since the Egyptians and Mesopotamians first successful efforts to control the flow of water thousands of years ago, the application and study of hydraulics has evolved. The term "stream restoration" is often erroneously used to refer to any type of stream corridor manipulation. "Restoration" refers to the return of a degraded ecosystem to a close approximation of its remaining natural potential (U.S. Environmental Protection Agency, 2000). Stream restoration is defined as one or more conservation practices used to overcome resource impairments and accomplished the identified purposes based on client objectives for a conservation management unit (CMU) containing, in whole or part, the stream corridor needing treatment (USDA–NRCS, 2007). Stream restoration is a growing area within hydraulic engineering practice encompassing a wide range of activities (Shields Jr. et al., 2003). Stream restoration can increase flow storage and energy dissipation of passing flood waves (Scott et al., 2004). Conceptually, stream restoration has the potential to augment the ability of an incised or channelized reach to reduce peak discharges and disperse flood waves via enhanced energy dissipation and increased channel capacity (Emmett, 1970; Dunne and Dietrich, 1980). This has led to the development of innovative stream structures as block ramps, rock chutes, check dams, plunge and stepped pools, drop shafts, rock sills, spillways, riprap lining, etc.because of their low environmental impact. The concept of harnessing natural materials in stream restoration has gained importance respectively from ecological and economic considerations. Block ramps have proved to be a cost-effective and potential assembly in stream restoration projects. Block ramps also play a fundamental role in stabilization of streams downstream of water resources projects which houses overflow dams, spillways, weirs, conduits, escape channels, etc. The application of this structure in India is still in an inert stage where numerous water resources projects have been constructed to meet the demands of a huge population and a developing nation.

1.3 STREAM RESTORATION

Stream restoration design has focused on restoring stable cross-sectional, profile and plan form geometry to create and maintain riffle-pool spacing and sequencing, often disregarding

the effect of bed resistance on channel morphology (Scott et al., 2004). Rock ramp (riffle grade control) structures have been successfully applied to restore many stream channels and its effect on adjacent channel morphology has proved to be productive. These structures can be designed to function simply as grade control structures, such as in White Marsh Run in Baltimore County or nature-like fish ways such as the rock ramps constructed in the Northwest Branch of the Anacostia River in Hyattsville, USA. The United States Department of Agriculture –Natural Resources Conservation Service (USDA–NRCS, 2007) describes a stream corridor that includes the stream and extends in cross section from the channel's bank full level towards the upland (perpendicular to the direction of stream flow) to a point on the landscape where channel-related surface and/or soil moisture no longer influence the plant community. In the idealized cross-sectional stream corridor segment (Fig. 1.1), biota may habitat in all dimensions (riparian, in-channel, hyporheic and/or ground water zone). Inundation and desiccation of the 'blue shaded area' occurs as the amplitude of the discharge increases and decreases under a natural flow regime. The variable "Sd" designates sediment deposition sites, and "Se" is a site of bank erosion. The solid line is the thalweg, and the broken lines indicate the different directions of flow and materials among in-channel, hyporheic, and ground water zones.

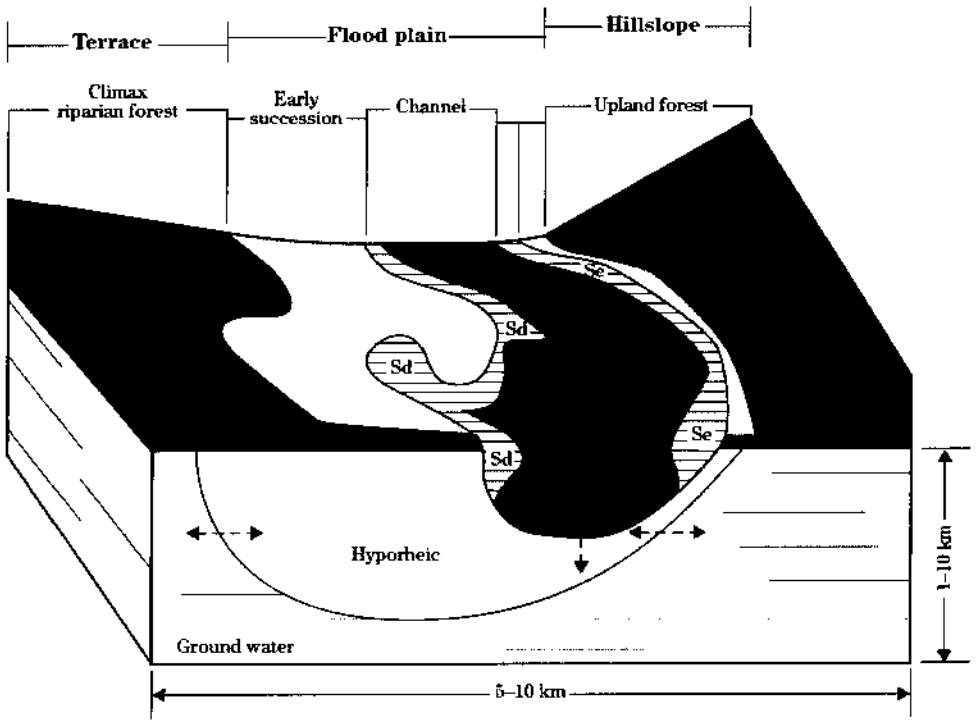

Fig. 1.1 Generalized section of stream corridor in three spatial dimensions (USDA–NRCS, 2007)

Stream restoration work historically has concentrated on redesigning the dimension, pattern and profile of impacted stream reaches. Designs often are patterned after reference-reach streams and focus on reducing bank erosion and providing effective sediment-transport. Restoration and enhancement projects generally also address the restoration of the riparian canopy. However, the restoration of in-stream habitat has not been addressed as thoroughly as channel stability and riparian vegetation. It is known that many benthic organisms can seasonally prefer one type of microhabitat and that certain fish species require specific habitat types. Good in-stream habitat is structurally complex and is composed of both inorganic and organic components. A working group for stream restoration (FISRWG, 1998) has worked upon various stream restoration process and procedures, and presented a handbook under the title "Stream Corridor Restoration: Principles, Processes, and Practices". The North Carolina State University Stream Restoration Institute, USA, conducted a workshop (NCSRI, 2004) on stream restoration and discussed methodologies on the in-stream structures and other stream and floodplain habitat features that can be incorporated into the restoration design process. The USDA – NRCS (2007) has formulated a handbook of stream restoration design taking physical and ecological considerations for the stream projects. The overall design procedure advocates that stream designs may include a variety of solutions ranging from upland watershed and riparian area management practices that may be needed, large scale re-constructions of entire stream reaches, localized applications that can involve earth materials, live and inert flora materials, as well as manufactured materials.

The recent upsurge in stream restoration practices has brought to numerous laboratory investigations, with the aim of defining suitable criteria for the design of innovative stream structures, with different characteristics with respect to the conventional training works.

1.4 BLOCK RAMPS

Block ramps are structures used for river bed stabilization to gradually overcome height differences of the river bed while controlled energy dissipation can be achieved. They are also termed as stream restoration structures applied to maintain the morphological continuity of the stream especially in mountainous reaches of rivers and are created by superimposing one or more rock layers on the original river bed. Block Ramps are grade control structures constructed to mitigate the negative impacts of artificial barriers and to conserve riparian habitat. A typical schematic representation of block ramps is given in Fig. 1.2.

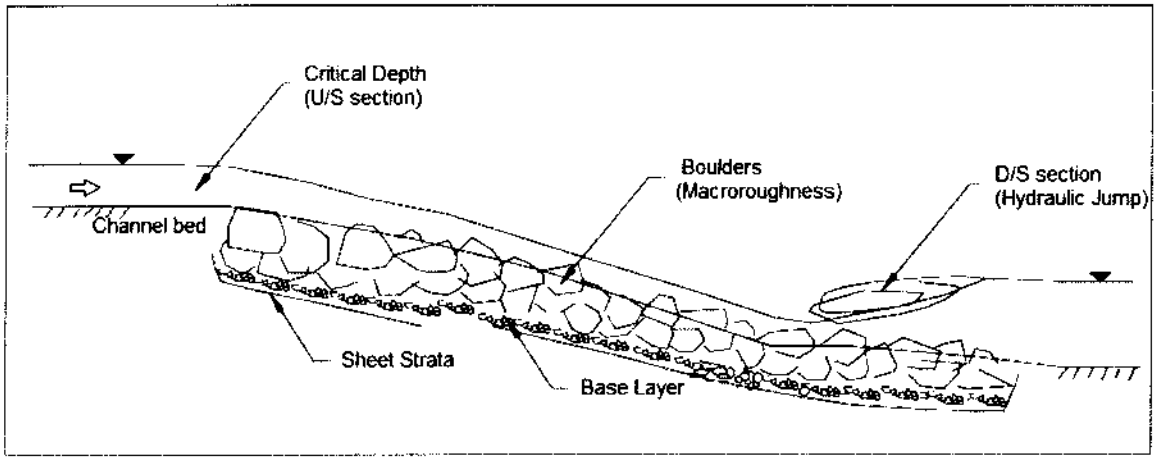

Fig. 1.2 Schematic sketch of a block ramp

Block ramps are generally adopted where there is an appreciable fall in the river grade. These are made of natural boulders whose mean diameter varies between 0.3 m and 1.5 m. These structures are an answer when it comes to preserving the morphological continuity and longitudinal connectivity of the river systems. Block ramp structures are also defined as stone structures installed within the bed of a stream channel intended to emulate the physical attributes of natural riffles within a stream system (Shamloo et al., 2001; Scott et al., 2004). Block ramp application in the Landquart and Goldach rivers, respectively in Switzerland and Germany, are shown in Figs 1.3 and 1.4. The effects of these structures on improving flow diversity may indicate the ability of block or rock ramp structures to stabilize and mimic natural riffle-pool sequences in urban stream systems.

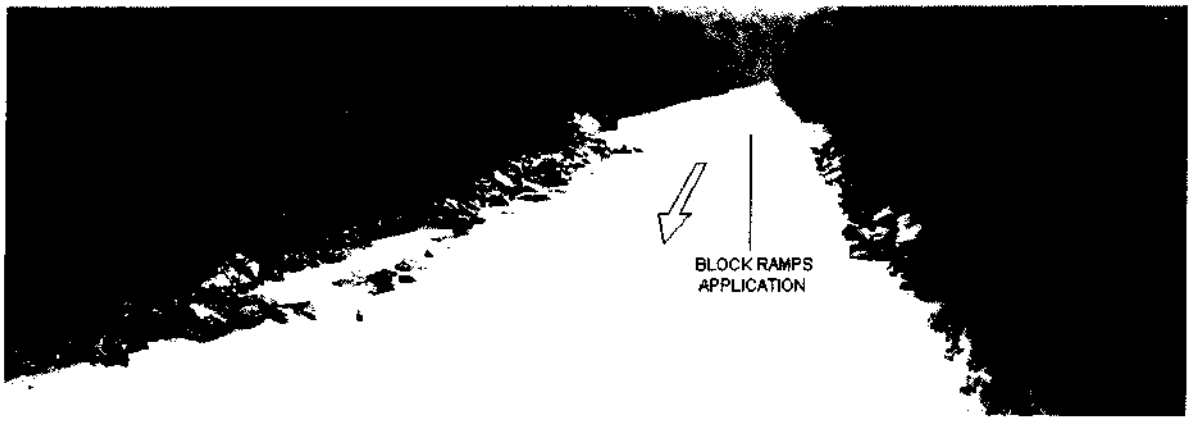

Fig. 1.3 Block ramp application in Landquart river in Switzerland

Fig.1.4 A typical block ramp application in Goldach river, Germany

Several investigators have pointed out that block ramps act as an excellent energy dissipator (Whittaker and Jäggi, 1986; Peruginelli and Pagliara, 2000; Pagliara and Dazzini, 2002; Semadeni et al., 2004; Pagliara and Chiavaccini, 2006a, 2006 b; Aberle, 2007). From the environmental point of view, block ramps do not act as barriers, as the hydrodynamic conditions on the ramp can be generally compatible with the characteristics of dynamism of the stream riparian habitat and fauna (Keller and Haupt, 2000). Block ramps or rock chutes present many advantages from an ecological point of view and for this reason, they are considered as low environmental impact hydraulic structures. The gradually change of geodetic height combined with moderate flow velocities enable for riparian habitat preservation as passage of fish and other fauna (USDA–NRCS, 2005; Tamagni et. al., 2011) as illustrated in Fig. 1.5.

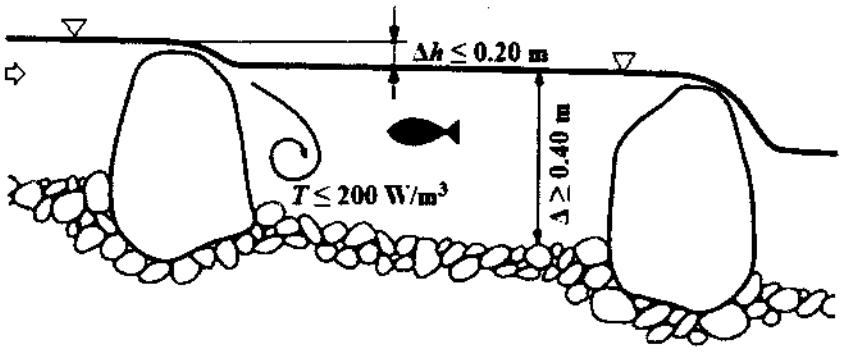

Fig.1.5 Ecological continuity of stream flow using block ramps (Δh = drop height, T = turbulence, and Δ = minimum pool depth to guarantee habitat migration) (FISRWG, 1998)

In the last decades many existing drops and sills have been replaced by block ramps and many more are planned (Tamagni et al, 2011). However, restoring stream structure and function demands a combined knowledge of hydrologic, hydraulic and geomorphic processes.

1.5 OTHER STREAM RESTORATION STRUCTURES AND ENERGY DISSIPATORS

Similar structures adopted in stream restoration as energy dissipators are rock chutes, step-pools and plunge pools, stepped channels/cascades, spillways (overflow, chute, stepped, siphon, etc.), stilling basins, gabion weirs, rock riprap, stream barbs, drop chutes, drops, etc. have been investigated. Stepped Gabion weirs were found to be efficient energy dissipators (Peyras et al. 1992). Abundant research in stepped spillways, overflow weirs and other energy dissipatorshave concentrated mainly on large dams or hydraulic structures (Chanson, 1993a, 1993b, 1999, 2002; Matos, 2000, 2002; USACE, 1990; Bombardelli et al., 2011). Christodoulou (1993) found that in stepped spillways, the relative energy loss increases with the number of steps at a certain ratio of the critical depth to the step height. Peyras et al., (1999) found stepped gabion weirs to be excellent in energy dissipation action and can withstand floods of upto 3 $m^3/s/m$ without The USDA–NRCS (2005) reported hydraulic analysis of stream barbs and gave design recommendations for barb slope, height and rock sizing for stream corridor protection works. Weichert (2006) conducted an in-depth study of the energy dissipation in plunge pools, dividing the water flow body into three energy dissipating regions as shear, impact and mixing dissipation regions of energy. Chinnarasri and Wongwises (2006) studied flow patterns and energy dissipation over various stepped chutes with emphasis on providing an effective dissipation basin for powerful hydraulic structures in steep mountain topography. Step-pools and its dissipative analogies have been studied by Canovaro et al. (2007).

1.6 ENERGY DISSIPATION OF FLOW

Every moving fluid particle or drop of water loses some of its hydraulic energy along its trajectory. This loss is a result of friction or drag forces that are closely related to turbulence production in hydraulic energy dissipation. The process of energy dissipation can be usefully divided into two cases as:

(i) A particle of water within a water current, and

(ii) A drop of water in an air current

In the first case, the energy dissipation is related to energy–consuming eddies which are mainly generated in the shear zones or in zones of large velocity gradients. To induce a considerable loss of energy, the creation of high turbulence zones is, therefore, important. In the second case, the energy dissipation results from the air resistance exerted on the drop of water. The magnitude is large if the drop is small and the relative velocity between the drop and the ambient air is high. Block ramps implement the energy dissipation characteristics of the first case.

Energy dissipators are adopted whenever the velocity of flow leaving a water management structure exceeds the erosion velocity of the downstream channel system. Bed armoring controls bed degradation and scour and the increased hydraulic roughness of the bed control structure may dissipate a minor amount of hydraulic energy (USACE, 1983). Block ramps serve as a cost-effective therapy for scour and other unwanted effects of flowing water downstream of the structures. A hydraulic control structure is designed to function by reducing the energy slope along the degradation zone to the degree that the stream is no longer competent to scour the bed. Dissipation of the kinetic energy is essential for bringing the flow into the downstream river to the normal condition in a short distance as possible. This is necessary, not only to protect the riverbed and banks from erosion, but also to ensure that hydraulic structures (dam, hydroelectric powerhouse, canal, etc.) are not undermined by the high velocity turbulent flow. Efficient energy dissipation is a process of disturbing the flow of water either by increasing its turbulence or diffusing it into spray. An economical energy dissipator is designed to affect such an impact within a comparatively small region.

Energy dissipation structures may be used for both sub-critical and super-critical upstream channel flow conditions. Excess energy of flow is usually dissipated to control erosion and /or scouring in open channels. Generally energy-dissipating devices are designed in conjunction or downstream of hydropower units, spillways, outlet works etc., utilizing blocks, sills, or other roughness elements to impart additional resistance to the flow and reduce energy of flow. The energy dissipation structures in open channels are based on: (a) Impact type or head-on impact on a solid obstruction element, and (b) Hydraulic jump type or creation of a stable hydraulic jump. The impact-type of energy dissipation is considered to be more efficient than the hydraulic jump-type as it diverts the flow in many directions resulting in formation of eddies and dissipative wakes which reduces the energy in the flow. Also the impact-type energy dissipaters are smaller and more economical structures. Block ramps are

characterized with high turbulent flow on large graded natural roughness resulting in energy dissipation, and therefore may be grouped under the "impact-type" of energy dissipators.

As described in previous sections, the potential of block ramp structures as optimal energy dissipators downstream of the water resources projects as trench weir, overflow dams, spillways, etc. are a cost-cutting measure or alternative to the construction of big and expensive dissipation structures such as stilling basins, plunge pools, end sills, chute blocks, etc. at the downstream reaches.

1.7 BRIEF REVIEW OF LITERATURE AND NEED OF THE STUDY

A wide variety of structures has been employed to provide grade control in river channel systems. The goal of this study is to provide a subjective description of block ramps over other common types of grade control structures that are frequently used in stream restoration works and describe the various design considerations that should be used when selecting and placing these grade control structures. To examine the rationale of the present study and identify the gaps, a critical assessment of the studies and postulations by various researchers has been done.

Notably, Pagliara and Chiavacinni (2004, 2006) and Pagliara et al., (2008, 2009) have studied block ramps intensively and postulated energy loss relations on different conditions of block ramps (Fig. 1.6). Janisch and Weichert (2006) studied unstructured and structured block ramps with the objective of improving the river bed morphology and stability of steep channels. Hunziker et al. (2008) presented a project design manual report on block ramps. Ahmad et al. (2009) studied energy dissipation of flow over block ramp with protruding boulders with staggered arrangement. Tamagni et al. (2010) investigated unstructured block ramps and provided design principles along review of past formulations. Oertel and Schlenkhoff (2012) simulated flow over crossbar block ramps and investigated the flow regimes, energy dissipation process, friction factor and drag forces associated with this structure. To get a preliminary insight on the energy dissipation formulations, some of the significant ones are explained.

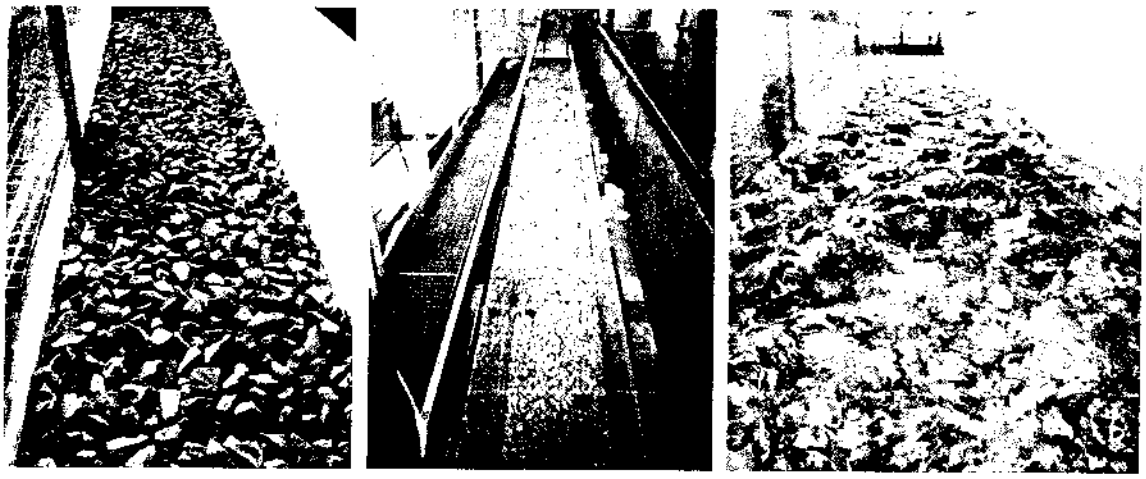

Fig. 1.6 Study of block ramps in various models in the laboratory (Pagliara et al., 2008)

Energy dissipation on the block ramps depends on the height of the ramp, size of the base material, size and arrangement of the boulders on the ramp. The energy loss (ΔE) over the ramp = (upstream energy E_o – downstream energy E_t) of the ramp. The relative energy loss (ΔE_r) is written as

$$\Delta E_r = \frac{\Delta E}{E_o} = \frac{E_0 - E_t}{E_0} \tag{1.1}$$

Based on the experimental study, Pagliara and Chiavaccini (2006a) proposed the following equation for energy dissipation on smooth ramp and ramp with base material:

$$\Delta E_r = \frac{\Delta E}{E_o} = A + (1 - A)\exp^{(B+C.S)\frac{h_c}{H}} \tag{1.2}$$

where$H$ = ramp height, S = ramp slope, h_c = critical depth of flow, and A, B, C are coefficients, which depend on the roughness characteristics of the ramp. For $h_c/d_{50} < 2.5$, A = 0.33, B= -1.3, and C= -14.5; for $2.5 < h_c/d_{50} < 6.6$, A = 0.25, B= -1.5, and C= -12; and for $h_c/d_{50} > 6.6$, A = 0.15, B= -1.0, and C= -11.5. For the case of a smooth ramp, which represents a limiting condition when mean size of base material d_{50} tends to 0, A = 0.02, B= -0.9, and C= -25.0.

When boulders or macro-roughness elements are introduced on the smooth or base material, there is a significant change in the roughness boundary. Pagliara and Chiavaccini (2006b) modified the relations for the base material and postulated the following equation accounting for macro-roughness boulders in rows and random arrangements,

$$\frac{\Delta E_{rB}}{\Delta E_r} = 1 + \frac{\Gamma}{(E + F\,\Gamma)} \tag{1.3}$$

ΔE_{rB} represents the relative energy dissipation of block ramp with protruding boulders. A combined relationship for the relative energy dissipation for base and reinforced block ramp is presented in the form (Pagliara and Chiavaccini, 2006b)

$$\Delta E_{rB} = A + (1 - A)\exp^{(B+C.S)\frac{h_c}{H}}\left(1 + \frac{\Gamma}{E + F\,\Gamma}\right) \tag{1.4}$$

where, coefficients E and F are functions of arrangement and roughness of the boulders. For random arrangement and rounded boulders (river stones), E = 0.6 and F = 13.3; for row arrangement and rounded boulders, E= 0.55 and F = 10.5; for random arrangement and crushed boulders (quarry stones) E = 0.55 and F = 9.1; and for row arrangement and crushed boulders, E = 0.4 and F = 7.7. The boulder concentration (Γ) is calculated as

$$\Gamma = \frac{N_B \Pi\, D_B^{\,2}}{4\, W\, L_R} \tag{1.5}$$

Ahmad et al., (2009) found that energy loss in staggered arrangement of boulders on the ramp is more than the random or row arrangements. They proposed E = 0.60 and F= 7.9 $(D_B/h_c)^{-0.9}$ for staggered arrangement which will be used in Eq. (1.4). Ghare et al., (2010) correlated the step height ratio of stepped chute with representative base material size (d_{50}) of block ramp under identical hydraulic conditions.

From the review of the studies cited, it can be noted that the energy dissipation depends mainly on the boulder concentration, disposition or arrangement of boulders, relative submergence, and ramp slope. The effect of Froude number and Reynolds number has been considered negligible in the studies conducted, so far. Undoubtedly, the roughness of the elements modifies the dissipation and the within the boulder arrangement or disposition, the random arrangement is systematically found less dissipative than the rows disposition.

The effect of row and random arrangement of boulders has been investigated by Pagliara and Chivaccini (2006) upto a certain extent (further discussed in Chapter 2). Other structured forms of block ramps as staggered arrangement have not been fully investigated upon. The slope and wider range of flow as well as boulder configuration needs to be examined for characterizing the energy dissipation. The present study is directed to exemplify these hydraulic parameters with various boulder sizes and higher range of submergence and flow discharge.

1.8 OBJECTIVES OF THE STUDY

The manifold parameters characterizing energy dissipation on block ramps are to be examined with an experimental model to ascribe their relative effects. The findings of previous studies are to be investigated in terms of the critical factors as boulder concentration, boulder size and geometry, flow parameters, etc. Some of the prime focuses motivated in this study are:

- To examine the manifold hydraulic parameters characterizing energy dissipation on block ramps with an experimental model.
- To simulate the effect of various permutations and combinations of boulder concentration, size and spacing with respect to relative energy dissipation on the ramp. The present study is focused on finding optimum configuration of boulders in staggered pattern.
- To study the effect of slope with different configuration of boulders on the ramp, and the variation in resultant energy dissipation.
- Test the applicability of the existing relationship for the estimation of energy dissipation on the block ramp with various arrangements of the macroroughness elements. The relationship for the evaluation of energy dissipation on smooth ramp, ramp with base material and ramp with boulders in staggered arrangements of boulders of different sizes on base material is to be validated with the experimental dataset derived in the present study.
- To develop relationship for the energy dissipation incorporating ramp & boulder physical parameters and flow parameters.
- To develop design rules and recommendations to protect water resources and hydraulic structures using ramps.
- To study of air concentration and stability of the block ramps.

1.9 LIMITATIONS OF THE STUDY

Following are the limitations of the present study:

(i) Energy dissipation on block ramps has been studied for clear water flow in the channel. It is likely that the presence of sediment in the flow may affect the energy dissipation process. This aspect has not been covered in the present study.

(ii) The outcome of the study is applicable for the range of dimensionless parameters (viz., h_c/H, hydraulic flow variable; D_B/h_c and d_{50}/h_c, relative submergence variables; Γ, boulder concentration; etc.). Proper care should be taken while using the outcome of this study beyond the range of these dimensionless parameters studied therein.

(iii) The present study is limited to energy dissipation on base materials, protruding boulders with base material in staggered and row (structured) arrangements. The relationships adopted and formulated are thereby applicable only for these configurations.

(iv) The outcomes of the study are applicable to the block ramps provided in the straight reach of the river.

1.10 STRUCTURE OF THE REPORT

This thesis is concerned with the description of energy dissipation for steep open channel flow over large-scale roughness over varying ranges of configurations and determination of the flow parameters in view of implementing this structure in the field. For lucid presentation of the work carried out in the thesis, it is divided into six chapters: Chapter-1 outlines briefly a description of block ramps, stream restoration and energy dissipation principles, summary of previous studies, objectives and conceptualization of the study. Chapter-2 presents the basic theory of block ramps and objective examination of literature that is concerned with the quantification of energy dissipation. The hydraulic factors and relations associated with the energy dissipation function are discussed in detail in this chapter. The limitations and gaps in previous studies have also been identified. Chapter-3 presents the details of experimental programme and test procedures adopted in the study. Chapter-4 provides the important experimental results and the details of data analysis, equations for energy dissipation for staggered arrangement and outlays validation to the relation. Chapter-5 presents the design recommendations of block ramps with protruding boulders for staggered configuration from a hydraulic perspective. Chapter-6 summarizes the major conclusions from the present study and identifies some of the future research needs.

THEORY AND REVIEW OF LITERATURE

This chapter describes the hydraulic entity of block ramps and emphasizes upon the factors consequent for energy dissipation. Review of the various studies carried out for block ramps and similar structures as for steep rough channels are examined in detail. This chapter objectively examines the postulated relations for the estimation of dissipation of energy for block ramps as well as other related hydraulic structures under the prescribed boundaries of flow, so that it can be refined and applied to the present study. The sensitivity of each hydraulic variable is subjectively examined to arrive at selection of critical parameters that should be concentrated upon in the experiment set up and prime observations that are to be made in order to address the study objectives. The review presented is maintained in chronological order as far as possible and in order of hydraulic parameters dealt upon.

2.1 ENERGY DISSIPATION PRINCIPLES

Energy dissipation is generally achieved in various means as expansion and deflection, counter flow, rough channels and cascades, vortex devices, air entrainment, jet diffusion, etc (Vischer and Hager, 1995). A rough channel can dissipate a large part of the flow energy within a comparatively short distance. The subject of this present study falls within this category. The use of large roughness elements as block ramps, baffled aprons, rock chutes, etc. have become popular in river engineering (Whittaker and Jäggi, 1986). In close resemblance to the block ramps, baffled apron or baffled chute are used to dissipate the energy in the flow at a drop and are mostly often used on canal escapes or drops and they require no initial tail water to be effective. It further defines that blocks, baffle piers, friction blocks and control blocks are obstructions set in the path of high velocity water, such as piers, on the apron of an overflow dam, weir or drop and to dissipate energy thereby preventing scour downstream to control the position of hydraulic jump. Chute blocks are provided at the entrance of the stilling basin to stabilize the formation of hydraulic jump, to increase effective depth, to break up flow into a number of water jets, to create turbulence and to lift the jets off the floor to reduce basin length.

To summarize the numerous techniques used for the evaluation of dissipation of flow energy, and according to the mechanism of the processes, energy dissipation can be grouped under two main categories as:

(i) Provoking large velocity gradients and thus increasing turbulence in the water current with devices as,

- Sudden expansions,
- Sharp deflections,
- Sills and end sills,
- Chute blocks, baffle piers and beams,
- Counter flows,
- Rough boundaries,
- Vortex chambers.

(ii) Creating extended and turbulent interfaces between the water and the surrounding air by devices that,

- create free jets, and
- split free jets.

The energy dissipation structures in open channels are broadly based on: (a) Impact type or head-on impact on a solid obstruction element, and (b) Hydraulic jump type or creation of a stable hydraulic jump. Block ramps resemble this category of energy dissipation. The special feature of these structures is that no tail water is required for their functioning.

The principal forces contributing to energy dissipation are shear and turbulence. Dissipation of energy by impact requires inclusion of devices like friction blocks and baffles. The objective is to prevent undue acceleration of the flow, thus limiting the velocity to a magnitude that can be handled easily.

One of the ways to limit velocity is to use simple roughness elements on the bed of the chute, utilizing size and spacing to induce what is termed as the tumbling flow regime in the channel (Khatsuria, 2005). Block ramps resemble this energy dissipating composition. Tumbling flow consists of a series of hydraulic jumps in which the flow oscillates from subcritical to supercritical and then, through the jump, back to subcritical as it passes each roughness element. The large scale roughness induced into the flow stream give rise to eddies and vortices with generation of turbulent kinetic energy that substantially dissipates in to other

forms and tranquil into the downstream flow. In mountain streams, as the water flows over the steep bed, the enhanced roughness and the momentum transfer within the stream promote the energy dissipation rate.

2.2 BLOCK RAMPS AND OTHER RELATED STRUCTURES

To get a coherent concept on the energy dissipation principle on block ramps, it is necessary to comprehend the structures associated closely to block ramps both in morphological and functional characteristics. Block ramps are structurally composed of large scale or macro-scale roughness generally in the form of river-bed stones and boulders, in steep channel beds (Fig. 2.1). When the roughness is not present, the smooth ramp is very closely representative to a chute or minor overflow spillway. Therefore, the interlacing of hydraulic theories of macro-scale roughness bed form and steep channel flows are a laconic feature of the block ramp energy dissipation function.

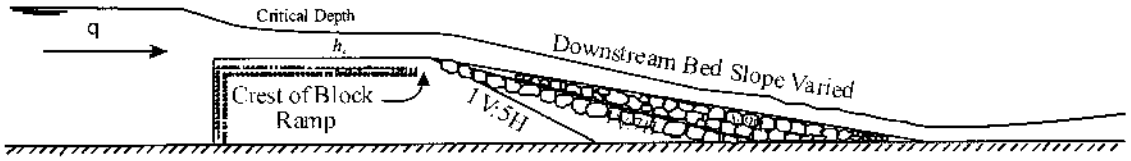

Fig. 2.1 Schematic profile of a block ramp

In urban streams block ramps are usually designed with uniform geometry, because of their low elevation. The ramp can be partially covered with boulders, if it is necessary to increase ramp roughness. From the hydraulic point of view, a ramp is a steep reach preceded and followed by the relatively milder ones. At the upstream end of the ramp the critical depth occurs while at the downstream end, a hydraulic jump may occur. It has been pointed out by Pagliara and Chiavacinni (2004) that the energy dissipation generally increases with the decline of the bed slope, and the differences tend to diminish with decreasing discharges.

Depending on the morphological structure and configuration of macro roughness elements, block ramps may be classified in two main types: (a) block carpet and (b) block cluster, within which other sub-classes are identified as shown in Fig. 2.2. Block clusters generally comprises of structured, unstructured, or self-structured blocks. For unstructured blocks, the

boulders are randomly arranged as were studied by Pagliara and Chiavaccini (2006c) and Janisch and Tamagni (2008).

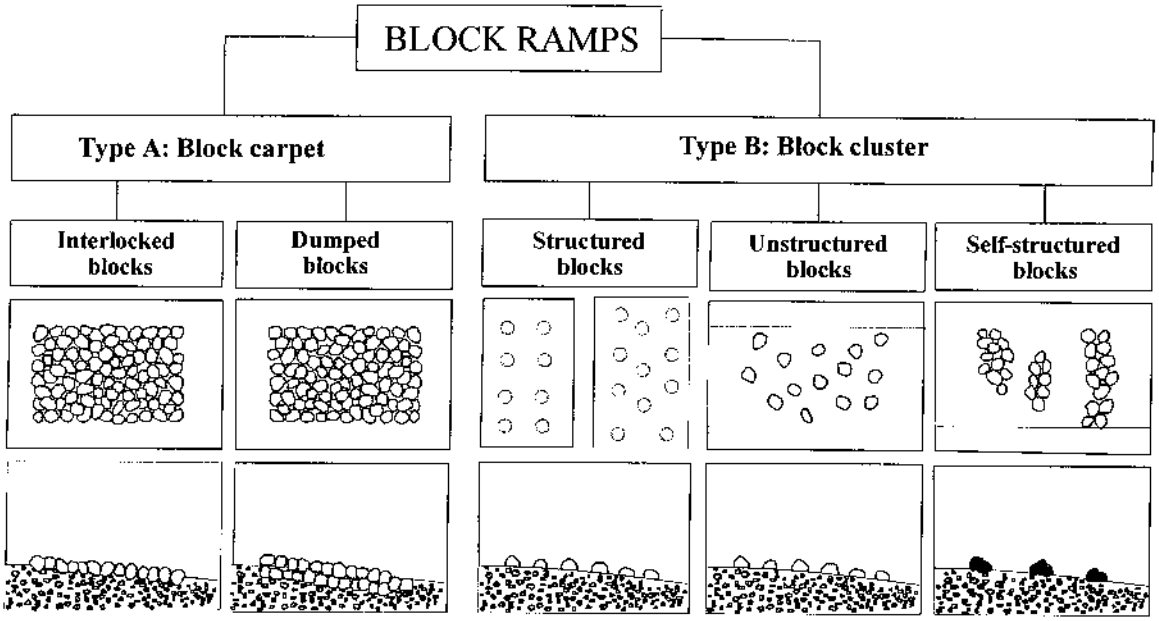

Fig.2.2 A morphological and structural classification of block ramps (adapted after Lange, 2007 and Tamagni et al., 2011)

Flows over macro-scale roughness are found generally in mountain streams (Bathurst, 1985), overland flows and inundation of floodplains (Järvelä, 2002). Several well-known field studies have considered overland flow hydraulics on rough surfaces (Emmett, 1970; Dunne and Dietrich, 1980; Abrahams and Parsons, 1990) and more recent work has focused on the relative importance of various contributions to frictional resistance (Rouse, 1965; Yen, 2002). Dunne and Dietrich (1980) based the analysis of their field data on the assumption of an explicit dependence of friction factor on Reynolds number and suggested that the variability in the coefficient associated with this dependence is due to differences in the surface roughness at each site. Lawrence (1997) pointed out that in states of partial inundation the local Froude number of the flow will most likely be highly variable, with numerous transitions between supercritical and subcritical flow, as the flow is diverted around surface roughness elements. These transitions will conserve flow momentum, but dissipate energy, thus increasing the effective frictional resistance to flow, so that the tendency for wave drag will be strongly related to the inundation ratio (h/k) and other measures of the surface

roughness, such as the percentage stone cover. He expressed a dimensionless grouping for the assessment of overland flow in terms of the Reynolds Number, inundation ratio and the sine function of the surface slope.

2.2.1 Studies carried out on Block Ramps and Similar Structures

Various studies have been conducted in order to determine a relationship for calculating the magnitude of the energy dissipation on the ramp and similar-other structures. Chamani and Rajaratnam (1999a,1999b), Peyras et al. (1992) and Christodoulou (1993), Chinnarasri and Wongwises (2006) and Chanson (1999) amongst other authors, investigated the energy dissipation on stepped channel which hydraulic behavior, in case of skimming flow, is similar to the block ramp one.

In mountain reaches riffle pool and step pool are widely used for stream restoration. They are typically adopted with well confined (urban), high-gradient channels with slopes greater than 3%, having small width to depth ratios, and bed material dominated by cobbles and boulders (Maryland Dept. of the Environment, 1999). Step pools generally function as grade control structures and aquatic habitat features by reducing channel gradients and promoting flow diversity. They are characterized by a succession of channel-spanning steps formed by large grouped boulders that separate pools containing finer rock as shown in Fig. 2.3. The design of these structures has not been fully reinforced on a standard platform.

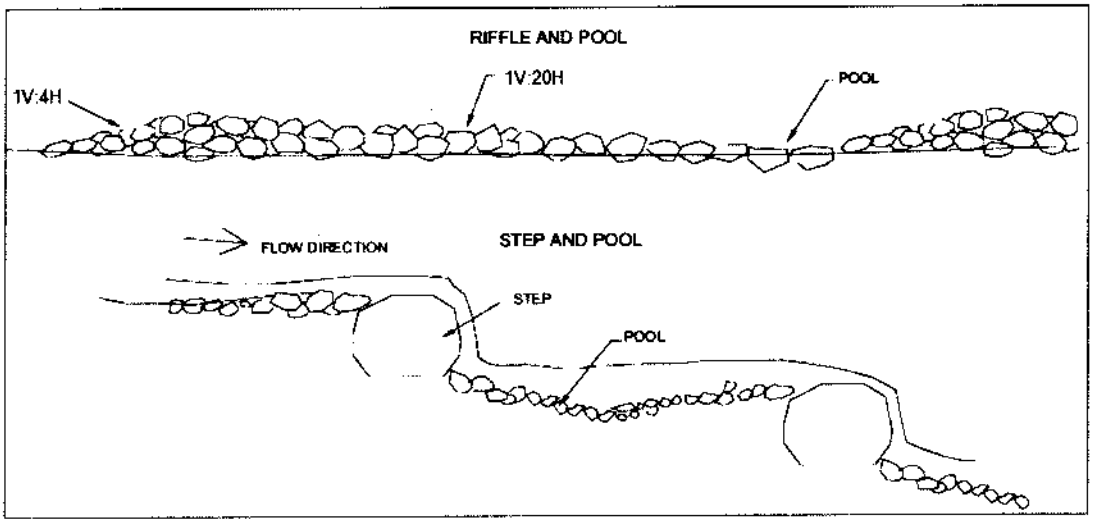

Fig. 2.3 Sketch of a riffle pool and step pool structure (Pagliara and Chiavacinni, 2004)

In close relation to block ramp, Canovaro and Solari (2007) investigated flow resistance developed by macro-roughness pebbles positioned on a granular layer according to a regularly spaced stripe pattern on steep bed slopes. Flume experiments under various geometrical and hydraulic conditions were carried out and the authors showed that flow resistance reaches a maximum and is mainly due to form drag when the spacing between macro-roughness stripes is about 10 times the average macro-roughness height.

In another perspective, Pagliara and Pozzolini (2003) stipulated that energy of flow in mountainous stream is dispensed in providing bed stabilization that might otherwise be available for sediment erosion. Other authors (Whittaker and Jäggi, 1986; Abrahams et al., 1995) have suggested that step–pool streams evolve toward a maximum flow resistance condition in order to achieve maximum bed stabilization. In particular, Abrahams et al.(1995) recommended that maximum flow resistance occurs when $1 < (k/\lambda)/S < 2$, where k is the step height, λ the step–pool wavelength and S the average bed channel slope (Fig. 2.4). More recent field investigations have somewhat extended the validity of the results of Abrahams et al.(1995), suggesting that where average channel slope is below 5–7% the $(k/\lambda)/S$ ratio is greater than 2.0. These recommendations will be put into check with the observations of the present study. Although several field and laboratory studies of step–pool geometry have been carried out (Wilcox, 2005; Church and Zimmermann, 2007), very few data are available about the behavior of hydraulic variables and so very little is known about the flow resistance developed by step–pool streams (Carling, 1991; Aberle and Smart, 2003; Wilcox et al., 2011). Wyrick and Pasternack (2008) had asserted that this lack of hydraulic data may be attributed to the difficulties of measuring low-frequency high-magnitude formative discharges, especially when step–pool sequences occur in rugged, mountainous and often inaccessible terrain.

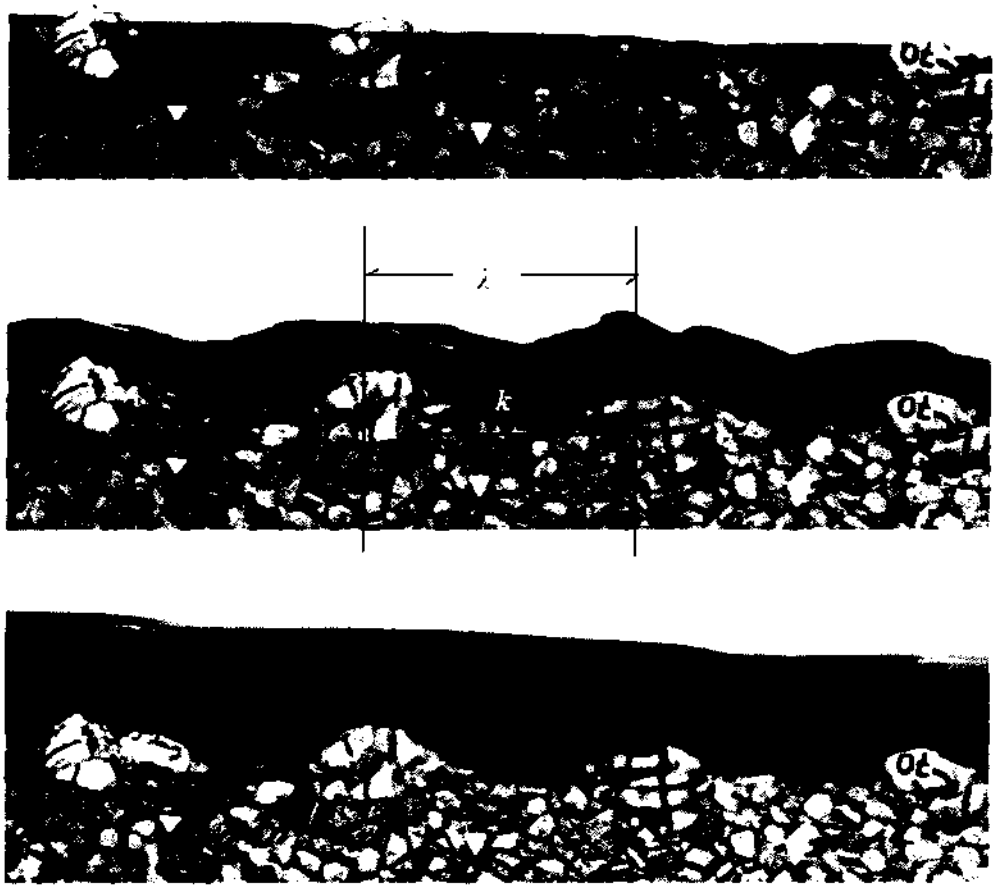

Fig.2.4 Various flow profile structures in step–pools (*adapted*, Janisch-Breuer, 2006)

Steep and short rough channels, such as rock chutes, were also used in river restoration as grade stabilization structures. The stability of these channels can be increased using boulders placed over the base material. The boulders can be placed with different configurations such as randomly or in rows. In each case, their presence affects the geometry of the channel and modifies the hydraulic resistance. Pagliara and Chivaccini (2006c) conducted laboratory test to evaluate the flow resistance in terms of both Manning's coefficient and Darcy-Weisbach friction factor, for a chute with steep slopes ($S \geq 0.40$) and short reach lengths, where protruding boulders were introduced for stabilization the river bed. In an interesting finding, Peruginelli and Pagliara (2000) and Pagliara and Dazzini (2002) showed that block ramps produced the highest energy dissipation among the studied configurations of various structures as stepped channels (in various configurations: smooth steps with and without end sill, plastic grass on the tread), drop, rock chutes, smooth ramp and block ramps. They illustrated this finding by plotting collected data for rock chutes, smooth and block ramps as given in Fig. 2.5. For napping flow and skimming flow regime, and based on the regression curves obtained from the data analysis,

Pagliara and Dazzini (2002) presented two relations between relative energy dissipation (ΔE_r) and the flow parameter (h_c/H) for the smooth ramp as given in Eqs. (2.1) and (2.2). Here, the parameter H represents the step or drop height, as well as height of the ramp; h_c is the critical flow depth for that discharge condition.

$$\Delta E_r = \frac{\Delta E}{E_0} = 1 - \frac{2 + 10.34(H/h_c)^{0.83}}{6.54(H/h_c)^{0.28} + 4.36(H/h_c)^{1.28}} \quad for (H/h_c) < 40,\ S = 1V:2H \tag{2.1}$$

$$\Delta E_r = \frac{\Delta E}{E_0} = 1 - \frac{2 + 10.01(H/h_c)^{0.63}}{6.46(H/h_c)^{0.21} + 4.31(H/h_c)^{1.21}} \quad for (H/h_c) < 40,\ S \geq 1V:4H \tag{2.2}$$

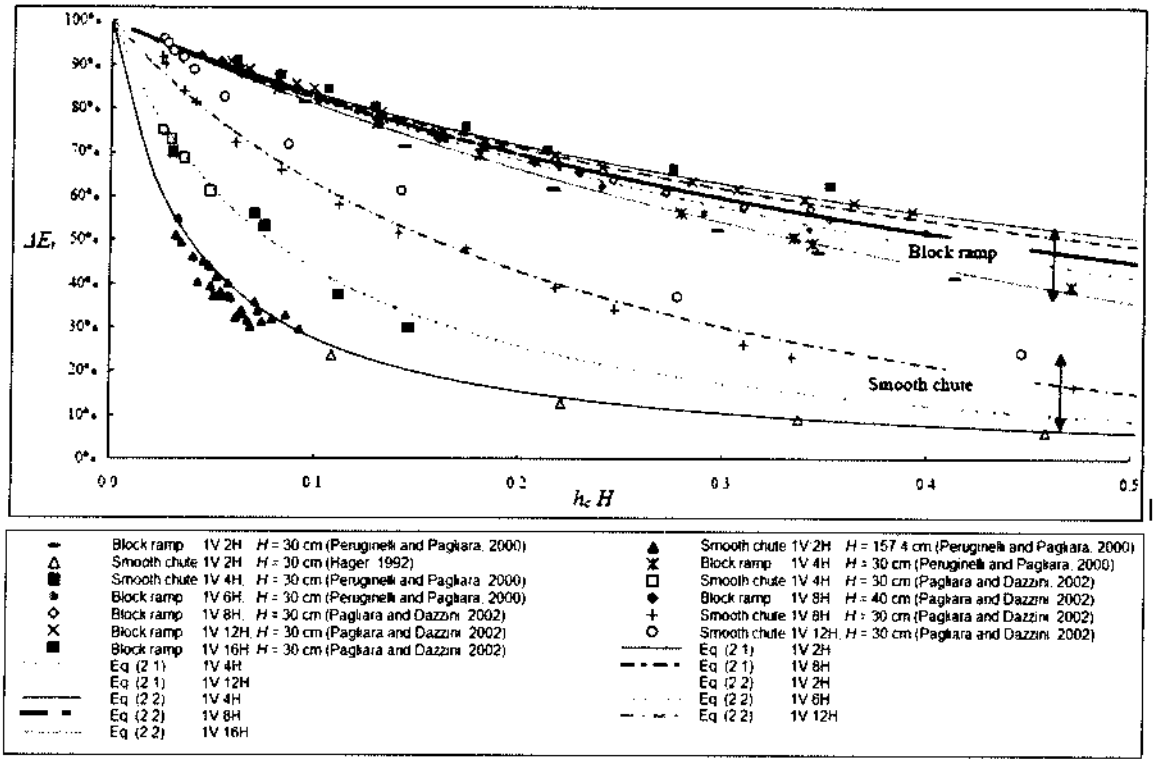

Fig. 2.5 Comparison of relative energy dissipation of block ramps with rock chutes of various types (Pagliara and Dazzini, 2002)

Spillways and chutes which transmit upstream flow down a slope have been adopted widely in water resources projects. The hydraulics of stepped channel was investigated Chanson (1994), and the author postulated the equations for the energy dissipation in condition of nappe and skimming flow (Eq. 2.3) between the entrance and toe of a chute.

$$\Delta E_r = 1 - \frac{h_u \cos\theta + h_c^3}{1.5h_c + H} \tag{2.3}$$

Flow resistance has also been investigated in term of Manning coefficient and Darcy–Weisbach friction factor for rock riprap in mountain streams with steep slopes. Abt et al. (1987, 1988), Anderson et al. (1970); Jarrett (1984, 1988); Ugarte and Madrid–Aris (1994); Soto and Madrid–Aris (1994); Rice et al. (1998); and Golubtsov (1969) conducted the test to estimate flow resistance in terms of the Manning's coefficient, while Bathurst (1985) and Rice et al. (1998) conducted the test to estimate out the flow resistance in terms of the friction factor. Chanson (1999) studied ancient Roman drop shafts structures and postulated a relation for modern design after re-analysis with physical model tests (Eq. 2.4). These drop shafts have been projected to have better water cushion to prevent scour than the modern vortex drop shafts.

$$\frac{\Delta E}{E_o} = 1 - \left[\frac{0.54\left(\frac{h_c}{\Delta z}\right)^{0.275} + \frac{3.43}{2}\left(\frac{h_c}{\Delta z}\right)^{-0.55}}{1.5 + \left(\frac{\Delta z}{h_c}\right)} \right] \tag{2.4}$$

where, Δz is the drop crest elevation above the level of downstream toe.

Pagliara and Chiavaccini (2006a, b) postulated energy loss equations for smooth, base material and reinforced configurations. Janisch and Weichert (2006), Tamagni et. al. (2010) studied unstructured and structured block ramps with the objective of improving the river bed morphology and stability of steep channels. Unstructured block ramps (Fig.2.6a) are loose unstructured blocks distributed on the rough-textured bed material and were investigated for the possibility for linking two rivers (Janisch and Weichert, 2006). The laboratory investigation of such block ramps is still undergoing (Fig. 2.6b).

Fig.2.6a Unstructured block ramp application study on Landquart river (Janisch and Weichert, 2006)

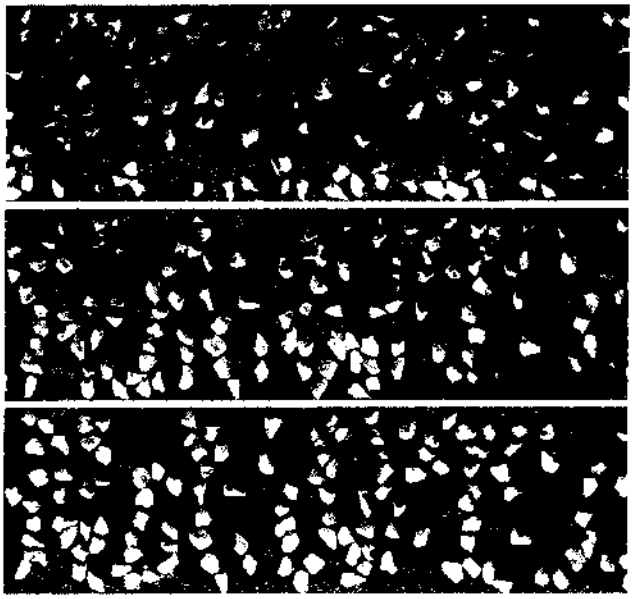

Fig.2.6b Unstructured block ramp in the laboratory study (Janisch and Tamagni, 2008)

Structured block ramps (Fig. 2.7) were tested to find an optimum combination of step length, pool depth and ramp by (Janisch and Tamagni, 2008).

Fig.2.7 Structured block ramps with boulders (Janisch and Tamagni, 2008)

Oertel (2010) investigated both physical and numerical models of cross-bar block ramps and described it as part of the structured ramp family and separate a river bottom slide into several basins with adequate velocities and acceptable water levels. He compared the numerical *FLOW-3D* results with the physical model (Fig. 2.8), and found a good conformity for every discharge regime; the stepped as well as the waved flow and, for very high discharges, quasi-uniform flow were reproduced in an accurate way especially for discharges ranging above 0.05 m^3/s.

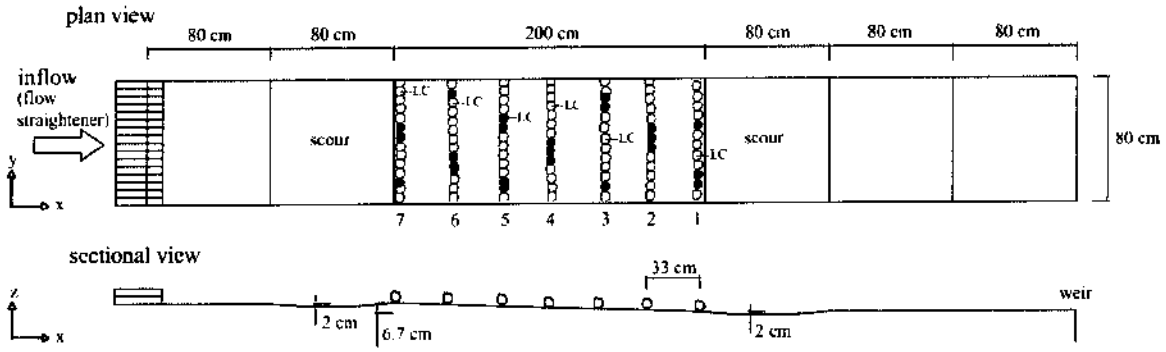

Fig.2.8 Schematic plot of physical crossbar block ramp model (Oertel and Schlenkhoff, 2012)

Oertel and Schlenkhoff (2012) stated that the main parameters used to calculate the relative energy dissipation for the given representative crossbar block ramp structures are the discharge and the slope. The effects of boulder's roughness or the bottom material were not analyzed in detail because the energy loss due to the crossbars was the leading parameter within their study. However, to analyze the drag forces on single boulders on the crossbar block ramp, a special arrangement was used by vertically placing load cells (LC) to measured the drag forces directly (Fig. 2.9). They concluded that bigger boulder sizes of D_B = 9 cm, yielded higher relative energy dissipation by approximately 5% compared to smaller boulder sizes of D_B = 6 cm. In contrast, increasing crossbar distances (i.e. longitudinal spacing) have no major influence on the relative energy dissipation. They developed exponential formulae for a flow system with crossbars as the main flow resistance to estimate the relative energy dissipation using physical and numerical model results, which was in parallel with that proposed by Pagliara and Chiavacinni (2006a) as in Eq. (1.2) with the parameters A,B and C determined by best fit as in Eqs. (2.5a, 2.5b and 2.5c),

$$A = 0.17 - \frac{0.0017}{S} \tag{2.5a}$$

$$B = -0.7 + \frac{0.0073}{S} \tag{2.5b}$$

$$C = -4.9 - \frac{0.26}{S} \tag{2.5c}$$

The authors postulated that crossbar block ramps can be constructed with slopes of approximately S = 1:10 to 1:50, prescribing that S should be less than 1:20 for stability and ecological considerations. Figure 2.9 shows a practical application of crossbar block ramps.

Fig.2.9 Crossbar block ramp application in the Wupperriver, Germany (Oertel and Schlenkhoff, 2012)

2.3 HYDRAULICS OF BLOCK RAMPS

A subjective understanding of the hydraulic characteristics is essential to factor the appropriate parameters involved in the energy loss process to comprehend the efficiency and energy dissipation characteristics of block ramp. The hydraulic properties of block ramp structures and how they relate to channel morphology preservation theories have been studied, such as the velocity reversal hypothesis (Keller, 1970) and sediment transport discussions through riffle-pool sequences (Carling, 1991). The armoring of riffle features by constructing rock ramps increases the resistance of the bed and further influences the structure of the riffle pool sequences (Fig. 2.10), potentially improving the ecological health and habitat diversity of the effected stream channel (Scott et al., 2004). The use of boulders gives different advantages: they can increase the energy dissipation caused by the ramp acting as macro-roughness elements and can facilitate stream fishes passage across the ramp, as their presence create on the ramp a cycle of swifter and slower flow zones more favorable to the biologic exchanges (Pagliara & Pozzolini, 2003).

Fig. 2.10 Close view of flow profile over an unilateral macro-roughness element (Aberle and Smart, 2003)

The flow over the ramp is generally characterized by an approach flow (generally stating critical flow depth at the transformation of slope, upstream crest) with a non-aerated or developing flow region circumscribing growth of a boundary layer, then accelerating down the slope to an inception point where the boundary layer growth meets the flow surface to give rise to an aerated flow region. A fully developed flow generally persists much the slope

becomes moderate or gentle. This is illustrated in Fig. 2.11 and may vary in case of large scale roughness and flow conditions.

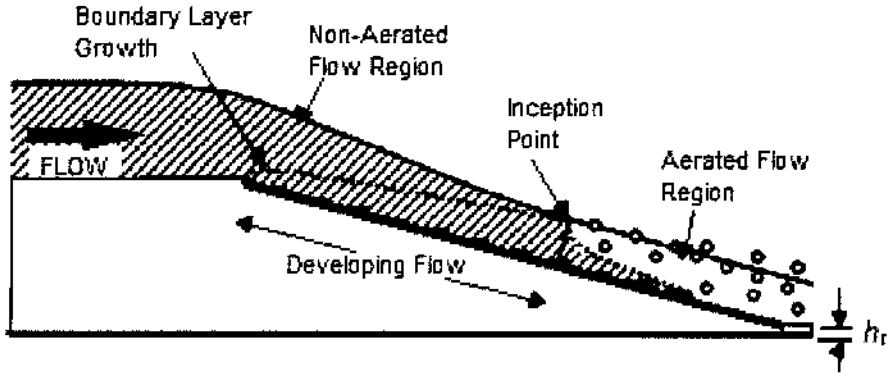

Fig. 2.11 Schematic turbulent flow profile on a rough ramp or chute

Peterson and Mohanty (1960) stated that roughness is an appreciable portion of the depth of flow in steep channels. Turbulent flow fields with different contents of vortices and coherent structures were identified by submergence ratio and concentration of roughness (Lyn, 1993). It is seen that when the macro-roughness boulder elements are introduced, turbulence is dominated by the interactions between the wakes, generated downstream of the boulders, and the jets generated in between the boulders (Nikora et al., 2001, 2004). Characteristics of flow on ramp with base material and boulders are shown in Figs. 2.12 and 2.13.

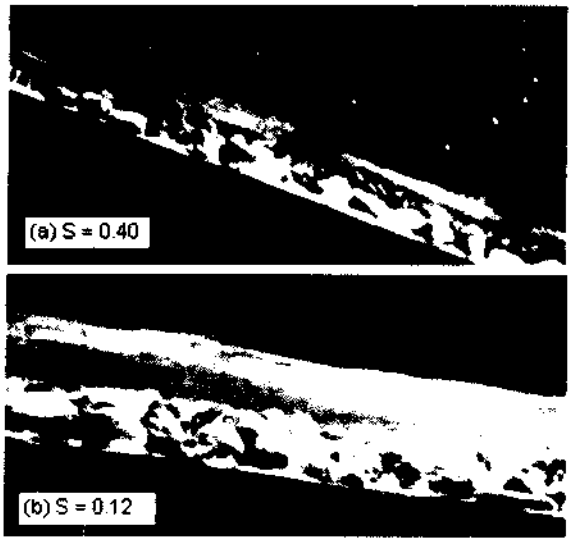

Fig. 2.12 Flow profile on uniform base material on the ramp
(Pagliara and Chiavaccini, 2006c)

Fig.2.13 Flow profile on base material with boulders:
(a) smooth, and (b) rough surfaces (Pagliara and Chiavaccini, 2006c)

2.3.1 Classification of Flow

For better understanding of the flow over the block ramps and quantifying the energy dissipation, it is necessary to classify the flow over the ramps and similar structures. This section deals with various type of flow that are likely to happen over the ramps. Aberle (2007) classified the flow on block ramps of type A in four typical categories depending on discharge and tail water level. It was assumed that critical flow occurs on the ramp head (flow conditions change from subcritical to supercritical) and a hydraulic jump occurs at the ramp toe or, depending on the tail water level, somewhere on the ramp. Janisch and Tamagni (2008) classified undulating flow conditions with Froude numbers close to unity, mostly for unstructured block ramps of type B (Fig. 2.2). Oertel et al., (2011) presented a rather complex classification based on the relative water level (water depth to boulder height), the obstruction ratio (sum of boulder widths to channel width), the boulder configuration (interaction of boulders in rows or columns and their spacing), and sub- or supercritical flows.

Despite the annals of research on free-surface flow over rough channel bed, a holistic approach considering the whole flow field from the channel bottom to the free-surface is relatively not systematically classified especially for free-surface flow over steep channels with rough beds (Mohanty, 1957; Erpicum et al., 2009). This is a necessity to understand and categorize the governing hydraulic variables for such channel studies. Based on the prerogative of the present research and adapting from studies on high-gradient or mountain

streams (Jarrett, 1984; Bathurst, 1985; Aguirre-Pe and Fuentes, 1990; Aberle, 2007) and experimental studies on steep channels (Morris, 1955; Peterson and Mohanty, 1960; Hartung and Scheuerlein, 1967; Aberle and Smart, 2003; Canovaro and Solari 2007) flow conditions on the block ramps may be categorized into the following four types.

2.3.1.1 Tumbling or undulating flow

When the distance between the boulders is relatively high, then a condition of flow dominated by scattered regions of alternate acceleration and deceleration through critical flow over the boulders in a cyclic order gives an appearance of water to "tumble" over the boulders (Fig. 2.14). Localized hydraulic jumps in between the boulders may take place but no wake interaction occurs. In such case, flow resistance is proportional to the number of boulders. At lower discharges, the standing wave-like pattern associated with the hydraulic jumps subsides, and the flow transits into a tranquil state even above the tops of the boulders.

The velocity at the outlet of the channel is nearly equal to the critical velocity, which can be handled safely by a stilling basin of smaller size. The efficiency of this device is dependent on the height and spacing of the elements that ensure succession of hydraulic jumps. For a representative roughness height (k), sketch of a tumbling flow profile is given in Fig. 2.15, where λ representing length of a wave in the flow denotes the centre to centre (c/c) spacing between the roughness elements or boulders.

Fig.2.14 Undulating or tumbling flow conditions in an unstructured block ramp application on Wyna River, Switzerland

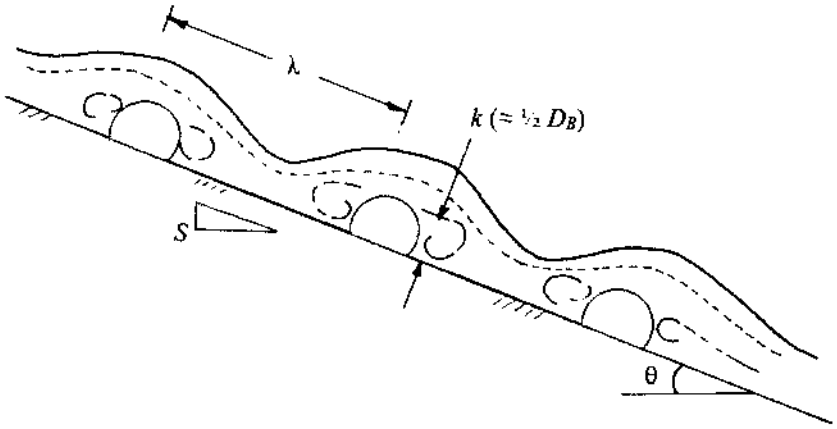

Fig. 2.15 Tumbling flow profile over large roughness elements (boulders)

2.3.1.2 Wake interference flow

When the elements are sufficiently close together and the wake behind each roughness element overlaps with the next element, flow resistance is no longer given by the sum of the single effects, since the vortex generation and dissipation phenomena associated with each wake will interfere with those of the adjacent roughness elements. This type of flow also occur in amalgamation with tumbling flow when the flow conditions and macro-roughness spacing do not permit a clear asymptote profile of either flow types.

2.3.1.3 Quasi-smooth or skimming flow

When the boulders are spaced so closely as to form a more or less smooth pseudo-wall composed of the boulder crests, or at higher stages the sub-critical depth pools below the boulders are swept out by the increased momentum, the flow skims over the boulders at super-critical velocity. Within the enclosed pockets of "dead fluid", there are stable vortices, unable to separate and mingle with the bulk flow because of the closeness of the downstream boulders.

2.3.1.4 Protruding flow

In the case of mountain streams, due to the presence of large rocks and boulders protruding from the steep channel bed, the flow depth is typically analogous with roughness size, as also indicated by Canovaro et al. (2007). Under similar conditions in the laboratory flume, when the relative submergence decreases especially for large roughness boulder elements, the flow relatively travels viscously between the macro-roughness boulders and the boulders seem to

protrude out of the flow. This flow type is generally a characteristic of block ramps with macro-roughness boulders.

2.3.2 Turbulence and Velocity Distribution

While it is important to have conceptual understanding and quantitative description of turbulent flows, their random nature makes a deterministic solution of equations of motion unattainable. Given their engineering importance and also their complexity, turbulent flows on rough channel beds have been extensively studied by Patel (1998), Nikora et al., (2001, 2004), and Jimenez (2004). Jimenez (2004) summarized from his studies that sufficiently large roughness modifies the whole flow. Although most of the turbulent energy is generated close to the wall, large roughness affects the turbulence structure throughout the flow depth (Chen, 1992). The effect of wall roughness on the turbulent flow characteristics increases with the increase of the roughness size (k or D_B). For flow over large-scale roughness with size of the same order of the flow depth (h), it is expected that the flow structures and velocity distribution are highly dependent on the roughness geometry. The mean velocity profiles in channels over rough beds differ considerably from the profile over a smooth bed since the bottom drag is significantly larger when roughness elements are present (Polatel, 2006).

In view of the flow separation and reattachment (Fig. 2.16), flow regions with localized wakes and adverse pressure gradients, detachment and reattachment of the boundary shear layer, etc., applications of the ideal flow principles will be rough engineering approximations (White, 1991). The empirical formulations need to be based on sound and multi-varied measurements in the laboratory.

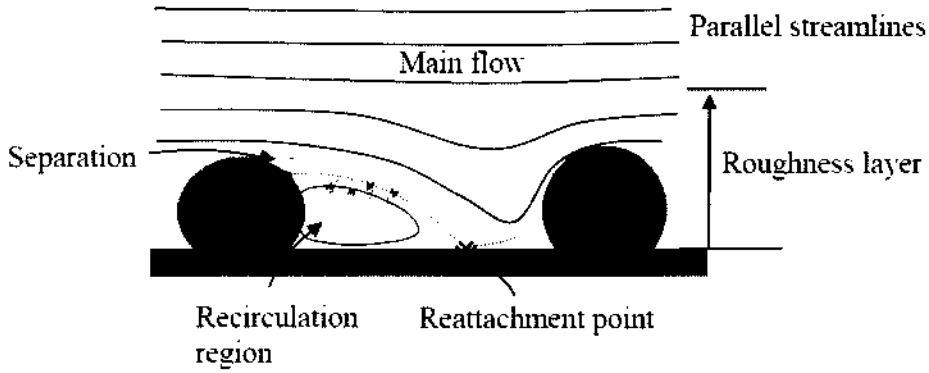

Fig.2.16 A schematic representation of flow turbulence on block ramps with boulders

Each boulder or macro-roughness element is a source of vortices, which may be delineated into two orders: (i) those with vertical axes, and (ii) those with horizontal axes. The vortices are generated by the accelerated flow around the upstream faces of the boulders and dissipate in the retarded flow in the wakes downstream from the boulders. At high boulder concentration, each upstream boulder produces vortices that interfere with each other consequently influencing the drag on the boulder immediately downstream (Fig. 2.17a). For low concentrations, the wake of an upstream boulder is diffused so greatly that the downstream boulder is subjected to the flow distribution that is produced by the entire block pattern (Fig. 2.17b). When the free surface impact over the boulder tips, it is possible to observe the formation of stable stream-wise oriented vortex (drag vortex) in the flow, which becomes more stable for relatively low flow depths (Pagliara et al., 2009). Moreover, shear vortex is also present between the boulders.

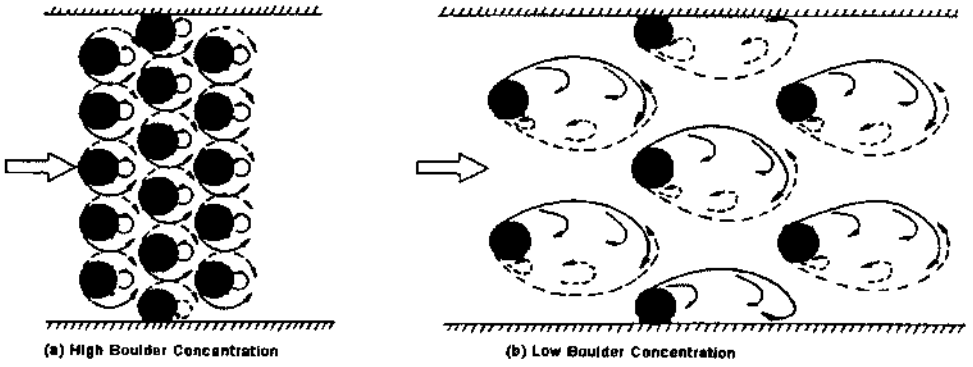

Figure 2.17 Schematic illustration of vortices and wake generation in flow on block ramps with protruding boulders in staggered arrangement

Lawrence (1997) studied the effects of the roughness elements on the overall structure of the flow and stated that the effects are not fully accounted for by a model that is based on flow around individual elements that uses a coefficient of drag originally developed for fully submerged objects in an otherwise uniform flow field. Oertel et al., (2011) stated that the flow over a boulder is a complex 3-dimensional free surface flow problem, and that calculation of mean water levels and velocities on block ramp structure can vary considerably due to the interaction processes with the macro-roughness boulders. He thereby proposed the following empirical relation to determine the drag coefficient (C_D).

$$C_D = -2.0\times10^{-11}\,\mathrm{Re}^2 + 2.2\times10^{-6}\,\mathrm{Re} + 1.4 \qquad (2.6)$$

Field and laboratory measurements of velocity profiles in high gradient gravel bed streams (Marchand et. al., 1984; Baiamonte et al., 1995) suggest that the velocity takes an ''S-shaped'' profile and at least two flow regions can be identified in the flow field: a near bed region characterized by relatively low flow velocity dominated by the loss of flow momentum due to drag around the bed material and an upper region, in proximity to the water surface, characterized by significantly higher velocities distributed according to a profile which deviates from a logarithmic law.

2.4 ENERGY DISSIPATION FACTORS FOR BLOCK RAMPS

With an insight into the energy dissipation mechanism and hydraulic composition of block ramps, the various critical factors relative to the process are further assessed.

2.4.1 Flow Resistance

Many researchers have postulated theories to relate flow resistance to the energy loss in the flow (Rouse, 1965; Bathurst, 1985; Ugarte and Madrid, 1994; Baiamonte and Ferro, 1997). Rouse (1965) classified flow resistance into four components: (i) surface or skin friction, (ii) form resistance or drag, (iii) wave resistance from free surface distortion, and (iv) resistance associated with local acceleration or flow unsteadiness. By using the Weisbach resistance coefficient or friction factor f, he expressed flow resistance as the following dimensionless symbolic function as given in Eq. (2.7).

$$f = \phi(\mathrm{Re}, K, \eta, N, \mathrm{Fr}, U) \tag{2.7}$$

where Re = Reynolds number; K = relative roughness, usually expressed as k_s/R, where k_s is the equivalent wall surface roughness and R is hydraulic radius of the flow; η = cross-sectional geometric shape; N = non-uniformity of the channel in both profile and plan; Fr = number; U = degree of flow unsteadiness; and φ represents a function. Smart et al. (2002) stated that the formulas for predicting flow resistance are empirical or theoretically based and described the term ''flow resistance'' broadly by the ratio U/U^* (where U= mean flow velocity) and similar friction indicators such as the Darcy–Weisbach friction factor f, Chezy's coefficient C, and Manning's coefficient. These were all interrelated as in the classical flow resistance law (Eqs. 2.8 and 2.9).

$$\left(\frac{U}{U^*}\right)^2 = \frac{8}{f} = \frac{C^2}{g} = \frac{R^{1/3}}{gn^2} \tag{2.8}$$

In terms of other flow parameters,

$$\left(\frac{U}{U^*}\right)^2 = \frac{\mathrm{Fr}^2}{S} = \frac{Q_p U}{\tau_o A_f} \tag{2.9}$$

where, Fr = Froude number, Q_pU = flow momentum flux, τ_o = shear force per unit area in the plane of the bed of the channel, and A_f = cross-sectional area of flow. Several approaches to the quantification of flow resistance in gravel-bed streams have also been based on the boundary layer theory. These approaches are generally of the form (Eq. 2.10):

$$\sqrt{\frac{8}{f}} = \frac{1}{\kappa} \ln\left(\frac{h}{d_{84}}\right) + b_0 \tag{2.10}$$

where κ = von Karman constant, h = mean water depth, b_0= constant. The value of the von Karman constant is normally taken as $\kappa = 0.41$.

The dependence of flow resistance on the relative submergence was investigated by Bathurst (1978, 1985) and Bathurst et al., (1981). They found that the flow resistance decreases as the relative submergence increases. Several authors have postulated relations to determine flow resistance in terms of $\sqrt{8/f}$ or n with respect to the relative submergence in the form of the general flow resistance equation (Eq.2.10) or in terms of correlation derived from their experimental studies. Table 2.1 and Table 2.2 present a list of the equations postulated which are in close relation to the present study and accounting macro-roughness elements in terms of the flow resistance factors viz., Darcy–Weisbach friction factor and Manning's roughness coefficient, respectively. In the following relations, for Eq. 2.15, the relationship between Γ and α for given e (= D_{50}/d_{50}) values (Ferro, 1999) is given in Fig. 2.18.

Table 2.1 Flow resistance relations postulated by various investigator(s) in terms of Darcy–Weisbach friction factor

Sl.	Investigator (s)	Relation / equation	Description	Eq. No
1	Bathurst (1985)	$\sqrt{\frac{8}{f}} = 5.62 \log\left(\frac{h}{d_{84}}\right) + 4.0$	range of the resistance variation for channels with slopes,S ≤ 0.4%	2.11
2	Aguirre-		κ (universal Von Karman	2.12

	Peand Fuentes(1990)	$\sqrt{\frac{8}{f}} = \frac{1}{\kappa}\ln\left(\frac{h}{\gamma d_{mean}}\right) + B - \frac{1}{\kappa}$	constant) = 0.41, γ (texture factor related to Nikuradse standard) = 3.0 for hemispheres, B = 8.5 for high shear velocity	
3	Lawrence (1997)	$f = \frac{8gh\sin\theta}{v^2} = 50\left(\frac{k}{h}\right)^2\kappa^2 \approx 10\Lambda^{-2}$ where, Λ (Inundation ratio) $= \left(\frac{h}{k}\right)$	θ= angle of the surface slope, k= characteristic height of roughness elements, κ (Von Karman constant) = 0.41	2.13
4	Rice et al. (1998)	$\sqrt{\frac{8}{f}} = 5.1\ \log\left(\frac{h}{d_{84}}\right) + 6.0$	Angular rock riprap: $0.025 < S < 0.333$, $0.052\text{ m} < D_m < 0.278\text{ m}$	2.14
5	Ferro (1999)	$\sqrt{\frac{8}{f}} = 15.74\ \log\left(\frac{h}{d_{84}}\right) + b_0$	$b_0 = -1.5$ for $\Gamma > 50\%$, $b_0 = (-0.2590 - 0.1189\,\alpha - 0.01711\,\alpha^2 + 0.00117\,\alpha^3)$ For , $\Gamma < 50\%$, and α for various e (= D_{50}/d_{50}) from Fig. 2.20	2.15
6	Bathurst (2002)	$\sqrt{\frac{8}{f}} = 3.84\left(\frac{h}{d_{84}}\right)^{0.547}$	derived with field data for 9 sites	2.16
7	Aberle and Smart (2003)	$\sqrt{\frac{8}{f}} = 3.54\ \ln\left(\frac{h}{d_{84}}\right) + 4.41$	derived with experimental data with d_{90}= 64 mm and d_{10}= 32 mm randomly placed at S = 8 to 10%.	2.17
8	Pagliara and Chiavacinni (2006c)	$\sqrt{\frac{8}{f_{tot}}} = 3.5(1+\Gamma)^c S^{-0.17}\left(\frac{h}{d_{84}}\right)^{0.10}$	value of parameter c obtained from experimental investigation and listed in Table 2.3	2.18
9	Wang et al. (2011)	$f = 1.0083\left(\frac{h}{d_{50}}\right)^{-0.622}(\log \mathrm{Re})^{-0.622}$	experimental derivation for gravel bed channels	2.19
10	Oertel and Schlenkhoff (2012)	$\sqrt{\frac{8}{f}} = \left(4.4 + \frac{0.09}{S}\right)\log\left(\frac{h}{D_B}\right) + \left(2.2 + \frac{0.0023}{S}\right)$	derived for crossbar block ramps with boulder height of crossbars as D_B	2.20

Table 2.2 Flow resistance relations postulated by various investigator(s) in terms of Manning's roughness coefficient

Sl.	Investigator (s)	Relation / equation	Description	Eq. No
1	Jarret (1984)	$n = 0.39\, S_f^{0.38} R^{-0.16}$	0.002 <S<0.04 m/m	2.21
2	Soto and Madrid–Aris (1994)	$n = \left[0.183 + \ln\left(\frac{1.7462\, S_f^{0.1581}}{\mathrm{Fr}^{0.2631}}\right)\right] + \frac{(d_{84})^{\frac{1}{6}}}{\sqrt{g}}$	$0 < \frac{R}{d_{84}} < 1.0$, (large scale roughness) and for Q_{max} = 10.3 m^3/s	2.22
3	Palt (2001)	$\frac{n_r}{n_{tot}} = 0.15\, S^{-0.36}$	Developed from field data of Himalayan mountain streams, 0.002 <S<0.12 m/m ; n_r is a roughness coefficient for skin friction only	2.23
4	Wong and Parker (2006)	$\frac{1}{n_r} = \frac{(d_{90})^{\frac{1}{6}}}{23.2}$	Using flume experimental data	2.24
5	Rickenmann et al. (2006)	$\frac{n_r}{n} = 0.185\, S^{-0.22} \left(\frac{h}{d_{90}}\right)^{0.55}$	For S> 0.008 and using Palt (2001)	2.25
8	Pagliara and Chiavacinni (2006c)	$n_{tot} = 0.064\,(1+\Gamma)^e \times (d_{50}\, S)^{0.11}$	Value of parameter $e$obtained from experiments and listed in Table 2.3	2.26

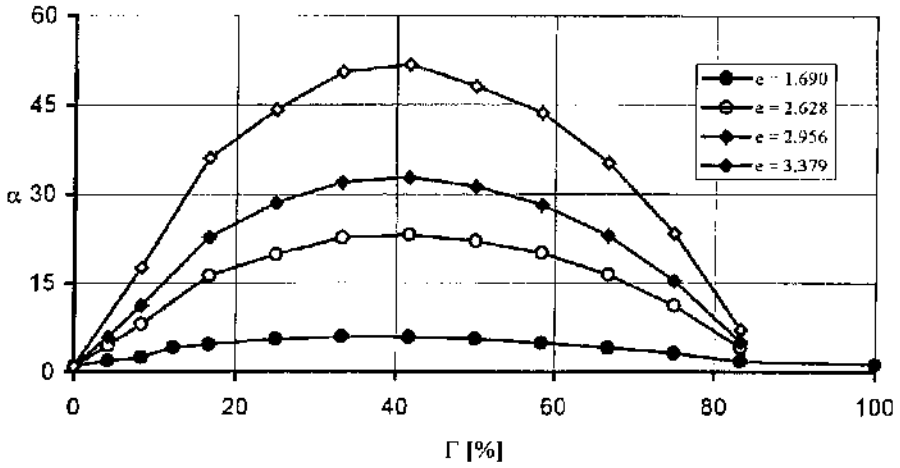

Fig. 2.18 Relationship between Γ and α for given e (= D_{50}/d_{50}) values (Ferro, 1999)

Pagliara and Chiavacinni (2006c) and Pagliara et al. (2008c) postulated that flow resistance is caused by the presence of the boulders, its concentration and disposition. Canovaro et al. (2007) asserted that flow resistance is a function of not only the relative submergence but also additional parameters related to the roughness geometry, such as spatial density (or concentration) and arrangement of macro-roughness elements. The effect of the presence of large roughness on flow resistance was investigated by Morris (1955), Mohanty (1957), Herbich and Shulits (1964), Sayre and Albertson (1961), Lawrence (1997), Baiamonte and Ferro (1997), Aberle and Smart (2003), Canovaro et al., (2007) etc.

Abt et al. (1987) correlated the median stone diameter (d_{50}) and the bed slope S to Manning's coefficient n as given by Eq. (2.27),

$$n = 0.0456 \times (d_{50} S)^{0.159} \tag{2.27}$$

where, d_{50} ranges between 26 to 157 mm, and S between 0.01 to 0.20. Rice et al., (1998) calculated "n" for a loose rock riprap as given by Eq. (2.28),

$$n = 0.029 \times (d_{50} S)^{0.147} \tag{2.28}$$

where d_{50} is in mm and range of S = 0.10 to 0.40.

Lawrence (1997) expressed the friction factor as the dependent dimensionless quantity in terms of Froude Number (Fr) and the channel slope θ (in degrees) as,

$$\mathrm{Fr} = \frac{8 \sin\theta}{f} \tag{2.29}$$

Assuming that roughness elements are fully covered by the flow and a logarithmic profile extends to the surface, Smart et al. (2002) presented a flow resistance parameter in terms of depth averaged velocity Eq. (2.30).

$$\frac{U}{U^*} = \frac{1}{\kappa}\left[\frac{R_v}{R_v - Z_o}\ln\left(\frac{R_v}{Z_o}\right) - 1\right] \tag{2.30}$$

where U = mean flow velocity at elevation Z, κ = von Karman's constant (κ = 0.4), and Z_0 describes the hydraulic roughness of the boundary (the height above the z datum where

stream wise velocity is zero), R_v = volume of overlying water per unit plan area of bed which we will refer to as the volumetric hydraulic radius.

Ferro (1999) carried out an experimental investigation using a ground layer constituted by bed particles having a characteristic diameter d_{50}, on which N_B number of boulders having a characteristic diameter D_{50} were arranged. He established the following flow resistance equation (Eq. 2.31).

$$\sqrt{\frac{8}{f}} = b_0 + 15.74\left(\frac{h}{d_{84}}\right) \tag{2.31}$$

in which for Γ values less than 50 per cent the intercept b_0 of the flow resistance law depends on both the median size ratio D_{50}/d_{50} and the concentration while for $\Gamma > 50$ per cent b_0 is constant and equal to $-1{\cdot}5$.

Pagliara and Chiavacinni (2006c) studied flow resistance in terms of both Manning coefficient and Darcy–Weisbach friction factor (f) for a rock chute with steep slopes upto 0.40 and expressed the total flow resistance relationship (for both base material and boulders) f_{tot},

$$\sqrt{\frac{8}{f_{tot}}} = 3.5(1+\Gamma)^{c} S^{-0.17}\left(\frac{h}{d_{84}}\right)^{0.10} \tag{2.32}$$

where, Γ is the boulder concentration, h is the flow depth, d_{84} is the size of the base material for which 84% of the material is finer. Also, they proposed a total Manning's coefficient n_{tot} by incorporating the influence of boulders concentration as,

$$n_{tot} = 0.064\,(1+\Gamma)^{e} \times (d_{50}\,S)^{0.11} \tag{2.33}$$

in which c and e are coefficients derived from experimental measurements and observed data, and their values are listed in Table 2.3.

Table 2.3. Values of coefficient c and e to be used in Eq. (2.32) and Eq.(2.33) (Pagliara and Chiavacinni, 2006c)

Coefficient	Random disposition, Rounded agg.	Row disposition, Rounded agg.	Random disposition, Crushed agg.	Row disposition, Crushed agg.
c	–1.60	–1.80	–2.40	–3.00
e	1.00	1.20	1.80	2.30

Using the relation of energy dissipation between entrance and toe of a chute (Chanson, 1994), equation of continuity and Darcy–Weisbach equation, Pagliara and Chiavacinni (2006a) derived a relation for relative energy dissipation of block ramps in terms of friction factor (f) adopting similar scale roughness conditions for the chute (Eq. 2.34).

$$\Delta E_r = 1 - \frac{\left[\left(\frac{f}{8S}\right)^{1/3}\cos\theta + \frac{1}{2}\left(\frac{f}{8S}\right)^{-2/3}\right]\frac{h_c}{H}}{\left(1.5\frac{h_c}{H}+1\right)} \qquad (2.34)$$

2.4.2 Flow Conditions and Characteristics

Gradually varied flow to rapidly varied flow plays a dominating role in flow over the ramp. Uniform flow depth is attained at the toe of the ramp for $0 < h_c/H < 1.2$, where h_c is the critical flow depth and H is the ramp height (Pagliara and Chiavacinni, 2006a). Particularly, at greater slopes as 1V:4H, it is difficult to obtain uniform flow conditions in the laboratory flume. In the reinforced block ramp, boulders modify the water profile that becomes more irregular and consequently flow depths become greater and a general reduction in velocity is observed as also reported by Pagliara and Chiavacinni (2006b). Kucukali and Cokgor (2008) found that the streamwise velocities (along the longitudinal direction of the ramp) add up to 10% faster than the surrounding flow and secondary currents are of the order of 5% of the mean streamwise velocity, for rough beds with crushed stone aggregate of d_{50} = 5.7 mm.

2.4.3 Channel and Bed Slope

Energy dissipation of block ramps varies inversely with ramp slope Pagliara and Chiavacinni (2006c). However, Pagliara and Chiavaccini (2006b) found that the slope do not increase energy dissipation in the reinforced block ramp. Rouse (1965) concluded that it is not the individual non-uniformities caused by the boulders but the overall channel slope that determines the cumulative rate of energy loss since a local increase in resistance will simply cause a local change in surface configuration. The slope must be adequate such that the form drag of the roughness elements and the shear on the channel bed can be surmounted by the water prism weight parallel to the bed (Peterson and Mohanty, 1960).

2.4.4 Flow Depth and Submergence

The depth of flow over the crests of the roughness elements (boulders) will control in part the vertical extent of the surface region with high turbulence and wakes. Pillai (1979) suggested that the effective depth, h_e should be evaluated by accounting for both the volume of the roughness elements and its concentration. Thus, more the number of roughness elements of a size in a given length and its concentration, less should be the effective depth. The effective depth may not be always equal to the average depth. A depth correction was proposed by Golubtsov (1969) for the flow depth measured for arriving at effective depth. The adapted form of the relation for block ramps with semi-hemispherical boulders is given in Eq. (2.35),

$$h_e = \left(h - \frac{D_B}{2}\right) - \left\{\frac{D_B}{6}\left(\frac{D_B}{2S_x}\right)^{-0.3}\right\} \qquad (2.35)$$

2.4.5 Macro-roughness Boulders and Concentration

Roughness elements are introduced on the block ramp under two considerations:

2.4.5.1 Micro-roughness or base material

Granular material with a uniformity coefficient (expressed by the ratio between d_{60} and d_{10}) close to 1.0 is laid on the smooth ramp bed. The smooth bed is composed of a geotextile layer to prevent filtration condition (Pagliara and Chiavaccini, 2006a) or a simple concrete trowel finish (Ahmad et al., 2009). The term "block ramp" takes shape when stones or granular bed material alike are packed on the ramp bed in an array or through different configurations.

2.4.5.2 Macro-roughness boulders

Boulders are introduced as macro scale roughness elements to achieve more energy dissipation and stability on the base material ramp. Boulders produce form drag forces which increase the flow resistance. Herbich and Shulits (1964) found that the shape of the macro-roughness elements is of secondary importance. Rouse (1965) concluded that the concentration of roughness elements is as essential as their size in determining resistance and energy loss; an optimum concentration 15% to 25%, depending upon element shape and arrangement, yields a maximum roughness effect. When the concentration is high (Γ approaches 1.0), the influence of the roughness pattern on the flow field fades since all the patterns collapse into the same configuration. The diameter of the boulders used in the studies

by Pagliara and Chiavaccini (2004) by were three times bigger than the base material with the boulders projected from the base material of about half its diameter. The same investigators used boulder sizes of 0.029 m, 0.038 m and 0.042 m in their study (Pagliara and Chiavacinni, 2006b). According to Ferro (1999) and Lawrence (1997), optimum flow resistance occur below a concentration, Γ=50%. Curran and Wilcock (2005) pointed that when the boulder concentration is more, the dissipation of energy by jets is predominant whereas for low boulder concentration, the dissipation of energy by vortices is predominant.

Pagliara and Chiavacinni (2006c) showed that as the boulder or macro-roughness concentration increases, the energy dissipation increases with a maximum of 10% to 12% for a concentration of ranging from 30% to 35%. Figure 2.21 shows smooth, rough and natural boulders adopted by the authors in their experimental investigation.

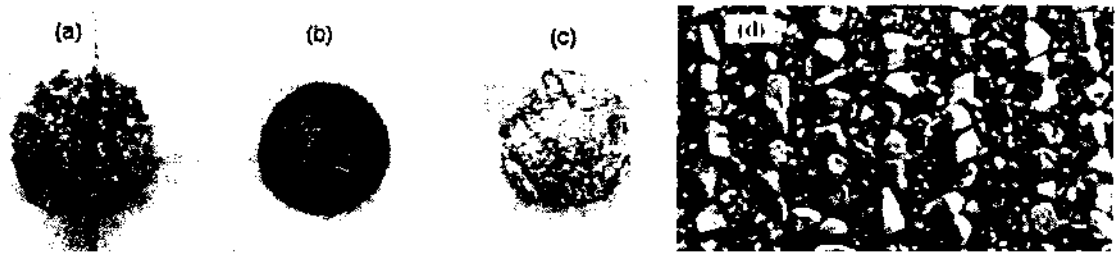

Fig. 2.19 Hemispheres replicating boulders: (a) covered with sand, (b) smooth, (c) covered with film of aluminum, and (d) natural stones placed over base material (Pagliara and Chiavacinni, 2006c)

2.4.6 Boulder Spacing and Geometry

Pagliara and Chiavacinni (2006c) conducted tests on ramps with rows and random disposition of boulders and found that random arrangements were less dissipative than the row arrangements. However, no spacing criteria for both arrangements were suggested. The same authors (2004) stated that the presence of the boulders improves the stability conditions on the block ramp, and the effect depends not only on the concentration but also on the planimetric arrangment used. Rouse (1965) indicated that in the case of regular dispositions of uniform and artificial roughness, the existence of an optimum value of spatial density produces the maximum of flow resistance.

Staggered arrangement with hemispherical-shaped boulders was studied by Ahmad et al. (2009) for boulder sizes and spacing as: for D_B = 5.5 cm, S_x/D_B= 4.0, 3.0, and 1.5 and S_y/D_B=1.23 (S_x and S_y represent the longitudinal and transverse spacing of boulders,

respectively); for D_B = 6.5 cm, S_x/D_B= 3.0, 2.0, 1.5, and 1.0 and S_y/D_B=0.81; and for D_B = 10 cm, S_x/D_B= 2.0, 1.5, and 1.0 and S_y/D_B=1.0. Non-uniform longitudinal spacing (lesser number of boulders on upper portion of the ramp and more number of boulders on the lower portion, and vice versa) pronounces a different impact on the energy dissipation, as was also studied by Ahmad et al., (2009).

However, Sayre and Albertson (1961) proposed that energy dissipation can be directly related to the boulder spacing. Herbich and Shulits (1964) related the transverse and longitudinal spacing by a roughness parameter, ξ, which is similar to the boulder concentration. The adapted relations are modified for block ramps with protruding boulders and given in Eqs. (2.36a) and (2.36b) as follows:

(i) when depth of flow, h > boulder height (skimming or submerged flow)

$$\xi = \frac{N_B \pi D_B^{\,2}}{8\sum(S_x + D_B)\sum(S_y + D_B)} \tag{2.36a}$$

(ii) when depth of flow, h < boulder height (protruding flow)

$$\xi = \frac{N_B h D_B^{\,2}}{\sum(S_x + D_B)\sum(S_y + D_B)} \tag{2.36b}$$

In similitude to block ramps, the use of roughness elements (square-blocks) on chutes was extensively studied by Morris (1968). It was shown that the optimum spacing (c/c) of elements was related to the critical spacing for maximum friction factor for flow in closed conduits or tranquil flow in open channels. He presented some guidelines that: (i) for roughness elements of square cross-section, the height k may be calculated in terms of the critical depth and slope of the chute (Eq. 2.37),

$$k = \frac{1}{(3 - 3.7S)^{2/3}} h_c \tag{2.37}$$

(ii) For cubical roughness elements, with cubes staggered in adjacent rows, and with a maximum transverse element spacing of 1.5 k the roughness height is given by Eq. (2.38).

$$k = 0.7 h_c \tag{2.38}$$

The height of the roughness element obtained from the above equations (Eqs. 2.36 and 2.37) is the minimum size to ensure tumbling flow. Morris (1968) further suggested an alternate

method is to use only five rows of elements at the downstream end of the chute, preceded by a single large leading roughness element for economical considerations (besides normally using the roughness elements throughout the entire length of the chute). The large element establishes one large hydraulic jump and the five following elements are then adequate to establish uniform tumbling flow for the given discharge from the leading element's overfall. The size, k_1, of the leading element is given by Eq. 2.39.

$$k_1 = \left[\sqrt{\left\{ \frac{2}{(1-S)^2} \left(\frac{h_c}{h_0} \right) - (1-S)^2 \right\}} \right] h_c \qquad (2.39)$$

Besides the above factors relating to the spatial density and geometry of macro-roughness boulders to the energy dissipation process, an important parameter that seem to link these parameters further with the macroscale roughness–induced flow resistance can be extracted from the studies of Canovaro et al. (2007) and Canovaro and Solari (2007). If the number of macro-roughness elements interacting with the lower layer of the flow is considerable, Bathurst (1987) asserted that the assumption of a logarithmic velocity profile is no longer valid, and the classical expression of flow resistance formulae cannot be applied. Thereby, a reduction coefficient (ψ) for the bottom layer flow velocity is introduced as a function of the macro-roughness spatial density and planimetric arrangement of boulders. The same is robustly adopted in the present study.

The reduction coefficient (ψ) is always smaller than 1, and is defined as the ratio between the cross-sectional area occupied by the flow among the macro-roughness elements in the lower layer and the total cross-sectional area of the lower layer (Fig. 2.20). Generally, in the case of a random planimetric arrangement with the macro-roughness placed with the short axis perpendicular to the channel bed and the long axis parallel the channel axis, ψ can be estimated as given by Canovaro et al., (2007) in Eqs. (2.40a and 2.40b).

$$\psi = 1 - \frac{\Pi}{4} D_m \sqrt{N_u} \quad \text{for } h_b \le D_s \qquad (2.40a)$$

$$\psi = 1 - \frac{\Pi}{4} \frac{D_s}{h_b} D_m \sqrt{N_u} \quad \text{for } h_b > D_s \qquad (2.40b)$$

where, D_s and D_m are the short and median axis diameters of the macro-roughness elements, approximated with ellipsoids, and N_u is the number of macro-roughness elements arranged on

an unit bed area. Adopting for block ramps with protruding boulders, the reduction coefficient is calculated as given in Eq. (2.41).

$$\psi = 1 - \frac{\Pi}{4}\frac{D_B}{2}\sqrt{N_u} \text{ where } N_u = (N_B/WL_R) \tag{2.41}$$

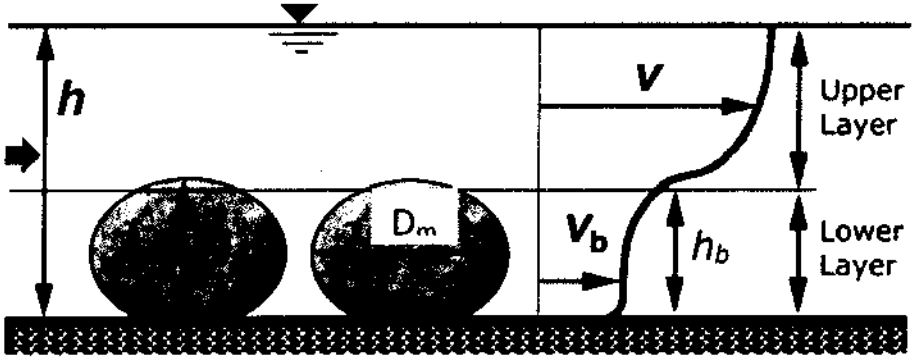

Fig. 2.20 Free surface flow over a bed with macro-roughness boulders (Canovaro et al., 2007)

2.4.7 Air Entrainment

Air entrainment does not affect the measurements of flow parameters significantly in macro-roughness channels (Peterson and Mohanty, 1960). However, Pagliara et al. (2009a) reinstated that entrained air can affect the performance evaluation of the block ramps as the bulk properties of the air-water mixture gets altered. As flow accelerates down the slope, a boundary layer develops from the crest and after fully developed flow is established, air entrainment takes place due to high velocities (Tullis and Larchar, 2011) and flow interference with the roughness elements producing considerable flow bulking. Kucukali and Cokgor (2008) further stated that a boulder-flow interaction can trigger air-water mass transfer and there is an interrelation between the aeration efficiency and the energy dissipation when the boulders are submerged.

However, the inheritance of the mean air concentration with energy dissipation characteristics on block ramps is taken negligible. Chanson (1993b) gave an estimate of the air entering the flow in terms of the bed slope of the chute as,

$$C_m = (1.44 \times \sin\theta - 0.08) \tag{2.42}$$

In the present experimental study, as also affirmed by Pagliara and Chiavacinni (2006a), for steep slopes no white water conditions were practically observed in the flow. Citing the same reasons whereby the contribution of air concentration and then of the Weber number or other parameters, which becomes significant when two-phase flow occurs, air entrainment factor is not taken into consideration.

2.5 ESTIMATION OF ENERGY DISSIPATION ON BLOCK RAMPS

Various relations to calculate the relative energy dissipation for different configurations of block ramps have been postulated from the experimental studies, and the same are described below. In most cases the kinetic energy correction factor or Coriolis coefficient has been assumed equal to unity.

2.5.1 Smooth Ramp

A smooth ramp is highly representative of a chute in terms of hydraulic behaviour. According to Chanson (1994), the energy dissipation between the inlet and the toe of a smooth ramp chute is given by the following relationship (Eq. 2.43):

$$\Delta E_r = 1 - \left(\frac{h_u \cos\theta + h_c}{1.5h_c + H} \right) \tag{2.43}$$

where, ΔE_r = relative energy dissipation, $\Delta E = (E_0 - E_t)$; E_o and E_t are respectively the energy at the upstream crest and at the toe of the ramp chute, and h_u= uniform flow depth.

Peruginelli and Pagliara (2000) adopted base material of d_{50} ranging from 0.085 to 0.105 m and proposed the following similar relationships between relative energy dissipation and the parameter, H/h_c based on regression curves as given in Eqs. (2.1) and (2.2). Pagliara and Dazzini (2002) alternatively proposed the following equation (Eq. 2.44) for very rough ramps,

$$\Delta E_r = 1 - \left[\frac{(0.925 \times S + 1.931)\frac{h_c}{H}}{(10.595 \times S^2 - 6.817 \times S + 2.417)\frac{h_c}{H} + 1} \right] \tag{2.44}$$

The form of the above equations did not fit the experimental data satisfactorily and a refined form for the energy dissipation on smooth ramp and ramp with base material was postulated by Pagliara and Chiavaccini (2006a) as given in Eq. (1.2). The values of the roughness

factors *A*, *B*, and *C* decrease with the scale of roughness, with the exception of *C* for a smooth ramp case.

2.5.2 Block Ramp with Base Material

The term "block ramps" generally takes shape with the introduction of base material in the form of granular stone pebbles (both rounded and crushed stone aggregate) on the smooth ramp bed. This formation was designed to represent river-bed material imparting roughness in the channel flow. Pagliara and Chiavaccini (2006a) studied the configuration on similar lines with the smooth ramp and presented roughness coefficients which are given in Table 2.4.

Table 2.4 Roughness scale conditions

Roughness condition	h_u/d_{84} (Bathurst, 1978)	h_c/d_{50} (Pagliara and Chiavaccini, 2006a)
Large scale roughness (LR)	$h_u/d_{84} < 1.2$	$h_c/d_{50} < 2.5$
Intermediate scale roughness (IR)	$1.2 < h_u/d_{84} < 4.0$	$2.5 < h_c/d_{50} < 6.6$
Small scale roughness (SR)	$h_u/d_{84} > 4.0$	$6.6 < h_c/d_{50} < 42$

Pagliara and Chiavaccini (2006a) further carried out the test on the block ramp with base material for various slopes 1V:4H, 1V:6H, 1V:8H and 1V:12H and varying the size of the base material such as d_{50} and d_{84} ranging from 1.0 mm to 88.0 mm and 1.3 mm to 105.0 mm respectively. The grain size was chosen with a uniformity coefficient (expressed by the ratio between d_{60} and d_{10}) close to unity.

From the studies, it was found that energy dissipation on block ramps with base material yield higher energy dissipation than the smooth ramp (Fig. 2.21) and that ΔE_r depends on the value of the dimensionless parameter h_c/d_{50} which could be considered as the relative submergence. Three different ranges were investigated by Pagliara and Chiavaccini (2006a) and are given in the Table 2.5. Relative energy dissipation was found to be higher in the large scale roughness conditions as shown in Fig. 2.21. The range intervals differ considerably from those indentified from by Bathurst (1985) because of the different parameters used. The critical depth h_c differs from the uniform flow depth h_u and the characteristic particle size is not d_{84} but d_{50}.

Table 2.5 Roughness coefficients for base material to be used in Eq. (1.2)

Roughness Condition	A	B	C
Large scale roughness (LR)	0.33	-1.3	-14.5
Intermediate scale roughness (IR)	0.25	-1.2	-12.0
Small scale roughness (SR)	0.15	-1.0	-11.5
Smooth Ramp	0.02	-0.9	-25.0

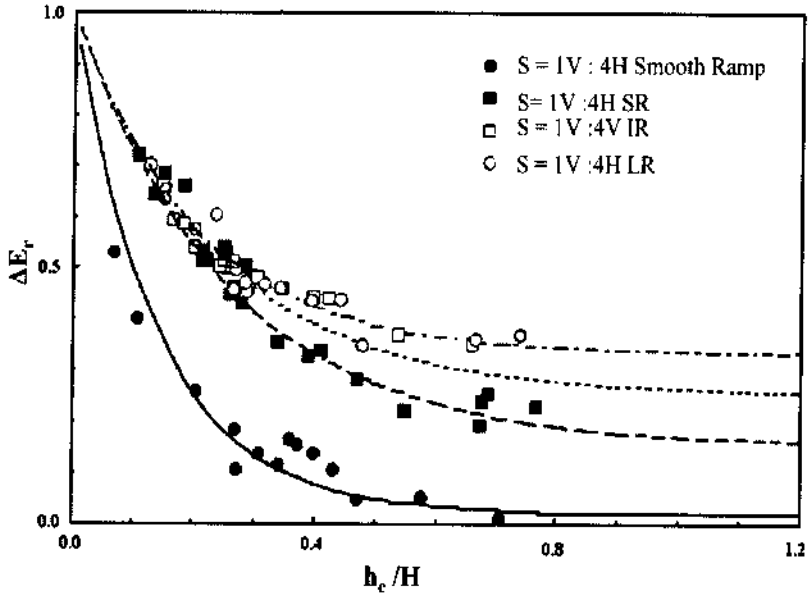

Fig. 2.21 Relative energy dissipation for smooth ramp, ramp with base material under different roughness conditions (Pagliara and Chivaccini, 2006a)

2.5.3 Block Ramp with Protruding Boulders on Base Material

When boulders or macro-roughness elements are introduced on the smooth or base material, there is a significant change in the roughness boundary and complexity of flow. It is in similitude to the baffled aprons or blocks used in spillways. Pagliara and Chiavaccini (2006b) adopted hemispheres representing mountain boulders with a protruding part equal to half the diameter in the range of 29 and 38 mm in diameter. The surface of the boulders was smooth or rough. A large range of D_B/d_{50} values was investigated. The rough hemispheres were obtained by covering the smooth ones with sand having a mean diameter of 2 mm or covering them with a thin film of aluminum to make it smooth. Quite reasonably, the rough ones induced more energy dissipation than the smooth ones. In the experimental range, the Reynolds number Re was between 1.2×10^4 and 1.5×10^5, while the Froude number Fr

(calculated at the ramp exit) was between 0.95 and 3.9. The other test parameters and variables were in the following range: $0.08<S<0.33$, $1.75< (D_B/d_{50}) <19$; $0< \Gamma <0.33$; and $0.04< (d_{50}/h_c) <0.98$. They proposed a new functional relationship for energy dissipation due to the presence of protruding boulders as given in Eq. (2.45).

$$\frac{\Delta E_{rB}}{\Delta E_r} = f\left(\frac{d_{50}}{h_c}, \frac{D_B}{d_{50}}, \frac{H}{h_c}, \Gamma, S, \mathrm{Re}, \mathrm{Fr}, \varepsilon, disp\right) \qquad (2.45)$$

where, ε = roughness of the boulders (smooth or rough), *disp* = arrangement (random or rows), and other variables denoted as earlier. Tests were performed to define which of the parameters plays a major role in the energy dissipation process. With a subjective examination of the experimental test results, they found that the parameters S, Re, Fr, d_{50}/h_c and D_B/d_{50} were negligible in the tested range, and they simplified Eq. (2.45) to the following form as,

$$\frac{\Delta E_{rB}}{\Delta E_r} = f(\Gamma, \varepsilon, disp) \qquad (2.46)$$

They further postulated the refined equations accounting for macro-roughness boulders as given in Eqs. (1.3) and (1.4).

Ahmad et al. (2009) have also found that energy loss in staggered arrangement of boulders on the ramp is higher than the random or row arrangements and proposed a relation to evaluate the roughness parameters for staggered arrangement of boulders on block ramps. These values were validated with the experimental observations of the authors within a ± 3% error line. Adopting the roughness parameter E = 0.60 (for random disposition and rounded boulders, as river stones), the value of F can be determined using the following relation.

$$F = 7.9\left(\frac{D_B}{h_c}\right)^{-0.9} \qquad (2.47)$$

Pagliara and Chiavacinni (2006b) have omitted the submergence factor by using the factor of relative energy dissipation for base material.

2.5.4 Submerged Block Ramps

Energy dissipation in different ramp submergence conditions due to tail water depth was studied by Pagliara et al., (2008) along with the scour of bed at the toe of the ramp (Fig.

2.22). It was found that the maximum energy dissipation for a fixed value of L/L_T takes place for LR (large scale roughness) followed by IR (intermediate scale roughness) and SR (small scale roughness) conditions which imply that for the same value of h_c/H, the relative energy dissipation increases with the roughness condition. Here, L is the horizontal distance at beginning of jump from the toe of ramp, and L_T is the horizontal length of the ramp.

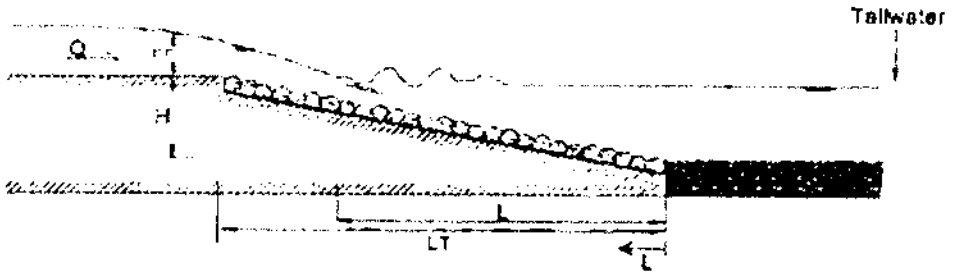

Fig. 2.22 Typical L-profile of block ramps in submerged condition (Pagliara et al., 2008)

An exponential relationship (Eq. 2.48) for the relative energy dissipation in the case of L/L_T =1/3 and 2/3 was proposed for the submerged block ramps case by substituting appropriate values for the coefficients A and B as,

$$\Delta E_r = A + (1 - A)\exp^{\left(B\frac{h_c}{H}\right)} \qquad (2.48)$$

Coefficients A and B depend on scale roughness and are given in Table 2.6:

The above relation is stipulated to be valid in the range: $0 < L/L_T < 0.7$, $0.1 < h_c/H < 1.2$, and ramp slope varying between 0.25 to 0.125.

Table 2.6 Roughness coefficients in submerged block ramps (Pagliara et al., 2008a)

Roughness condition	A	B
Small scale (SR)	0.239 exp {-2.323 (L/L_T)}	- {10.70 (L/L_T) + 1.729}
Intermediate scale (IR)	0.249 exp {-1.618 (L/L_T)}	- { 9.95 (L/L_T) + 1.863}
Large scale (LR)	0.256 exp {-1.245 (L/L_T)}	- { 8.475 (L/L_T) + 1.931}

Ghare et al., (2010) proposed a mathematical model for the design of block ramp system by correlating the step height ratio of stepped chute with representative base material size (d_{50})

of block ramp under identical hydraulic conditions. The authors presented a relation for calculating the step-height ratio, H^* (as longitudinal spacing-roughness height ratio) for block ramps in dimensionless form as given in Eq. (2.49) where using Eqs. (2.50, 2.51 and 2.52), the values of the coefficients ε, ζ, and γ are calculated respectively.

$$H^* = \varepsilon\left(\frac{h_c}{d_{50}}\right)^2 + \zeta\left(\frac{h_c}{d_{50}}\right) + \gamma \tag{2.49}$$

$$\varepsilon = -12.213 \times \ln(S) - 8.03 \tag{2.50}$$

$$\zeta = 18.893 \times \ln(S) + 17.288 \tag{2.51}$$

$$\gamma = 6.829 \times \ln(S) + 5.632 \tag{2.52}$$

The relation is valid in the bed slope range of 0.75 to 2.0. The findings need to be examined on the adaptation philosophy from stepped chute to block ramp hydraulics.

From the review of the studies cited, it can be noted that the energy dissipation depends mainly on the boulder concentration, disposition or arrangement, relative submergence, and slope. The effect of Froude Number and Reynolds Number has been considered negligible in the studies conducted so far. Undoubtedly, the roughness of the elements modifies the dissipation and the rough hemispheres were more dissipative than the smooth ones. With regard to boulder arrangement or disposition, the random arrangement is systematically found less dissipative than the rows disposition.

2.6 STABILITY OF BLOCK RAMPS

Stability is an important aspect in the design of block ramps/chutes. In fact, to ensure chute functionality the rocks should remain stable during design flood events. Rock chutes have been used in various forms in river engineering and hence it is very important to study its design aspect prior to its application aspect. The stability of a rock chute has been investigated by various researchers. Ibash (1936) developed a relationship relating the minimum velocity necessary to move stones of a known size and specific gravity. Abt et al. (1987) and Abt and Johnson (1991) tested angular and rounded stone in their study and found that rounded stone failed at a unit discharge of approximately 40% less than angular shaped stones of the same median stone size. They developed a design criterion for median stone sizes between 25 to 152 mm on slopes ranging between 1 to 20%. Maynord (1988) developed a riprap sizing method for stable open channel flows on slopes of 2% or less. He used d_{30} as

the characteristic size in his design method, which was based on average local velocity and flow depth. The various factors like rip-rap gradation, thickness and shape were also taken into consideration. Frizell and Ruff (1995) examined riprap with characteristic size d_{50} of 380 mm on slope of 50%. They studied riprap for embankment overtopping protection.

The minimum unit discharge that fails the rock chutes as per Whittaker and Jaggi (1986) is

$$q_c = 0.257 S^{-1.167} \left(g \left(\frac{\gamma_s}{\gamma_w} - 1 \right) d_{65}^3 \right)^{0.5} \tag{2.53}$$

in which q_c is the failure unit discharge (m^2/s), S the slope of the ramp, g the acceleration due to gravity, γ_s is the rock specific weight, γ_w is the water specific weight and d_{65} is the rock diameter for which 65% of the sample is finer. They considered a layer of rocks, placed over sand or gravel bed in their experimental set up. The failure was considered when one or more rocks left the ramp with the uncovering of the underlying bed and the following destruction of the structure.

Robinson *et al.* (1997) investigated the stability of rock chutes on slopes between 10 and 40 % and obtained the following relationship

$$q_c = (d_{50} S)^{\left[1.40 + 0.213/\sqrt{S}\right]} \exp(-11.2 + 1.46/\sqrt{S}) \tag{2.54}$$

in which d_{50} (mm) is the rock size for which the 50% of the sample is finer. The rock layer thickness in the chutes was $2d_{50}$ and placed over a geo-textile layer. In this case, failure was considered when scour holes were observed in the rock layer.

Pagliara and Chiavaccini (2004) studied the effect of protruding boulders over the base material for increasing the ramp stability. It was demonstrated that the boulders create a disturbance in the flow pattern which results in irregular water surface profile. Mean flow depths become greater compared to base condition resulting in reduction of the flow velocity. They also investigated reinforced ramps with different boulders dispositions (rows, randomly or arc configuration) and proposed the following relationship which indicates increase in failure discharge in reinforced ramps compared to the base ramp.

$$\frac{q_{cb}}{q_c} = \left[1 + 0.084\Gamma\right]^{2.7} \tag{2.55}$$

where q_{cb} is the critical failure discharge for the reinforced chute, and Γ is the boulders concentration expressed by

$$\Gamma=\frac{N_B \pi D_B^2}{4WL_R} \tag{2.56}$$

where L_R is length of the ramp, W is width of ramp, D_B the diameter of protruding boulders and N_B the number of the protruding boulders. They indicated that the ramp failure occurs in three different stages: (a) the "initial movement" of the base material, in which the base rocks begin to vibrate and the transport of some isolated elements occur; (b) the "local failure (LF)" in which one or more elements leave their position simultaneously, producing a well defined circular or semicircular scour hole; and (c) the "global failure" of the ramp in which different local failures happen: the ramp presents large longitudinal holes. Among the various stages of failure observed in their experimental studies, LF was considered representative due to the fact that ramp begins to change its original geometry at this stage.

Pagliara and Chiavaccini (2007) analyzed the stability of the rock ramp in terms of densimetric Froude number for both the base and the reinforced ramp condition in order to evaluate the bed evolution of the rock chute. For the base condition, they used data from Whittaker and Jäggi (1986) and Robinson et al. (1995) experimental results to determine a new relationship. They expressed Particle Froude number F_d corresponds to boulder size d_{xx} as;

$$F_{d_{xx}} = \sqrt{\frac{8}{f}} \frac{(SR)^{0.5}}{((s-1)d_{XX})^{0.5}} \tag{2.57}$$

where d_{xx} is rock diameter for which xx% of the mixture is finer, R is the hydraulic radius, f is friction factor, and s is relative specific weight of rock. The critical densimetric Froude number on rock ramps, both in presence and in absence of reinforced boulders was given as

$$F_{dc} = 1.98S^{0.18}\left(\frac{h}{d_{84}}\right)^{0.36}(1+\Gamma)^{a_1} \tag{2.58}$$

where a_1 depends on the boulders disposition and can be read from Table 1 for different arrangement/deposition of the boulders.

A direct relationship to evaluate the unit flow rate value (m^2/s) for local failure was given by Pagliara and Chiavaccini (2007) as

$$q_c = 1.8S^{(-0.52+b_1)}d_{50}^{1.5}(1+\Gamma)^{b_2} \tag{2.59}$$

where b_1 and b_2 depends on the boulders disposition (Table 2.7), d_{50} is the rock diameter for which 50% of the mixture is finer.

Table 2.7 Value of coefficients used in Eq. (2.58) and (2.59)

Boulder disposition	a_1	b_1	b_2
Rows	-2.2	-0.2	1.7
Random	-2.0	-0.27	0.8
Arc	-2.6	-0.17	1.2
Reinforced Arc Type 1	-2.6	-0.17	1.2
Reinforced Arc Type 2	-2.8	-0.3	0.4

Pagliara and Lotti (2007) presented the first relationship of specific discharge for local failure of base block ramps on the basis of their experimental results, which is the function of hydraulic and geometric parameters as below;

$$q_c = (-4.96\times10^{-6}S + 4.28\times10^{-6})d_{50}^{*\,(-0.32S+1.42)} \tag{2.60}$$

where d_{50}^* is the dimensionless grain diameter defined as $d_{50}^*=d_{50}(g\,\Delta/\nu^2)^{1/3}$, g=acceleration due to gravity; $\Delta = s\text{-}1$; ρ_s=mass density of block; ρ=mass density of water; ν= kinematic viscosity of water. This relationship is valid within the tested range ($1/8<S<1/3$; $350<d_{50}^*<1000$; $2400<\rho_s<2700$).

2.7 CONCLUDIG REMARKS

Based on the comprehensive review of literature, various parameters have been identified for estimating the energy dissipation on block ramps specially emphasizing for that with protruding boulders reinforced over the granular base material. Steep and short rough channels, such as rock chutes, were used in river restoration as grade stabilization structures. The relative energy dissipation of block ramps can be increased using boulders placed over the base material. As it had been observed that as the staggered arrangement finds merit over the other configurations as unstructured, dumped, self-structured, rows or random, this particular arrangement pattern has been selected for detail investigation in the laboratory. For general nomenclature, the study has generally been referred as "Energy Dissipation on Block Ramps".

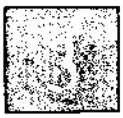

EXPERIMENTAL PROGRAMME

This chapter describes the laboratory experiments conducted on block ramps and their energy dissipation characteristics for different configurations such as smooth condition, ramp with base material and ramp with protruding boulders over the base material. The experimental set up, test conditions and data collection procedures are described in this chapter. The observations made during the experiment runs along with the equipments and instruments used are discussed. Different boulder sizes were used to replicate macro-roughness conditions in varying scales and the relative energy dissipation for each configuration was evaluated. The tested ranges of hydraulic variables are listed in the end of the chapter.

3.1 EXPERIMENTAL SET-UP AND INSTRUMENTATION

Experiments were carried out at the Hydraulics Laboratory of the Department of Civil Engineering, Indian Institute of Technology Roorkee, India. A variety of equipments and instruments were utilized in the present study to measure flow characteristics. Experiments were performed on a concrete flume having a rectangular ramp of width (W) 0.30 m, horizontal length 4.0 m with side walls of height 0.45 m. Three ramp slopes (S) i.e., 1V:5H, 1V:7H and 1V:9H were investigated. A broad crested weir of width 0.20 m was provided at the upstream most section of the ramp with a curvilinear finish (radius 0.10 m) to facilitate smooth water flow. A schematic diagram of the experimental set-up and its isometric representation are shown in Figs. 3.1 and 3.2, respectively.

Water flow was supplied from an overhead tank to an inlet tank (1.85 m ×1.10 m ×1.75 m) through a carbon steel pipe with internal diameter 210 mm and pipe thickness 6 mm, serving as the main inlet supply pipe. The overhead tank was maintained at overflow conditions to retain a constant water level in the inlet tank. An ultrasonic flow meter (transit-type portable), with transducer fittings, was used to measure the instantaneous discharge through the supply pipe and

the observations were used for the calibration of the broad crested weir. The ultrasonic flow meter instrument measures the flow of fluid with the help of signals transmitted by the transducers without interrupting the flow. The instrument consists of transducers, digital flow meter, and steel scale along with chain for mounting the transducer on the pipe (Fig. 3.3).

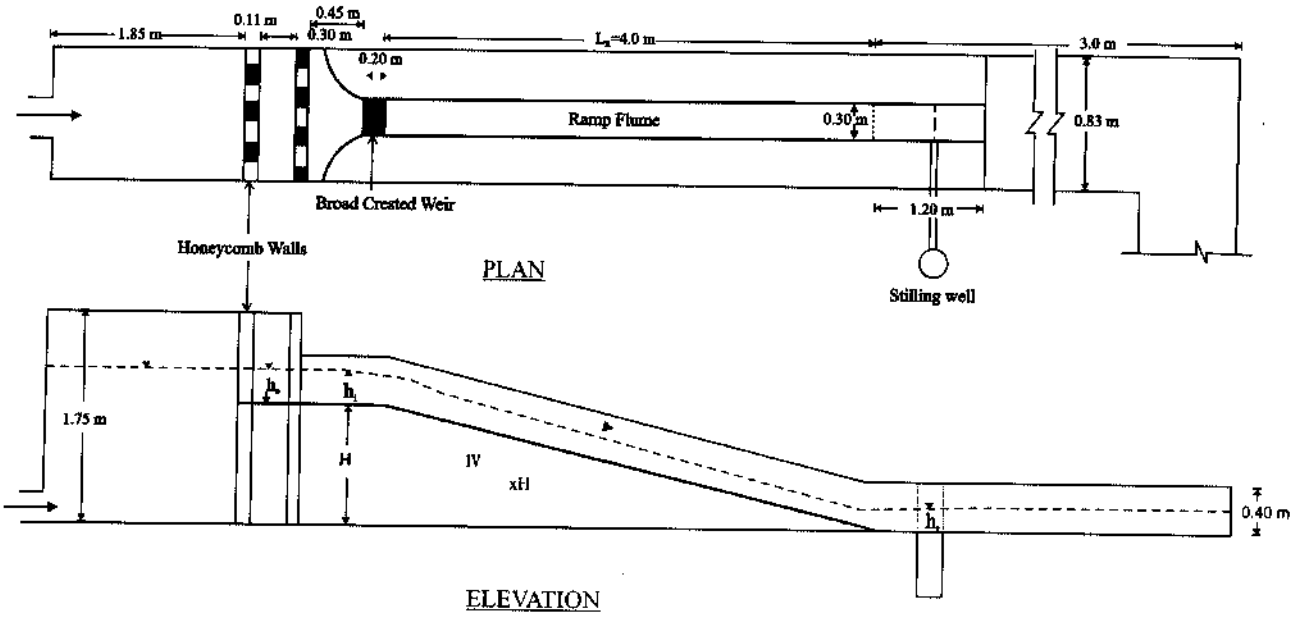

Fig.3.1 Schematic plan and elevation of the experimental set up (not to scale)

A bendmeter assembly with inclined manometer (at 15° with horizontal) was also fitted to the supply pipe to measure the discharge. To dampen large scale turbulence and for stabilizing the entrance flow, the inlet tank (via the supply pipe) was gated with two series of honeycomb walls consisting of a stack of brick masonry meshing, prior entry to the flume section (Fig. 3.5). A wave suppresser made of a wood grid (Fig. 3.6), was floated and used in the inlet tank to dampen oscillations and other disturbances in the supply of water from the pump.

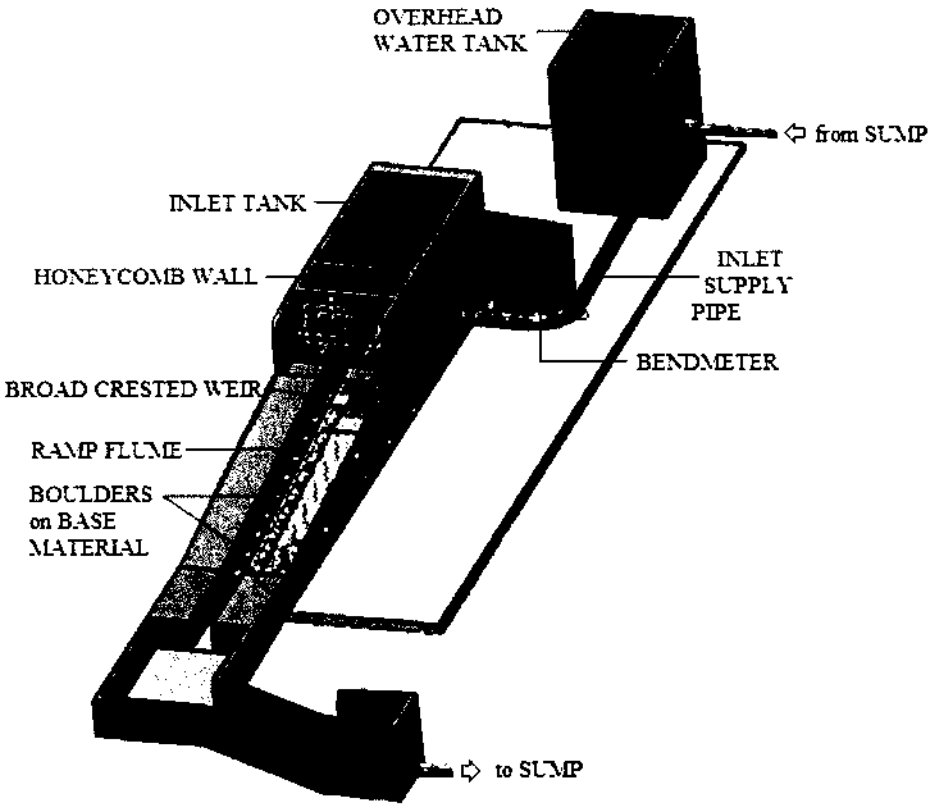

Fig.3.2 Isometric view of the experimental set up (not to scale)

Water level measurements were taken with the aid of digital and manual pointer gauges as shown in Fig. 3.7. At the downstream section of the ramp (approximately 1.0 m downstream from where the ramp slope ends), a stilling well assembly (Fig. 3.8) was used for the measurement of tail water depth. As per United States Bureau of Reclamation (1983) recommendations, the tube connecting the flume or channel to the stilling well should be about $1/10^{th}$ of the diameter of the stilling well. A stilling well made of carbon steel circular pipe (180 mm inner diameter) with PVC connecting tube of outer diameter 21.6 mm was installed. Three intake holes of 1 cm diameter (Fig. 3.9) at the channel bed were used for the measurement depth of flow. The mean flow velocity at the toe section of the ramp was recorded by means of a Pitot tube assembly at the downstream toe of the ramp as shown in Fig. 3.10.

Fig.3.3 Ultrasonic Flow Meter with transducers

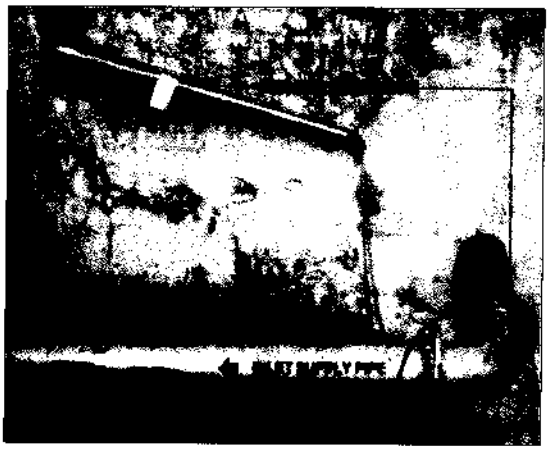

Fig.3.4 Bendmeter at main supply pipe

Fig.3.5 Honeycomb walls in the inlet tank

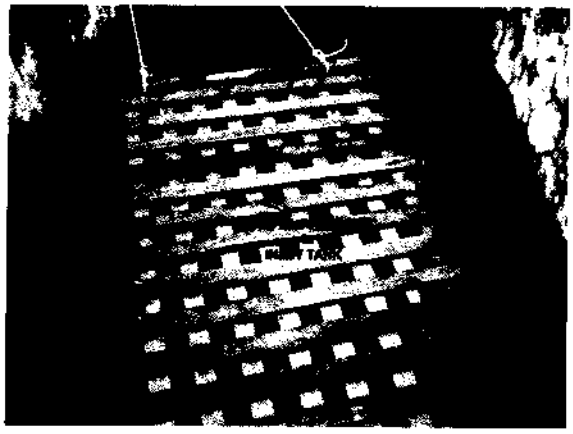

Fig.3.6 Wave Suppresser used in inlet tank

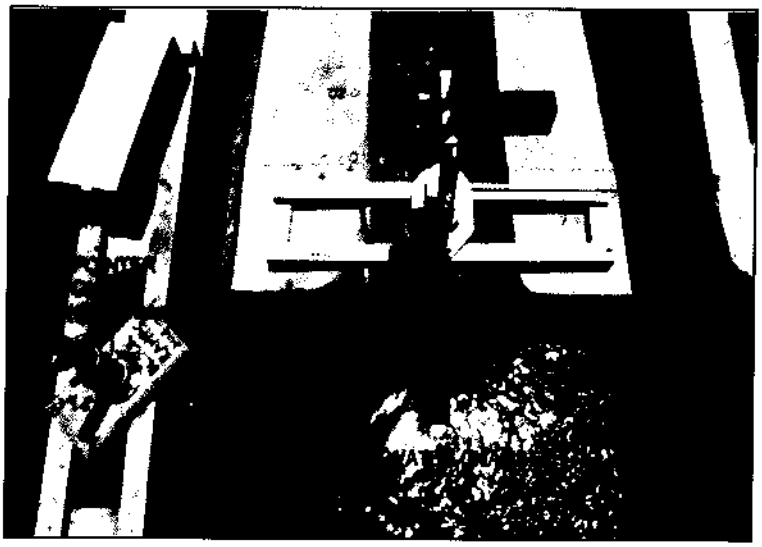

Fig.3.7 Digital and manual pointer gauges

Fig.3.8 Stilling well

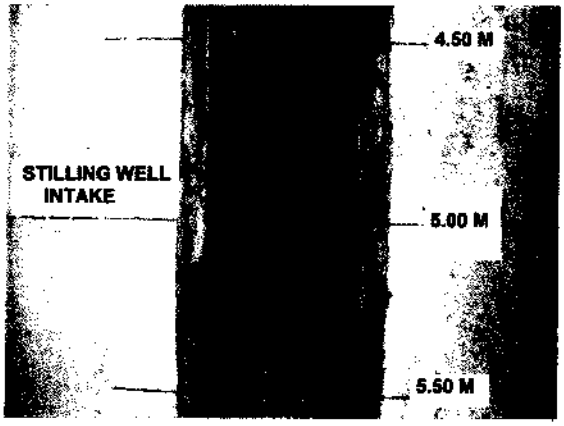

Fig.3.9 Intake holes for stilling well

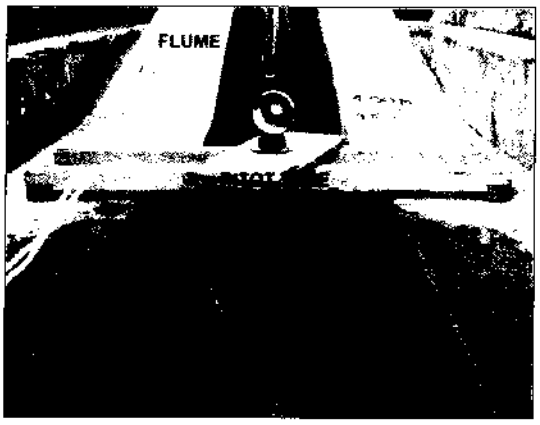

Fig.3.10 Pitot tube assembly at D/S section

3.1.1 Observation Sections

To facilitate the measurement of water level at different sections of the ramp, the ramp flume was marked at certain intervals starting from the trailing edge of the broad crested weir (Fig. 3.11). This section was denoted as X0. This section was taken as the reference or starting section for the longitudinal distance marking along the ramp flume. A spacing of 0.20 m for the upstream 1.00 m inclined length of the ramp was adopted for water level observations at closer intervals to account for the flow variability and transition in flow profile as a result of developing boundary layer. The remaining length was sectioned X1 to X11 at 0.50 m interval till the end of the inclined length. The toe section was marked XT and located at further 1.00 m downstream of section X11. The elevation of bottom of the cross section and the details are outlined in Fig. 3.12. Section X1 corresponded to a water depth measurement of h_1 and so forth.

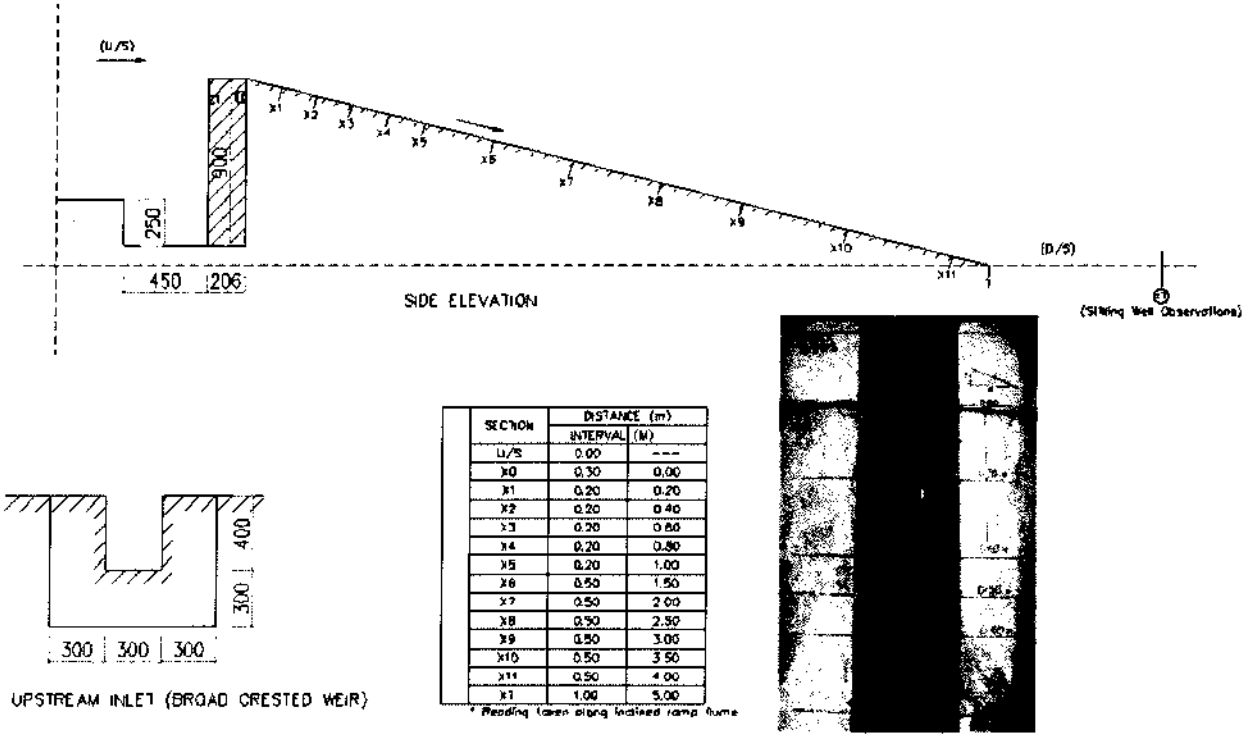

SECTION	DISTANCE (m)	
	INTERVAL	(M)
U/S	0.00	---
X0	0.30	0.00
X1	0.20	0.20
X2	0.20	0.40
X3	0.20	0.60
X4	0.20	0.80
X5	0.20	1.00
X6	0.50	1.50
X7	0.50	2.00
X8	0.50	2.50
X9	0.50	3.00
X10	0.50	3.50
X11	0.50	4.00
X1	1.00	5.00

* Reading taken along inclined ramp flume

Fig. 3.11 Longitudinal section and cross section of the ramp flume (dimensions in mm unless specified)

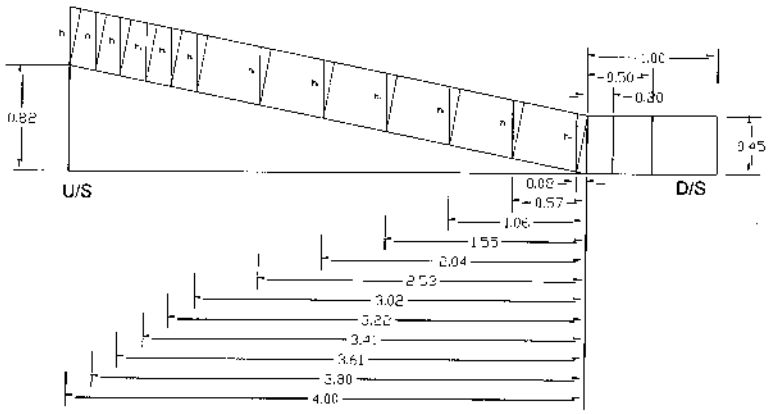

1V:5H

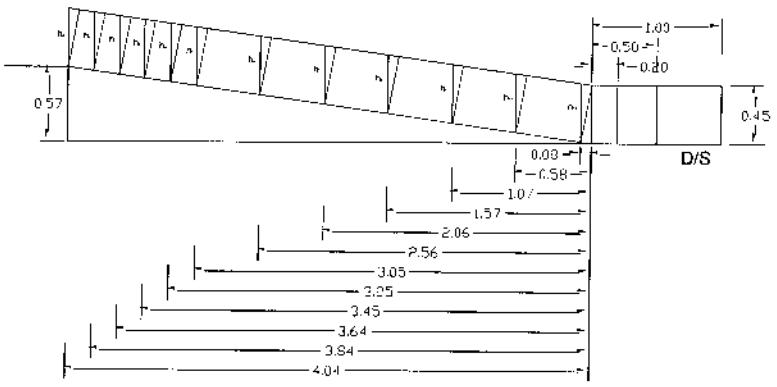

1V:7H

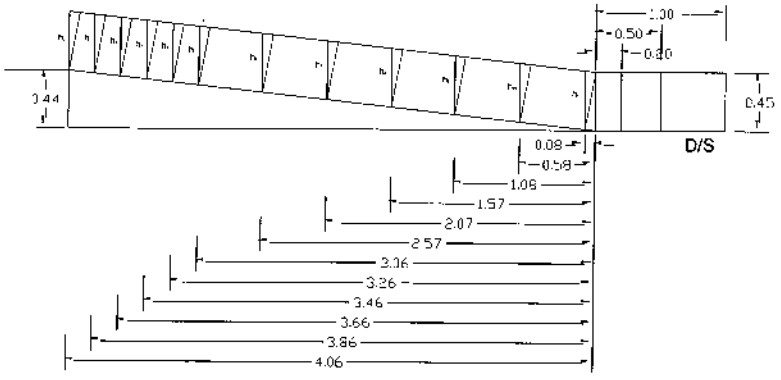

1V:9H

Fig. 3.12 Typical longitudinal profile of the ramp showing sections where water level measurements were measured (all dimensions in m)

3.2 EXPERIMENTAL PLAN AND ORGANIZATION

The experiments were first conducted on ramp slope 1V:5H (S = 0.20) followed by 1V:7H (S = 0.1428) and 1V:9H (S = 0.1111). For the each slope, the sequence of test followed was: smooth condition, ramp with base material, and ramp with boulders on base material (smallest to biggest size boulders) in various configurations. The framework of the experimental plan in the present study is given in Table 3.1.

Table 3.1 Experimental organization and plan

Set	Bed Slope	Ramp Condition	Arrangement	Spacing (longitudinal)	Remarks
I	1V:5H	Smooth			
		Base material d_{50}= 0.020 m			for angular and rounded
		Boulder sizes: 0.042 m 0.055 m 0.065 m 0.080 m 0.10 m	staggered rows*	$1.0D_B$, $1.5D_B$ $2.0D_B$, $3.0D_B$ NU-1, NU-2, NU-3, NU-4	Non-uniform arrangement comprised of 2 S_x/D_B spacings
II	1V:7H	Smooth			
		Base material d_{50}= 0.020 m			for angular and rounded
		Boulder sizes: 0.042 m 0.055 m 0.065 m 0.080 m	staggered	$1.0D_B$, $1.5D_B$ $2.0D_B$, $3.0D_B$ NU-1, NU-2, NU-4	Non-uniform arrangement comprised of 2 S_x/D_B spacings
III	1V:9H	Smooth			
		Base material d_{50}= 0.020 m			
		Boulder sizes: 0.042 m 0.055 m 0.065 m 0.080 m	staggered	$1.0D_B$, $1.5D_B$ $2.0D_B$, $3.0D_B$ NU-1, NU-2, NU-4	Non-uniform arrangement comprised of 2 S_x/D_B spacings

*conducted for 0.055 m diameter size

The smooth condition of ramp is similar to a case of chute spillway with a quasi-smooth bed (concrete trowel finish on the bed). Sorted stone aggregate were partly grouted on the ramp bed to cover the entire inclined bed of the ramp bed – referred as block ramp. The next configuration forms the crux of the study. When casted concrete semi–hemispherical blocks (replicating boulders in mountain streams) are placed on the block ramp with base material, then a macro-roughness–induced flow regime characterizes the "boulder block ramp", which imparts high energy dissipation on the flow. The description of the spatial arrangement and various configurations of boulders on the ramp as listed in the above table are presented in the following sections.

3.2.1 Configuration and Distribution of Boulders

The spatial arrangement of boulders on block ramps was configured to symmetric or axisymmetric patterns in the present study. Two structured configuration of boulders, described as "row" and "staggered" patterns, were tested in the study and are illustrated in Fig. 3.13. It can be noted that the boulders are symmetric about the longitudinal mid-axis XX' in both the cases. The random arrangement has been investigated by several authors, and corresponded to a non-symmetric configuration. In the present study, the "staggered" pattern in uniform and non–uniform arrangement of boulders along the L-section of the ramp flume has been investigated in detail. The boulders were placed on the block ramp in various concentrations (Γ) under varied longitudinal and transverse spacing in staggered arrangement over the base material.

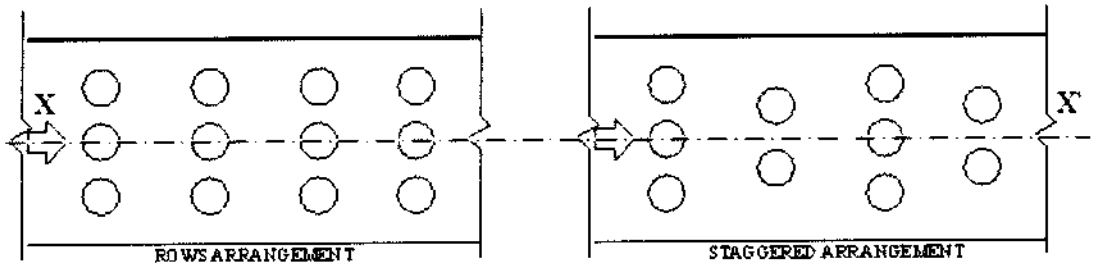

Fig. 3.13 Structured arrangements of boulders on block ramps (not to scale)

Few experimental runs were conducted for the rows arrangement to compare its energy dissipation trend with the staggered arrangement. For the rows arrangement, the boulders were placed in regular and clear longitudinal (S_x) and transverse (S_y) spacing with the boulders

oriented behind one another starting from the upstream X1 section (Fig. 3.14). In the staggered arrangement, the boulders were also placed in regular and clear longitudinal (S_x) and transverse (S_y) spacing with the boulders aligned behind the gap between the two preceding upstream boulders (in the transverse axis) as illustrated in Fig. 3.15. Further in the staggered arrangement, two boulder spacing and distribution configurations viz., uniform and non-uniform, were adopted which are further described in the following section 3.2.2.

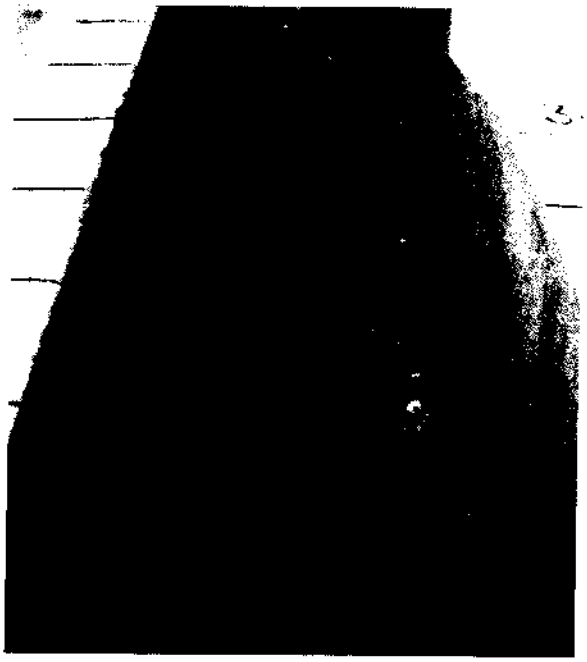

Fig.3.14 Boulders in row arrangement over the base material

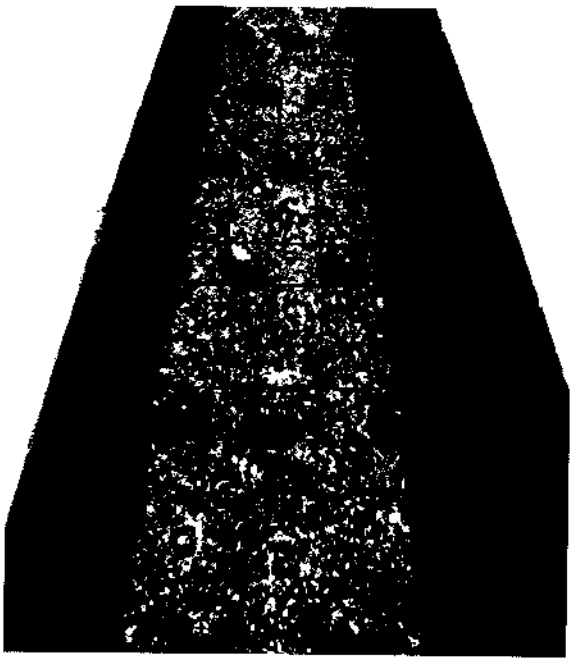

Fig.3.15 Boulders in staggered arrangement over the base material

3.2.2 Spacing of Boulders in Staggered Configuration

The staggered arrangement of boulders on the ramp was tested under two spacing distributions:

(i) Uniform distribution: boulders placed at uniform clear longitudinal (S_x) and transverse (S_y) spacing throughout the ramp bed, and

(ii) Non-uniform distribution: boulders placed with closer spacing on the upstream portion (denoted by S_{x1}) of the ramp bed, and higher spacing on remaining downstream portion (denoted as S_{x2}), and vice versa.

The first row of the boulder on ramp in both cases was placed such that it should not impede the flow of water in the upstream boundary of the ramp. The uniform staggered arrangement is denoted by its relative spacing with the boulder size, as "$x.D_B$". For example, $2.0D_B$ implied a uniform staggered arrangement with clear L-spacing (S_x) equal to 2 times the boulder size in terms of its diameter. The non-uniform staggered arrangement is denoted by the term "NU" with two types of relative spacing: S_{x1} for the upstream section and S_{x2} for the remaining downstream section. A schematic elevation profile of the uniform and non-uniform staggered arrangement of boulders is shown in Fig. 3.17. A sketch of the two staggered arrangements in the plan view of the ramp flume, highlighting the spacing of boulders in each respective configuration, is illustrated in Fig.3.18. It may be distinctly noted that there is discontinuity in the longitudinal spacing in the non-uniform pattern, while the transverse spacing (S_y) is kept equal for both the uniform and non-uniform configurations.

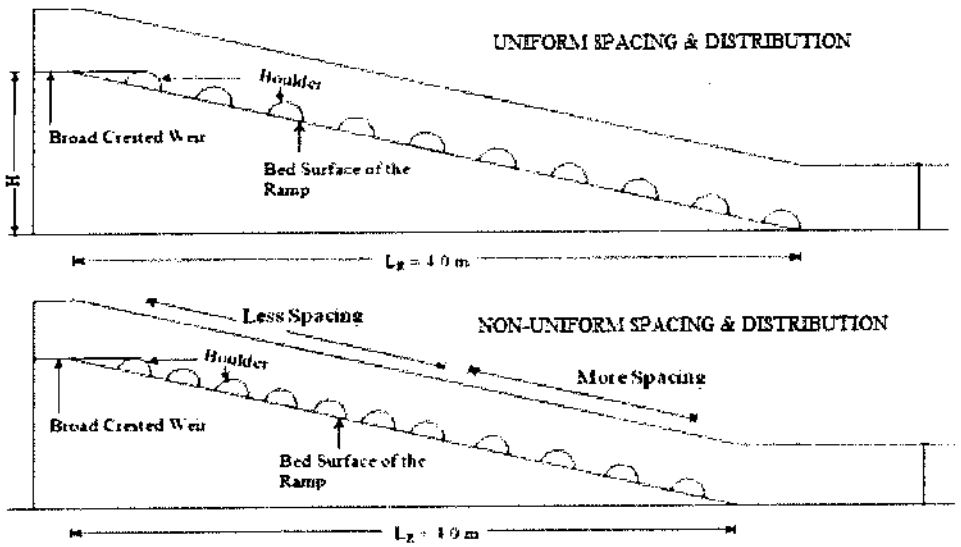

Fig. 3.16 Schematic elevation profile of uniform and non-uniform arrangement of boulders

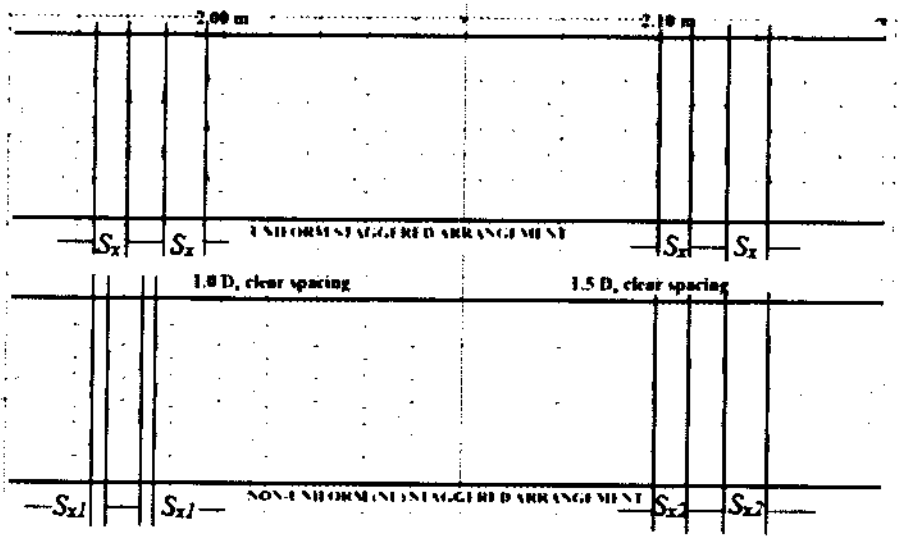

Fig.3.17 Sketch showing uniform and non-uniform staggered arrangement of boulders

It has been illustrated that the boulder spacing is based on the clear spacing in terms of the boulder diameter to express it as a dimensionless factor. Four non-uniform staggered configurations investigated in the study are described in Table 3.2 and illustrated correspondingly in Fig. 3.18.

Table 3.2 Description of non–uniform configuration of boulders used in the experiments

Sl	Notation	Configuration	Description
1	NU–1	Non-uniform spacing –1	1.0 D_B clear spacing of the boulders covering 0.85 m upstream length of the ramp, followed by 1.5 D_B for remaining length of the ramp
2	NU–2	Non-uniform spacing –2	1.0 D_B clear spacing of the boulders covering 2.0 m upstream length of the ramp, followed by 1.5 D_B for remaining length of the ramp
3	NU–3	Non-uniform spacing –3	(reverse order of NU-2)
4	NU–4	Non-uniform spacing –4	Alternate 1.0 D_B and 1.5 D_B clear spacing of the boulders throughout the length of the ramp

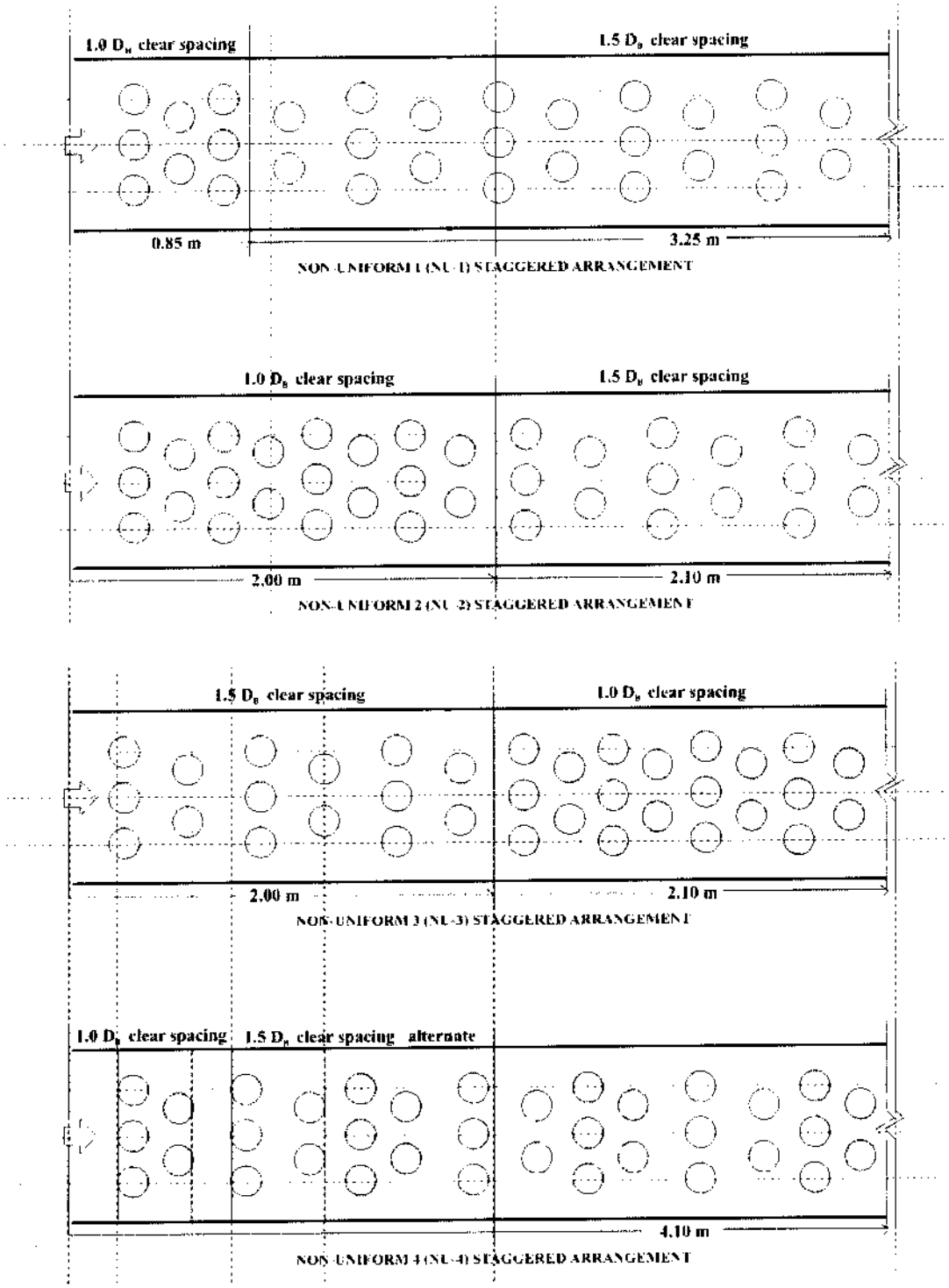

Fig.3.18 Schematic representation of non-uniform staggered configurations of boulders: NU–1, NU–2, NU–3 and NU–4 on the ramp (not to scale)

3.2.3 Rationale of testing the Non-uniform Distribution

As it was observed that the developing flow region generally prevailed up to approximately $1/3^{rd}$ to $1/4^{th}$ of the upstream portion of the ramp in the tested conditions. Beyond this upstream portion, a developed turbulent flow regime was observed in most of the test conditions as shown in Fig. 3.19. The resistance imparted by the roughness elements in the form of Darcy–Weisbach friction factor f have been related to the energy loss and has significant factors in the developing and developed flow regimes (Hartung and Scheuerlein, 1967). The non-uniform arrangement was fabricated to introspect and compare the energy dissipation function with the uniform arrangement, by perturbing the homogeneity of flow characteristics that were invoked by macro-roughness boulder distribution on the block ramp under the same flow conditions that prevailed for the uniform configuration. The notion was whether a differential longitudinal spacing of the boulders along the block ramp could result in higher dissipation of energy.

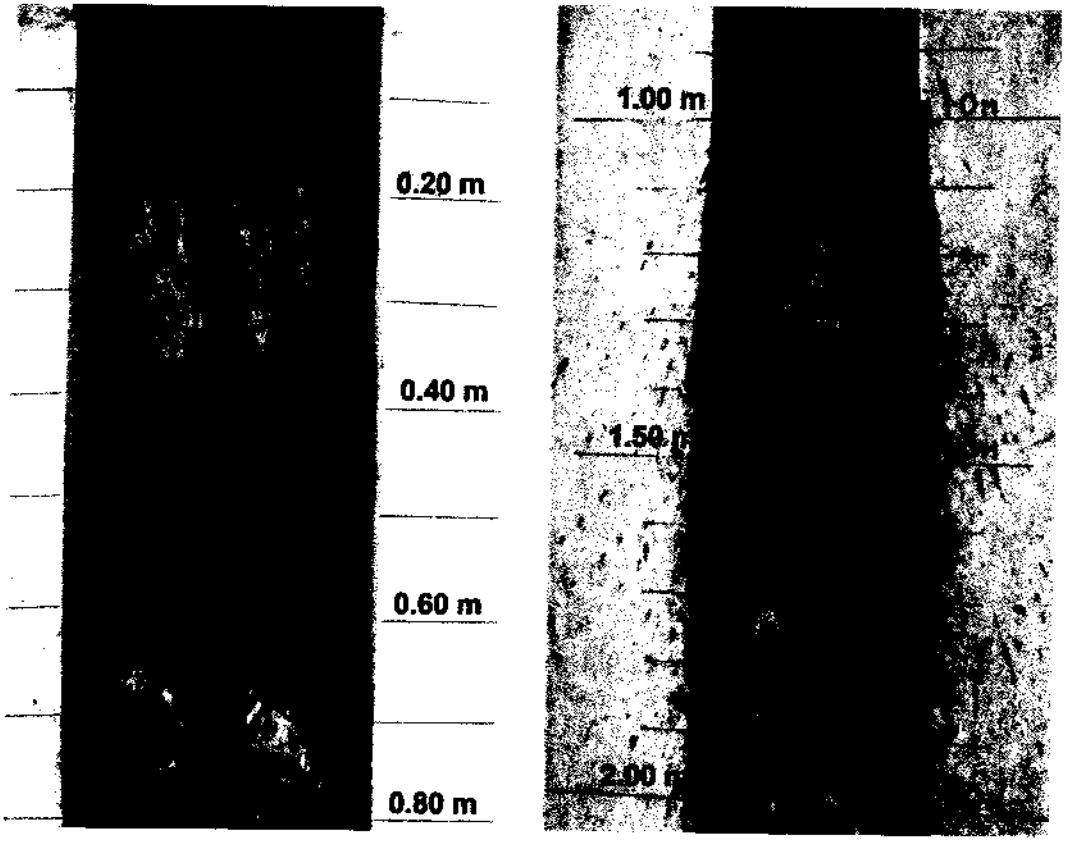

Fig. 3.19 Typical developing and developed flow on boulder block ramps

3.3 EXPERIMENTAL PROCEDURE AND TEST CONDITIONS

Experiments were carried out for each set of ramp configuration starting with the steepest slope i.e. 1V:5H. For each slope, test was conducted on smooth ramp in the beginning. Then, the ramp was laid evenly with base material for the next test configuration. As described earlier, two types of base material were investigated upon: first with the rounded river-bed stone aggregate, followed by the angular or crushed stone aggregate. The median diameter (d_{50}) of the aggregate has been taken as the representative size of the base material. In the next sequence, the hemispherical blocks representing boulders of various sizes (in terms of D_B), were laid over the block ramp for specific configurations in uniform and non-uniform patterns. This sequence involved the various permutations and combinations of boulder arrangement over the block ramp, and comprised of the maximum number of test runs. Each experimental set ranged from 8 to 15 runs depending on the ramp configuration and flow discharge.

3.3.1 Calibration

The bendmeter fitted in the supply pipe was calibrated using ultrasonic flowmeter as shown in Fig. 3.20.

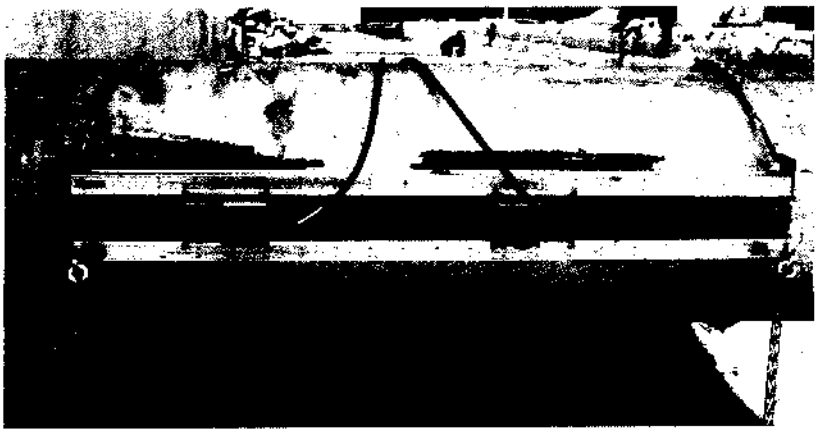

Fig.3.20 Mounting of transducers on the main inlet supply pipe

The calibration chart of bendmeter is shown in Fig. 3.21.

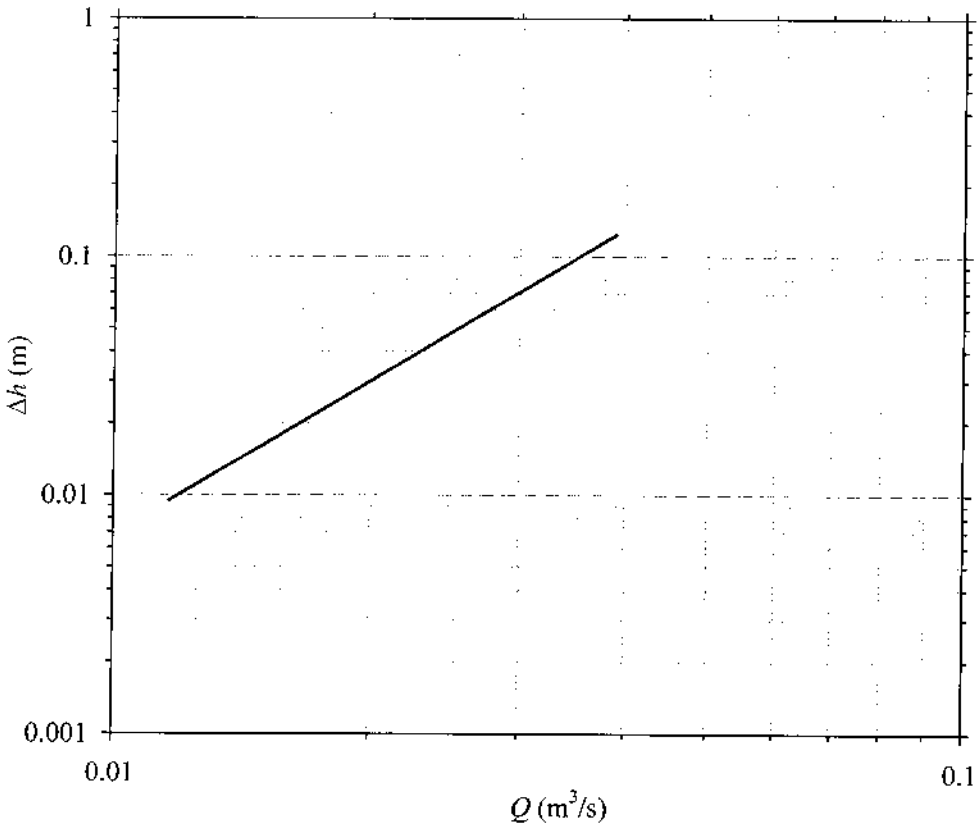

Fig.3.21 Calibration of bend meter

The calibration equation for computing discharge in all the experimental runs is obtained by the a power fit which yielded the following relation (Eq. 3.1) within a 95 % prediction limit (R^2 = 0.99),

$$Q = 0.104 \times (\Delta h)^{0.47} \tag{3.1}$$

where Q is in m^3/s and Δh is in m.

The above Eq. (3.1) is thereby adopted to quantify flow discharge in the whole set of experimental runs recorded in the study.

3.4 RAMP CONFIGURATIONS

As pointed earlier, three ramp conditions were conceived for the present study. The details of the sequence of various ramp configurations used in the study are described in the following sections.

3.4.1 Smooth Ramp

For each slope studied in the experiments, smooth or plain condition of the ramp was the first set to be tested. The smooth ramp has been taken as the reference or pre-restoration condition prior configuration of a block ramp structure. The smooth bed was prepared using a cement concrete trowel finish over the bed of the flume section (Fig.3.22). The objective was to assess the energy dissipation characteristics on the ramp in comparison with other similar structures as chutes, inclined drops, etc. The slope of the ramp flume bed was initially set at 1V:5H (S = 0.20), with the upstream crest at 0.815 m above the reference datum of the experimental set-up. Water was allowed to flow on the ramp by opening the regulating valve of supply pipe. After stabilizing the flow over the ramp, the head above the crest on the weir and depth of flow (normal to the bed) was measured at different sections. Discharge was varied by regulating the supply valve and observations were taken for the test runs. The next set of observations were taken for ramp slopes 1V:7H (S = 0.1428) and 1V:9H (S = 0.1111), respectively.

3.4.2 Ramp with Base Material

After performing the experiment for smooth ramp, granular stone aggregate was laid on the smooth ramp bed by grouting with a fine cement grout layer. Stone aggregate with representative median size d_{50} = 0.020 m and specific gravity in the order of 27.0 kN/m^3, were used in the experiments. The experiment was performed in the similar way as it was done in a smooth ramp with runs ranging between 9 to 15 runs for S = 0.20, 0.1428 and 0.1111, respectively. River bed pebbles with uniform spherical shape and distribution were taken as the 'rounded' base material and laid on the ramp bed as shown in Fig. 3.23. This arrangement represents the "dumped block" type of block ramps. In the second arrangement, for comparative test of the effect of sphericity and granularity factor of micro-roughness on energy dissipation on the ramp, 'angular' base material selected from crushed stone aggregate was also investigated

(Fig. 3.24). The objective was to find out whether an interlocked granular micro-roughness composition imparts higher resistance and energy loss than the river-bed aggregate.

In the first case, natural river–bed pebbles passing through 25 mm sieve and retained on the 16 mm sieve was taken as the "rounded" base material (b-I). The median diameter d_{50} = 20 mm was adopted as the representative size of the base material. Similarly, for the second case, crushed granular stone aggregate passing through 25 mm sieve and retained on the 16 mm sieve was taken as the "angular" base material (b-II).

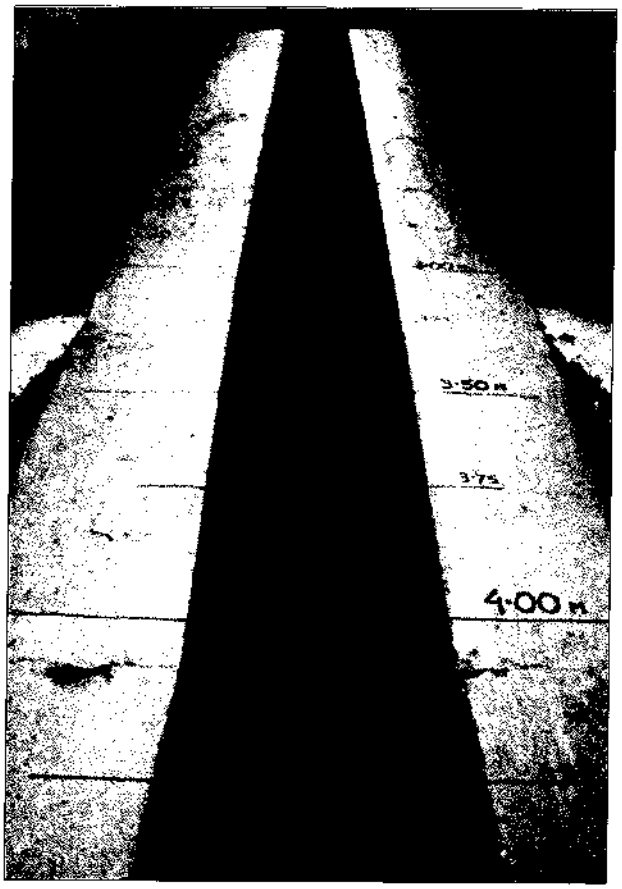

Fig.3.22 Smooth ramp used in the study

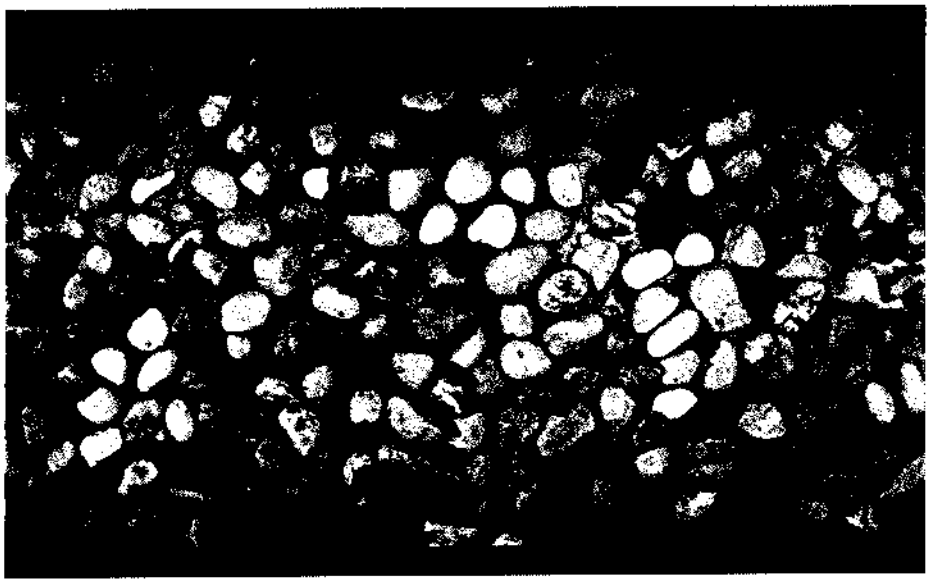

Fig.3.23 Rounded river–bed aggregate as base material (16 mm $\leq d_{xx} \leq$ 25 mm)

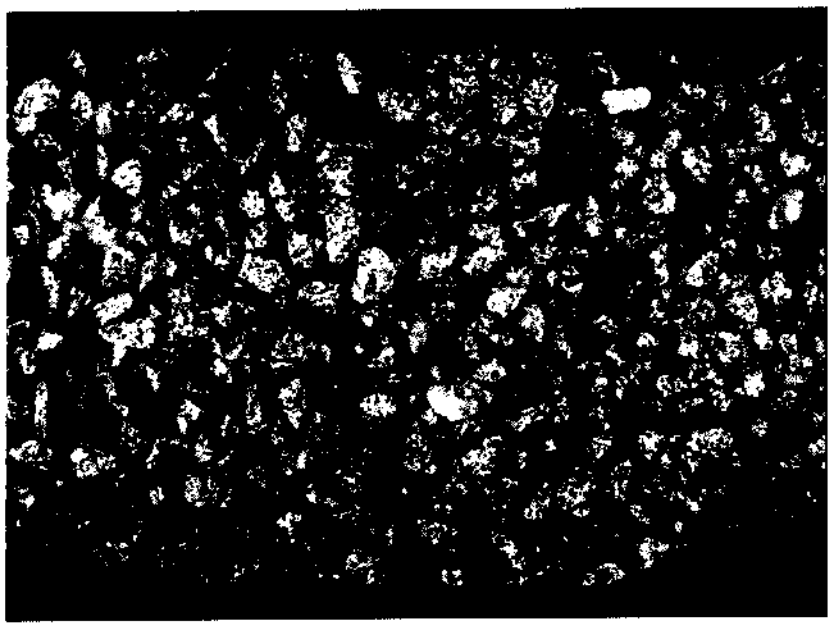

Fig.3.24 Angular crushed aggregate as base material (16 mm $\leq d_{xx} \leq$ 25 mm)

3.4.3 Ramp with Protruding Boulders on Base Material

Semi–hemispherical concrete blocks were placed over the base material on the ramp representing boulders in mountain streams. The semi–hemispherical structure facilitated such that the height of the boulder blocks (i.e. half of the boulder diameter) laid on the ramp bed was such that it replicated the mountain stream boulders that are armored over the stream bed

naturally as shown in Fig. 3.25. Semi–hemispherical blocks casted with concrete of diameter 4.2 cm, 5.5 cm, 6.5 cm, 8.0 cm and 10.0 cm were used to simulate varied boulder ranges that occur in natural mountain streams (Fig. 3.26). The surface of the semi–hemispherical blocks were finished with a fine cement paint coating to provide a quasi–smooth roughness structure when introduced in the flow.

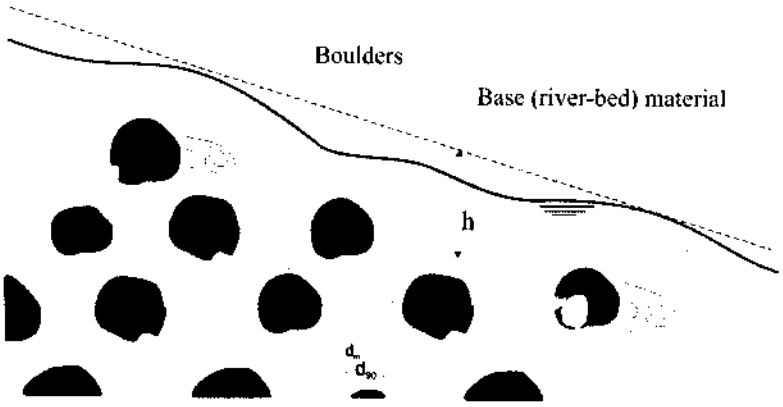

Fig.3.25 Conceptualization of boulder block ramp in the study

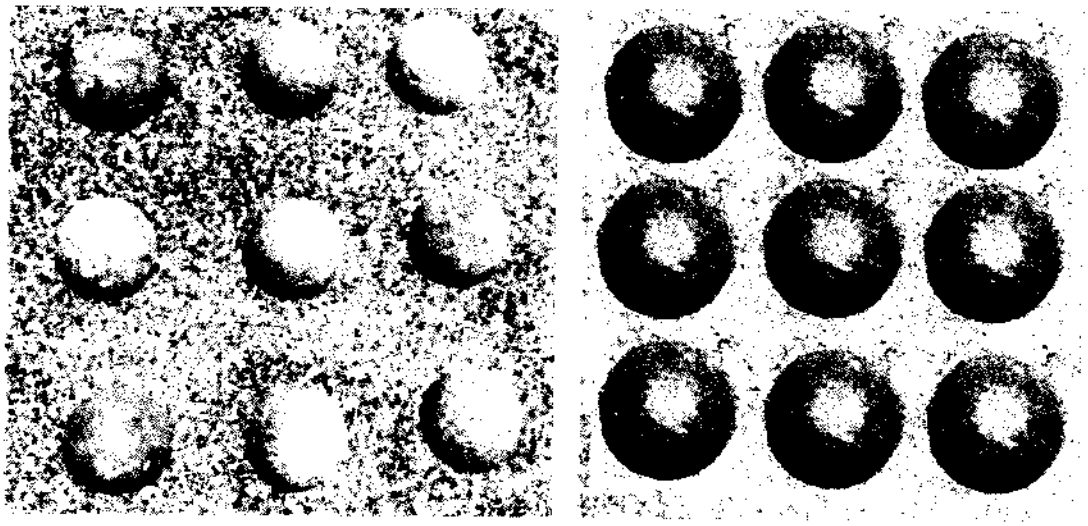

Fig.3.26 Boulder semi–hemispheres of various sizes (D_B = 0.055 and 0.80 m dia respectively)

The boulders were laid on the block ramp with base material using a cement mixture paste in various arrangement patterns and configuration following a symmetric geometry as shown in Fig. 3.27. Experiments were performed in the sequence as first for the steepest slope 1V:5H

with the smallest size boulder i.e. D_B = 4.2 cm. Thus for the first experimental set under this element configuration, various clear spacing in terms of the boulder diameter were used to test the effect of macro-roughness geometry and configuration in the energy dissipation process. The generally adopted spacing patterns were $1D_B$ (denoting S_x/D_B = 1.0), $1.5D_B$, $2.0D_B$, $3.0D_B$ and so forth for the staggered uniform arrangement. After each spacing set of runs under varied discharges, the boulders were carefully removed from the ramp flume. Then the second spacing set was put into place for the next experimental set. To test the effect of the boulder geometry on the energy dissipation process apart from boulder concentration, a few runs were conducted for the "rows" arrangement also.

Fig.3.27 A typical arrangement of the boulder block ramp in the flume

After the experimental runs on uniform set, then specific non-uniform configurations were used for placing the boulders of the same size on the same ramp slope. It may be noted that, the non-uniform staggered configuration were designed in such a way that symmetry of boulder arrangement is preserved along the longitudinal mid-axis of the ramp flume. The adopted non-uniform configurations were denoted as NU–1, NU–2, NU–3 and NU–4. These configurations have been detailed earlier in section 3.2.2 of this chapter. Experimental runs were followed in similar way as the uniform arrangement in the order as NU–1, NU–2, NU–3

and NU–4. These comprised of a total experimental set for S = 0.20, D_B = 0.042 m configuration.

Likewise tests were performed for the sets for the other boulder dimensions under the same slope as: S = 0.20, D_B = 0.055 m; S = 0.20, D_B = 0.065 m; S = 0.20, D_B = 0.080 m; S = 0.20, D_B = 0.10 m, respectively. This completes one full experiment cycle for a particular slope 1V:5H.

Similarly, the experiments were carried out for the second and third full experiment cycles under slopes 1V:7H and 1V:9H in the same order of configuration and test conditions.

3.4.3.1 Spacing configuration of boulders

The arrangement of boulders on ramp was done in two major patterns: (i) Uniform distribution (boulders placed at uniform spacing throughout the length of ramp) and (ii) Non-uniform distribution (boulders placed with lesser spacing on upstream section of ramp and more spacing on downstream section, and vice versa). In both the arrangements, the first row of the boulder on ramp was placed at a distance downstream from the upstream crest such that it should not create a major disturbance in the flow at the upstream section as shown in Fig. 3.28.

Experiments were first performed for uniform spacing of boulders in staggered pattern for 4.2 cm diameter boulders at ramp slope S = 0.20 for S_x/D_B = 1.0, 1.5, 2.0, 3.0, and 4.0 along with four sets for non–uniform configuration of boulders: NU–1, NU–2, NU–3, NU–4. In the uniform arrangement, the longitudinal spacing (S_x) represents the clear longitudinal spacing between each rows of boulders at regular intervals throughout the inclined length of the ramp. In the non-uniform arrangement, for the first NU–1 set, up to 0.85 m upstream length of the ramp, the boulder spacing is S_x/D_B = 1.0 and for the remaining downstream length, S_x/D_B = 1.5. In the second NU–2 set, boulders were placed at S_x/D_B = 1.5 clear spacing up to 2.00 m upstream length of the ramp, and for the remaining downstream length S_x/D_B = 1.0. The third NU–3 set was arranged in a reverse order of the NU–2 set. In the fourth non-uniform configuration set, tests were conducted with the objective of eventuality of localized jump formation with a closer and higher spacing alternately. Thereby, boulders were placed alternately at S_x/D_B = 1.0 and S_x/D_B = 1.5 throughout the inclined length of the ramp.

Observations were recorded and this pattern was followed for the ramp slopes, $S = 0.1428$ and 0.1111 respectively during the study.

The boulder size 5.5 cm diameter hemispheres were investigated for the slope $S = 0.1428$ with uniform spacing: S_x/D_B = 1.0, 1.5, 2.0, 3.0 and 4.0 along with the four sets for non–uniform spacing of boulders, all in staggered pattern.

In the next set, experiments were performed for 6.5 cm size boulders at uniform arrangement: S_x/D_B = 1.0, 1.5, 1.7, 2.0, 3.0, and 3.4 along with the four sets of non–uniform spacing of boulders: NU–1, NU–2, NU–3, NU–4, in staggered pattern.

For 8.0 cm size boulders, experiments were performed for the three slopes first at uniform spacing: S_x/D_B = 0.5, 1.0, 1.5 and 2.0 along with the four sets of non–uniform spacing of boulders: NU–1, NU–2, NU–3, and NU–4 in staggered pattern. Considering scale factor that the boulder size is large with the flume dimensions, higher spacing above $S_x/D_B > 2.0$ were not tested. Spacing of $S_x/D_B = 0.5$ is adopted to test the energy dissipation on the ramp with compact spacing.

Similarly, experiments were conducted for the boulder semi–hemispheres of 10.0 cm diameter on $S = 0.20$ slope, for uniform spacings: S_x/D_B = 1.0, 1.5 and 2.0 along with the three sets of non–uniform spacing of boulders: NU-1, NU-2 and NU-3 in staggered pattern. The large scale roughness induced in the flow was studied to test its significance on energy dissipation.

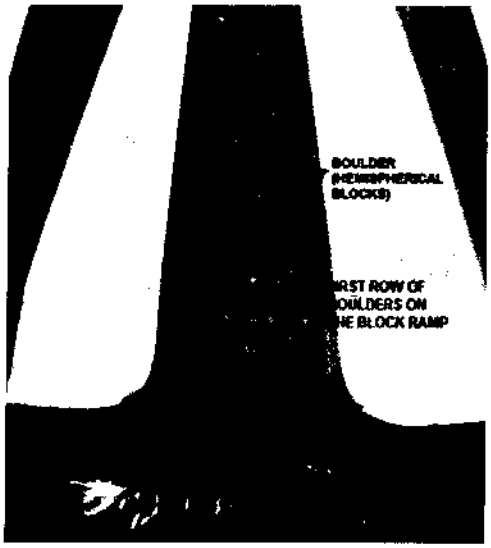

Fig.3.28 Typical approach flow condition at the upstream section with boulders on block ramps

3.4.3.2 Test for specific boulder configurations

To test the effect of boulder concentration (Γ) for the same configuration in imparting flow resistance and energy dissipation, specific arrangements were investigated. As a case configuration, for the same arrangement pattern and longitudinal spacing, the number of boulders in rows were varied alternate 5 and 4 numbers of staggered-arranged blocks in one set was compared with alternate 3 and 2 numbers of staggered-arranged blocks in the another set for the same longitudinal spacing $4D_B$. Further, to investigate the effect of boulder disposition and concentration, for the same clear L-spacing, S_x/D_B = 4.0, two sets were examined: (i) "4 D_B–Staggered (I)" with alternate 3 and 2 numbers of boulders row-wise (N_B = 40, Γ = 7.76 %), and (ii) "4 D_B–Staggered (II)" with alternate 4 and 3 numbers of boulders row-wise (N_B = 56, Γ = 10.87 %). Then, in another specific configuration, to test the boulder arrangement factor, for the same S_x/D_B = 4.0, two sets were tested in "row" arrangement as: (i) "4 D_B–Rows (I)" with 3 number of boulders row–wise (N_B = 48, Γ = 9.31 %), and (ii) "4 D_B–Rows (II)" with 4 number of boulders row–wise (N_B = 64, Γ = 12.42 %).

The spacing of S_x/D_B = 3.4 (i.e. S_x = 3.4 x 6.5 = 22.10 cm) was deployed to test the effect of boulder size under same spacing, by correlating with S_x/D_B = 4.0 (i.e. S_x = 4.0 × 5.5 = 22.00 cm) for the boulders of size 5.5 cm diameter. Similar tests were done for S_x/D_B = 1.7 spacing with the same objective. For ramp slope, S = 0.1428, one set for "row" arrangement was tested with S_x/D_B = 3.0 with 3 number of boulders row-wise (N_B = 60, Γ = 16.43 %).

3.4 DATA CHARACTERISTICS

The experimental data collected in the present study are listed in the Appendix-I under the major hydraulic parameters and the range of the data are listed in Table 3.3. Besides the range of dimensionless parameters adopted in the discharge, Reynolds number (Re) was used to exemplify the turbulent flow regime on block ramps.

Table 3.3 Range of the data of present study

Sl	Parameter	Unit	Range of data for ramp bed slopes:		
			1V:5H	1V:7H	1V:9H
1	Discharge (Q)	m^3/s	0.0073 – 0.0308	0.0128 – 0.0339	0.0176 – 0.0387
2	Head at the upstream broad-crested weir (h_0)	m	0.0504 – 0.1223	0.0807 – 0.1625	0.1057 – 0.1859
3	Depth of flow at downstream toe (h_t)	m	0.0095 – 0.0565	0.0185 – 0.0728	0.0226 – 0.0591
4	Base material size (d_{xx}) (micro-roughness)	mm	16 – 25	16 – 25	16 – 25
5	Boulder size (D_B) (macro-roughness)	cm	4.2 – 10.0	4.2 – 10.0	4.2 – 10.0
6	Boulder concentration (Γ)	%	7.76 – 32.07	13.72 – 28.74	16.52 – 28.86
7	Reynolds Number (Re) ($\times 10^4$)	–	2.55 – 7.47	4.55 – 9.29	5.86 – 10.68

3.6 EXPERIMENTAL STUDIES FOR STABILITY OF RAMPS

Tests were carried out at the hydraulics laboratory of the Department of Civil Engineering, Indian Institute of Technology Roorkee, India in a rectangular chute of width (W) = 0.83 m, height (H) =1.0 m and length (L_R) = 3.049 m, 4.971 m and 6.082 m for ramp slopes of 1V:2.88H, 1V:4.87H and 1V:6H, respectively. A broad-crested weir of the length 0.20 m was provided upstream of the chute and joined to the chute with a curved of radius 0.10 m. Electromagnetic flow meter was used to measure the discharge with a precision of 10-5 m^3/s. Loose boulders were placed on the concrete bed of chute in closer arrangement with minimum voids. Three sizes of boulders designated as β_1, β_2 and β_3 were used during the experimental study. They possessed irregular and smooth geometry as shown in Fig. 3.29a, b.

Fig. 3.29 (a) Different sizes of investigated boulders; (b) Irregular and smooth geometry of boulders used in the present study.

Using volume displacement method (Aguirre et al. 2003), the size of each boulder was calculated and discrete approach was used to arrive at boulder distribution function which is given below;

$$F_d(d) = \frac{m}{N+1} \tag{3.2}$$

where m = ranking number and N = number of boulders taken in the samples from boulder population.

The granulometric curves of the boulders used in the present study are shown in Figure 3.30 and the geometrical characteristics of boulders are given in Table 3.4.

The uniformity coefficient C_u is given as; $C_u = d_{60}/d_{10}$, which represent the degree of uniformity of the boulders. For uniformly graded boulders, C_u is nearly unity. As per Table 3.4, the boulder size β_1 is more uniform followed by β_3 and β_2.

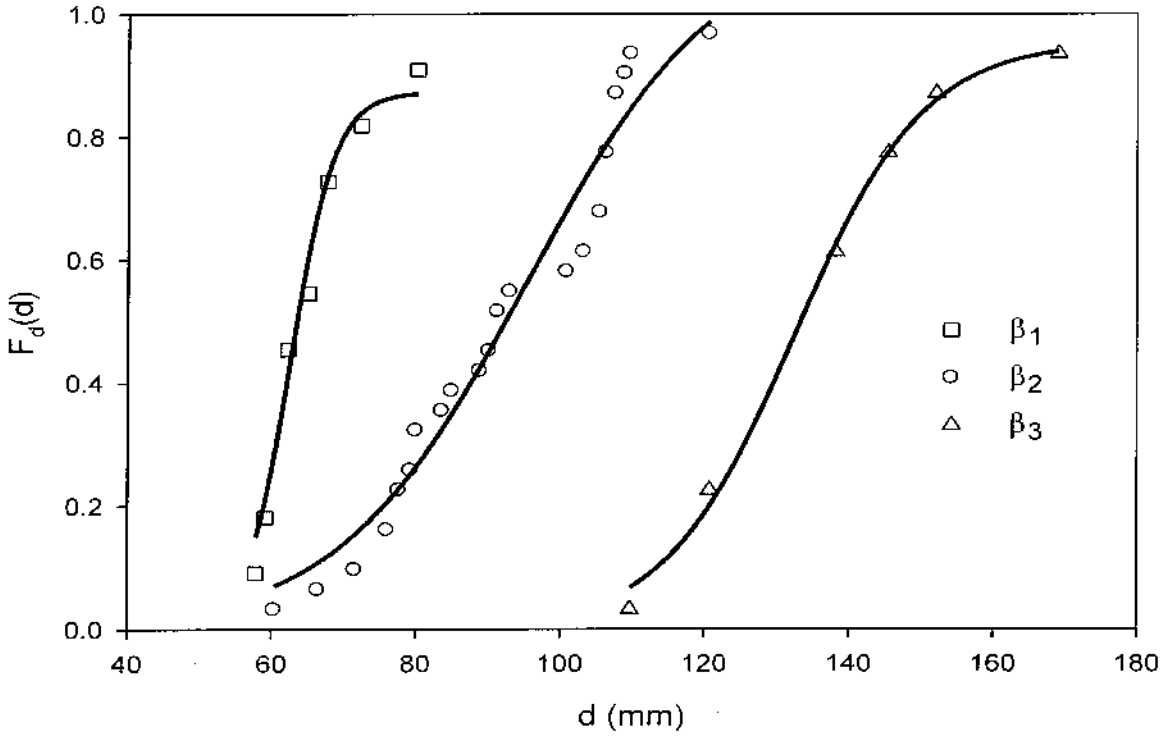

Fig. 3.30 Granulometric curves of the used boulders.

Table 3.4 Geometric characteristic of the used boulders

Parameter →	d_{10}	d_{50}	d_{60}	d_{84}	$\sigma = \sqrt{d_{84}/d_{50}}$	C_u
Unit	mm	mm	mm	mm	_	_
Sample β_1	57.7	64	66	74	1.075	1.14
Sample β_2	72	91.3	103.1	107	1.085	1.43
Sample β_3	113	133.8	138	150	1.059	1.22

In all the channel arrangements the boulders were placed on a concrete bed prepared to a desired slope. Boulder samples β_1, β_2 and β_3 were placed over the entire ramp during the each stability test unlike that of Pagliara & Chiavaccini (2007) who used large rocks at the beginning of the

ramp entrance to avoid scouring phenomenon due to impinging jet. To take into account the effect of impinging jet in the present study; boulders were closely packed together like a rocky layer or in one piece construction. A triangular sill was provided downstream end of the chute to prevent the skidding of the boulders over the chute. A schematic drawing of the experimental set up is shown in Fig. 3.31.

The discharge was regulated with the valve fitted on the inlet supply until the discharge provoking the chute instability was reached. Each discharge step was maintained for at least 8 minute in order to stabilize the bed evolution

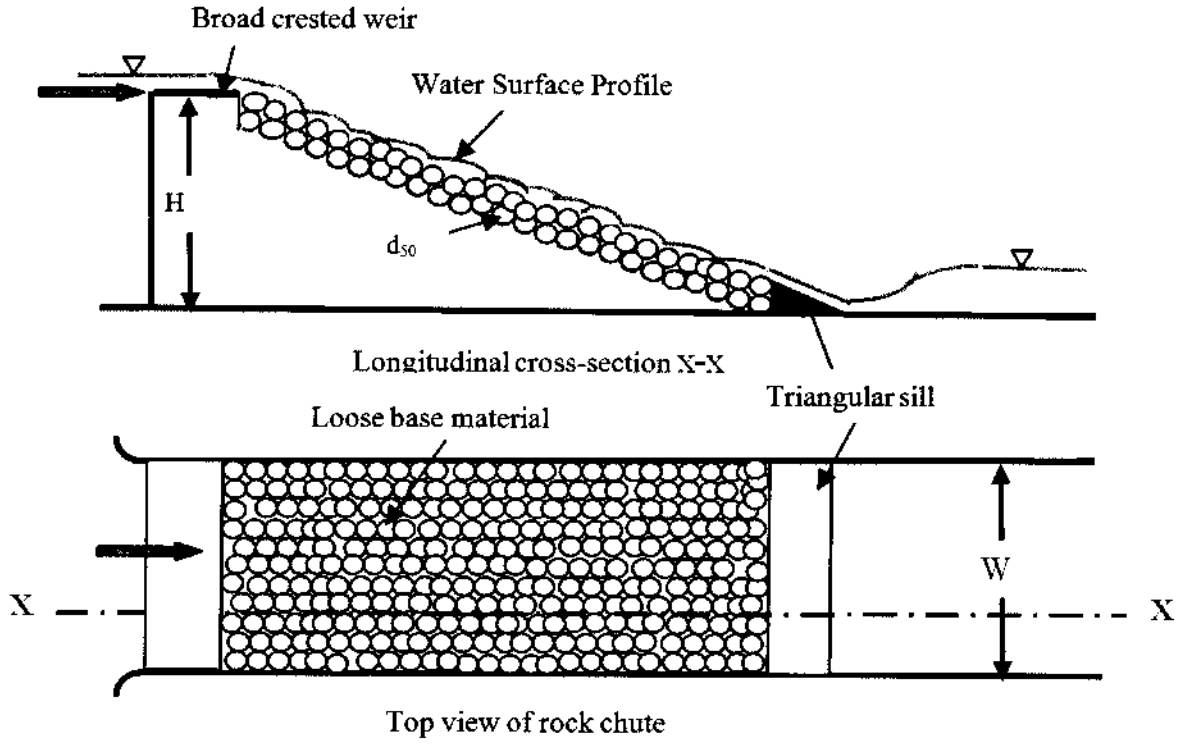

Fig. 3.31 Schematic sketch of the experimental set up.

During the stability tests, the main focus was to estimate the critical discharge causing local failure; because local failure is considered as a stable or equilibrium condition, unlike global failure which is a beginning of the total collapse of the chute, hence can't be regarded as an equilibrium condition.

At earlier stages of discharge, the boulders begin to vibrate and single boulder leaves the chute. This type of movement called initial movement of the ramp (Fig. 3.32a) and considered as stable or a normal condition because it doesn't affect ramp configuration. For high discharge values, few boulders leave the chute and number of boulders subjected to movement increase significantly. This movement was identified as the local failure (Fig. 3.32b) and the correspondingly unit flow discharge was referred as critical failure discharge q_c. As the discharge was further increased, many local failures occurred over the ramp. Once created scour hole loosened the surrounding boulders and with the event these boulders try to roll down and in this way one scour hole gets connected with another causing channelization over the face of the ramp. This type of failure was called global failure (Fig. 3.32c).

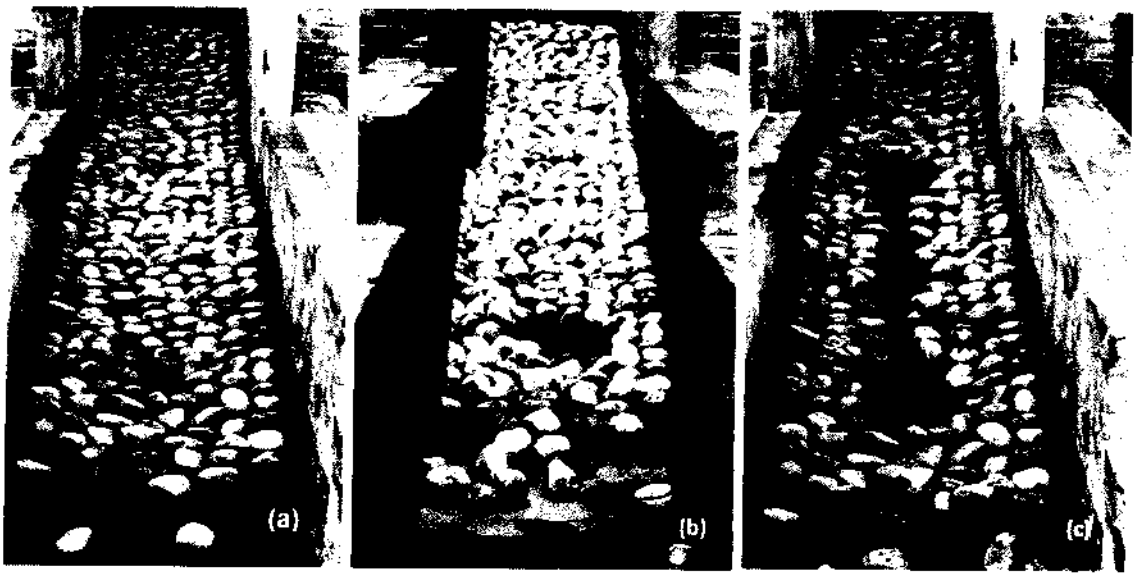

Figure 3.32 Various stages of base chute failure; (a) Initial movement; (b) Local Failure and (c) Global failure observed in the present study.

3.6 CONCLUDING REMARKS

The experimental dataset for various configurations of block ramps investigated in the present study were recorded for various flow conditions. The experiments entailed a range of flows with Reynolds number of 25,500 to 106,800 under three ramp slopes with varied boulder spacing and arrangement covering S_x/D_B = 1.0 to 4.0. Observations for each specific configuration and boulder geometry under different permutations and combinations of boulders were noted with

the objective of ascribing its differential effect on the relative energy dissipation. Each boulder configuration represented a boulder block ramp entity with that particular arrangement for which flow discharges were computed with the calibration equation as derived. Primarily, the energy heads at the upstream section and downstream toe of the block ramp were computed using the depth of flow at the respective section to evaluate the overall energy dissipation in the test runs. These data were systematically tabulated for subjective analysis and composed for projecting a relation to determine the relative energy dissipation on block ramps with staggered boulders in the next chapter. The validity of findings of the present study is limited to the range of data as reported in Table 3.3.

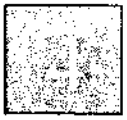

ANALYSIS OF DATA

This chapter elaborates the analysis of data recorded in the experiments conducted for studying energy dissipation on block ramps. First, the discharge and depth of flow observed from the experimental work was used for computing the total energy at the upstream and downstream sections of the ramp. Then the relative energy loss was calculated for various configurations of block ramps under varying flow conditions. The analogy of flow resistance and roughness-induced flow are examined using the postulations of various authors. This chapter also describes the various statistical procedures used to examine the multitude and dimensionality of the observed dataset. The selection of optimal hydraulic variables and the dataset which best fitted the relative energy dissipation curve is also discussed. Further, the chapter explicated the existing relationships prescribed for energy dissipation on block ramps along with associated variables using the experimental dataset of the present study, following which new relations are proposed for the computation of relative energy dissipation on block ramps with boulders in staggered configuration.

4.1 ENERGY DISSIPATION AND FUNCTIONAL RELATIONS

4.1.1 Energy Dissipation

For understanding the behaviour pattern of varying roughness dimensions and the relative energy dissipation on block ramps, the analysis of data were done in the ascending order of boulder size and spacing from the steepest to mildest slope tested.

During the experimental test runs and observations recorded, certain assumptions within the asymptotes of free surface flows were made. They are listed below:

(a) It is assumed that hydrostatic pressure prevailed on the ramp.

(b) The localized jumps and flow disturbances are also under hydrostatic pressure distribution. Because of the small curvature of the flow at the toe of the ramp, these conditions could be considered satisfied as was also assumed by Pagliara and Chiavacinni (2006a).

(c) The kinetic correction factor (α) is assumed equal to unity. Chen (1992) found different values of this parameter in his experiments with a typical range of 1.05–1.08. Pagliara and Chiavacinni (2006a) has showed that this variation will not practically influence the results in their experimental findings in quantification of relative energy loss.

(d) Wall roughness factor of the channel flume is not taken into account considering that the boundary of the prismatic flume is smooth.

(e) In all the observations, clear water conditions have been considered. Local effects of scour and mobile bed were considered negligible within the test conditions on the ramp flume.

(f) The effect of air entrainment in the flow over the ramp was considered negligible due to the short length of the ramp in the test conditions. It may be cited that Pagliara and Chiavacinni (2006a) had found a mean air concentration varying from 0.04 to 0.22 (for S = 0.125 to 0.25 respectively), which are relatively small to affect the friction factor for flow on block ramps.

(g) Scale effects are considered not to be affected with respect to the width and length of the experimental channel flume, taking that the flow is approximately two dimensional (Pagliara and Chiavacinni, 2006a). Further, high Reynolds number of flow was also maintained to sustain turbulent flow.

The energy dissipation on the block ramp is evaluated in terms of the energy per unit weight of water volume, generally termed as the head and having the same dimensions of length. In the present study, the head loss between the upstream section and downstream toe section is taken as the energy loss of flow over the block ramp. The outline of computational steps is listed below:

(i) At the point where the ramp slope starts, it is considered that critical flow conditions prevail and the critical flow depth (h_c) is thereby computed using the flow discharge as (Eq. 4.1a),

$$h_c = \left(\frac{q^2}{g}\right)^{\frac{1}{3}} = \left(\frac{Q^2}{W^2 g}\right)^{\frac{1}{3}} \qquad (4.1a)$$

(ii) The upstream total energy or head is then calculated with the critical flow condition factor as (Eq. 4.1b),

$$E_0 = H + \frac{3}{2}h_c \qquad (4.1b)$$

(iii) The downstream flow depth (h_t) for the flow over the block ramp is measured via the stilling well. Then the specific energy at this section (XT) is calculated using the simple relation (Eq. 4.1c),

$$E_t = h_t + \frac{q^2}{2gh_t^2} \tag{4.1c}$$

(iv) The relative energy dissipation at the downstream toe section of the ramp with respect to the upstream measured head is the ratio of difference of energy heads between the two sections (ΔE) and the upstream energy as given in Eq. 4.1d.

$$\Delta E_r = \frac{E_0 - E_t}{E_0} = \frac{\Delta E}{E_0} \tag{4.1d}$$

The relative energy dissipation term is denoted by ΔE_{rB} for the case of block ramps with boulders over base material. In general, ΔE_r denotes the relative energy dissipation term for the smooth ramp case or ramp with base material.

(v) For flow depths at other sections on the ramp (h_i), the specific energy at each respective section was calculated using Eq. (4.1e). The geometric mean of the measured flow depth across the three transverse sections was assumed as the flow depth at that section.

$$E_i = h_i + \frac{q^2}{2gh_i^2} \tag{4.1e}$$

Subsequently, the analysis of the variables related to the energy dissipation function, were based on the above calculations.

4.1.2 Functional Relations

Using the basic principles of steep channel flow and roughness-induced flow hydraulics (Chow, 1959; Hartung and Scheuerlein, 1967; Jarret, 1984; Whittaker and Jäggi, 1986; Pagliara and Chiavacinni, 2006a), a functional relationship (Eq. 4.2) for a ramp of height H and slope S was developed to delve upon the various probable hydraulic variables associated with the relative energy dissipation on block ramps in the present study.

$$F\left(\Delta E_r, Q, H, L_R, W, S, D_B, d_{50}, S_x, S_y, f, \tau, \mu, \sigma, \rho, g\right) = 0 \tag{4.2}$$

where F is a functional symbol; ΔE_r is the relative energy dissipation term; Q is the flow discharge; L_R and W represent the ramp channel dimensions of length and width respectively; D_B is the macroroughness element or boulder size in terms of median diameter; d_{50} is the median size of the microroughness element or base material; S_x and S_y are the clear

longitudinal and transverse spacing of boulder elements; f is the roughness–related friction factor; τ is the shear stress due to turbulence effects; along with the main fluid properties; μ is the dynamic viscosity; σ is the surface tension; ρ is the specific mass or density of water; and g is the acceleration due to gravity constant. The parameters have been chosen considering all the factors ascribing the hydraulic boundaries of the presence of macroroughness boulders and base material on the ramp. The relative energy dissipation term is denoted by ΔE_r for block ramps with microroughness base material or ramps in smooth condition, and ΔE_{rB} for the block ramps with macroroughness boulders placed over the base material. In both cases, the term ΔE_{rB} or ΔE_r is expressed by the ratio ($\Delta E/E_0$) as given in Eq. (4.1d).

Applying the Buckingham Π theorem, the functional relation can be represented in terms of dimensionless grouping variables as h_c/H, h_c/D_B, h_c/d_{50}, D_B/d_{50}, and W/h_c. The basic flow properties such as viscosity (μ), mass density (ρ), surface tension (σ), and shear stress (τ) are taken care of by Reynolds Number and Froude Number which govern the viscous, gravitational and inertial forces of the flow. The boulder concentration factor Γ (Ferro, 1999) and reduction coefficient ψ (Canovaro and Solari, 2007) were introduced to account for the number of boulders, spacing and arrangement on the ramp. The functional relationship is expressed explicitly using a function Ω in terms of ΔE_{rB} as,

$$\Delta E_{rB} = \Omega_1\left(\frac{h_c}{H}, \frac{h_c}{D_B}, \frac{h_c}{d_{50}}, \frac{D_B}{d_{50}}, \frac{W}{h_c}, f, \mathrm{Re}, \mathrm{Fr}, \Gamma, \psi, C_m\right) \tag{4.3}$$

C_m is the non-dimensional mean air concentration or air entrainment factor. In the above relation Eq. (4.3), the parameter W/h_c can be neglected as it has been found there were no differences in the test results for experiments conducted on ramps of different widths (Pagliara and Chiavacinni, 2006a). Regarding the effect of air entertainment in energy dissipation, flow appeared with practically no white water conditions though bubbles seem to be significant at lower submergence (Pagliara and Chiavacinni, 2006a). The contribution of air concentration (C_m) which becomes insignificant when two-phase flow occurs, have thus been neglected in the present study. The friction factor was investigated explicitly as only a range of base material size was tested and not much variation could be noted in the experimental conditions for block ramps, thereby the term is excluded from the relation. However, the relative roughness terms as h_c/D_B and h_c/d_{50} were considered. Reynolds number was included as viscous forces were predominant in the test conditions of the present study, and Froude number of approach flow was neglected, as inertial forces were found to have less

correlation with the relative energy dissipation factor (as was also found by Pagliara and Chiavacinni, 2006a). The relative energy dissipation can be further expressed as (Eq. 4.4).

$$\Delta E_{rB} = \Omega_2\left(\frac{h_c}{H}, \mathrm{Re}, \Gamma, \psi, \frac{S_x}{D_B}\right) \tag{4.4}$$

4.2 FLOW RESISTANCE AND ROUGHNESS CRITERIA

Hydraulic flow resistance has been an important criterion for roughness related effects for studies on open channels. It can be generally conceived that higher resistance in the course of flow in rough open channels will impart higher drag and other resistive forces, which in turn relatively retards the energy of flow. To understand this effect, roughness has to be scaled in terms of the hydraulic geometry and flow parameters. Generally three roughness conditions were considered in flow hydraulics of rough bed channels (Bathurst, 1978; Bathurst et al., 1981): (i) small scale roughness (SR) which occurs for relative submergence greater than 4 (where, relative submergence is the ratio of the uniform flow depth h_u to characteristic particle size d_{84}), intermediate scale roughness (IR) which occurs for relative submergence between 1.2 and 4, and large scale roughness (LR) which occurs when the relative submergence is less than approximately 1.2. In the present study, roughness criteria for flow on block ramps were adopted as per the criterion adopted by Pagliara and Chiavacini (2006a) as given in Table 4.1.

Table 4.1 Roughness categorization for block ramps (Pagliara and Chiavacinni, 2006a)

Roughness	Notation	h_c/d_{50}
Large Scale Roughness	LR	$h_c/d_{50} < 2.5$
Intermediate Scale Roughness	IR	$2.5 < h_c/d_{50} < 6.6$
Small Scale Roughness	SR	$6.6 < h_c/d_{50} < 42.0$

It was observed that in most cases of the experimental test conditions, intermediate scale roughness prevailed. It may be recalled that natural mountain streams and torrents characterize this type of roughness condition. This conformity is also with the experimental findings of Afzalimehr and Anctil (2001). Though the median grain size is the denominative of the roughness and relative submergence criteria, the critical depth h_c is a key deciding factor for describing the flow parameter.

Different power and log laws have been used to describe flow resistance at different relative roughness as the R/d_{84} or h/d_{84} exponent. Various empirical relations have been proposed by different authors based on their experimental or field investigations, and the relations thereby were ideal to the hydraulic boundaries of the experimental or field conditions. To test the flow resistance condition of block ramps in the present study, few relations were selected which pertain to large scale roughness with steep channels. Observed data of the present study were used to evaluate the resistance function $(8/f)^{1/2}$ as per the equations postulated by various authors and plotted with the observed $(8/f)^{1/2}$ factor as shown in Fig 4.1. The resistance functions were plotted with respect to the relative submergence parameter h_c/d_{50}. It can be inferred that a logarithmic variation follow in most cases. In the present study, three distinct scatter following respective three asymptotes can be observed for the tested slopes. The scatter is almost representative to that depicted by the Lawrence (1997) relation, where the resistance function remains almost at a constant state with respect to the relative submergence parameter h_c/d_{50}. The Pagliara and Chiavacinni's (2006c) total resistance function also showed a similar trend though at a higher margin of $(8/f)^{1/2}$ from that of the present study. The relatively lower values of the resistance function $(8/f)^{1/2}$ observed in the present study seemed to affirm that the prevailing hydraulic conditions prescribed higher energy dissipation as was also indicated by Ferro (1999).

It can be observed from the comparison plot that the observed dataset and test conditions of the present study were in parity with the formulations of various authors. The scatter of points in the case with Lawrence (1997) can be attributed to the slope factor in his postulation, which other authors did not consider directly. Also in the case with Ferro (1999), five distinct asymptotes can be noted characterizing the five different sizes of boulders tested in the present study.

The spatial variability of bed particles of a gravel-bed channel and the effects of the arrangement of coarse bed elements on the flow resistance law was experimentally investigated by Baiamonte and Ferro (1997). The roughness elements on a gravel-bed channel vary in size and shape (as the base material on block ramps), and do not equally project into the flow, thereby giving rise to differential form drag. As a consequence, the flow resistance law is strongly affected by the roughness geometry, which is primarily a function of the arrangement and concentration of boulders (Ferro, 1999). Pagliara and Chiavacinni (2006c) stated that boulders produce form drag forces which increases the flow resistance and that the boulder concentration is the main parameter affecting the flow resistance.

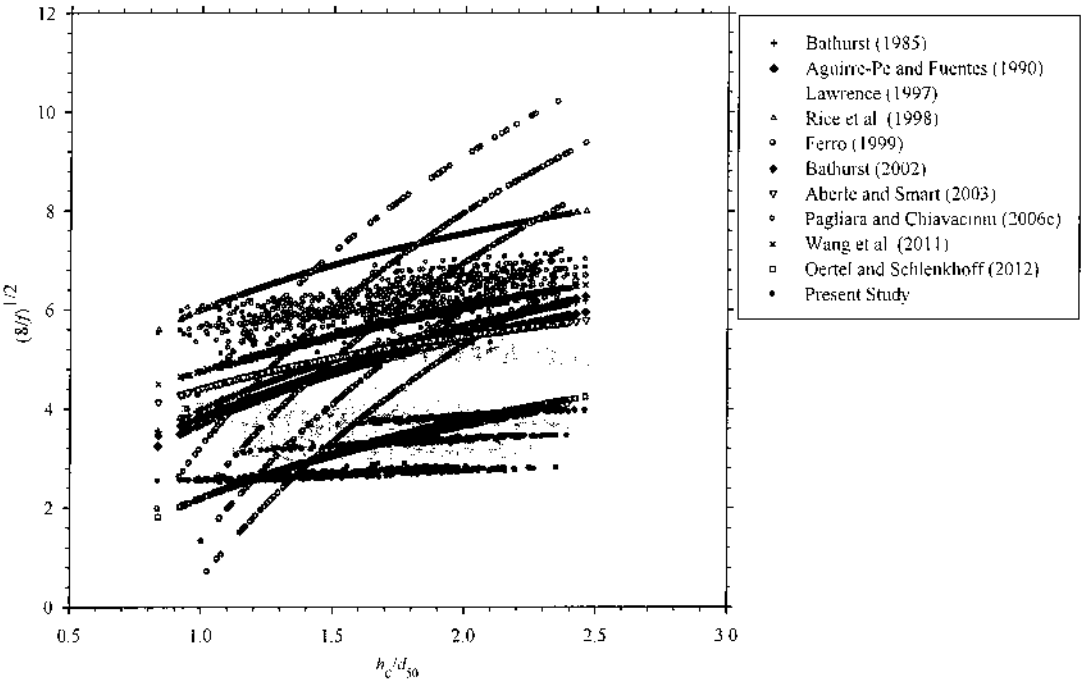

Fig. 4.1 Comparison of flow resistance factor in the present study using relations of various authors

A flow resistance relation considering the boulder concentration factor is formulated for block ramps with staggered boulders adopting a similar functional relationship presented by Pagliara and Chiavacinni (2006c) based on the observed dataset as given by Eq. (4.5).

$$\sqrt{\frac{8}{f_{tot}}} = a\,(1+\Gamma)^{b}\left(\frac{h_c}{H}\right)^{b}\left(\frac{h_c}{d_{50}}\right)^{0.10} \tag{4.5}$$

where a and b are parameters for correlation. As was noted that the present dataset marked a distinct correlation for each tested slope, the values of parameters a and b were found to be characteristic to the particular slopes tested, and given in Table 4.2. The above equation can used to evaluate the flow resistance function for staggered boulder configuration for a correlation of $R^2 = 0.92$ in the tested slope range.

Table 4.2 Values of parameters a and b in Eq. (4.5)

Slope	a	b
1V:5H	2.659	0.046
1V:7H	3.277	0.077
1V:9H	3.720	0.093

The flow resistance factor imparted by the macroroughness boulders over the base material and its possible analogy with energy dissipation on block ramps are further investigated and discussed in this chapter.

4.3 ENERGY DISSIPATION ON SMOOTH RAMP

Experiments have been carried out for the ramp initially for the smooth condition before application of any roughness material for each tested slope. The relative energy dissipation has been evaluated with respect to h_c/H as this dimensionless flow parameter represents the ratio of flow discharge and slope of the ramp. Pagliara and Chiavacinni (2006a) have also indicated that the relative energy dissipation depend on this parameter and slope for the same scale roughness conditions on block ramps. Flow over the smooth ramp was characterized with high velocity (2.85 to 3.58 m/s) and less depth of flow at the toe of the ramp because of the shooting nature of flow at the downstream section of the ramp. In order to find out and have a comparative assessment of the energy dissipation characteristics on block ramps, ΔE_r was evaluated for the smooth ramp case for the tested slopes as 1V:5H, 1V:7H and 1V:9H respectively. Figure 4.2 shows the relative energy dissipation trend for each slope.

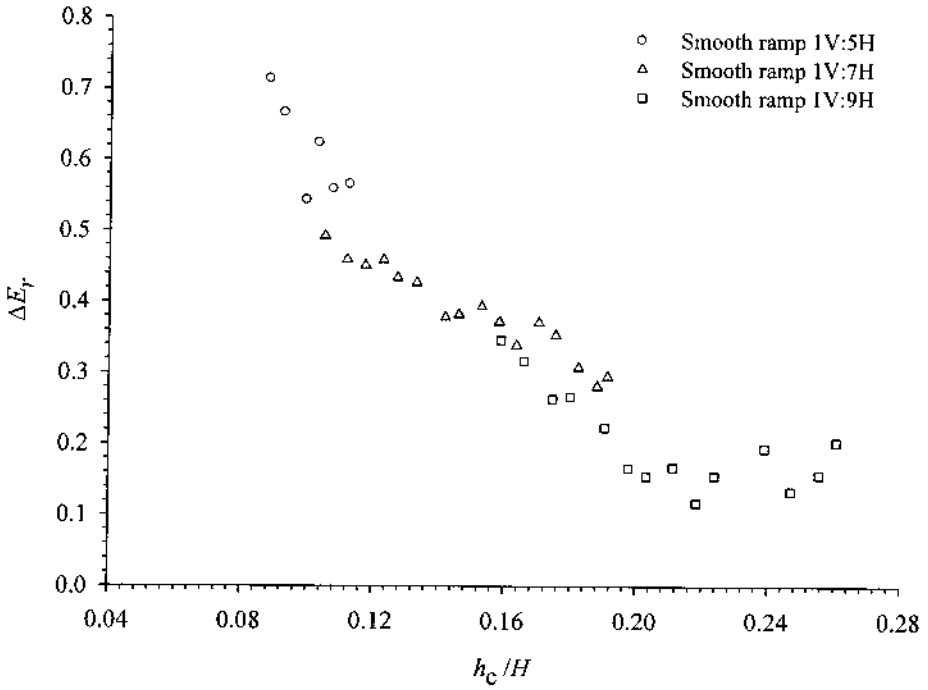

Fig. 4.2 ΔE_r for smooth ramp at various slopes

From the assay of the experimental results, it is found that on the ramp slope 1V:5H, for $0.07 \leq h_c/H \leq 0.11$, the optimum relative energy dissipation achieved is of the order of 54 to 71 %. It may be recalled that Pagliara and Chiavacinni (2006a) found a maximum relative energy dissipation of 54% in their experimental observations on a 1V:4H smooth ramp. Few anomalies in the precise measurement of the downstream flow depth cannot be ruled out due to the rapidly varying flow conditions on the smooth ramp. In the next tested slope 1V:7H, for $0.11 \leq h_c/H \leq 0.19$, the optimum relative energy dissipation achieved is of the order of 30 to 49%. There is a falling trend of ΔE_r as discharge increases. It can be noted that higher discharge prevailed as the slope gets milder in the test conditions of the present study. For the smooth ramp at slope 1V:9H, for $0.16 \leq h_c/H \leq 0.26$, the optimum relative energy dissipation achieved is of the order of 12 to 35%. One striking observation was that for similar h_c/H values, the relative energy dissipation is greater at steeper slopes. It may be deduced from the test results that the energy dissipation increases with steeper slopes, and that the trend gradually reclines as the slope gets milder. The overall range of the test results for relative energy dissipation on smooth ramps are reported in Table 4.3.

Table 4.3 Summary of the test results on smooth ramps

Parameter	1V:5H	1V:7H	1V:9H
velocity at toe section, v_t	2.85 – 3.58 m/s	2.93 – 3.93 m/s	2.93 – 3.82 m/s
h_c/H	0.07 – 0.11	0.11 – 0.19	0.16 – 0.26
ΔE_r	0.543 – 0.714	0.295 – 0.493	0.117 – 0.346

To test the adequacy of the observed dataset of the present study, the Pagliara and Chiavacinni (2006a) equation was used to compute the relative energy dissipation (parameters: A = 0.02, B = –0.9 and C = –25.0 for the smooth ramp condition). The comparative plots for each respective slope are given in Figs. 4.3a-c. The respective trend depicted that there is a close proximity for the respective ΔE_r values at 1V:5H slope smooth ramp. But at milder slopes the Pagliara and Chiavacinni (2006a) equation shows a higher relative energy dissipation trend from the observed values.

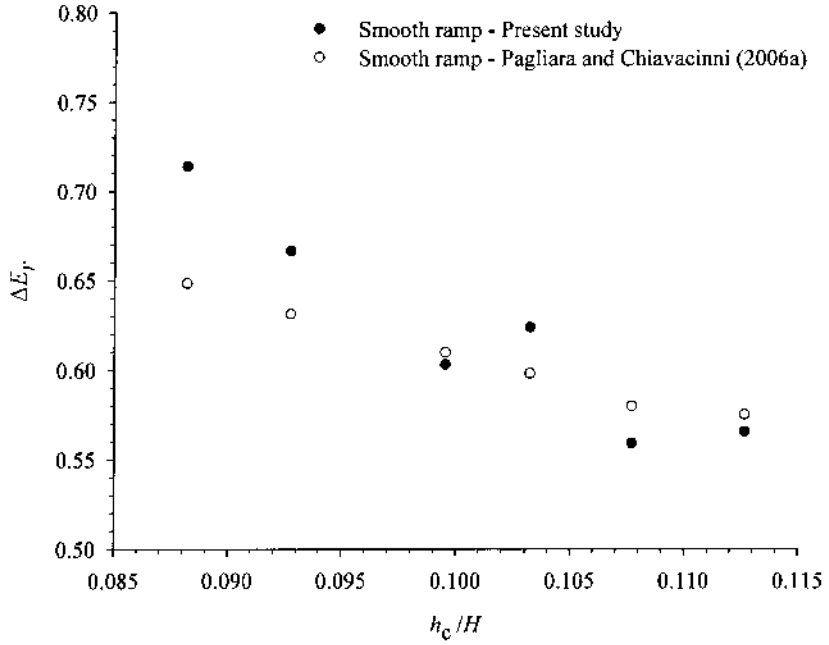

Fig. 4.3a Comparison of observed ΔE_r for smooth ramp (1V:5H) with that calculated using Pagliara and Chiavacinni's (2006a) equation

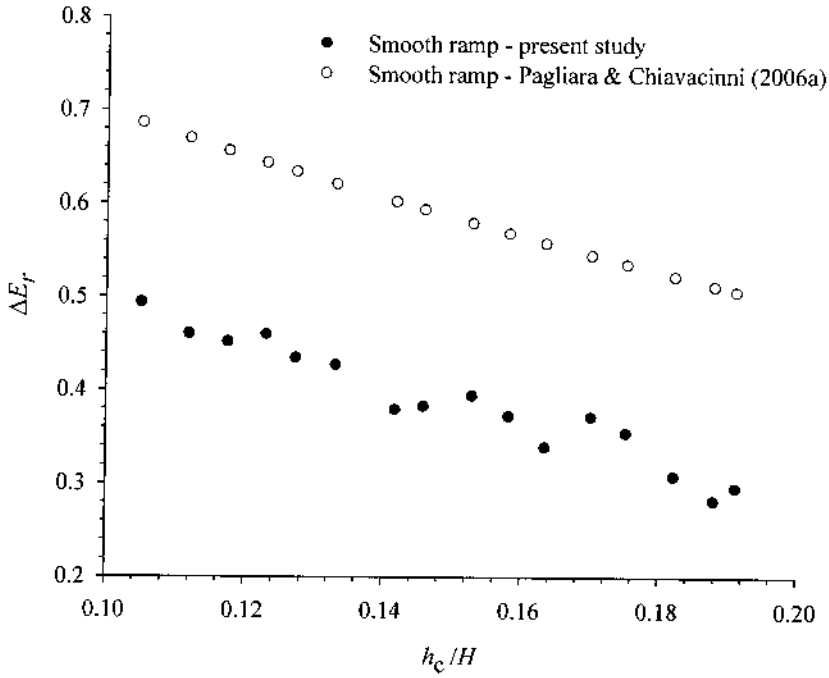

Fig. 4.3b Comparison of observed ΔE_r for smooth ramp (1V:7H) with that calculated using Pagliara and Chiavacinni's (2006a) equation

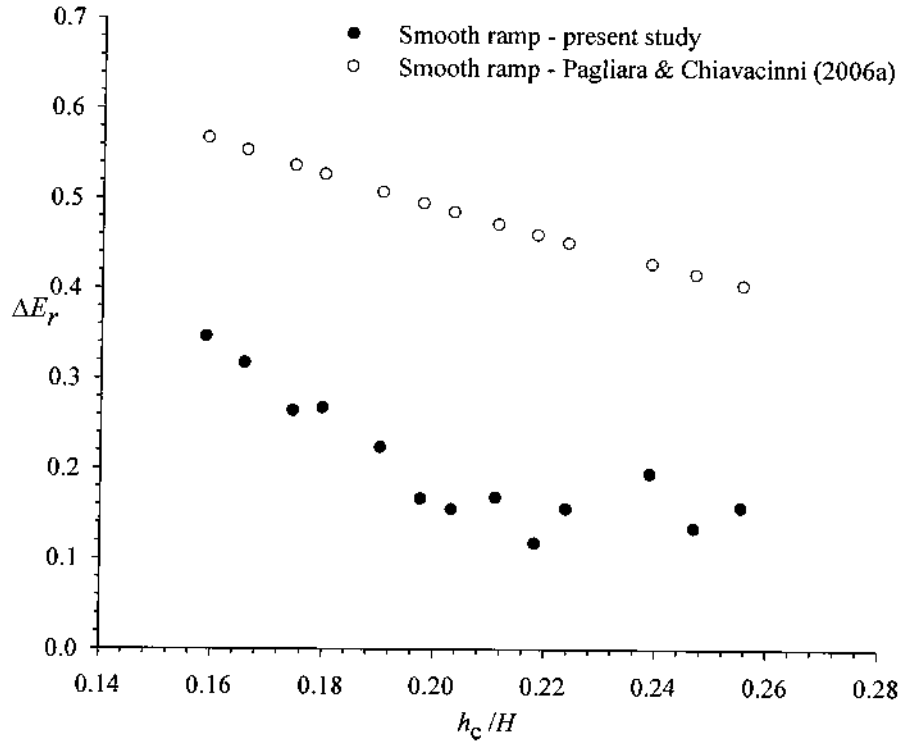

Fig. 4.3c Comparison of observed ΔE_r for smooth ramp (1V:9H) with that calculated using Pagliara and Chiavacinni's (2006a) equation

4.4 ENERGY DISSIPATION ON BLOCK RAMPS WITH BASE MATERIAL

The introduction of microroughness elements or base material on the smooth ramp significantly modifies the flow boundary. Then the "block ramp" structure takes shape. Uniformly sorted angular or crushed stone aggregate with size distribution in the range having d_{10} = 16 mm and d_{84} = 24 mm were chosen as the base material. The roughness factor h_c/d_{50} were in the range of 1.95 to 5.81 indicating intermediate roughness (IR) conditions on the tested block ramps as per the Pagliara and Chiavacinni (2006a) classification. The base material on ramp imparts bed roughness in the flow, which results in reduction in the flow velocity and increase in flow depth at the toe of the ramp. As the velocity of flow at the toe of the block ramp decreases, the energy loss for the base material is greater than the smooth ramp. The observed relative energy dissipation with respect to the flow parameter h_c/H for the tested slopes on block ramps is given in Fig. 4.4.

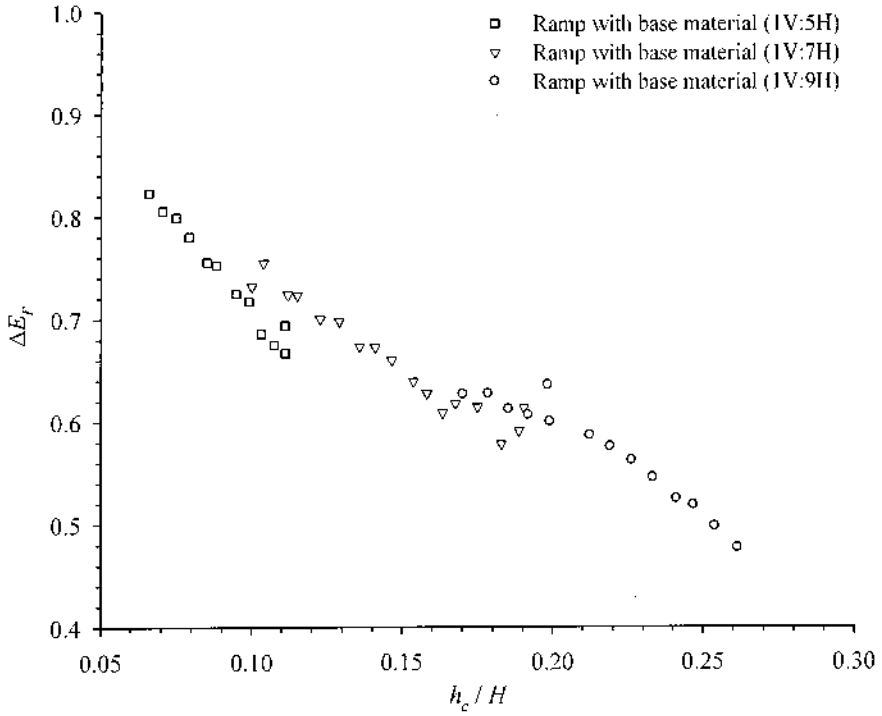

Fig. 4.4 Observed ΔE_r for block ramp with base material (angular) for the tested slopes

It can be seen from Fig. 4.4 that there are three distinct trends of relative energy dissipation with respect to the three tested slopes. Fig. 4.4 indicates that for similar h_c/H range (here in the observed data, when $h_c/H \approx 0.10$), that a less–sloping block ramp can dissipate more energy than a block ramp with steeper slope within the test conditions. It can also be deduced

that the optimal energy dissipation falls by 10% slope–wise. For instance, on the 1V:5H block ramp, ΔE_r is of the order of 67 to 82% ; on the 1V:7H block ramp, ΔE_r is of the order of 61 to 73%; and on the 1V:9H block ramp, ΔE_r is of the order of 48 to 63%. The range of the test results for relative energy dissipation on block ramps with base material are reported in Table 4.4.

Table 4.4 Summary of the test results on block ramps with base material

Parameter	1V:5H	1V:7H	1V:9H
roughness factor, h_c/d_{50}	1.95 – 3.74	2.86 – 5.44	3.78 – 5.81
velocity at toe section, v_t	1.95 – 2.81 m/s	1.72 – 2.85 m/s	1.56 – 2.90 m/s
h_c/H	0.07 – 0.11	0.10 – 0.19	0.17 – 0.26
ΔE_r	0.667 – 0.823	0.613 – 0.732	0.476 – 0.626

When compared with the smooth ramp for each respective slope (Fig. 4.5), there is a substantial increase in the energy dissipation within the tested range of flow discharge. The difference increases as the ramp slope decreases. At the steepest slope tested, there is a small difference in the ΔE_r values (for $0.08 \leq h_c/H \leq 0.11$) indicating that microroughness factor is marginally affecting the energy dissipation for the steep– sloped block ramp and smooth ramp. It can be also the reason that at steep slopes ($S \geq 0.20$), the microroughness factor has negligible effect due to the dominance of rapidly-varying and highly turbulent flow conditions. The test results were also compared with the ΔE_r values computed using the Pagliara and Chiavacinni (2006a) equation for block ramps with intermediate roughness condition (parameters: A = 0.25, B = –1.2 and C = –12.0). The plot (Fig. 4.6) showed that there is more than 5% difference of ΔE_r values computed using the Pagliara and Chiavacinni (2006a) relation with assignment of the appropriate parameters especially for the flatter slopes. The relation also depicted a continuation of the relative energy dissipation trend from 1V:5H to 1V:7H; though this continuity does not follow to the 1V:9H sloped block ramp. Thus the Pagliara and Chiavacinni (2006a) relation was found to overestimate the relative energy dissipation on block ramps as was the case with smooth ramp condition.

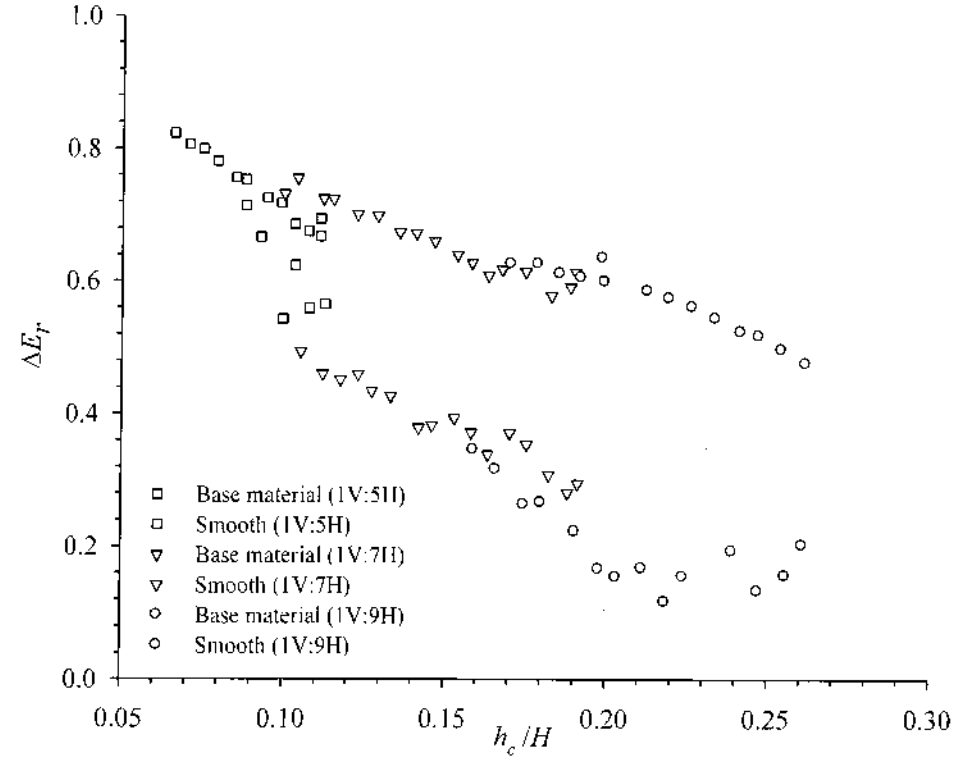

Fig. 4.5 Comparison of ΔE_r for block ramp with base material and smooth ramp

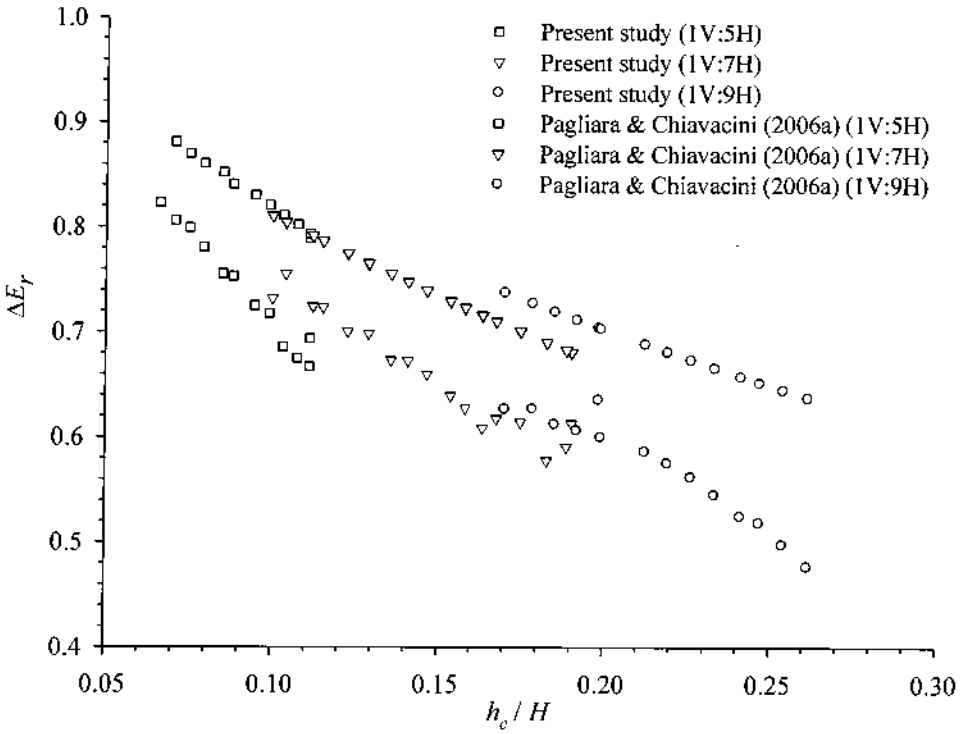

Fig. 4.6 Comparison of observed ΔE_r for block ramp with base material of the present study with that calculated using Pagliara and Chiavacinni's (2006a) equation

4.4.1 Comparison between Angular and Round Base Material

To examine the effect of sphericity of the base material aggregate, the energy dissipation on block ramps with river bed material of relatively uniform size (in the range d_{10} = 16 mm, d_{50} = 20 mm and d_{84} = 24 mm as for angular aggregate), representing "round" or spherical stone aggregate, were evaluated for two ramp slopes 1V:5H and 1V:7H. Figure 4.7 shows a comparative plot of the relative energy dissipation on block ramps with "angular" aggregate and "round" aggregate within the same size distribution. It can be observed that there is almost no variation in ΔE_r between the two types of base material in each respective slope, or in other words it can be concluded that there is no significant effect of the sphericity of the base material aggregate on the energy dissipation on block ramps in the tested conditions.

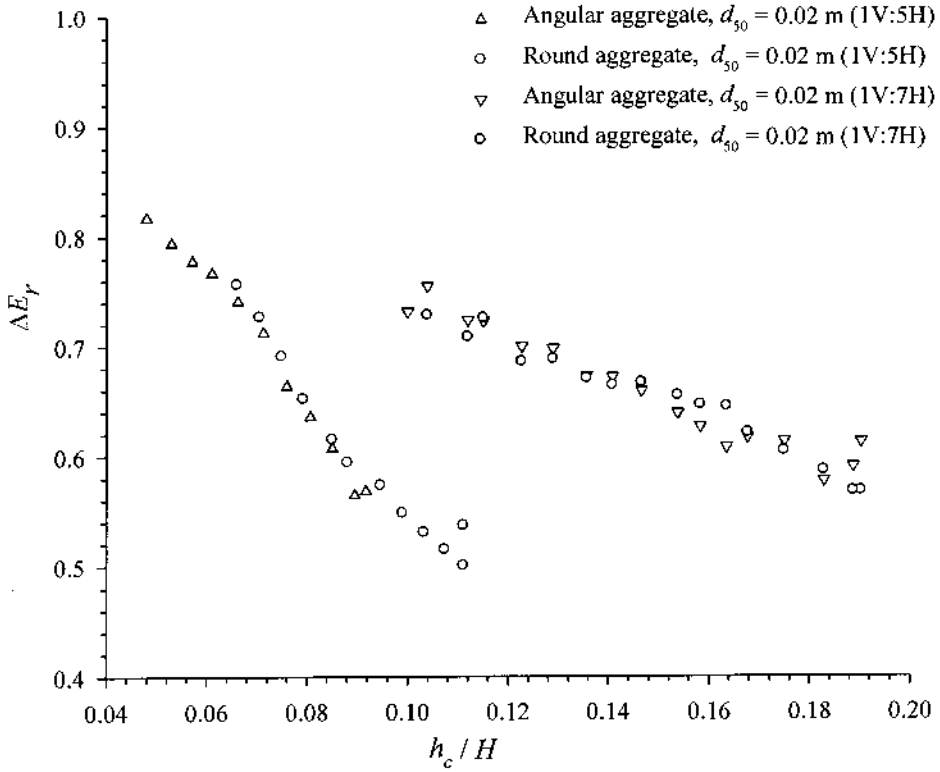

Fig. 4.7 Comparison of ΔE_r for angular and rounded stone aggregate as base material

4.5 ENERGY DISSIPATION ON BLOCK RAMPS WITH BOULDERS

When semi–hemispherical blocks are placed on the block ramp, then the element of macroroughness is imparted on the flow creating additional drag forces resulting in higher energy dissipation compared to the block ramps with base material. As this configuration represented protruding boulders in mountain streams, this element is generally referred to as

"boulder block ramps" and investigated exhaustively with the viability of its field application. Experimental data collected in the present study were analyzed to investigate the relative energy loss due to varied arrangements of the macroroughness boulders on the block ramp with base material. Staggered configuration of the boulders has been studied in detail as it was found to impart enhanced energy dissipation when compared with the rows or random arrangements (Ahmad et al., 2009). Further the random configuration of boulders has been pointed out to be systematically less dissipative than the rows configuration by Pagliara and Chiavacinni (2006b). Sayre and Albertson (1961) had proved that the staggered pattern of roughness elements (baffle blocks in their experiments) were extremely effective in maintaining large sediment concentrations in suspension without appreciable deposit on the channel bed. The spacing criteria for this structured arrangement of boulders have been examined as this factor seem to be a major governing factor for the energy dissipation on boulder block ramps.

4.5.1 Examination of the Dimensionless Flow Variables

As it is important to ascertain the dynamic similitude of the experimental test conditions, both the dimensionless Reynolds number (Re) and Froude number (Fr) were evaluated for all the test runs. The Reynolds number was found in the range 2.55×10^4 to 10.68×10^4 describing a highly turbulent flow regime on block ramps. There is a distinct association of Re for each tested slope with the flow parameter h_c/H as was also found by Patel (1998). In many configurations of the boulder block ramp, Re was found to have a good correlation with the relative energy dissipation ΔE_{rB} as shown in Fig. 4.8. This indicated that the contribution of viscous effects cannot be entirely neglected. Pagliara and Chiavacinni (2006a) had separately investigated to specially test the effect of Reynolds number and stated that for a variation of Re, the relative energy dissipation ΔE_r is almost constant and established that viscous effects are not an important parameter for energy dissipation on block ramps. The Froude number (Fr) was found to range from 1.64 to 3.98 signifying supercritical flow conditions in all the experimental runs. However, it indicated a low correlation with the relative energy dissipation ΔE_{rB} within the test conditions as depicted by the scatter of points in Figs. 4.9. Pagliara and Chiavacinni (2006b) had also found a low correlation ($R^2 < 0.2$) between Fr and the relative energy dissipation in their experimental test conditions.

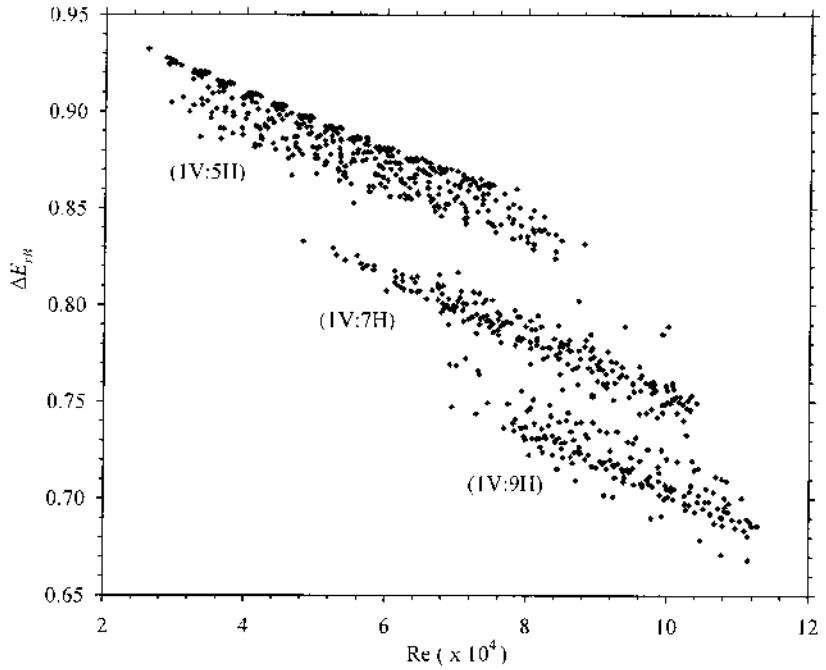

Fig. 4.8 Variation of the Reynolds number with ΔE_{rB} in the tested conditions

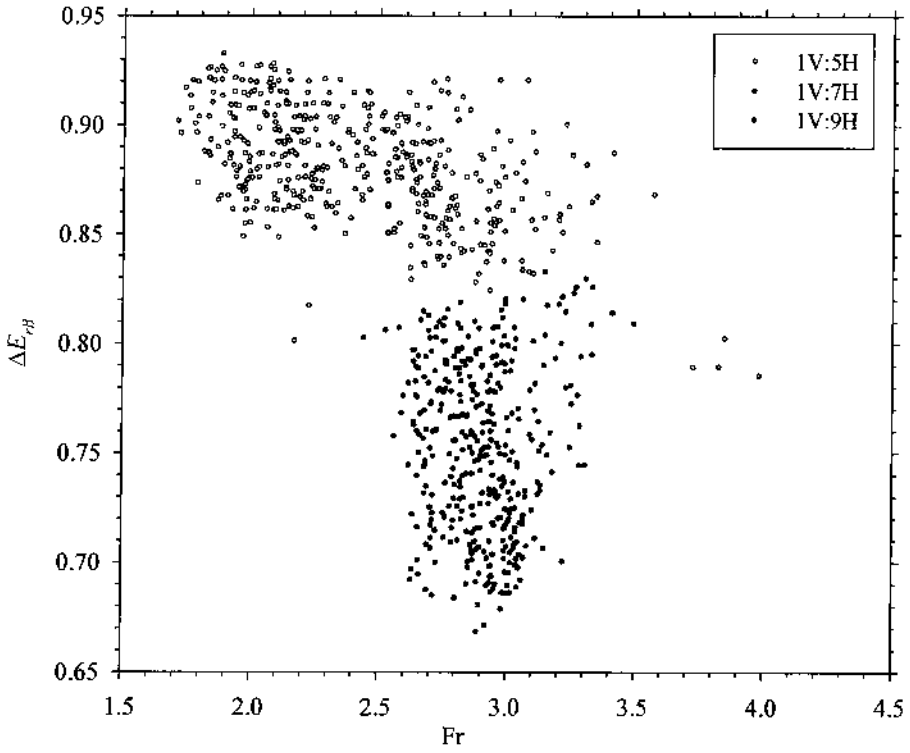

Fig. 4.9 Variation of the Froude number with ΔE_{rB} in the tested conditions

4.5.1 Boulders in Rows Configuration and Modification of Roughness Parameters (E, F)

To test the parity or similitude of experimental data collected for the tested conditions, four sets of observations were taken for boulders in the standard row arrangement in the present study. It may be recalled that for boulders in rows arrangement and rounded (smooth) boulders, Pagliara and Chiavacinni (2006b) have proposed E = 0.55 and F = 10.5, as the values of the two roughness parameters (functions of arrangement and roughness of boulders), to be used in Eq. (1.3) or (1.4). They have carried out their study within a flow discharge range of 0.0012 to 0.0104 m^3/s for three sizes of boulders D_B = 29 mm, 38 mm and 42 mm diameter respectively at the slope range $0.33 \leq S \leq 0.08$. Adopting the same functional relationship used by the authors, and combining the dataset with observed data of the present study for rows arrangement only which included boulder sizes D_B = 42 mm, 55 mm and 65 mm diameter, the modified values of the roughness and disposition parameters were obtained as E = 0.23 and F = 11.6 using observed data of the present study. The same is validated by using Eq. (1.4) to get the calculated ΔE_{rB} values using the modified values of E and F and plotted against the corresponding observed ΔE_{rB} values, within a ± 5% deviation from the line of perfect agreement as shown in Fig. 4.10. These modified values may be considered valid for larger boulders in rows configuration.

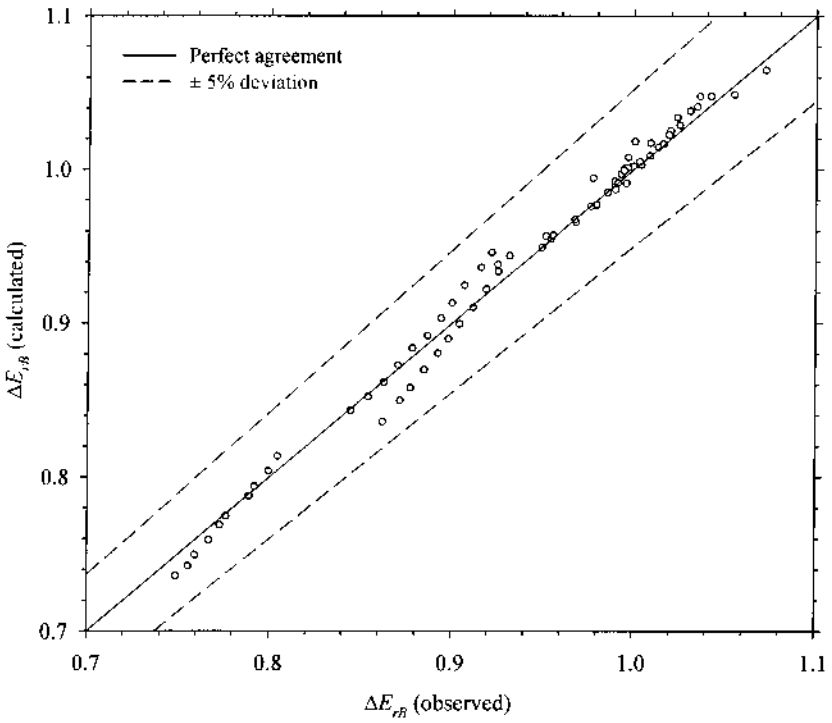

Fig. 4.10 Comparison between observed and calculated ΔE_{rB} for boulders in rows

4.5.3 Comparison between Rows and Staggered Configuration of Boulders

To test and compare the relative energy dissipation with row and staggered configuration of boulders on block ramps, boulders of the same size (D_B = 0.055m) were placed at the same longitudinal spacing (S_x/D_B = 4.0) on a 1V:5H ramp slope and tested under four experimental sets by varying the boulder concentration. Initially, 3 numbers of boulders were placed in each row for the row configuration (Γ = 0.093) and compared with alternate 3 and 2 numbers for the staggered configuration (Γ = 0.078). Likewise, 4 numbers of boulders were placed in each row for the row configuration (Γ = 0.124) and compared with alternate 4 and 3 numbers for the staggered configuration (Γ = 0.109). The comparative plot (Fig. 4.11) showed that the staggered configuration resulted in higher energy dissipation even at lower value of Γ. Though the row configuration with lesser boulder concentration falls asymptotically with those points for the staggered configuration, it may be due to the prominence of an isolated tumbling flow regime where boulder interaction with the flow is less. This can also be attributed due to the high form drag, wake vortices, localized jumps, and jet flow between the boulders as compared to the row and random configuration. Thus, it can be derived that a staggered configuration of boulders yields higher dissipation of energy as compared with rows arrangement, which are in parity with the conclusion of Ahmad et al. (2009). This is one of the reasons why the staggered configuration of boulders on block ramps is emphasized and delved in the present study.

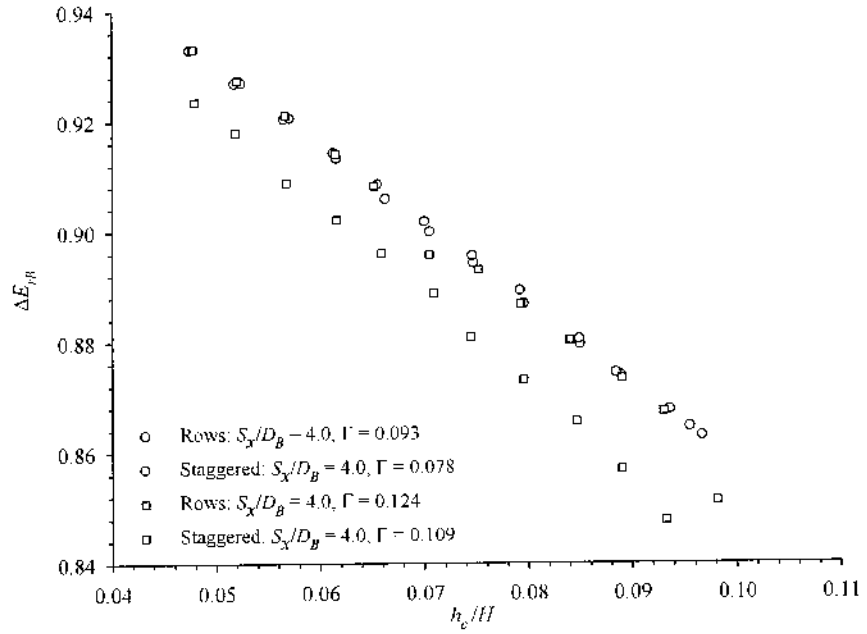

Fig. 4.11 Comparison between ΔE_{rB} for rows and staggered configuration of boulders for D_B = 0.055m and S= 1V:5H

4.5.4 Variation of Relative Energy Dissipation with Ramp Slope

As one of the key functional variables affecting the energy dissipation process on block ramps, the slope parameter is examined in detail. Pagliara and Chiavacinni (2006a) found that on block ramps, as the slope increases the energy dissipation decreases, and the variation tend to diminish with the decrease of the slope. However the same authors (2006b) pointed out that the slope did not seem to influence the increase in ΔE_{rB} in the case of boulder block ramps (or reinforced block ramps, as the authors termed it). This anomaly is required to be investigated with a meticulous assay of the other respective hydraulic variables in terms of the slope. Though the flow parameter h_c/H implicitly envelopes the slope factor, a subjective analysis is required to understand the dependence and interdependence of each variable related to the energy dissipation on boulder block ramps. A combined examination could not lucidly reveal the characteristics of the slope factor on ΔE_{rB}.

To start with, a variation of ΔE_{rB} with slope (S) for a representative boulder concentration (Γ= 0.23) was examined as shown by the Fig. 4.12a. This boulder concentration was chosen as it comprised of the whole range of boulder sizes under all the three slopes tested in staggered configuration. The plot indicated that energy dissipation increases with at steeper slope in the tested flow conditions. This variation is however not well defined when the same dataset is plotted with $\Delta E_{rB}/\Delta E_r$ which is the relative energy dissipation due to the effect of boulders only as shown in Fig. 4.12b. There is a random variation of the points (marked by the boulder sizes) along the asymptote line of each slope. Hence there is an interdependence of the macroroughness boulder size and distribution with $\Delta E_{rB}/\Delta E_r$ which is not fully governed by the slope parameter. An individual examination for each tested slope of the variables related to the energy dissipation function on boulder block ramps was conducted.

The variation of relative energy dissipation with respect to the main functional parameters as derived in Eq. (4.4), are analyzed for each tested slope. It may be noted that the differential and integral effects of boulder size, concentration and spatial distribution were hereby examined on the domain of ΔE_{rB} with respect to the flow parameter h_c/H.

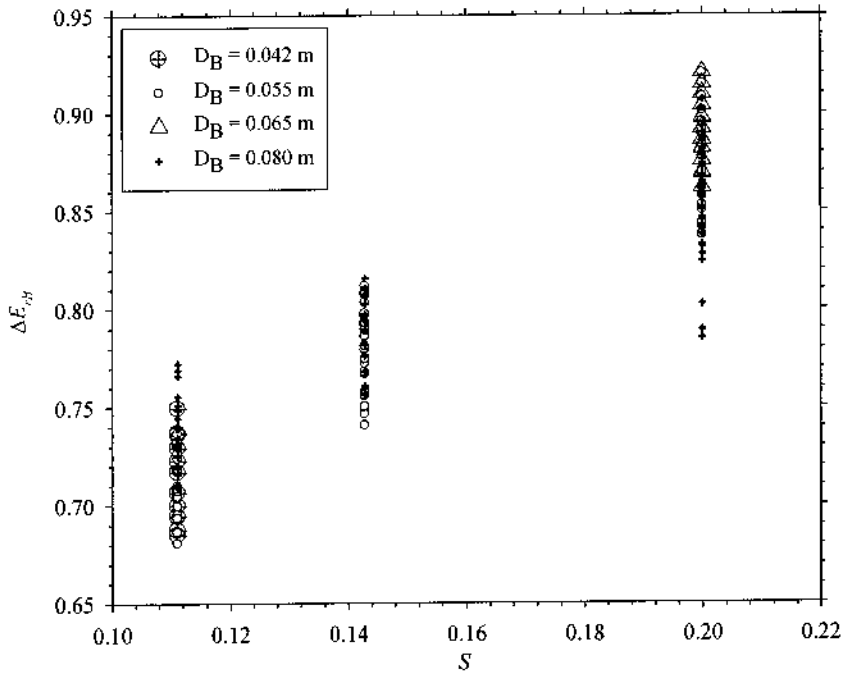

Fig. 4.12a Variation of ΔE_{rB} with S for Γ= 0.23 for different boulder sizes

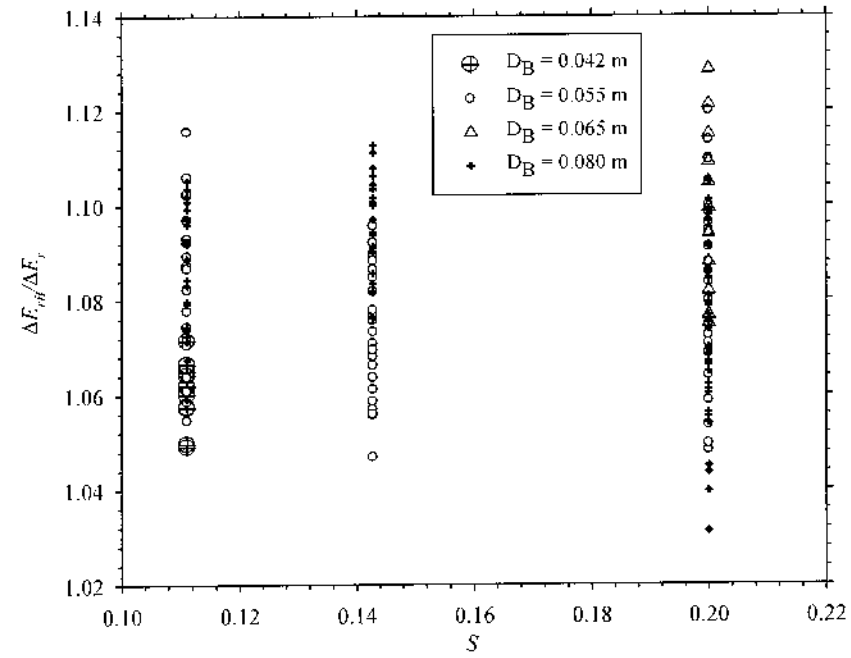

Fig. 4.12b Variation of $\Delta E_{rB}/\Delta E_r$ with S for Γ= 0.23 for different boulder sizes

4.5.4.1 Ramp Slope 1V:5H

Boulders of 0.042 m, 0.055 m, 0.065 m, 0.080 m and 0.10 m diameter were investigated under varied spacing in staggered configuration over this steepest ramp slope tested. To study the relative energy dissipation for each respective boulder under varied concentrations and spacing, the observed ΔE_{rB} values are plotted with respect to the flow parameter h_c/H as given in Figs. 4.13a-e. The plots were presented in respect of the boulder longitudinal spacing and distribution along with the boulder concentration factor Γ and reduction coefficient ψ. The reduction coefficient ψ (< 1.0) is a function of the both the number and planimetric arrangement of macroroughness boulders and depends on the effective bed arrangement (Canovaro and Solari, 2007). An examination of the plots indicated that closer spacing and certain non-uniform configurations exhibit higher dissipation of energy. Also bigger –sized boulders tend to produce higher ΔE_{rB}, though it may be noted that for some configurations, boulder sizes of 0.080 m diameter produced slightly lower energy dissipation as compared to that produced by the smaller-sized boulders of 0.055 or 0.065 m diameter. With the 0.10 m size boulders there is negligible effect of boulder configuration i.e. spacing and distribution, on the energy dissipation. That is why almost all the ΔE_{rB} point converges to almost the same location for the respective h_c/H. It can be also observed that the magnitude of scatter of points along the vertical profile (Y–axis) also reduces as the boulder size increases, indicating that the spacing factor of boulders does not play a significant role when the boulder dimensions are large relative to the flow depth. The coefficient ψ inversely vary with Γ, and indicated that lesser values imparted higher energy loss over the block ramp with boulders of 0.042 m diameter and a reverse case with the boulders of 0.065 and 0.080 m diameter.

From the observations made, there is no clear perception of the effect of boulder concentration on the relative energy dissipation for the tested slope ($S = 0.20$). The spacing of boulders, its distribution and size also seem to collectively influence the relative energy dissipation factor. Though it could be noted that the small spacing as $S_x/D_B = 1.0$, exhibited a steady energy dissipation profile among the tested configurations which indicate that closer boulder spacing is accountable for achieving stable energy dissipation along the section of the block ramp for this tested slope. For the largest boulder size tested ($D_B = 0.10$ m), it may be expressed in terms of the ratio of channel width to macroroughness size that for $W/D_B \leq 3.0$ (0.30 m/0.10 m = 3.0), any boulder size exceeding this ratio has no significant impact with respect to its spacing or distribution in describing the relative energy dissipation at this slope.

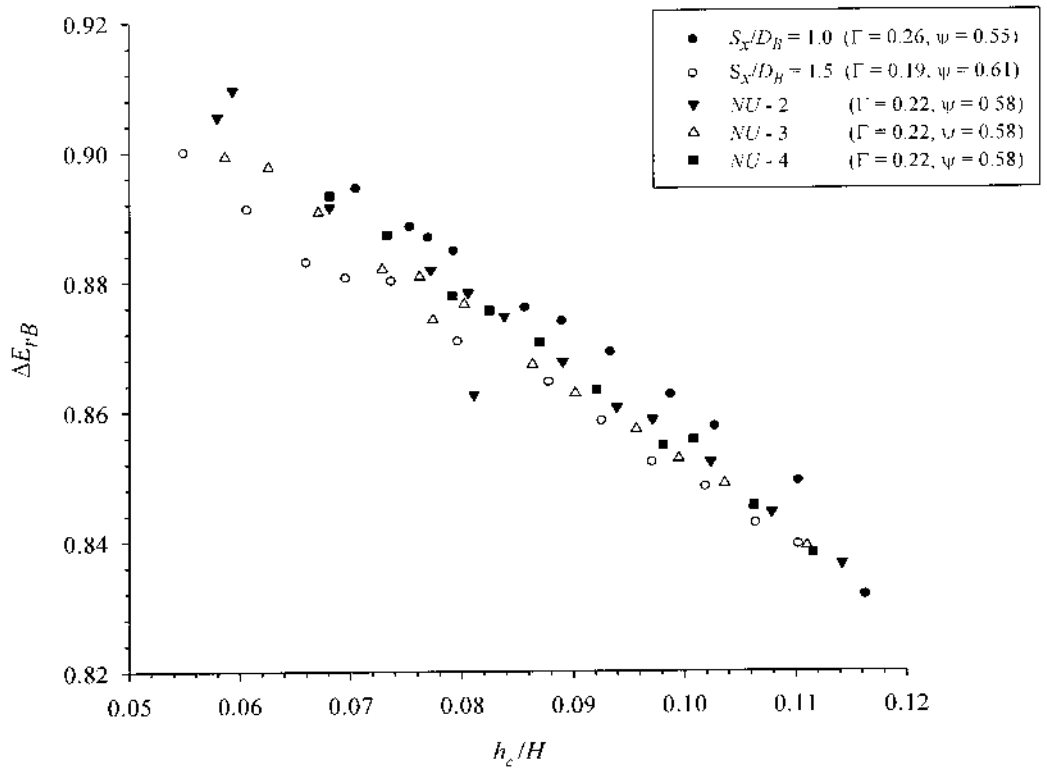

Fig. 4.13a Variation of ΔE_{rB} for $D_B = 0.042$ m in various staggered configurations (1V:5H)

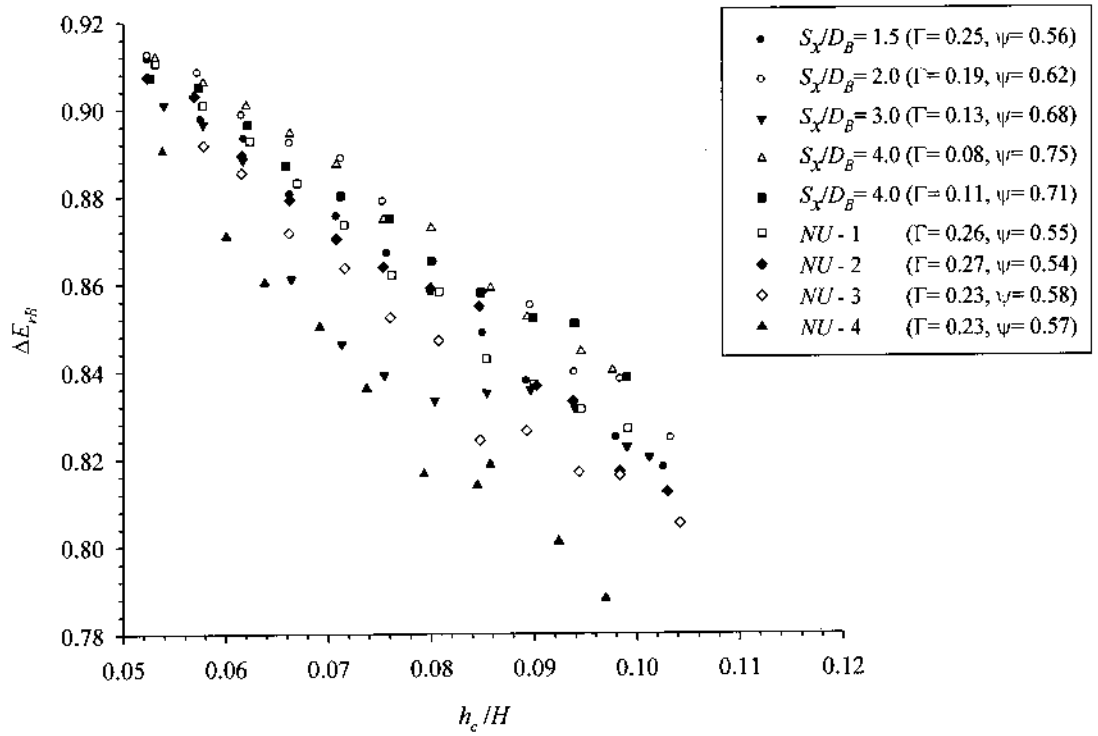

Fig. 4.13b Variation of ΔE_{rB} for $D_B = 0.055$ m in various staggered configurations (1V:5H)

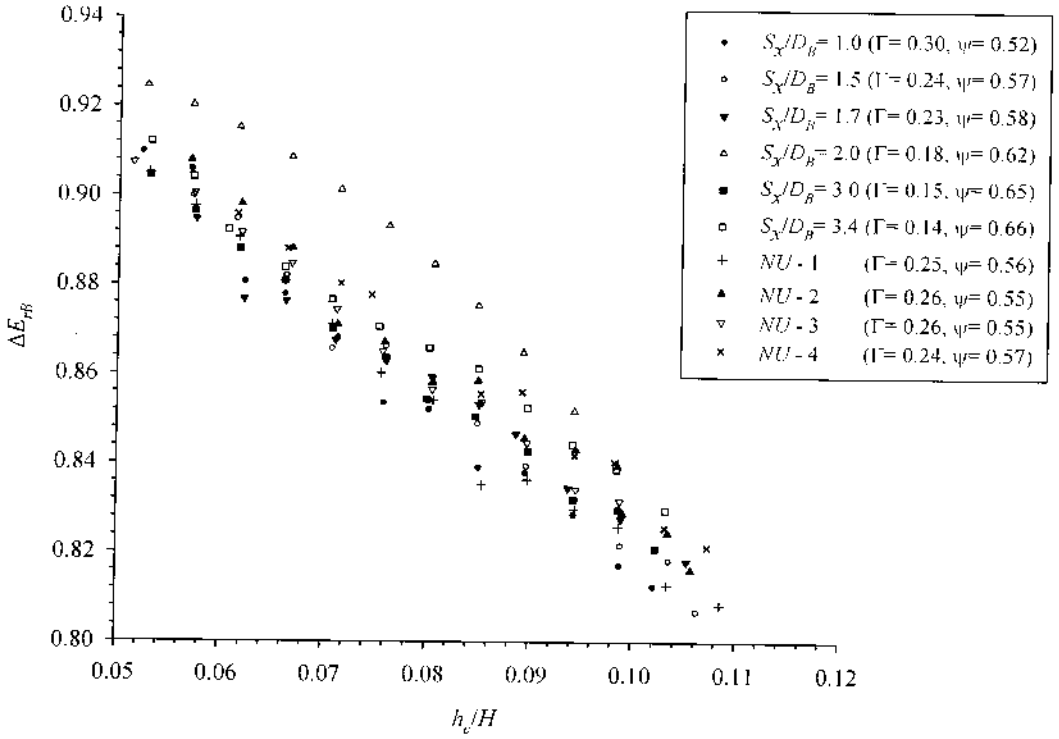

Fig. 4.13c Variation of ΔE_{rB} for $D_B = 0.065$ m in various staggered configurations (1V:5H)

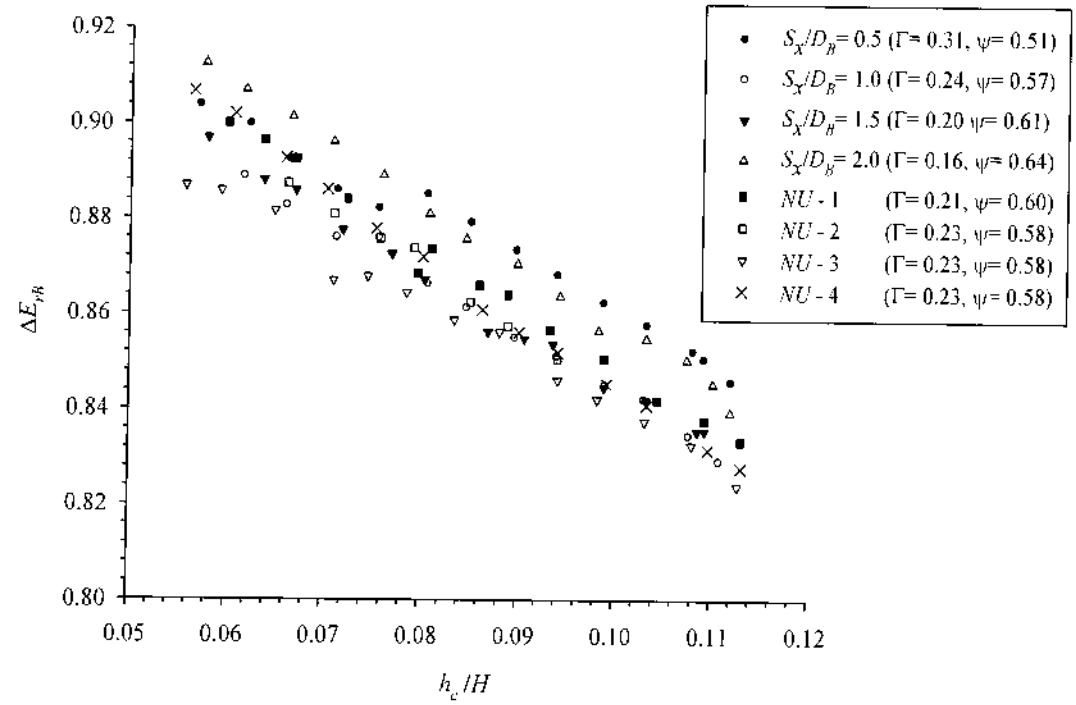

Fig. 4.13d Variation of ΔE_{rB} for $D_B = 0.080$ m in various staggered configurations (1V:5H)

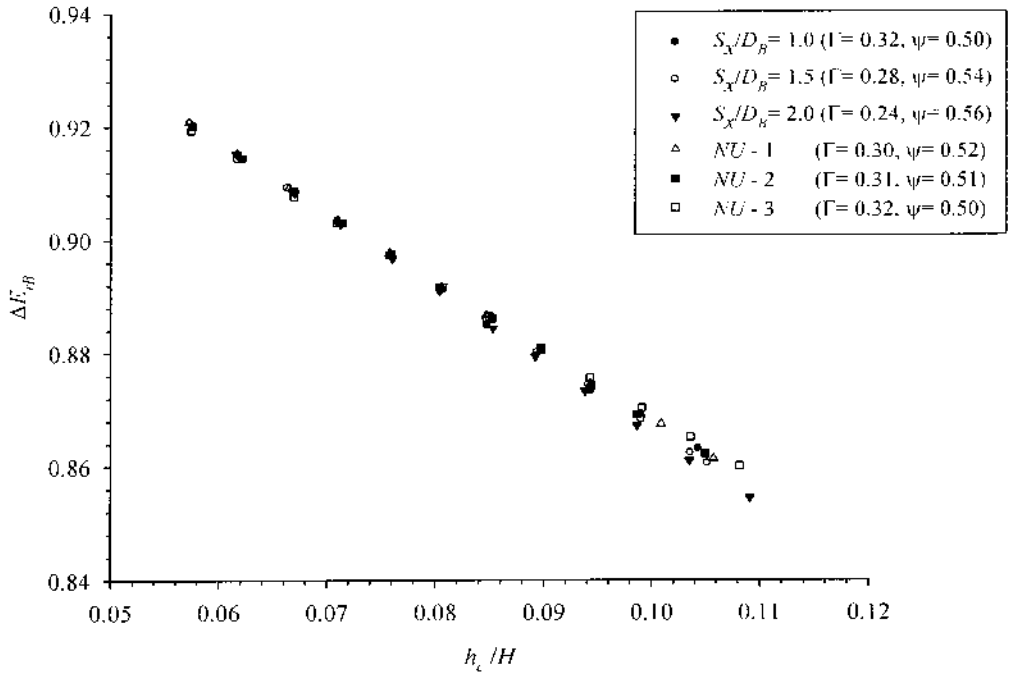

Fig. 4.13e Variation of ΔE_{rB} for $D_B = 0.10$ m in various staggered configurations (1V:5H)

To further test and examine closely the integral effect of flow parameter h_c/H and Γ (function of boulder size and spacing) on the relative energy dissipation function due to the presence of boulders, isolines of $\Delta E_{rB}/\Delta E_r$ are simulated using data analysis tools (MATLAB environment) using the dataset for each boulder size observed on 1V:5H slope ramp. The above plots showed the variations of ΔE_{rB} in a 2–dimensional array where the relative variation of Γ could not be compositely depicted. The derived plot revealed the multi–dimensional effect on the energy dissipation factor as presented in Figs. 4.14, as illustration. For clarity in distinguishing the isolines, the plots are presented in colour intensity scales. The general trend showed that $\Delta E_{rB}/\Delta E_r$ increases with relative increase of both Γ and h_c/H. However, it drops after a certain threshold boulder concentration (Γ = 0.22 to 0.25). The largest tested sized boulder ($D_B = 0.10$ m) did not show any relative effect of Γ.

The notable derivation from the above analysis is the threshold boulder concentration, beyond which the $\Delta E_{rB}/\Delta E_r$ function tend to decay or remain unaffected even after increase in Γ. The possible reason is that, beyond this boulder concentrations, the boulders are packed closely to virtually replicate a general block ramp roughness condition with lesser gaps to permit formation of large scale vortices to separate and intermingle with the bulk flow to cause significant drag forces. The close packing of the macroroughnes boulders formed a more or less smooth pseudo–wall composed of the boulder crests and the enclosed pockets of

dead fluid (Morris, 1959). Localized jumps may not take place, which are another major factor responsible for the energy loss function. The boulder size of 0.055 m diameter showed a progressive relative energy dissipation compared to the other sizes in the tested range for this slope. There are few indications that the flow parameter has peculiar effect on the $\Delta E_{rB}/\Delta E_r$ function as showed by syncline and anticline forms of the isolines. Also it can be concluded that for the boulders D_B = 0.10 m, the effect of boulder concentration is negligible in ascribing the relative energy dissipation within the tested range. This may be due to the large relative dimensional ratio (W/D_B = 0.30/0.10 = 3) in the experimental test conditions, creating a condition where flow stagnation may occur in the pockets between the boulders resulting in only a partial tumbling or skimming flow. So this boulder size has thereby been neglected in further experimental tests.

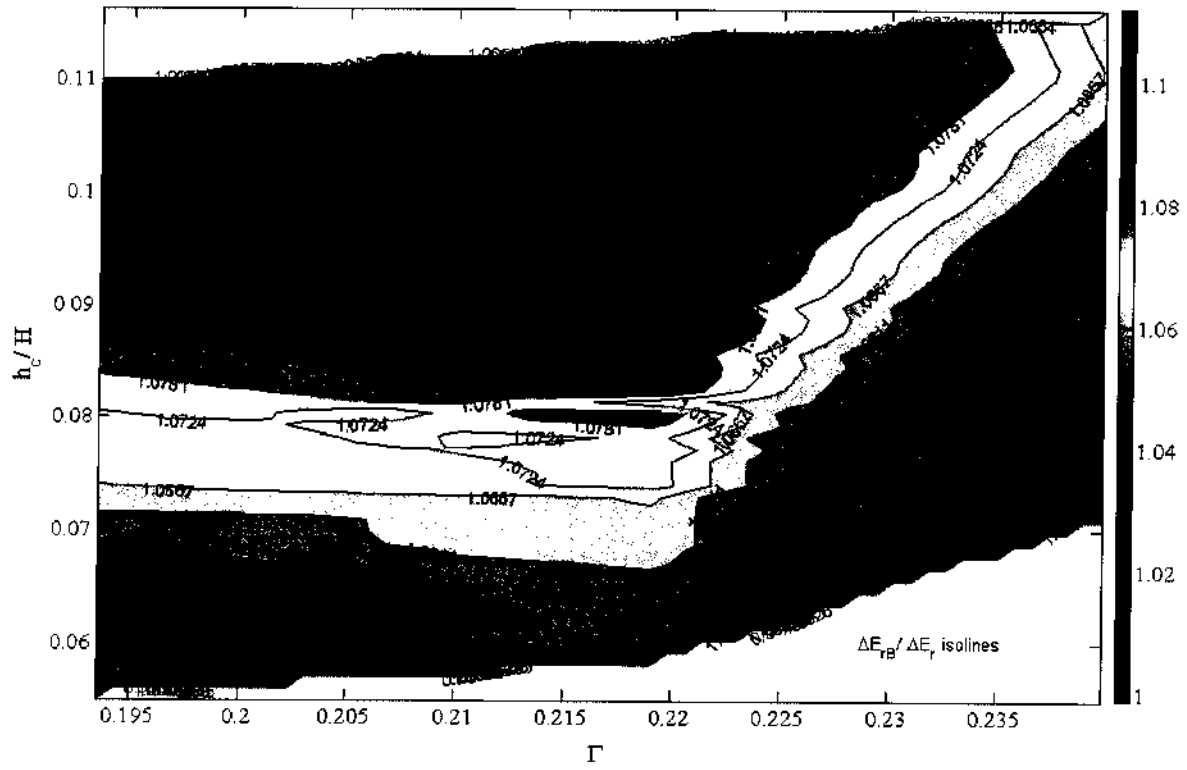

Fig. 4.14 Isolines of $\Delta E_{rB}/\Delta E_r$ w.r.t. boulder concentration and h_c/H for D_B = 0.042m (1V:5H)

On an average, the relative energy dissipation observed was between 73 – 92 % for the range $0.05 < h_c/H < 0.11$, and it was found that ΔE_{rB} decreases appreciably as the flow parameter h_c/H increases. The relative energy dissipation on block ramps with boulders of different sizes for 1V:5H slope are reported in Table 4.5.

Table 4.5 Summary of the test results on block ramps with boulders for 1V:5H slope

Parameter	D_B = 0.042 m	0.055 m	0.065 m	0.080 m	0.10 m
Γ	0.19 – 0.24	0.08 – 0.27	0.14 – 0.30	0.16 – 0.31	0.24 – 0.32
h_c/H	0.055 – 0.116	0.048 – 0.112	0.051 – 0.109	0.056 – 0.125	0.057 – 0.109
ΔE_{rB}	0.832 – 0.910	0.726 – 0.923	0.858 – 0.927	0.802 – 0.913	0.855 – 0.921

4.5.4.2 Ramp Slope 1V:7H

On this ramp slope, boulders of 0.042 m, 0.055 m, 0.065 m, and 0.080 m diameter were investigated under various staggered configuration. Higher discharge is achieved for the test conditions on this milder slope as compared with the 1V:5H slope, and the flow showed a smoother profile though it decelerates with increasing depth at the downstream toe.

To study the relative energy dissipation trend for each respective boulder under varied concentrations and spacing at the slope 1V:7H, the observed ΔE_{rB} values are plotted against the flow parameter h_c/H as shown in Figs. 4.15a-d for the four boulder sizes. An examination of the plots indicated that closer spacing do not exactly yield the maximum energy dissipation. There is an intermingling trend that intermediate L–spacing for the smaller-sized boulders ($D_B \leq 0.055$ m) exhibited slightly higher dissipation of energy than the closer spacing. It may be the reason that at this slope, the flow depth relative to boulder size (h/D_B) is high that only a larger spacing of the boulders could induce macroroughness effects and increment wake–interference and skimming flow conditions over the ramp. As the boulder size increases, the relative flow depth decreases, and the degree of scatter of points along the vertical profile (Y–axis) increases, with the indication that the spacing factor of boulders play a dividend role when the macroroughness size was large relative to the flow depth. The non-uniform configuration exhibited higher dissipation of energy than the uniform configuration especially in the case with 0.080 m diameter boulders. For the smaller–sized boulders tested (D_B = 0.042 m), there was converging trend that any variation in the boulder concentration or distribution is not likely to affect the scale of ΔE_{rB} at this slope. It may be expressed in terms of the ratio of channel width to macroroughness size that for $W/D_B \geq 7.0$ (0.30 m/0.042 m ≈ 7.0), there is no significant effect of boulder spacing or distribution. On the whole, with reduction in slope from 1V:5H, the increase in submergence denoted a substantial drop in relative energy dissipation.

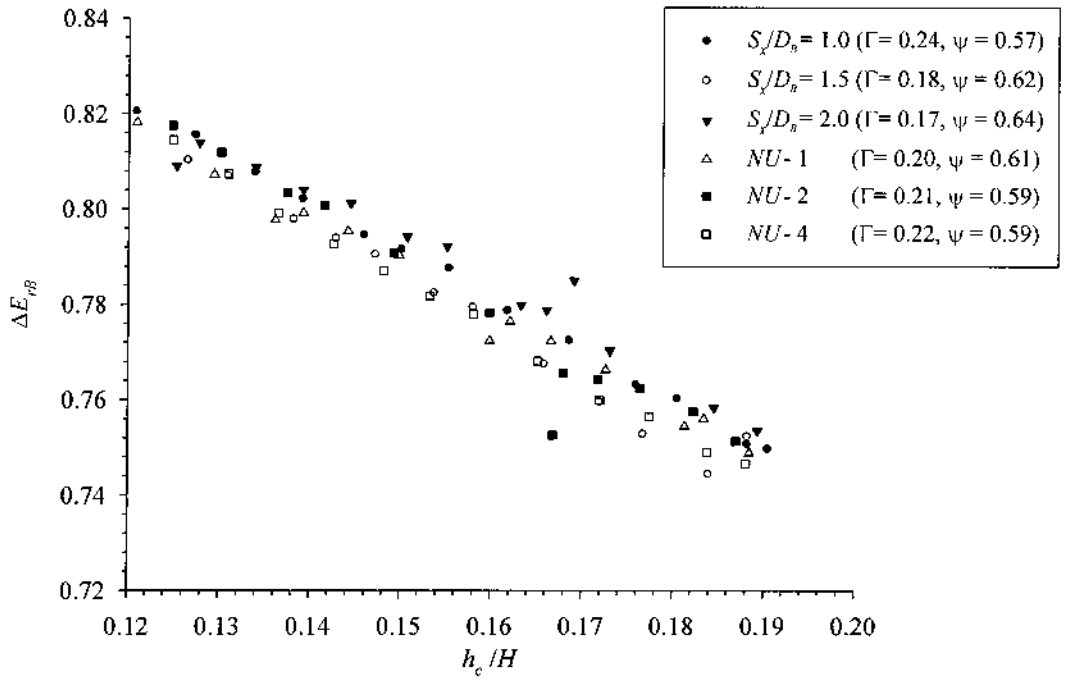

Fig. 4.15a Variation of ΔE_{rB} for D_B = 0.042m in various staggered configurations (1V:7H)

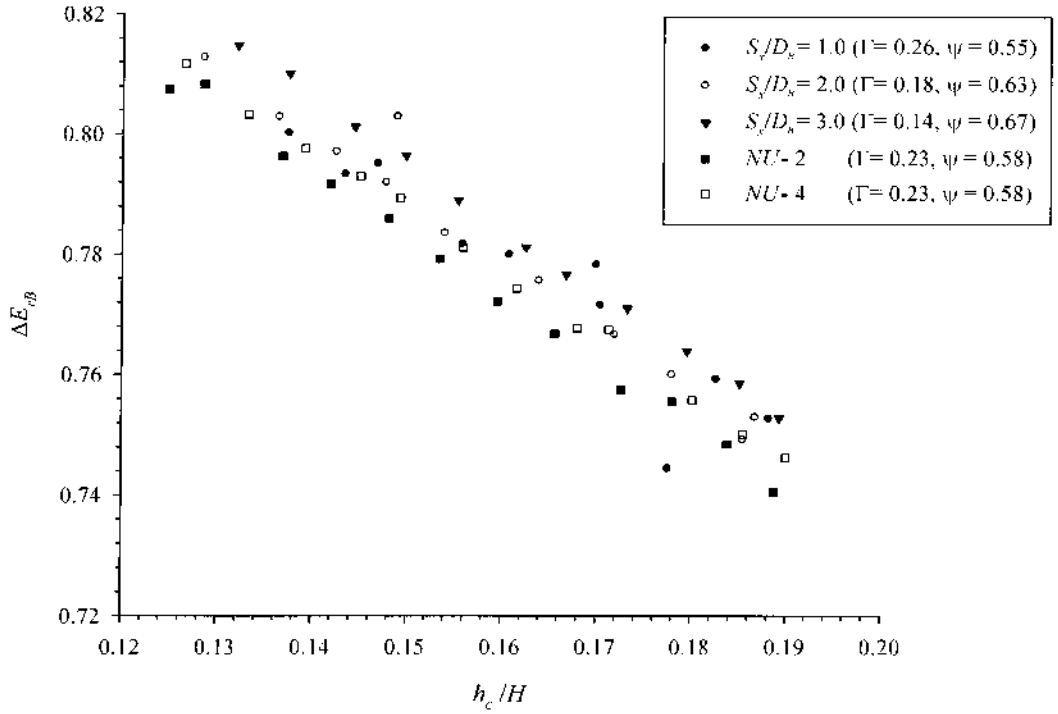

Fig. 4.15b Variation of ΔE_{rB} for D_B = 0.055m in various staggered configurations (1V:7H)

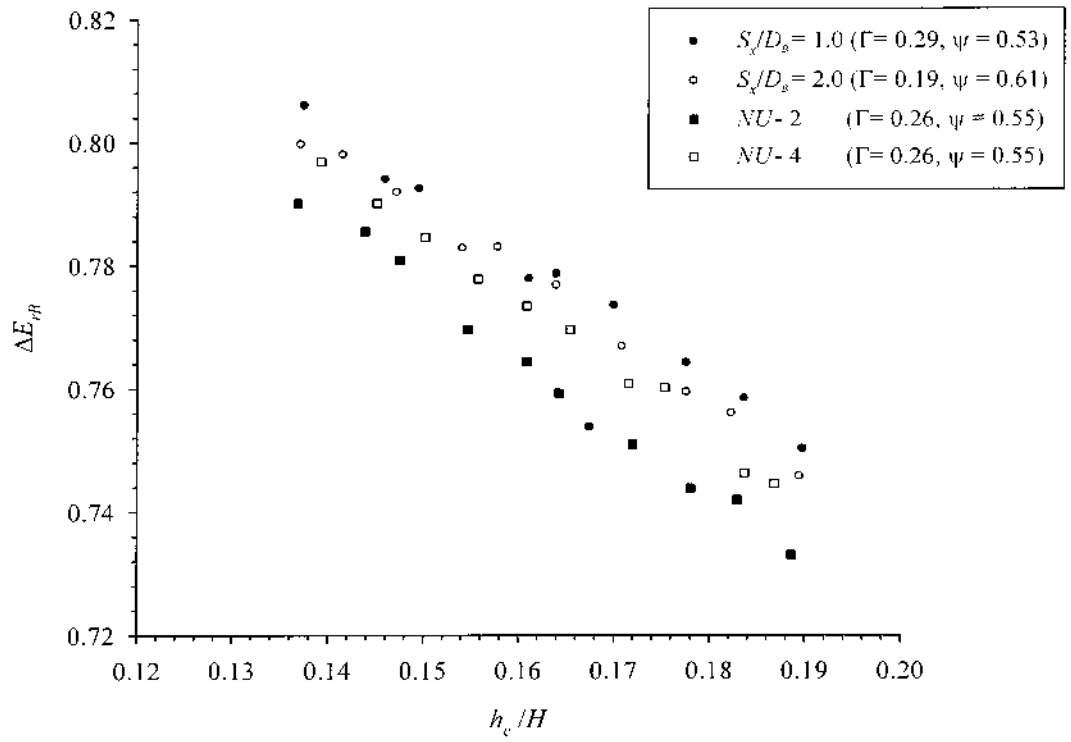

Fig. 4.15c Variation of ΔE_{rB} for D_B= 0.065m in various staggered configurations (1V:7H)

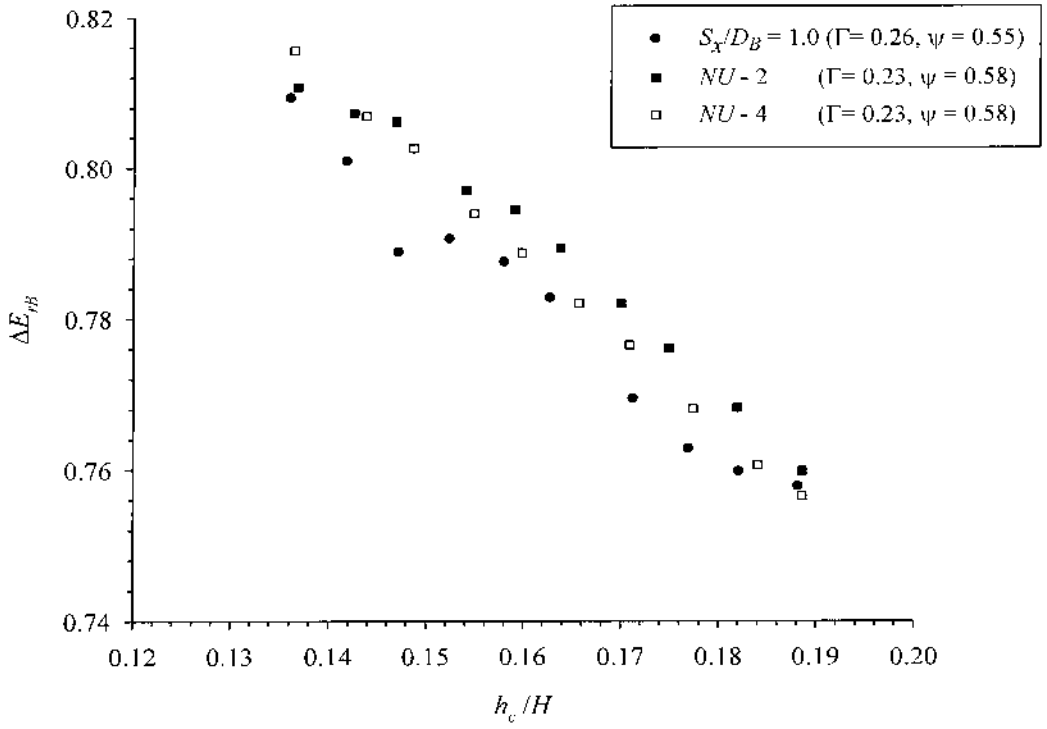

Fig. 4.15d Variation of ΔE_{rB} for D_B= 0.080m in various staggered configurations (1V:7H)

Similarly as carried out for the 1V:5H slope ramp, to examine the integral effects of flow parameter h_c/H and Γ on the relative energy dissipation function due to the presence of boulders, isolines of $\Delta E_{rB}/\Delta E_r$ are simulated for flow conditions for Q = 0.014 to 0.034 m^3/s discharges using the observed dataset for 1V:7H. The derived plot for D_B = 0.042 m is shown in Fig. 4.16, as illustration. The multi–dimensional effect of Γ and h_c/H on the energy dissipation factor showed distinctive trends with respect to each boulder size tested. The ratio $\Delta E_{rB}/\Delta E_r$ increases with increase of h_c/H and there is marginal effect of Γ. However, the trend gets distributed or congregated after the range of threshold boulder concentration (Γ = 0.22 to 0.25) as was observed in the 1V:5H slope boulder block ramp. As the energy dissipation trend in the 1V:7H slope block ramp reflect that there is not much effect of the boulder concentration factor as shown by the almost parallel isolines of $\Delta E_{rB}/\Delta E_r$ with Γ.

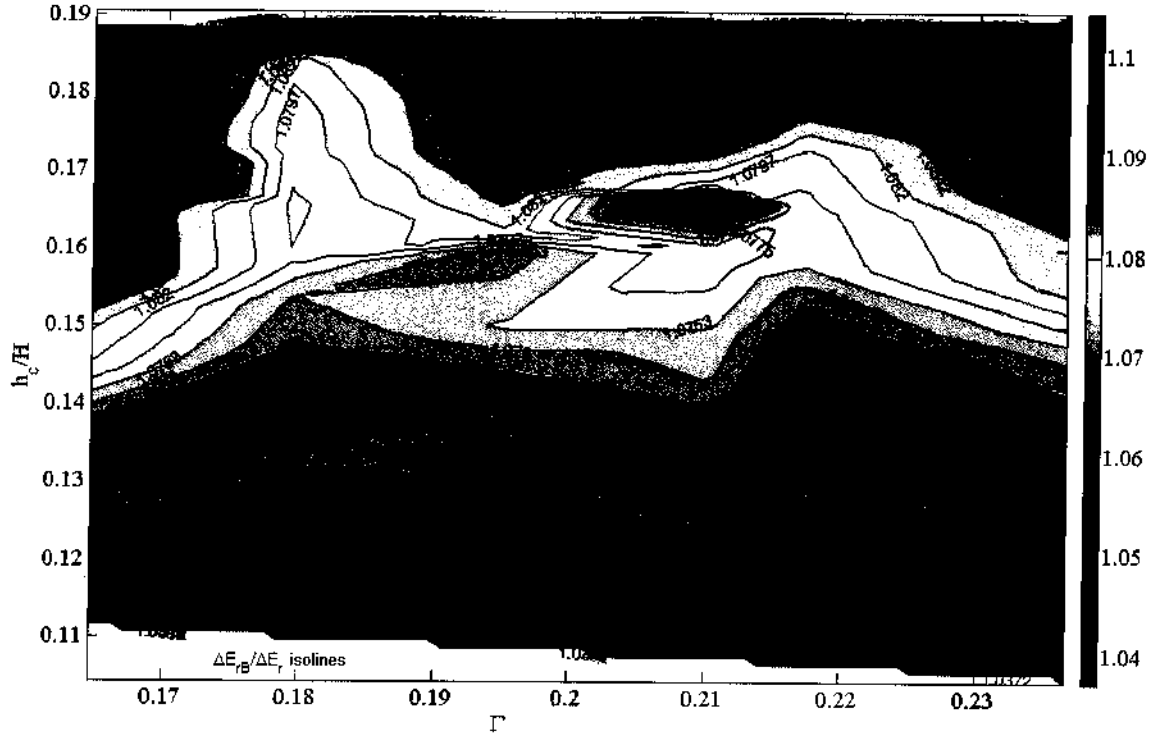

Fig. 4.16 Isolines of $\Delta E_{rB}/\Delta E_r$ w.r.t. boulder concentration and h_c/H for D_B = 0.042 m (1V:7H)

From the assay of test observations, thereby it can be deduced that there is no generalized indication that a particular boulder spacing or distribution yielded the optimum energy dissipation for the boulder block ramp on 1V:7H slope in common to all the boulder sizes, though there are indications that uniform spacing distribution produced higher ΔE_{rB} for boulder with $D_B \leq 0.065$ m. On the whole, the characterization of ΔE_{rB} can be said to

interdependent with the boulder size and distribution for the respective flow parameter. The average relative energy dissipation ΔE_{rB} was observed in the order of 74 to 83 % for $0.14 \leq h_c/H \leq 0.29$. The relative energy dissipation on block ramps with boulders of different sizes at 1V:7H slope are reported in Table 4.6.

Table 4.6 Summary of the test results on block ramps with boulders for 1V:7H slope

Parameter	D_B = 0.042 m	0.055 m	0.065 m	0.080 m
Γ	0.16 – 0.24	0.14 – 0.25	0.19 – 0.29	0.23 – 0.26
h_c/H	0.111 – 0.190	0.125 – 0.190	0.137 – 0.190	0.136 – 0.189
ΔE_{rB}	0.744 – 0.833	0.744 – 0.815	0.742 – 0.806	0.757 – 0.816

4.5.4.3 Ramp Slope 1V:9H

On this flattest ramp slope tested, boulders of 0.042 m, 0.055 m, 0.065 m, and 0.080 m diameter were investigated under various staggered configuration. Higher discharge at Q = 0.021 to 0.037 m^3/s prevailed for the test conditions as compared with the 1V:7H slope, and there was an appreciable flow depth.

For detailed examination of the relative energy dissipation trend for each respective boulder under varied concentrations and spacing at the slope 1V:9H, the observed ΔE_{rB} values are plotted against h_c/H as shown in Figs. 4.17a-d for each of the four boulder sizes. An examination of the plots indicated that close spacing ($S_x/D_B \leq 1.0$) yielded slightly lower energy dissipation as the boulder size increases. For the smallest boulder size tested (D_B = 0.042 m), all the points lie asymptotically indicating that there is no significant impact of spacing or distribution at larger flow depths, as was similarly found at 1V:7H slope. Dimensionally, it may be expressed in terms of the ratio of channel width to macroroughness size that, for $W/D_B \geq 7$ (0.30 m/0.042 m ≈ 7.0), the spacing factor is diminutive in describing the relative energy loss at this slope.

As the boulder size increases, the degree of variation of ΔE_{rB} along the vertical profile (Y–axis) segregates for each spacing and configuration, with the flow parameter. The spacing factor of boulders can be said to have a distributed function when the relative flow depth (h/D_B) is significant. Another interesting observation was that, the non–uniform (NU–4) configuration exhibited higher dissipation of energy than the other tested configurations in the case of bigger–sized boulders (for D_B = 0.065 m and 0.080 m) for this slope. It could be noted that NU–4 configuration is a recurring pattern of the boulder spacing in the order S_x

$/D_B$ = 1.0 and 1.5 all along the ramp longitudinal section, and this array may have generated cyclic interferences with the wake formation and flow boundary. It can also be observed that there is almost a similar percentage range (on an average 7%) of energy dissipation as flow traverses downstream of the ramp with the prominence of a quasi–skimming flow regime. Further it can be marked that, there are substantial drops of the NU–2 configuration with the 0.065 m size boulders and S_x/D_B = 1.0 configuration with the 0.080 m size boulders from the general ΔE_{rB} variation line for each case. This can be an indication that boulder distribution is a critical parameter for the ΔE_{rB} function across boulder block ramps, when relatively large boulders are used at flatter slopes. Dimensionally speaking, for $W/D_B \leq 4.5$ (0.30 m/0.065 m ≈ 4.5), the boulder distribution factor is explicitly related to the ΔE_{rB} function for the 1V:9H slope.

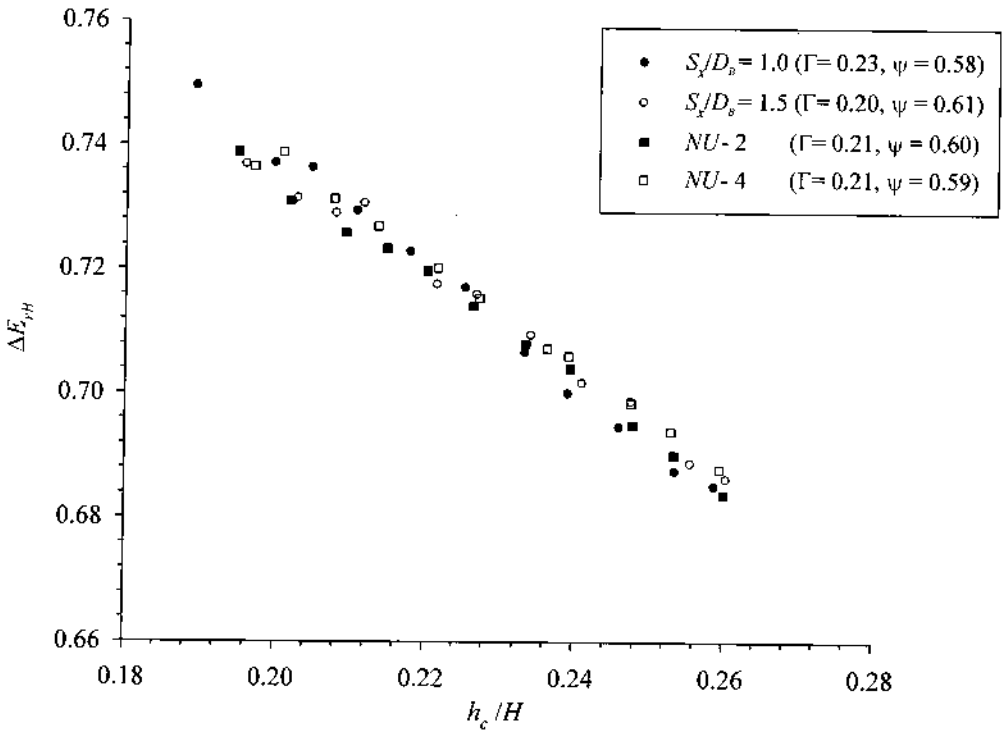

Fig. 4.17a Variation of ΔE_{rB} for D_B = 0.042 m in various staggered configurations (1V:9H)

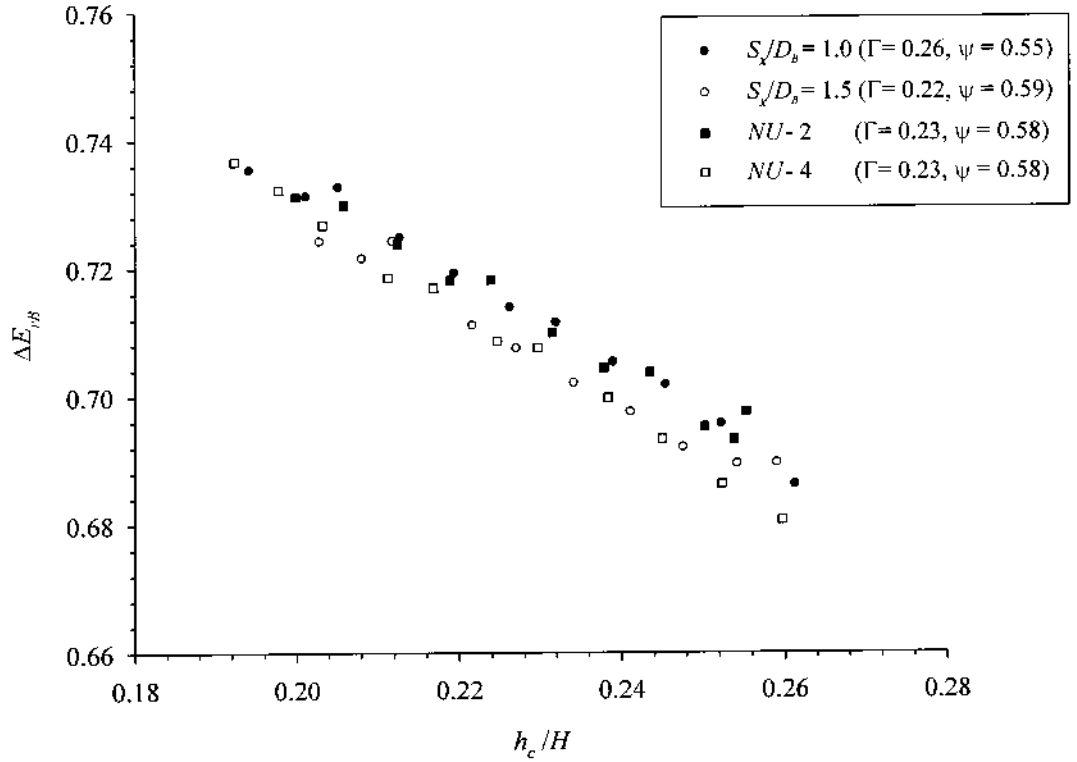

Fig. 4.17b Variation of ΔE_{rB} for D_B = 0.055 m in various staggered configurations (1V:9H)

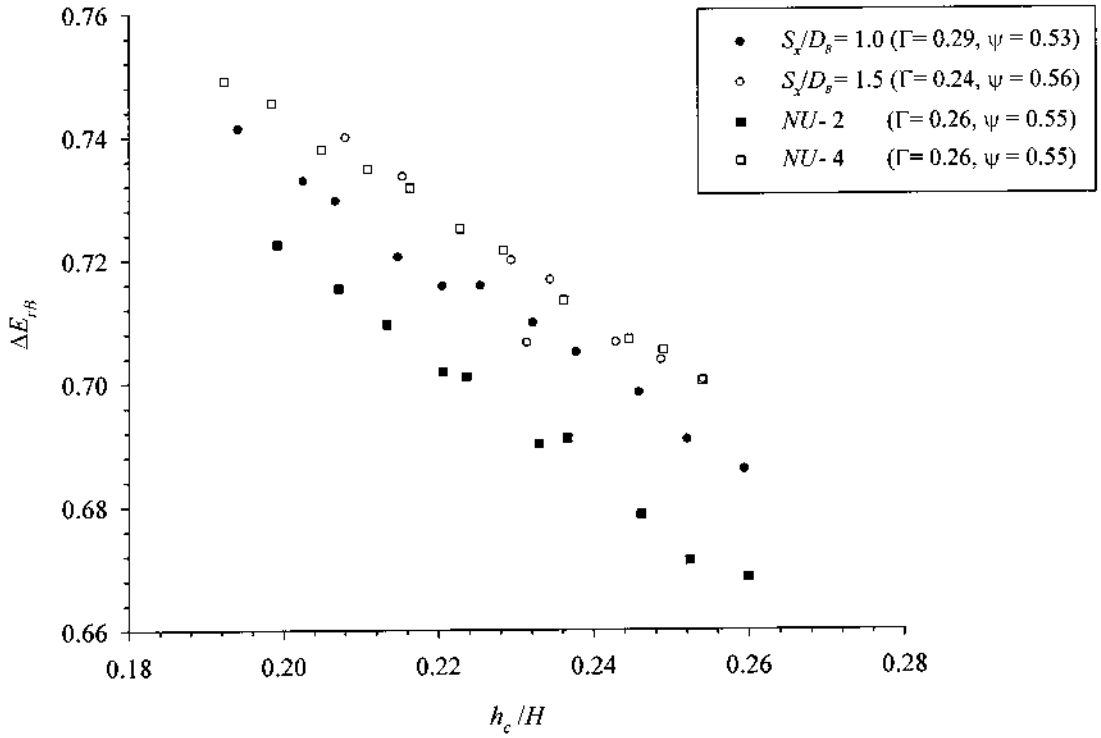

Fig. 4.17c Variation of ΔE_{rB} for D_B = 0.065 m in various staggered configurations (1V:9H)

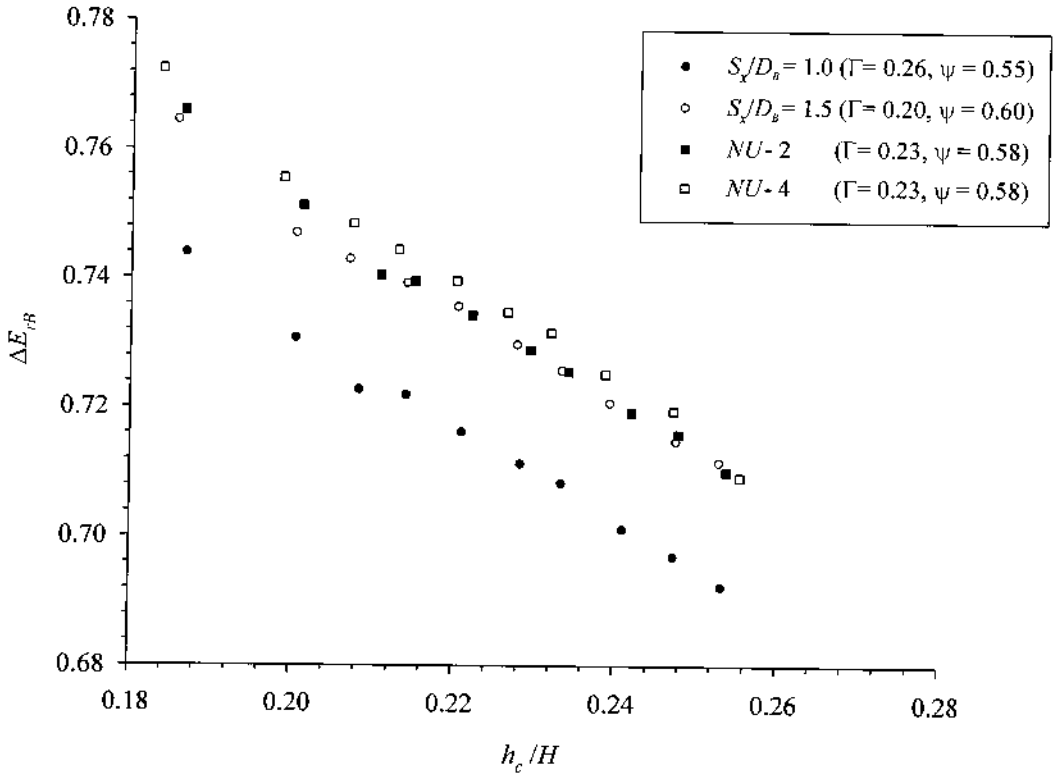

Fig. 4.17d Variation of ΔE_{rB} for D_B = 0.080 m in various staggered configurations (1V:9H)

To examine the integral effects of the flow parameter h_c/H and boulder concentration Γ on the relative energy dissipation function, isolines of $\Delta E_{rB}/\Delta E_r$ are simulated for flow conditions using the observed dataset for 1V:9H. The derived plot for D_B = 0.042m is presented in Fig. 4.18, as illustration. The energy dissipation factor showed distinctive trends with respect to each boulder size tested in similitude with that derived for the 1V:7H slope. There is not much effect of the boulder concentration factor as shown by the almost parallel isolines of $\Delta E_{rB}/\Delta E_r$ with the x-axis (Γ scale) for the boulders of 0.042 m and 0.055 m diameter.

On the whole, a substantial drop in relative energy dissipation was observed at the 1V:9H slope as compared with the previous two slopes. Here also, there is no clear distinctive trend that a particular boulder configuration yielded effective dissipation of energy for the boulders of smaller sizes. It may be deduced that for a channel width to macroroughness size ratio of $W/D_B \geq 5.5$ (i.e. 0.30 m\0.055 m ≈ 5.5), there was no appreciable effect of boulder concentration or spacing for the 1V:9H boulder block ramp under the test conditions. Non–uniform staggered configuration (particularly NU–4) resulted in stable relative energy dissipation as compared to the uniform configurations at this slope. The bigger-size boulders

(D_B = 0.080 m) yielded a higher rate of ΔE_{rB} with clear variations of the spacing and distribution. Thus at flatter slopes, bigger macro-roughness size can be adopted for efficient energy dissipation. Average relative energy dissipation ΔE_{rB} was observed in the range of 67 to 77 % for the flow parameter range $0.19 < h_c/H < 0.29$, and it decreases considerably as the flow submergence increases. The relative energy dissipation on block ramps with boulders of different sizes for 1V:9H slope are reported in Table 4.7.

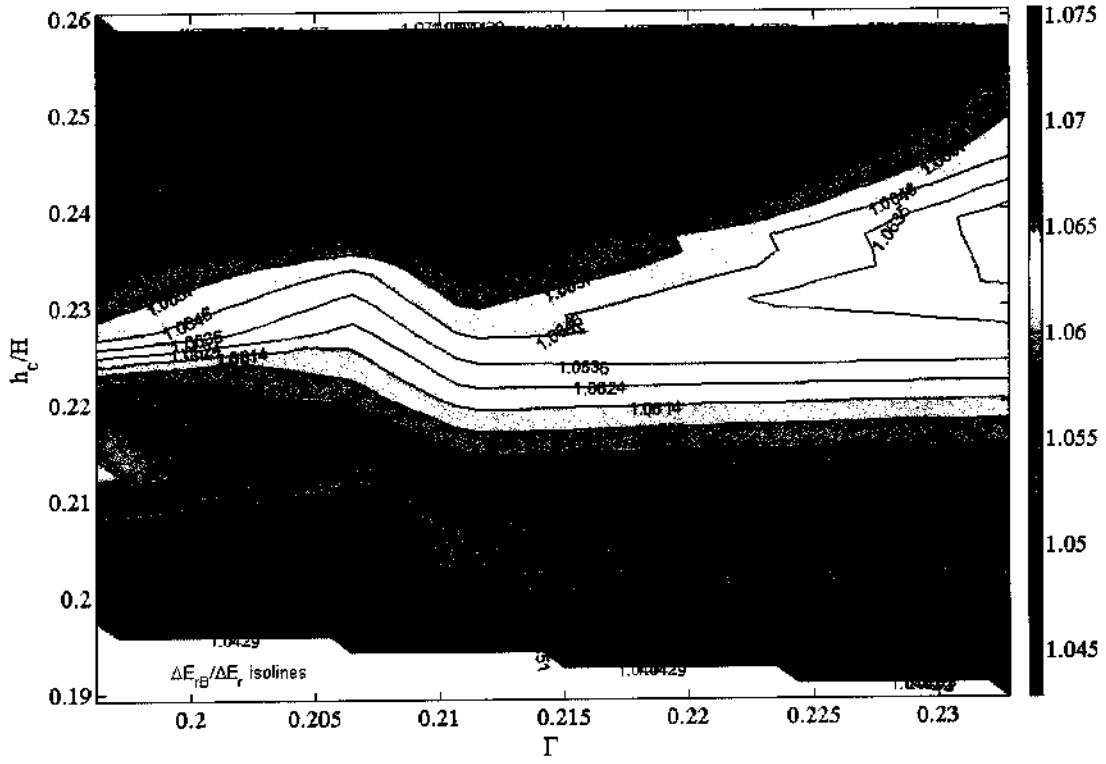

Fig. 4.18 Isolines of $\Delta E_{rB}/\Delta E_r$ w.r.t. boulder concentration and h_c/H for D_B = 0.042 m (1V:9H)

Table 4.7 Summary of the test results on block ramps with boulders for 1V:9H slope

Parameter	D_B = 0.042 m	0.055 m	0.065 m	0.080 m
Γ	0.19 – 0.23	0.21 – 0.26	0.24 – 0.29	0.20 – 0.26
h_c/H	0.190 – 0.260	0.192 – 0.261	0.192 – 0.260	0.179 – 0.255
ΔE_{rB}	0.684 – 0.749	0.686 – 0.737	0.671 – 0.749	0.692 – 0.769

Subjective examinations have been conducted on each particular slope for each tested boulder size to delve into the mechanism of how each variable related to the energy dissipation process. It is clear that the relative energy dissipation decreases as the slope gets flatter. The

notable finding is the threshold boulder concentration whereupon design applications can be built–upon to render efficient dissipation of energy on boulder block ramps. Other inferences were drawn as regarding the behaviour of the boulder spacing configuration in respect of the ratio of channel width to macroroughness size W/D_B or relative flow depth, that a value less than or greater than, influenced the ΔE_{rB} variation over the tested ramp slopes. Though this deduction may proclaim better with a wider range of boulder spacing for similar test conditions, each boulder configuration factor can be said to characterize a distinctive exponent on the energy dissipation process. The reduction coefficient ψ showed an inverse variation with the boulder concentration factor Γ on all the tested slopes and thus all findings relative to Γ inversely apply to the factor ψ in equivalent proportions. On the whole, the energy dissipation on boulder block ramps was observed to be much higher than the general block ramp condition with base material. If the upper limits of the ΔE_r are taken for each slope, then it can be concluded that there is an overall 10 % increase in the energy dissipation when boulders are placed in staggered configurations over the block ramp. Also, this scale seemed to amplify with decrease in slope as was marked by a 14 % increase for the 1V:9H slope. The overall summary of the test results are presented in Table 4.8.

Table 4.8 Overall summaries of the test results on block ramps with boulders

Parameter	1V:5H	1V:7H	1V:9H
Boulder concentration, Γ	0.08 – 0.32	0.14 – 0.29	0.19 – 0.29
h_c/H	0.048 – 0.125	0.111 – 0.190	0.179 – 0.261
ΔE_r	0.726 – 0.927	0.742 – 0.833	0.671 – 0.769

4.5.5 Variation of Relative Energy Dissipation with Boulder Concentration

After the slope factor, the boulder concentration Γ (spatial density of boulders) is considered to the next key parameter describing the energy dissipation on boulder block ramps. In the earlier section, detailed observations have been assessed based on this parameter based on the slope factor. To investigate the effect of Γ implicitly on the energy dissipation function, boulders in various configurations and distributions ranging between 8 to 32 % were examined with respect to each boulder size. It can be noted that boulders of different sizes in different spacing and distribution can have the same value of Γ. For instance, on the 1V:5H slope, boulders D_B = 0.055 m in staggered uniform configuration of S_x/D_B = 1.5 quantified a value of Γ = 0.25, which is also the same value for boulders D_B = 0.065 m in non-uniform

NU-1 configuration. Thereby, the variation of ΔE_{rB} with respect to Γ was studied for each tested boulder size. In parity to check the energy dissipation due to boulders only, variations of $\Delta E_{rB}/\Delta E_r$ with respect to Γ were also examined. Plots are shown for two of the boulder sizes (D_B = 0.055 m and 0.065) and the variations of Γ are also reflected in terms of slope as given in Figs. 4.19a-b.

It can be observed that the boulder concentration has no significant characterization with the ΔE_{rB} function. Boulders at steeper slopes indicated higher energy loss than those at flatter slopes irrespective of the boulder concentration. For example, for the same boulders size 0.055 m, a concentration of Γ = 0.14 at 1V:5H slope ramp yielded much higher energy dissipation than at a higher concentration Γ = 0.26 at both 1V:7H and 1V:7H slopes.

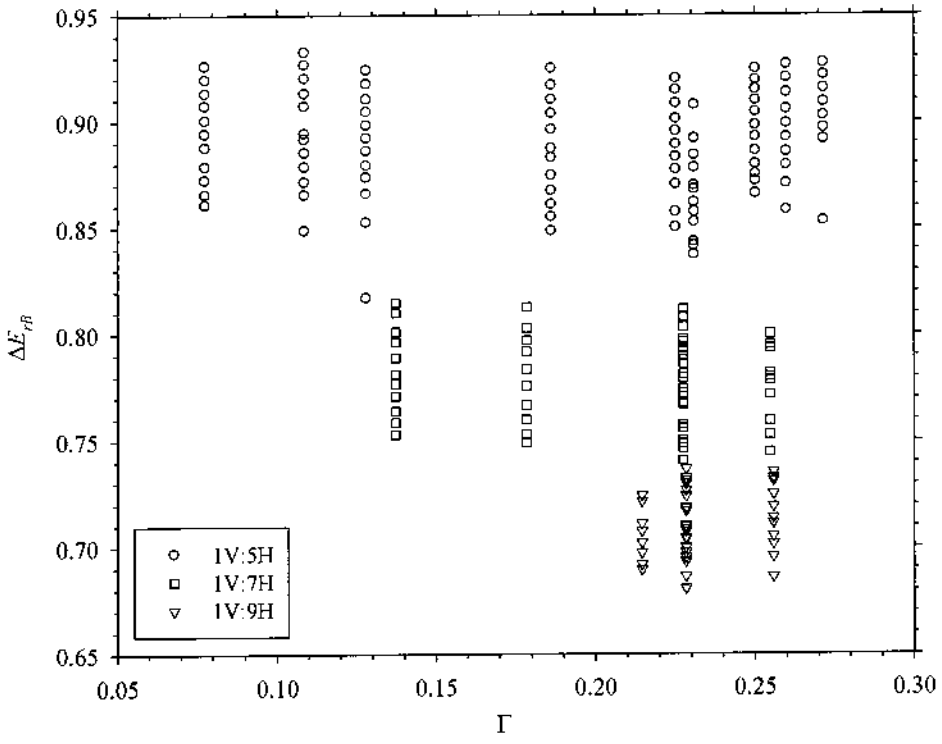

Fig. 4.19a Variation of ΔE_{rB} with Γ for a boulders (D_B = 0.055 m) at different ramp slopes

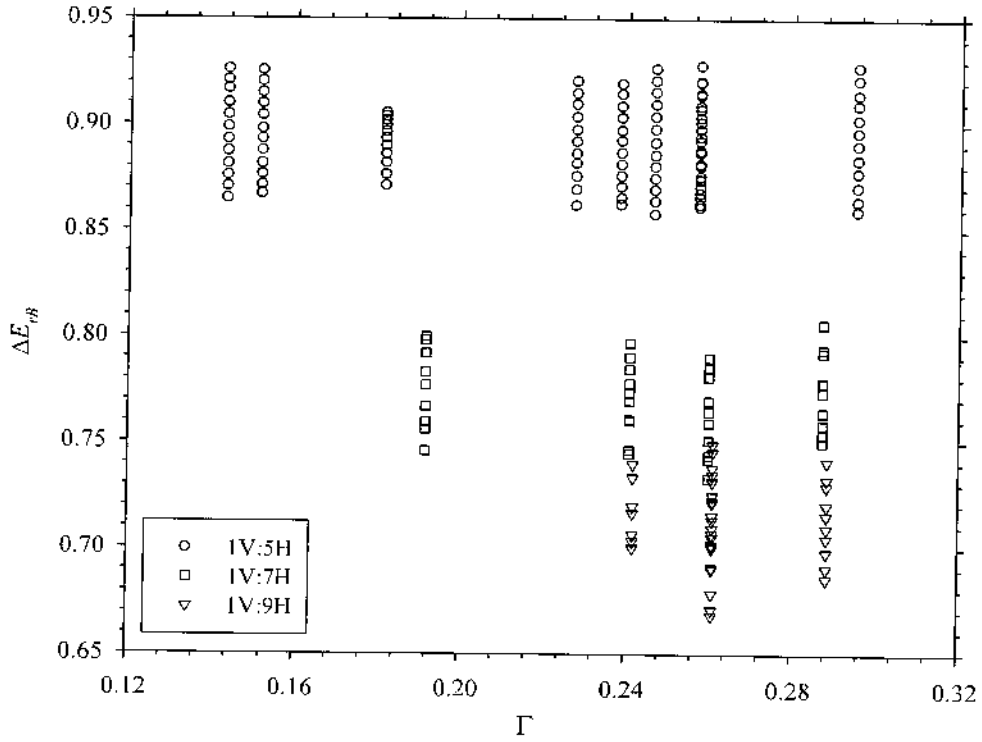

Fig. 4.19b Variation of ΔE_{rB} with Γ for a boulders (D_B = 0.065 m) at different ramp slopes

In this study under the tested conditions, the threshold range for Γ = 22 – 25 % is stipulated. Pagliara and Chiavacinni (2006b) had found a maximum increase in the energy dissipation by 10 – 12 % for an increase in boulder concentration of 30 – 35 %. The difference may be because of the smaller sized of boulders and arrangement pattern (rows and random) adopted by the authors in comparison with that used in the present study. For Γ greater than the threshold boulder concentration, the bed gets packed as closely and a common energy loss mechanism seemed to characterize the block ramp (Hunziker and Partner, 2008; Janisch and Tamagni, 2008). It may be resolved that an increase in Γ beyond the threshold lead to an identical hydraulic behavior with base materials where the roughness pebbles are packed so closely that the roller eddies and wakes formed, are only partially dissipated before it meets the next roughness obstruction.

4.5.6 Variation of Relative Energy Dissipation with Boulder size

Although the boulder concentration term Γ considers the boulder size factor, it is deemed important to understand the effect of macroroughness boulder size explicitly on the relative energy dissipation function. To examine this variation, observed dataset comprising boulders of different sizes in various spacing and distribution were sorted for the same or near – equal

boulder concentration under all the tested slopes. This categorization was done to delve the effect of D_B reciprocating the same boulder density on the ramp. The variation plots of ΔE_{rB} with boulder size are presented for Γ = 0.23 and Γ = 0.26 in Figs. 4.20a and 4.20b respectively. These boulder concentrations were chosen as they represented the maximum range of boulder sizes at the tested slopes.

It can be observed that there is an indication that the relative energy dissipation is not totally affected by the boulder size, though there are partial indications of marginal increase in ΔE_{rB} with larger boulder sizes. To have a closer examination with the integral effect of flow conditions, the variation plot Fig. 4.20b is transferred to a ΔE_{rB} against h_c/H plot with the same observed dataset for Γ = 0.23 as shown in Fig. 4.21. The plot depicted an asymptotic energy dissipation trend for the tested boulder sizes signifying a dependency on the flow conditions. Thereby, the boundaries ascribed by the ratio of channel width to boulder size (W/D_B) or the relative flow depth (h/D_B) as discussed earlier, could superimpose the effect of boulder dimensions on the relative energy dissipation function along with the concentration factor.

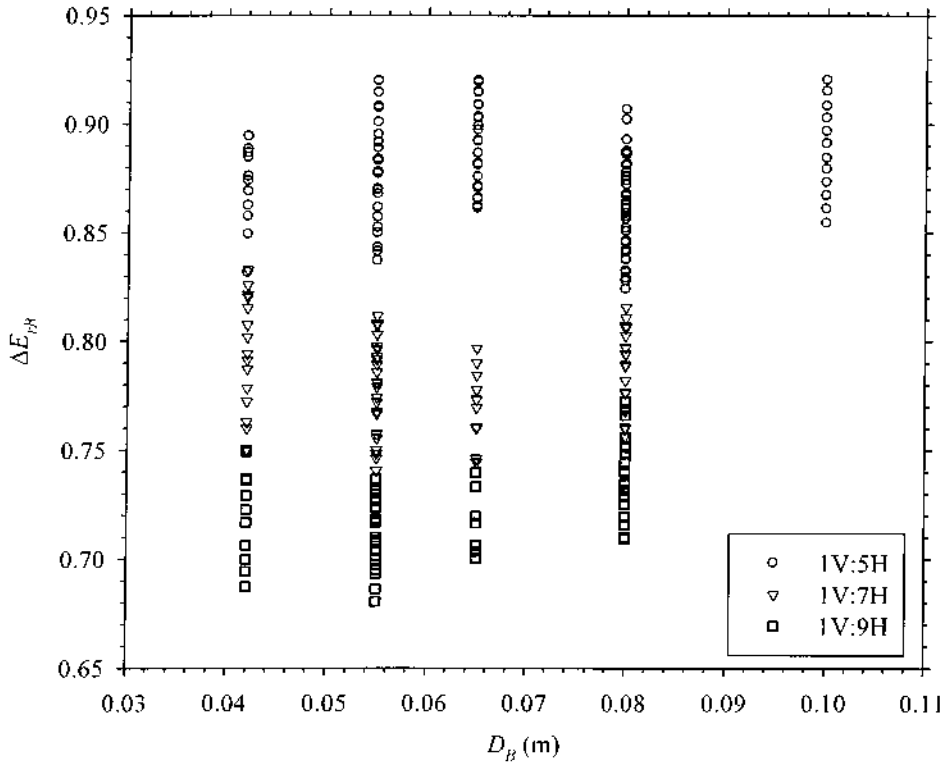

Fig. 4.20a Variation of ΔE_{rB} with boulder size for Γ = 0.23 at different ramp slopes

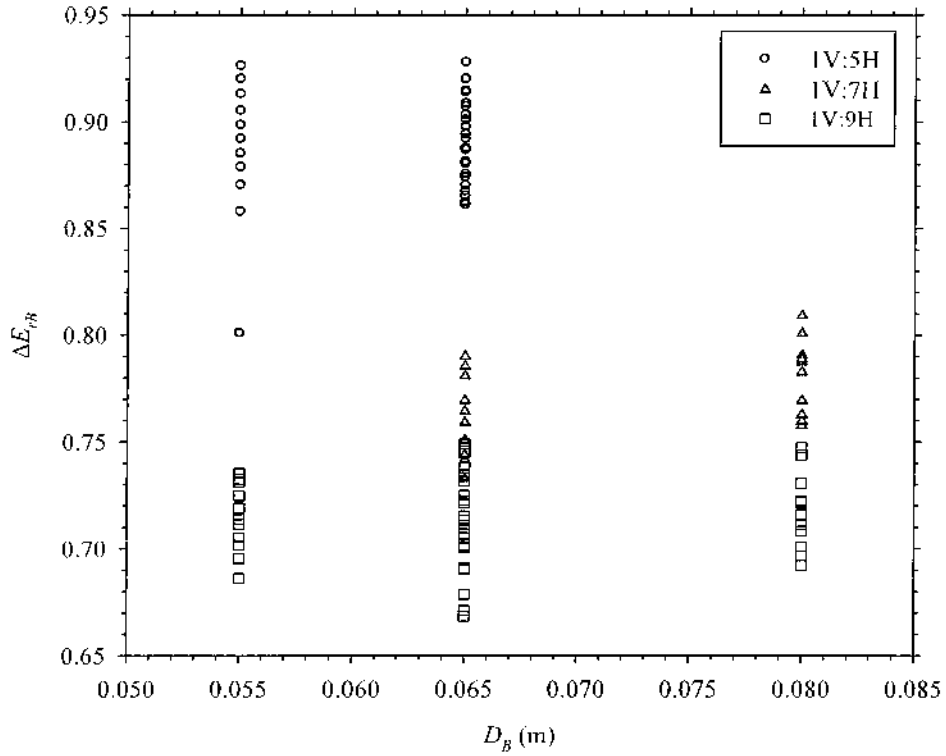

Fig. 4.20b Variation of ΔE_{rB} with boulder size for $\Gamma =$ 0.26 at different ramp slopes

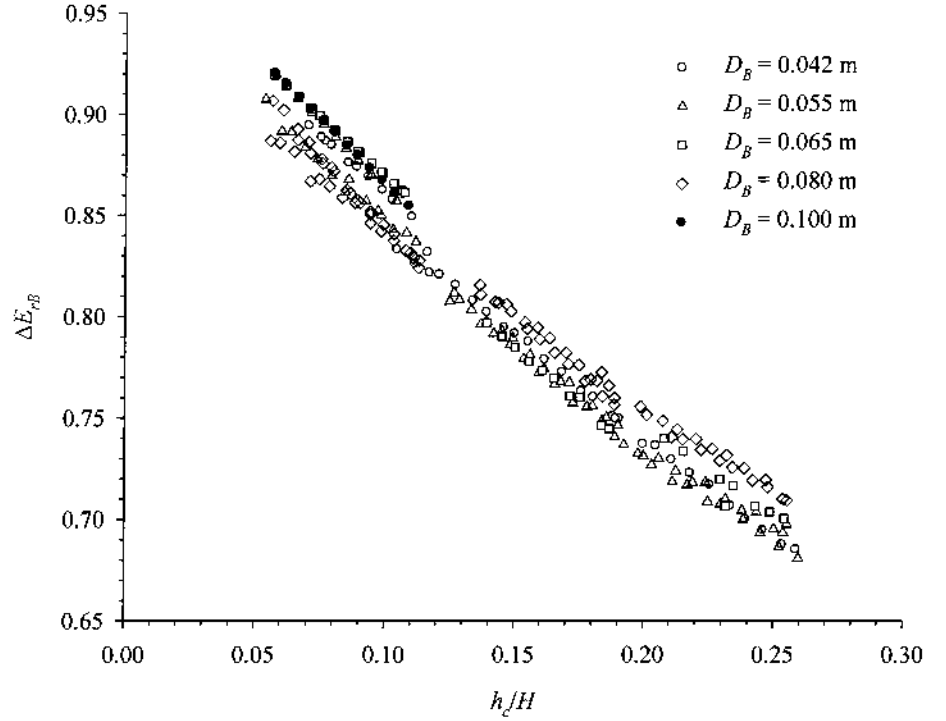

Fig. 4.21 Variation of ΔE_{rB} for $\Gamma \approx 0.23$ for all tested slopes

It can be noted that Pagliara and Chiavacinni (2006b) had investigated the variation of $\Delta E_{rB}/\Delta E_r$ with respect to D_B/d_{50} and found that the dependence of the energy dissipation on the factor D_B/d_{50} can be considered negligible. However, the effect of boulder size can be realized that each macroroughness element is a source of vortices which are generated by the accelerated flow around the upstream edges of blocks and dissipate in the retarded flow in the wake downstream from the blocks (Herbich and Shulits, 1964; Golubtsov, 1969).

4.5.7 Boulder Spacing Criteria

It has been observed from the assay of test results that the slope, boulder concentration and boulder size has integral and differential effects on the relative energy dissipation function on boulder block ramps. In some cases, closer spacing (in the order of $S_x/D_B \leq 1.0$) yielded higher energy loss, and in some cases the trend gets reversed. Similarly, regarding the boulder distribution, it was observed that particular non-uniform configurations resulted in efficient energy dissipation than the uniform configuration. Upto a certain extent, this was found to be characterized by the slope and W/D_B ratio within the envelope of the test conditions.

To test the consistency of the boulder spacing, observed data for boulders in uniform arrangement were selected with near-equal longitudinal clear spacing (S_x) and investigated for a particular ramp slope. The variation of $\Delta E_{rB}/\Delta E_r$ of boulders of different sizes and configuration with $S_x \approx 0.11$ m and $S_x \approx 0.22$ m with respect to the flow parameter h_c/H on 1V:5H slope ramp are shown in Figs. 4.22 and 4.23 respectively.The plots showed that the larger boulder sizes with higher boulder concentration factor resulted in higher relative energy dissipation irrespective of the spacing factor S_x/D_B for the similar S_x order. It can thus be noted that the Γ is a direct function of S_x/D_B parameter. It can be also inferred that the variation in the increase of energy dissipation for the same S_x becomes more prominent as with increase of the flow parameter h_c/H. This may be attributed to a transformation of partial skimming flow to developed– skimming flow conditions as the flow depth relatively increases with the margins of boulder dimensions.

The above tests show that the size of boulders is equally an important parameter while taking the spacing factor independently as a function of the relative energy dissipation. Thus the boulder size (D_B) has to be taken with appropriate modification with respect to its semi–hemispherical boundary in formulating a spacing criterion for boulders on the block ramp, while considering other parameters implicitly.

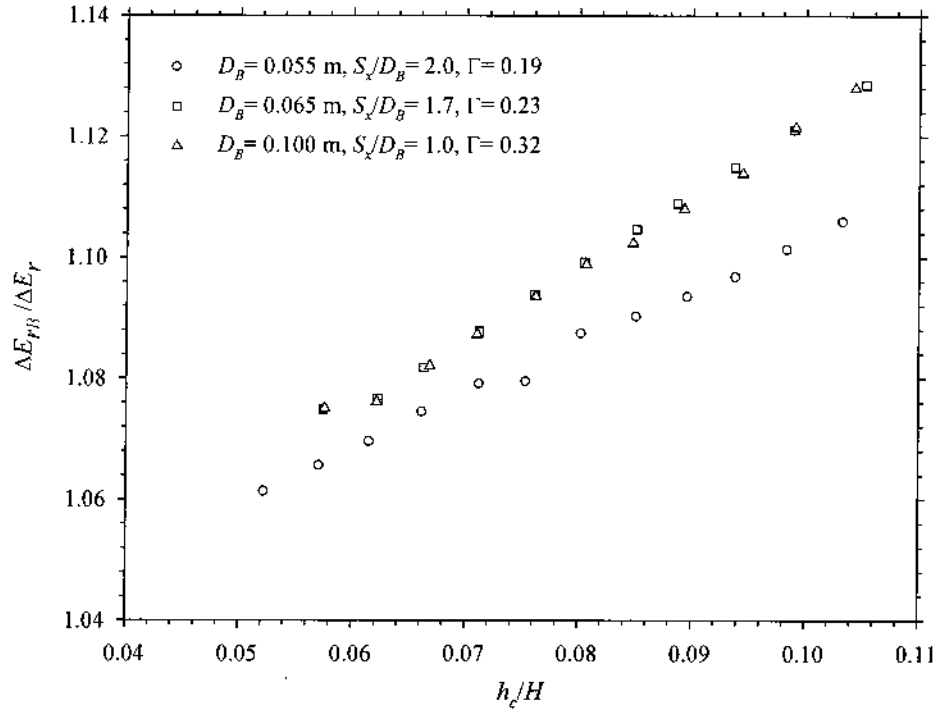

Fig. 4.22 Variation of $\Delta E_{rB}/\Delta E_r$ for equivalent L-spacing ($S_x \approx 0.11$ m) at 1V:5H ramp slope

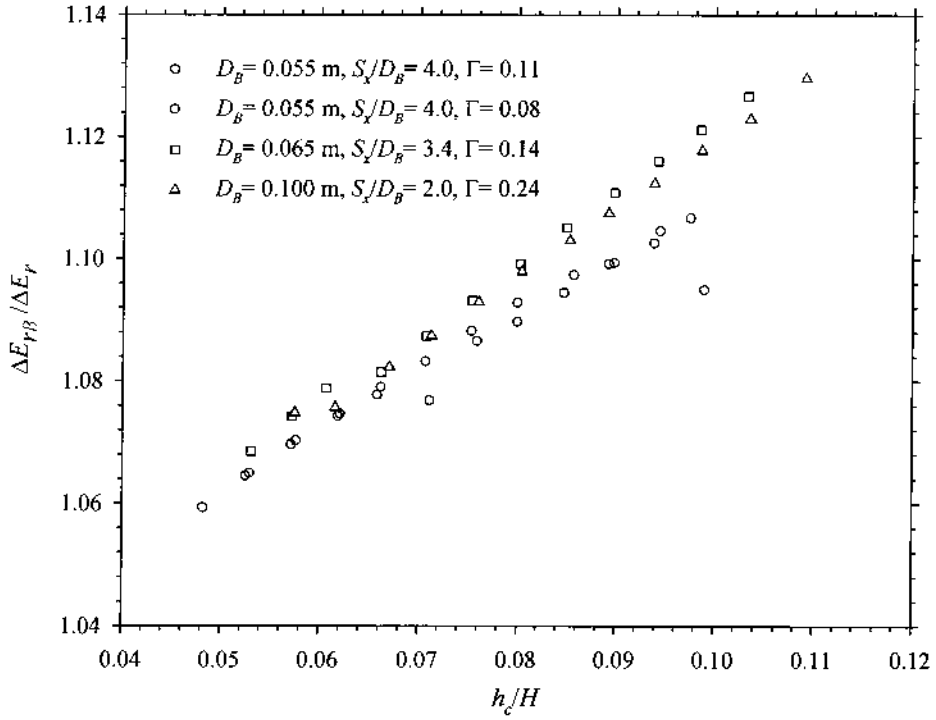

Fig. 4.23 Variation of $\Delta E_{rB}/\Delta E_r$ for equivalent L-spacing ($S_x \approx 0.22$ m) at 1V:5H ramp slope

Sayre and Albertson (1961) had investigated roughness spacing using baffle blocks placed at definite longitudinal and transverse intervals forming staggered symmetrical repeating patterns in their experiments. Though the authors did not consider the energy dissipation factor overtly, they presented a roughness parameter ascribing the flow resistance that was dependent only on the baffle spacing. Based on the authors' criterion for macroroughness spacing, the following relation (Eq. 4.6) is formulated in respect to the staggered uniform configuration for boulders on block ramps.

$$\Gamma = \frac{D_B^{\,2}}{2(S_x + D_B)(S_y + D_B)} \tag{4.6}$$

where S_x and S_y are the longitudinal and transverse clear spacing between the boulders respectively. It may be noted that S_x was generally kept equal to S_x for the configurations, except in the case of larger boulders i.e for D_B = 0.080 m and 0.10 m.

Since the above formulation was based on the rectangular-shaped baffles for the slope range 0.001 to 0.003, few ambiguities were observed and thereby the relation is further modified using the observed dataset of the present study. The respective scatter between the actual observed boulder concentration and the boulder concentration calculated using Eq. (4.6) was adapted using a power–fit at a correlation of 0.91 within ± 95% prediction line as shown in Fig. 4.24. The modified relation (Eq. 4.7) is thereby presented to evaluate the longitudinal and transverse spacing of boulders for a particular boulder concentration. Equation (4.7) may be satisfactorily used for block ramp applications for the range Γ = 5 to 35 %.

$$\Gamma(\text{calc}) = 0.86\left[\frac{D_B^{\,2}}{2(S_x + D_B)(S_y + D_B)}\right]^{1.11} \tag{4.7}$$

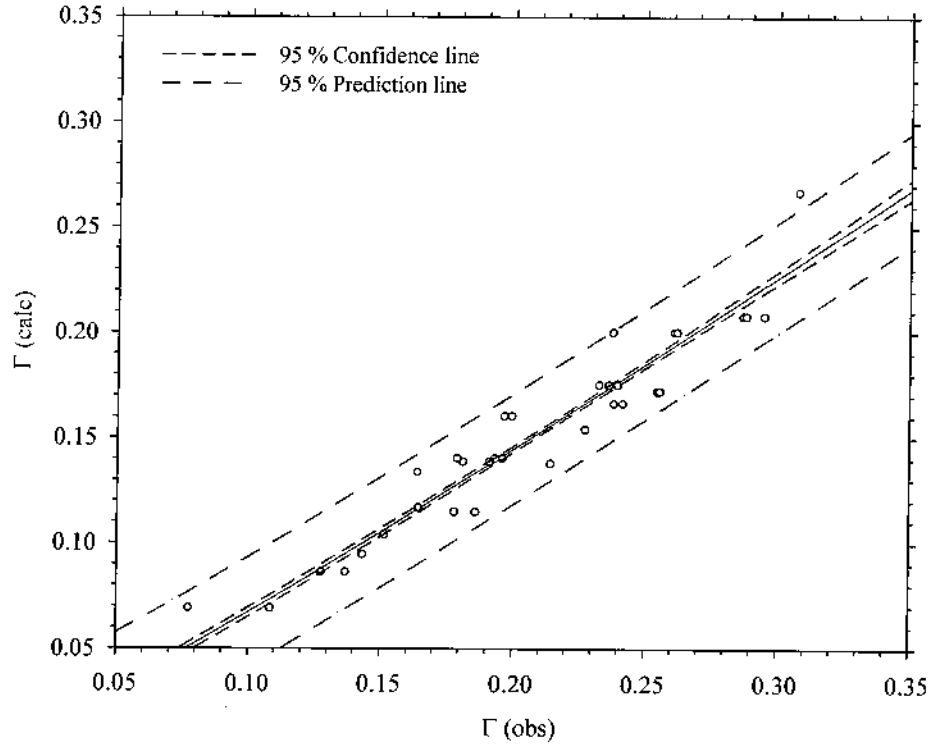

Fig. 4.24 Evaluation plot between Γ calculated (using Eq. 4.7) and Γ observed for staggered uniform configuration of boulders

4.5.8 Roughness Parameters for Staggered Configuration of Boulders and Validity

Pagliara and Chiavaccini (2006b) had postulated a relation (Eq. 1.3) to estimate the relative energy dissipation for block ramps with boulders in rows and random arrangements. The authors have presented the relation in terms of two parameters E and F that are the functions of the arrangement and roughness of the elements, along with the values of the two parameters with respect to the two arrangements for rounded and crushed boulders. Ahmad et al. (2009) had presented a relation for computing the roughness parameter F (Eq. 2.28) by using $E = 0.60$ that was designated for rounded boulders in random configuration (Pagliara and Chiavaccini, 2006b). Adopting an unbound condition for determining the value of these two roughness parameters which are critical in the estimation of relative energy dissipation for boulder block ramps, the roughness parameter values are found to be $E = -0.011$ and $F = 12.207$ deploying the same functional trend used by Pagliara and Chiavaccini (2006b). The relative energy dissipation was computed using these values in Eq. (1.4) and plotted against the observed values. It is observed that the points fall within a ± 5% deviation from the line of perfect agreement (Fig. 4.25). This can be considered satisfactory as the equation used in computing ΔE_{rB} is generally applicable to rows and random configuration and for a lower flow discharge range $Q \leq 0.011 m^3/s$. These new values can be adopted for staggered

arrangement of boulders within the above error margins and limits of test conditions used in the present study. The near-zero value of E showed that the relative energy dissipation function $\Delta E_{rB}/\Delta E_r$ is not absolutely dependent on the boulder concentration Γ. It has an integral variation with the flow parameter h_c/H.

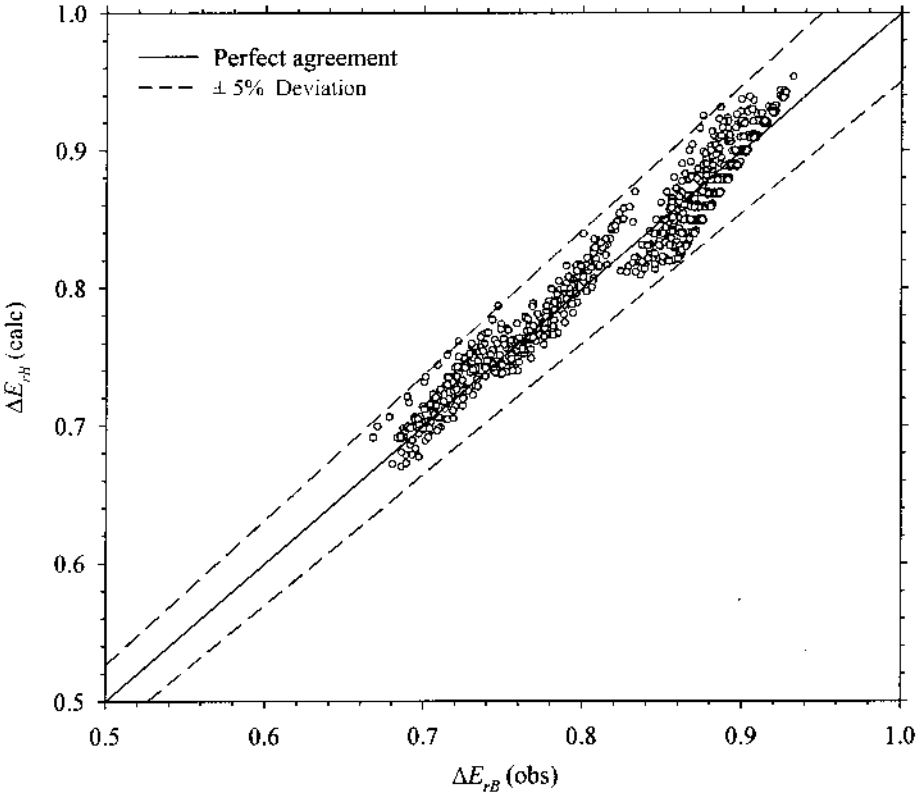

Fig. 4.25 Validation plot of the experimental dataset and check for E and F parameters

4.6 MULTI–LINEAR REGRESSION ANALYSES FOR THE ENERGY DISSIPATION FUNCTIONAL PARAMETERS

It is obvious that the combined effect of protruding boulders over the base material significantly increases the relative energy dissipation function. The functional relations as composed in section 4.1 were based on the unilateral composition factor of boulders and base material, and are not presented for the isolated case of presence of boulders only. In the present study, there is a lucid indication that flow separation and other turbulence properties are also inherent from the rough bed invoked by the granular base material.

It has been discussed in section 4.5.8 wherein the roughness parameters E and F (after Pagliara and Chiavacinni, 2006b) have been used to justify the observations for boulders in

staggered configuration, where $\Delta E_{rB}/\Delta E_r$ has been expressed as a function of the boulder concentration (Γ) term only in respect of the above two parameters.

The functional relation (Eq. 4.4) was based on the unilateral composition of boulders and base material, and not for the isolated case due to the presence of boulders only. It has been noted that a single parameter is not able to adequately correlate the energy dissipation. Considering the Reynolds number implicitly within the parameter h_c/H, the functional relation (Eq. 4.4) is presented in terms of ΔE_{rB} in respect of the influential parameters (Eq. 4.8): the flow parameter which takes care of the flow conditions and slope, h_c/H; the spatial density or concentration of the macroroughness boulders over the block ramp, Γ; the reduction coefficient which is function of both the number and planimetric arrangement of boulders, ψ; the longitudinal spacing of boulders for structured staggered arrangement, S_x/D_B.

$$\Delta E_{rB} = \Omega_3\left(\frac{h_c}{H}, \Gamma, \psi, \frac{S_x}{D_B}\right) \tag{4.8}$$

In the analyses, the complete dataset for all the three tested slopes, sizes and configuration of boulders, have been randomly sorted in such a way that about 80% of the dataset was used to calibrate the relations for each case of the dataset comprising at least one set for each boulder size for every slope tested. The remaining 20% dataset was kept segregated for validation.

(a) ΔE_{rB} with respect to Four Parameters

In the first case, the relative energy dissipation is taken as a function of the all the four parameters as given by Eq. (4.9). Adopting ΔE_{rB} as the dependent variable and the four influential parameters as the independent variables, the following relation (Eq. 4.9) is obtained.

$$\Delta E_{rB} = 1.239 - 1.895\left(\frac{h_c}{H}\right) - 0.126(\Gamma) - 0.449(\psi) + 0.028\left(\frac{S_x}{D_B}\right) \tag{4.9}$$

The coefficient of correlation (R^2) is 0.94. This equation includes the roughness spacing factor S_x/D_B of the boulders to check its sensitivity on other parameters describing ΔE_{rB}. The comparison plot (Fig. 4.26) for the observed values against the respective computed values of ΔE_{rB} as per Eq. (4.9) shows that few points are scattered marginally below the ± 10% error line. This may be attributed to the non-uniform configuration of boulders. Also it can be

inferred that the low coefficient associated with the roughness spacing factor showed less correlation with relative energy dissipation function.

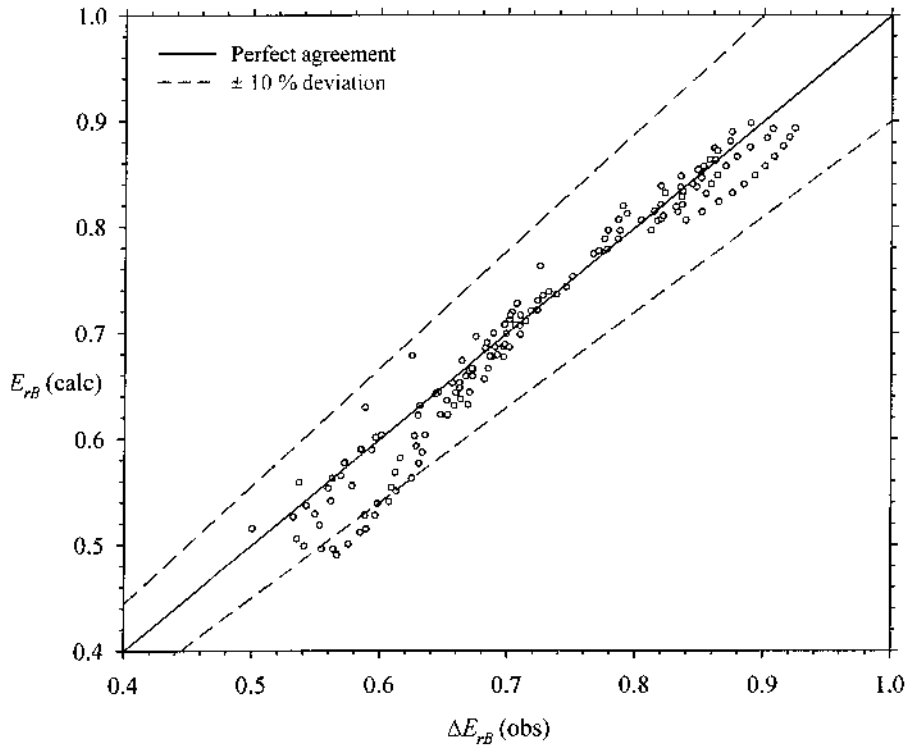

Fig. 4.26 Comparison between observed ΔE_{rB} and computed ΔE_{rB} as per Eq. (4.9)

(b) ΔE_{rB} with respect to Three Parameters

In the second case, the relative energy dissipation is taken as a function of the three parameters by neglecting S_x/D_B. Using the same confidence intervals with the dependent variable ΔE_{rB} as was conducted in case of four parameters, multiple regression analysis was performed and yielded the following relation (Eq. 4.10).

$$\Delta E_{rB} = -0.151 - 1.826\left(\frac{h_c}{H}\right) + 1.386(\Gamma) + 1.411(\psi) \qquad (4.10)$$

The coefficient of correlation (R^2) of the analyses is 0.95. The correlation coefficient in both the cases is nearly the same, though there is a marginal improvement after omitting the roughness spacing factor. This factor can be taken to be implicitly considered in the roughness concentration or reduction coefficient factors. The comparison plot (Fig. 4.27) for the observed ΔE_{rB} against the respective computed values of ΔE_{rB} as per Eq. (4.10) showed that all the points were almost confined within the ± 10% deviation line from the perfect agreement. This may be attributed to the omission of the roughness spacing criteria.

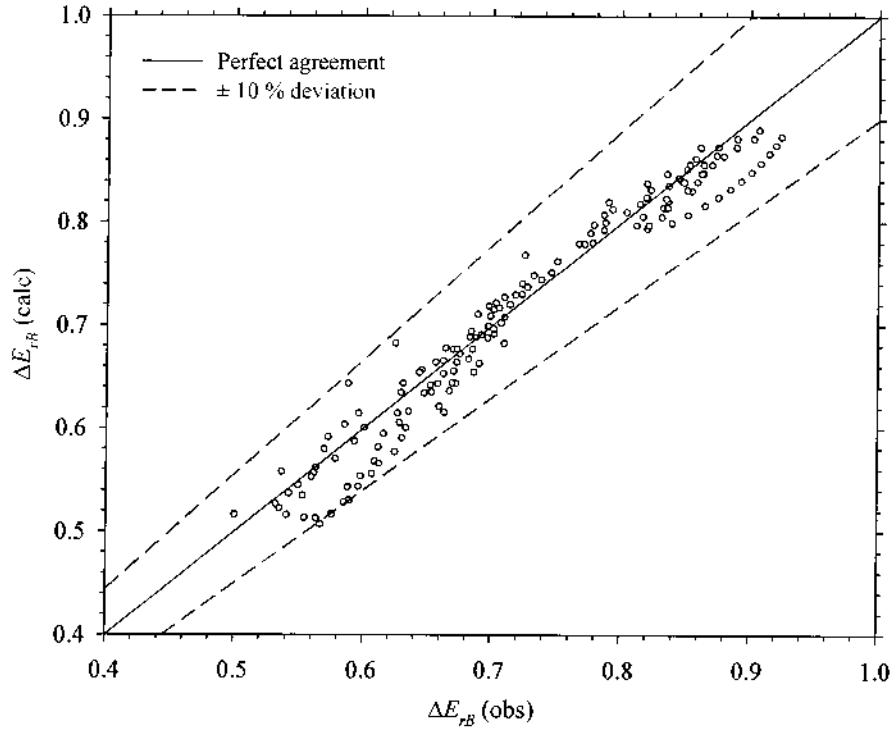

Fig. 4.27 Comparison between observed ΔE_{rB} and computed ΔE_{rB} as per Eq. (4.10)

(c) ΔE_{rB} with respect to Two Parameters

In the third case, the relative energy dissipation is taken as a function of the two parameters by omitting the reduction coefficient ψ. As both the terms Γ and ψ relate to the boulder configuration, and as it was observed that ψ had no significant variation then that depicted by the Γ factor, this term has been neglected. The multiple regression analysis yielded the following relation (Eq. 4.11).

$$\Delta E_{rB} = 0.987 - 1.853\left(\frac{h_c}{H}\right) - 0.005(\Gamma) \qquad (4.11)$$

The coefficient of correlation (R^2) in this analysis is 0. 95. Here one can see that there is a sharp drop in the coefficient associated with the boulder concentration factor from 1.386 to – 0.005 as compared to Eq. (4.10), and the intercept coefficient comes almost equal to 1.0. This seemed to indicate there an equivalent dependence of the ΔE_{rB} function on the parameters h_c/H and Γ. This comparison plot (Fig. 4.28) for the observed values against the respective computed values of ΔE_{rB} as per Eq. (4.11) also revealed that all the points are satisfactorily contained within the ± 10% deviation from the line of perfect agreement.

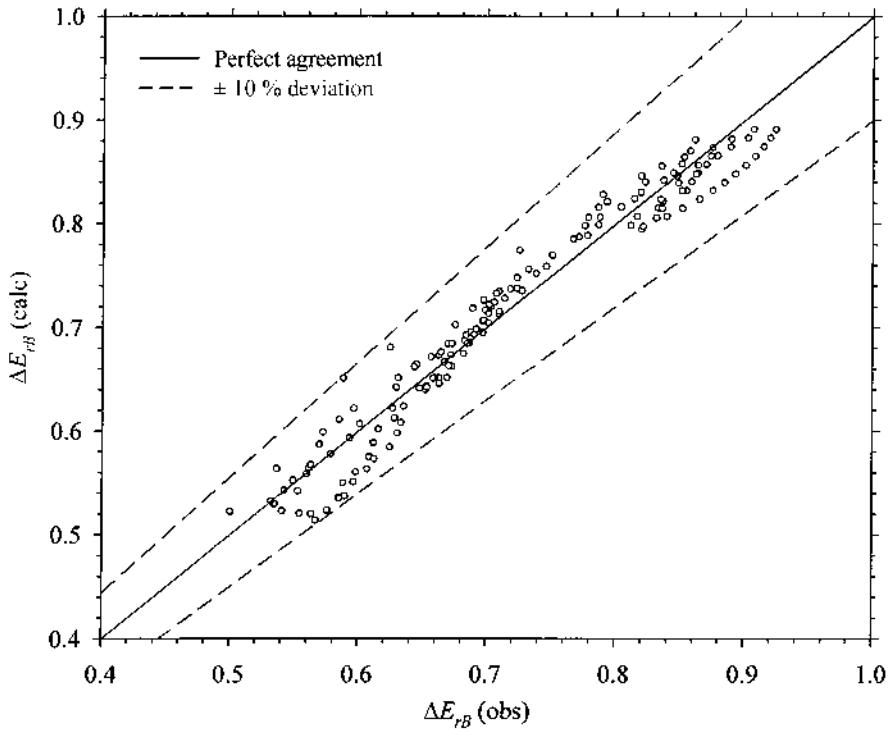

Fig. 4.28 Comparison between observed ΔE_{rB} and computed ΔE_{rB} as per Eq. (4.11)

4.7 MULTI–NONLINEAR REGRESSION ANALYSES FOR THE ENERGY DISSIPATION FUNCTIONAL PARAMETERS

The existing relations for computation of relative energy dissipation on block ramps with boulders considered the boulder concentration explicitly as the main factor. The relations postulated by Pagliara and Chiavacinni (2006a, 2006b) were derived for boulders in rows and random configurations by assigning roughness parameters. Ahmad et al. (2009) formulated a relation in terms of the roughness parameters E and F for staggered configuration of boulders. A new relation is formulated for computation of relative energy dissipation on block ramps with staggered boulders by considering the parameters Γ and h_c/H compositely. The inclusion of the flow parameter h_c/H was done to provide harmony with the inter–dependence of Γ factor governed by the h_c/H. From the optimal dataset, 75 % of the data were sorted randomly covering the range $\Gamma = 0.17$ to 0.30. Deploying a non–linear regression technique and using an exponential three–parameter decay function on the 75 % sorted dataset; an equation (Eq. 4.12) is derived. The coefficient of correlation of the analysis was 0.92 and most of the dataset were contained within the 95 % prediction line as shown in the analysis plot (Fig. 4.29).

$$\Delta E_{rB} = 0.086 \times L_R \, exp\left[\frac{0.131}{0.126 + \Gamma(h_c / H)}\right] \qquad (4.12)$$

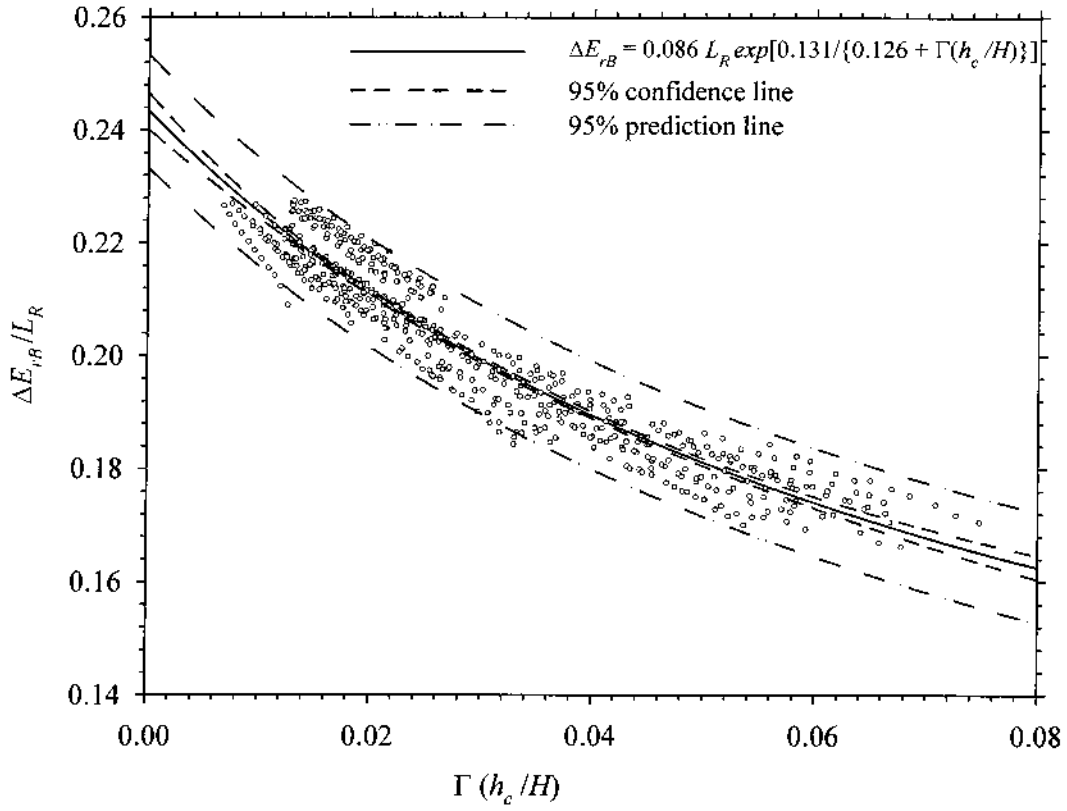

Fig. 4.29 Non–linear regression analysis plot of proposed equation (Eq. 4.12)

The proposed relation is validated using 25% of the remaining dataset that were sorted for Γ = 0.10 to 0.30. The above relation (Eq. 4.12) was used to compute the relative energy dissipation and plotted against the corresponding observed values. As was also indicated by the 95% confidence line (Fig. 4.29) and that the standard error of estimate was 0.005 in the analysis, the comparison plot depicted a near–confinement of the points within the ± 5% deviation from the line of perfect agreement as shown in Fig. 4.30.

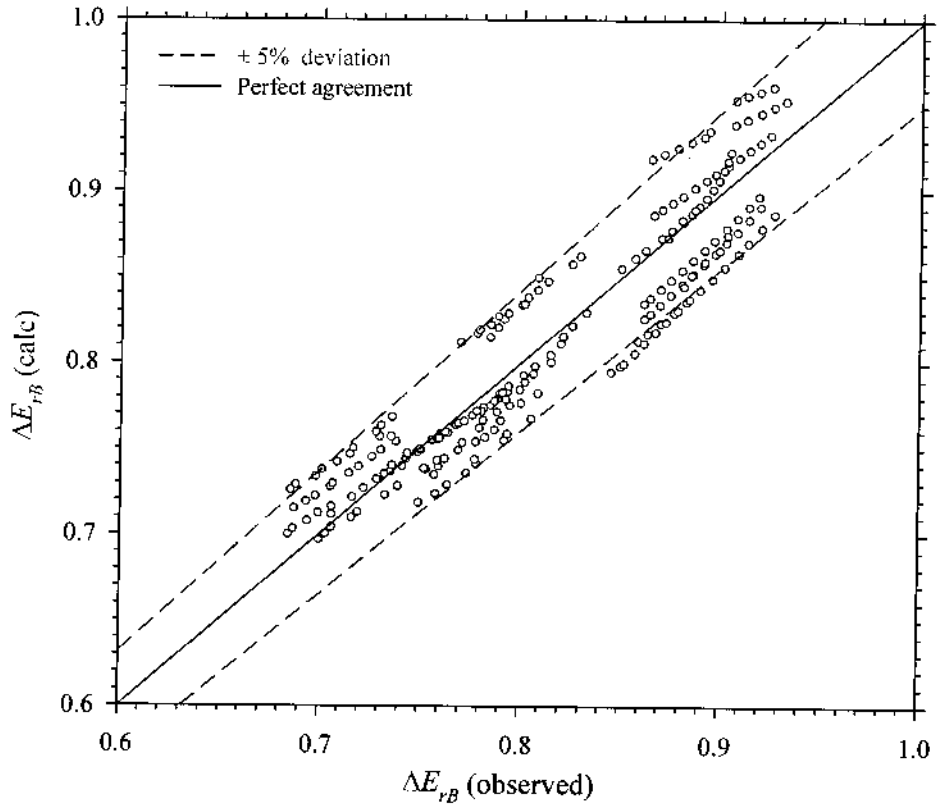

Fig. 4.30 Comparison between observed ΔE_{rB} and calculated ΔE_{rB} as per Eq.(4.12)

The validity of the proposed relation within ± 5% deviation from the line of perfect agreement may be considered satisfactory taking into consideration the multitude of varied boulder concentration with respective spacing of boulders and submergence flow conditions over block ramps in the tested range i.e, $\Gamma = 0.17 - 0.30$ and $0.05 < h_c/H < 0.29$.

It has been noted that, the points which were marginally scattered away from the ± 5% deviation line may be attributed to the slope and boulder concentration factor. It was also found that the coefficients vary with the boulder concentration term. So for a wider range of the applicability of the proposed relation, coefficients a_1, a_2 and a_3 can be used in Eq. (4.12) such that, these coefficients yielded the best fit correlations with respect to the range of boulder concentration used for both uniform and non-uniform staggered configurations. A common form of the relation is expressed as,

$$\Delta E_{rB} = L_R \times a_1 \, exp\left[\frac{a_2}{a_3 + \Gamma(h_c/H)}\right] \qquad (4.13)$$

where the coefficients a_1, a_2 and a_3 respectively, constitute the variability of the equation primarily in terms of boulder concentration and secondarily in terms of ramp slope, flow parameter, etc. The values of coefficients a_1, a_2 and a_3 for specific ranges of boulder concentration are given in Table 4.9. It may be noted that the values of the coefficients were not reported for the range $\Gamma = 0.30 - 0.32$. For this case, Eq. (4.13) may be used to estimate the value of ΔE_{rB}.

Table 4.9 Values of coefficients to be adopted in Eq. (4.13) for range of Γ

Sl	Γ	coefficient a_1	coefficient a_2	coefficient a_3	correlation R^2
1	0.17 – 0.19	0.110	0.053	0.064	0.98
2	0.20 – 0.21	0.020	0.834	0.332	0.99
3	0.22 – 0.24	0.051	0.323	0.207	0.96
4	0.25 – 0.26	0.074	0.173	0.140	0.98
5	0.27 – 0.30	0.012	1.616	0.530	0.99

4.9 STABILITY OF BLOCK RAMP

During the stability tests, the main focus was to estimate the critical discharge causing local failure; because local failure is considered as a stable or equilibrium condition, unlike global failure which is a beginning of the total collapse of the chute, hence can't be regarded as an equilibrium condition.

Variation of critical discharge with non-dimensional parameter d^*_{50} and chute slope is shown in Fig. 4.31, which indicates that the critical discharge increases with non-dimensional parameter d^*_{50} while decreases with chute slope. The existing equations for the estimation of critical discharge for the local failure of the rock chutes are checked for their accuracy using the present study data. The estimated critical discharge using various equations are compared with the observed ones in the Fig. 4.32, which indicates that equations proposed by Robinson et al. (1997) and Pagliara & Chiavaccini (2007) estimate the critical discharge up to some accuracy. Pagliara & Lotti (2007) relationship i.e., Eq. (2.60) shows large deviation from the observed data of the present experimental study as well as with data of other investigators. As none of the existing equations estimate the critical discharge with better accuracy, therefore, there is a need to propose a new relationship with use of available data and inclusion of some more parameters in the relationship. The observed data in the present study and the data of

Robinson et al. (1997) were used to arrive at a better relationship for the fair estimation of the critical discharge.

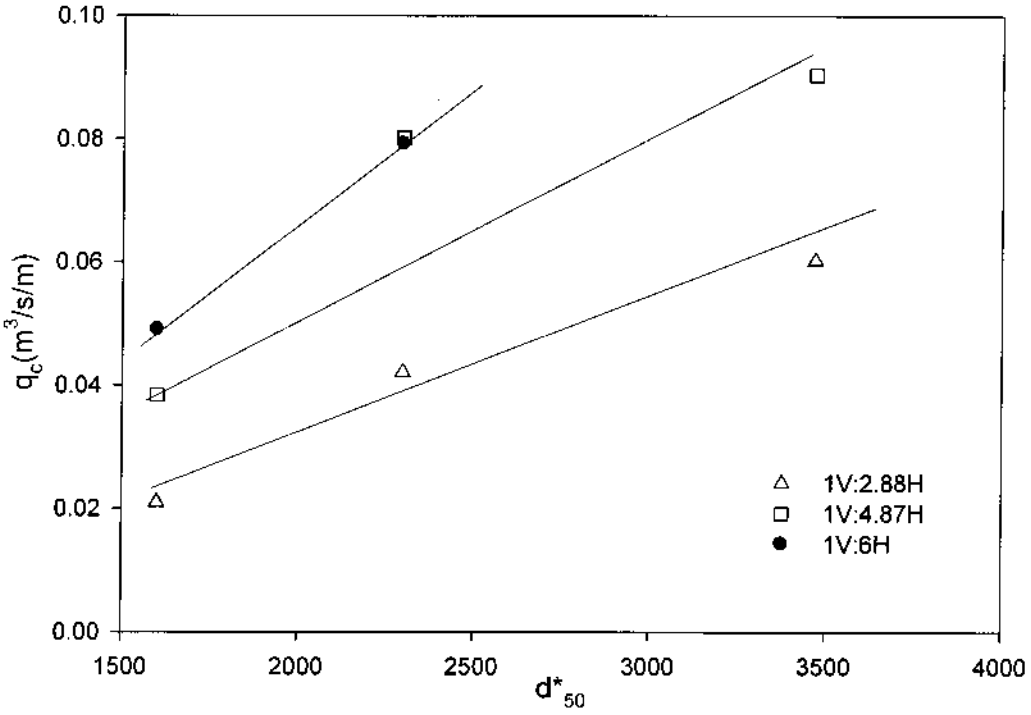

Fig. 4.31 Variation of critical discharge with dimensionless parameter d^*_{50} at different slopes.

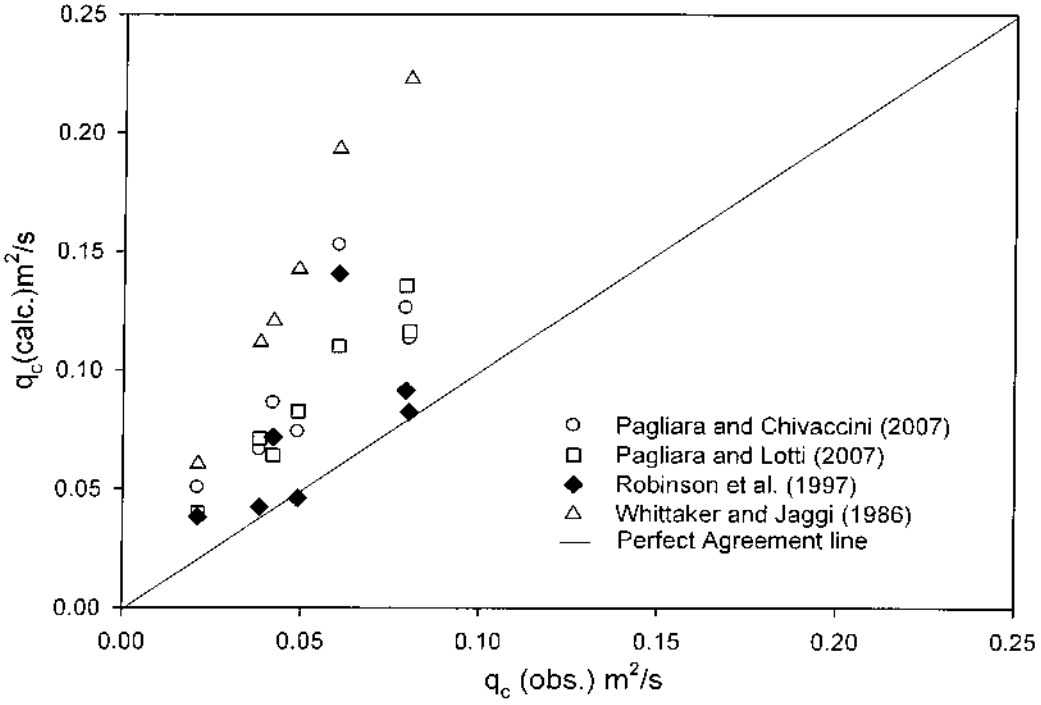

Fig. 4.32 Comparison between observed and calculated critical unit discharge for the local failure of the rock chute.

4.9.1 Relationship for Specific Critical Discharge at Local Failure

As per literature review and other aspects of flow over rock chute, the functional relationship for critical discharge q_c may be written as;

$$q_c = f(S, d_{50}, \gamma_s, C_u, g, v, C_a, h, \tau_c^*) \quad (4.14)$$

where C_a = percentage air concentration in flow; and τ_c^* = critical shear stress or Shields parameter. As per the present observed data and data of Robinson et al. (1997), the critical discharge increases exponentially with the increase in uniformity coefficient.

Hence q_c varies predominantly with d^*_{50}, S and uniformity coefficient C_u

$$q_c = f(d^*_{50}, S, C_u) \quad (4.15)$$

The other parameters like C_a can be supposed to have small effect in the estimation of critical discharge hence not taken in analysis. The most common approach to analyze the effects of relative submergence is to relate the dimensionless critical shear stress τ_c^* to relative depth h/d_{50}. Ashida & Bayazit (1973) showed that τ_c^* increases considerably as h/d_{50} becomes low or flow becomes shallower. Shvidchenko & Pender (2000) proved that for low bed slopes and h/d_{50}, the dimensionless particle diameter $d^*_{50}=d_{50}\ (g\Delta/\nu^2)^{1/3}$ play an important role in determining τ_c^*. As per the above discussion and literature review a relationship for critical discharge depending on three parameters viz. d^*_{50}, S and C_u is justified.

On the basis of observed data of experimental study and Robinson et al. (1997); the following relationship has been evolved

$$q_c = (-0.5952\times10^{-6}S + 0.5136\times10^{-6})e^{1.32C_u} \times d_{50}^{*\,(-0.32S+1.42)} \quad (4.16)$$

The proposed Eq. (4.16) is valid within the tested range (4 <S <40%; 850< d*$_{50}$ <4500; 25.4 <γ_s<28.2 kN/m^3) with an error of ±30%. The above relationship is dimensionally non-homogeneous; however this relationship has the greater advantage of directly giving specific critical discharge value which is expressed in m^2/s. The comparison between the calculated critical discharge by the proposed Eq. (4.16) and observed data is shown in Fig. 4.33, which indicates that the predicted critical discharge is within ±30% of the observed one.

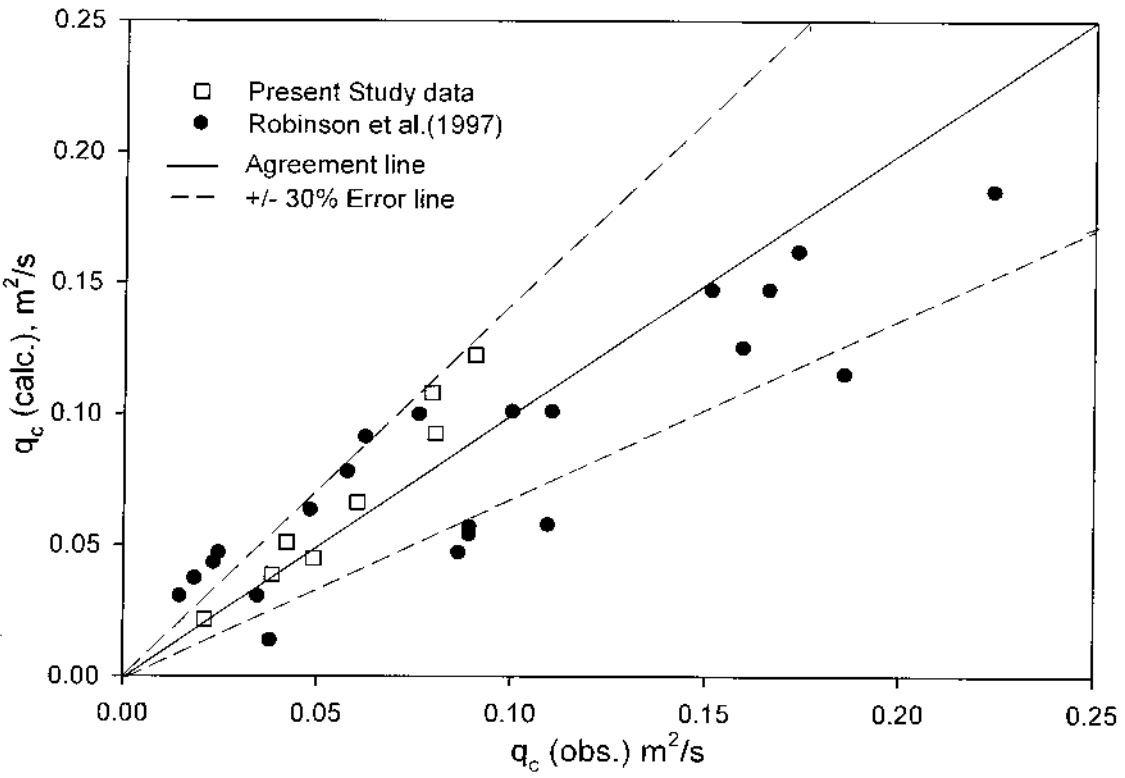

Figure 4.33 Comparison of predicted critical discharge by Eq. (12) with the observed one

As per Pagliara et al. (2010), the greater is the slope, the greater the average air concentration, and the greater the relative depth, the lesser the average air concentration. Air concentration C_a as assumed to have small effect on critical discharge estimation should be included in the relationship for discharge estimation. Hence further study is needed to arrive at for better prediction of critical discharge.

4.9 CONCLUDING REMARKS

Experimental data observed for block ramps in various configurations and with emphasis on the staggered configuration have been analyzed in this chapter. The effects of the various parameters related to the relative energy dissipation were investigated for smooth ramps, block ramps with base material and block ramps under various permutations and combinations of test conditions. The smooth ramp condition was examined to check the consistency of the boulder block ramps in dissipating energy and it was found that the smooth ramp yielded a maximum relative energy dissipation of 56%. Block ramps with base material were investigated in the next analysis, and it was found that this ramp condition yielded a maximum relative energy dissipation of 82%. The angularity of the base material was

analyzed using angular and round stone aggregates, and no prominent variation could be found in their energy dissipation characteristics within the range of tested data. The slope factor showed a dominant role and it was observed that maximum energy dissipation was realized in the steepest slope tested. For the block ramps with boulders, which formed the main component of the study, the variation of relative energy dissipation with respect to the related variables were exhaustively analyzed for each slope under various boulder concentration and configuration. A comparative examination of boulders in rows and staggered configuration reinforced that the staggered configuration generated higher relative energy dissipation. Within the staggered configuration, a subjective analysis was done for the boulder distribution in the form of uniform and non–uniform configurations. It was found that the behavior of the two boulder distributions had varied asymptotes and depended on the boulder size and concentration. From the sequence of analyses, a threshold boulder concentration beyond which there is negligible or diminishing effect on the relative energy dissipation could be earmarked. Certain deductions as the channel width to boulder size ratio were found to characterize the energy dissipation trend along with the boulder configuration for particular slopes. Specific examinations were done to test the variance of the major energy dissipation parameters and it was generally found that along with the flow parameter, the boulder concentration, spacing and size were vital in describing the energy dissipation trend. A relation to determine the longitudinal and transverse spacing of boulders could be derived using previous formulations. A statute analysis was also done to examine the analogy and possible relationship of flow resistance with the energy dissipation factor on boulder block ramps. It could be affirmed that low values of the resistance function depicted higher energy loss on the tested conditions. The multitude of the energy dissipation parameters were examined and analyzed using statistical techniques to select an optimal dataset which best reciprocated the relative energy dissipation function for block ramps with boulders in staggered configuration. The selected optimal dataset were tested for consistency with regard to the representation of the whole dataset observed in the present study. A boulder concentration of 0.23 was found optimal for deriving a relation to estimate the relative energy dissipation factor. Relations are proposed for computing the relative energy dissipation for block ramps with boulders in staggered and non-uniform arrangements using $3/4^{th}$ of the optimal dataset and the same is validated using the remaining $1/4^{th}$ of the dataset with ± 5% error. Conclusively the relations proposed for the estimation of energy dissipation on boulder block ramps with boulders in staggered configuration were validated along with existing relations, and thereby projected as the main outcome of the study.

DESIGN CONSIDERATIONS

This chapter presents the recommendations for the design and application of block ramps with boulders in staggered configuration based on the outcome of the present study. The results of the present study for different configuration of block ramps have been used to formulate design plots and to set guidelines for the respective hydraulic parameters to achieve efficient energy dissipation and aid practical application of block ramps. The existing relations for energy dissipation of flow over the ramp were also adhered while proposing the formulations. A case study, based on the proposed design considerations, is also presented to demonstrate the practical significance of adopting block ramps with staggered boulders for energy dissipation.

5.1 DESIGN APPROACH AND PARAMETERS

An efficient design of an energy dissipator is generally defined as one which provides a smaller and or cheaper structure for the optimum energy dissipation. This philosophy is tangible with block ramps, as these structures are cost–effective due to use of naturally available river stone aggregates or boulders. Design dimensions for energy dissipation structures are critical because an inappropriate design on the contrary, can aggravate erosion and or scouring, as has been manifested in the field and laboratory experiments. There have been cases in which the installation of an energy dissipation structure caused more erosion than that which occurred without it. Various design concepts and recommendations have been developed for block ramps. But no particular guidelines have been assayed with respect to the staggered configuration of boulders in uniform and/or non–uniform distribution. The present study has attempted on this particular aspect.

The theory of hydraulic models emphasizes the equality of all of the dimensionless variables between the model and the prototype as the requirement for full dynamic similarity. In a practical situation, however, this requirement cannot always be fully established and hence, some compromise has to be made for practical design considerations (Vischer and Hager 1995, Khatsuria 2005). In the present study as far as possible, similitude for flow conditions

with the Reynolds number is taken in to consideration as viscous forces were found to correlate healthily with the energy dissipation function on block ramps with boulders. The relative roughness of the macroroughness boulders has been taken acceptable with that simulated by the boulder blocks in the laboratory (Gordon et al., 2004). The boulder concentration and configuration were found to dominate the energy dissipation regime on block ramps in the present study. Within the range of the experimental test and the analyses conducted, the flow and energy dissipation characteristics were considered similar to the prototype because of fully–developed turbulence with only a minor effect on the drag forces (Oertel et al., 2011). It has also been prescribed that the most important scale effects encountered in the modelling of energy dissipators were those conditions that cannot be adequately simulated in the models such as friction, turbulence, air entrainment and release, fluid–structure interaction, etc (Peterka 1964, Khatsuria 2005). By expressing some of these processes implicitly as a function of the flow variables and employing the derivatives of the analyses with the tested conditions, the following design parameters were selected.

(a) Ramp Slope

It has been found that the relative energy dissipation is higher at steeper slopes and gradually decreases as the slope gets flatter. Simultaneously many variations were noted with regard to the energy dissipative trend on each tested slope with the configuration and concentration of boulders. Thereby, the slope of the ramp, though decided by the existing river bed profile, has to be fabricated with the relative consideration of both the boulder concentration and configuration.

(b) Base Material Size

As it was observed that block ramps with base material yielded energy dissipation in the range of 47 to 82 %, with a wider and higher range in the steepest slope tested ($S = 0.20$), the roughness boundary imparted by the angular base material is equally significant. The size distribution of the base material, generally in terms of the median size d_{50}, has to be considered for the bed factor aspect in application of block ramps.

(c) Boulder Size and Concentration

The boulder concentration Γ was found to be the key parameter ascribing the energy dissipation on boulder block ramps. As this factor is calculated from the number of boulders, boulder size in terms of the diameter and channel bed area, it reflects the spatial density of macroroughness elements in the flume (in the laboratory) and in the stream (in the field). The computation of relative energy dissipation has been directly related to this

factor. The boulder size was considered in terms of the flume width ratio (W/D_B) under which certain variants of energy loss magnitude were noted.

(d) Boulder Spacing and Distribution

The longitudinal and transverse spacing of boulders, S_x and S_y are explicit factors of the boulder concentration. However, it was observed that certain spacing of the boulders had characteristic impacts on the relative energy dissipation function for a ramp slope, even though they described a nearly equal concentration. Similarly, regarding the boulder distribution, it has been observed that in particular cases, the non-uniform configurations resulted in efficient energy dissipation than the uniform configurations. Thereby, the longitudinal and transverse spacing of boulders on the ramp have been succinctly considered.

Above all the flow parameter, which is the ratio of the critical flow depth to the effective height of the ramp, has been considered as the principal factor on which the above design parameters has to be selected.

Design discharge corresponds to 25 years frequency shall be taken in the non-urbanized area, however, it should be of 100 years frequency if block ramps shall be provided near the urbanized area.

5.2 DESIGN FORMULATION AND GUIDELINES

The formulation of design principles for block ramps with staggered boulders are based on the hydraulic imperatives derived from the present study. The design considerations assume conditions that are typical for mountain streams, i.e. rivers slope, S of approximately 10 to 20 %; base material size distribution ratio, d_{84}/d_{10} up to a value 1.5; submergence levels, h_c/d_{50} in the range of 1.95 to 5.80. The stability of the boulder blocks were taken with the similitude of boulders protruding with almost half of its height above the river bed in natural mountain streams. The following procedures have been devised with the relative energy dissipation as the primary function.

(a) River Topography and Flow Conditions

It has been stated that block ramps are adopted to provide morphological continuity of the river bed at steep reaches. A longitudinal bed profile of the river reach in consideration should be first prepared so as to mark the sub-reaches with the steepest descents in the river bed. The maximum discharge of the river is then taken to calculate the discharge per unit width of the river reach. Thereby, the critical flow depth can be evaluated. The

critical flow depth is adopted as in steep channel flow, uniform flow conditions do not generally prevail. The reach may require a single block ramp unit or intermediate sets of block ramp units as per the morphological conditions of the river reach. Wherever there are slopes generally greater than 10%, the block ramps with boulders are recommended for effective energy dissipation. The upstream and downstream depths of flow may be measured or computed to evaluate the extent of energy loss required to stabilize the flow.

(b) Dimensions of the Ramp

For general conditions, the height of the ramp may be kept equivalent to the difference in the river bed elevation where an abrupt fall in slope is noted. The height will also depend on the length of the ramp which can be kept equal to the distance of the line joining the two extreme bed elevation points where the drop is noted.

(c) Base Material

The bed of the ramp can be laid with crushed stone aggregate or locally available river-bed stone aggregate. A loose packing of the base material may be suitable for low values of the flow parameter. It is recommended to adopt a rigid packing in the form of grouting with the ramp bed, especially for steeper slopes. This can apply to a base material size distribution ratio, $d_{84}/d_{10} \leq 1.5$.

(d) Estimation of Flow Parameter and Relative Energy Dissipation

The flow parameter is calculated as the ratio of the critical flow depth to the height of the ramp. Initially a boulder concentration Γ between the range of 17 to 30 % can be assumed. Based on this assumed value of Γ and the flow parameter, by using Eq. (4.14) or the relative energy dissipation plot as provided in Fig. 5.1, an initial value of the relative energy dissipation may be estimated. This value may be compared with the energy loss requirement evaluated in (a). The value of Γ may be re-selected to attain to the nearest value of the relative energy dissipation required.

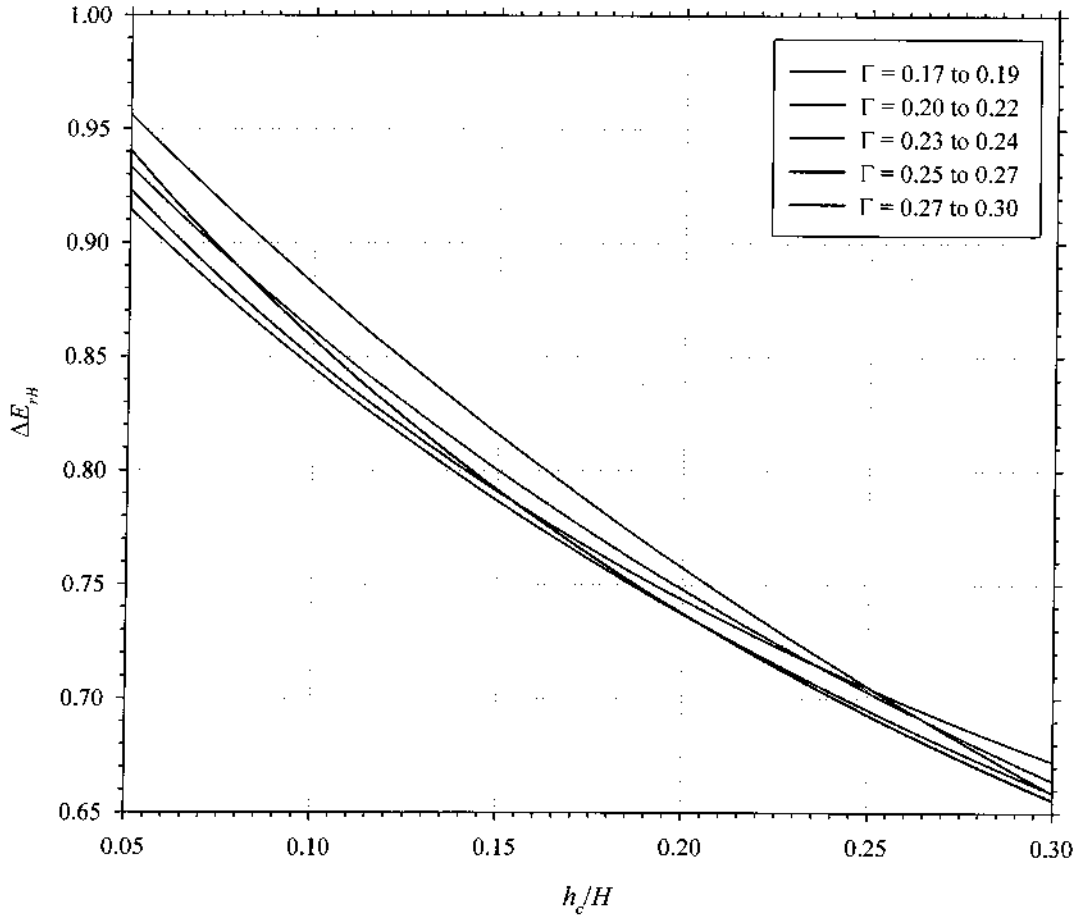

Fig. 5.1 Variation of relative energy dissipation for different boulder concentration.

(e) Boulder Concentration and Size

The selection of the boulder concentration as decided from (c) can be further adjusted with the boulder size in case a specific boulder size needs to be used. This can be done using Eq. (1.5) where the number of boulders can be ordered with the boulder size to suit the design requirements. The boulder size may be selected such that the ratio of width of the channel to the boulder size (W/D_B) is less than or equal to 7.0 to obtain similar conditions in the field as observed in the laboratory. As it has been observed that this ratio can describe the boulder configurations responsible for variant relative energy dissipation trends, W/D_B has to be given equal importance during the design process.

(f) Boulder Spacing and Distribution

The clear longitudinal and transverse spacing of boulders (S_x and S_y respectively) for staggered configurations can be evaluated holistically using Eq. (4.7) by assuming an initial value of S_y and using the value of boulder concentration derived in (d) or (e). However, this parameter has been found to produce different relative energy dissipation trends for a similar clear longitudinal spacing. The ratio of longitudinal spacing to boulder diameter, S_x / D_B was used to relate this parameter with the other dimensionless parameters. The boulder spacing can be adopted for a known boulder concentration with respect to the flow parameter using Fig. 5.2. This S_x / D_B should be selected upto a maximum of 4.0 to convene with the present design formulations. For steep slopes (as $S =$ 0.20), the boulder spacing criteria may not be applicable for boulders with $W/D_B \leq 3.0$. On flatter slopes, the non-uniform boulder distribution may be adopted when relatively large boulder sizes are to be used. For design practices, it is recommended to use smaller boulder distances in order to reduce boulder drag forces and reduce the flow velocity. Boulders are arranged in the staggered configuration to distribute the flow and create a recurring pattern of subcritical and supercritical flow state.

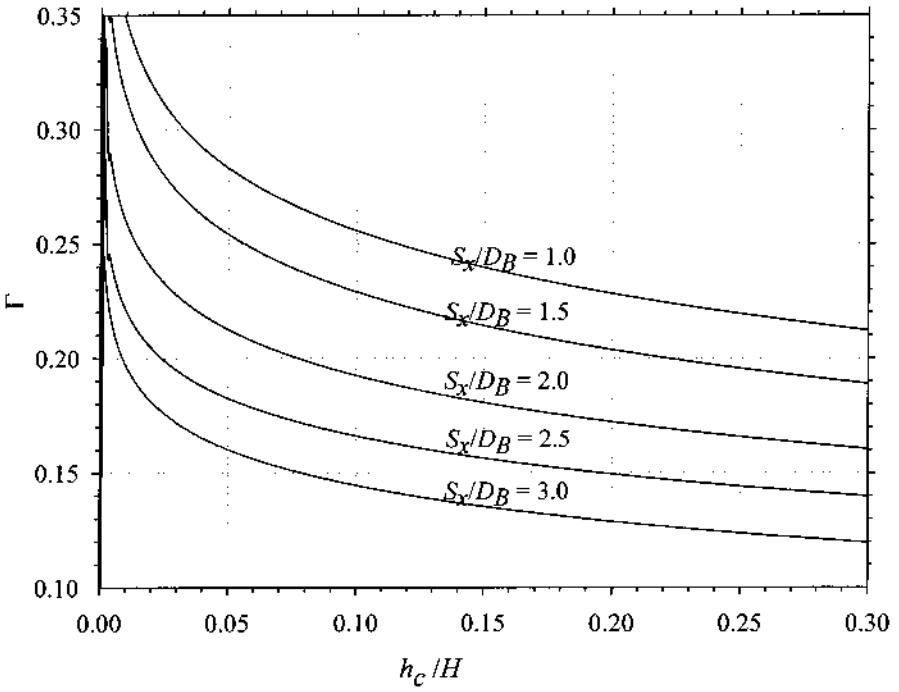

Fig. 5.2 Chart to determine the boulder spacing factor with respect to boulder concentration

5.3 CASE STUDY AND APPLICATION EXAMPLE

The Ranganadi river which is a major tributary of the Brahmaputra river, is ascribed with a perennial problem of flow instability due to recurrent flash flood flows and a hydroelectric power plant which regulates the flow in its upstream reaches. The river originates in the interlocked Nilam, Marta and Tapo mountain ranges of the state of Arunachal Pradesh at an elevation of 1124 metres above sea level and flows down to the valley of Lakhimpur district in Assam, India. A depiction of the river using a false colour composite (FCC) derived from satellite image (IRS LISS-3 MX) as acquired on 06–01–2010 is shown in Fig. 5.3. The river is characterized with a steep bed profile and abrupt drops in the river bed as shown in Fig. 5.4. Especially at the reach where the river descends into the plain valley region (shown by the yellow box in Fig. 5.3) there are abrupt drops in the river bed with gradients of the order of 12 % and this river reach may suitably be selected for the application of block ramps.

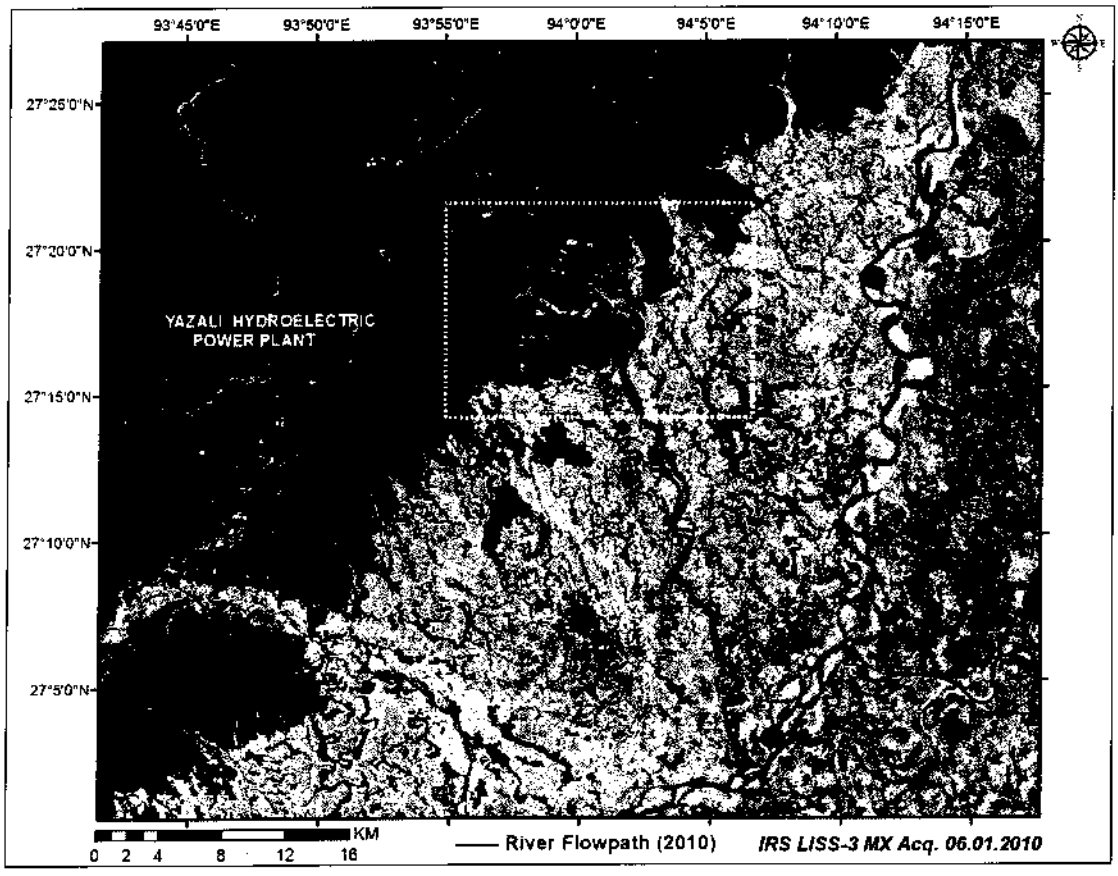

Fig. 5.3 Location of Ranganadi River and the selected river reach (highlighted in yellow box)

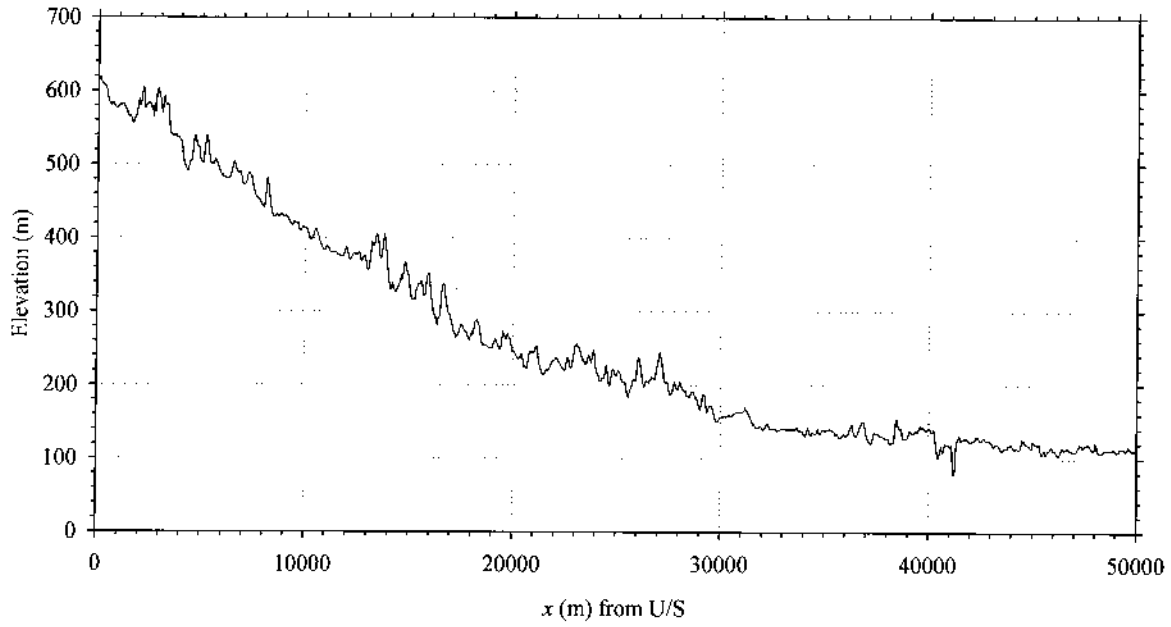

Fig. 5.4 Longitudinal bed profile of the Ranganadi River (U/S section taken at HEP site)

The river has undergone a lot of morphological changes with regard to its flow path and has been causing erosion at the downstream reaches affecting the livelihood of the people. The bed level has also undergone recursive aggradation and degradation posing challenges in the river management (Mahanta et al., 2011).

Application of Block Ramp:

The river is stipulated to have a design flood discharge of 73 m^3/s. A stretch of 50 m in the river reach with an abrupt gradient of 0.11 was selected for application of block ramps with boulders. The downstream portion of the selected river reach has a slope of 0.06 showing disturbed riparian conditions of the river. The river in this reach was presumed to have gravels and boulders in its natural state. The discharge per unit width was computed for the selected river reach taking a uniform river width of 30 m using the maximum design flood discharge. For the purpose of design calculations, it is presumed that uniform flow conditions were prevalent at the upstream and downstream of the selected reach.

The computations for evaluating the required relative energy loss with respect to the downstream section of the river reach and other design parameters under consideration are given as,

Slope of the river reach, S	=	0.11	
Length of the reach, L	=	50 m	
Manning's coefficient	=	0.035	(assumed arbitrarily)
Discharge per unit width, q	=	2.43 m^3/s /m	
Critical flow depth, h_c	=	0.85 m	
Flow depth downstream, h_t	=	0.53 m	(using normal depth conditions)
Energy at U/S section, E_0	=	7.27 m	(for a drop of 6 m)
Energy at D/S section, E_t	=	1.60 m	(using specific energy criteria)
Relative Energy Loss	=	(7.27 – 1.60)/7.27 = 0.78	

It can considered that block ramp with boulders can be applied to achieve the 78% relative energy dissipation required to maintain continuity in the flow conditions. Using either Eq. (4.14) or Fig. 5.1, for this relative energy dissipation and with respect to the flow parameter, the boulder concentration can be accordingly determined. Then the general relation, Eq. (1.5) can be used to evaluate the number of boulders and boulder size as suitable.

Block Ramp parameters (using boulders)

Slope of the ramp, S	=	0.11	
Length of the ramp, L_R	=	50 m	
Height of the ramp, H	=	6.00 m	
Flow parameter, h_c/H	=	0.85/6.0 = 0.14	
Base material size, d_{50}	=	0.05 m	
Boulder concentration, Γ	=	0.23	(using Fig. 5.1 or Eq. 4.14)
Boulder diameter, D_B	=	0.60 m	(using Eq. 1.5)
Number of boulders, N_B	=	1220	
Spacing of boulders, S_x/D_B	=	1.5	(using Fig. 5.2)
Spacing of boulders, S_y/D_B	=	0.7	(taking half of S_x/D_B, or using Eq.5.2)
Configuration/Distribution	=	Staggered/Uniform	

It can be noted that the application of boulders in staggered configuration are generally for packed conditions on the block ramps with base material grouted on the river bed. The downstream depth of flow as computed and attainable after the block ramps application should provide a higher specific discharge to maintain the continuity of flow. It can be further checked if these alterations in the flow conditions will be viable with the actual site conditions, and the process may be repeated to arrive at a site–suitable design.

5.4 CONCLUDING REMARKS

The derivations and findings of the present study have been used to frame design parameters and plots for block ramps with boulders for practical applications. The presumptions and relevance of each parameter were presented with the design recommendations with the relevance on energy dissipation. Guidelines for the application of block ramps have been listed along with the suitable criteria or values of the respective parameters. The significance of the design guidelines and effectiveness of boulder block ramps for field application was demonstrated with a case study.

Placement of the boulders on the ramp of designed slope shall be placed as per the designed configuration so that ramp should not fail due to poor quality of construction.

CONCLUSIONS AND SCOPE FOR FUTURE STUDY

The present study was endeavored to delve the energy dissipation characteristics on block ramps. Experiments were conducted and tailored to meet the objectives of the study. The analyses for different configurations of block ramps under varying flow conditions were carried out to arrive at the primary hydraulic variables that ascribed the energy dissipation on block ramps. The present study has been focused on the staggered configuration of boulders on block ramps in variant permutations and combinations of boulder spacing and with the statute that it has higher energy dissipation characteristics than the rows or random configuration. The existing relationships and associated parameters for energy dissipation on block ramps were tested using the collected dataset. The variables were examined and analyzed implicitly or explicitly for its effect on the energy dissipation, from which deductions were made to select the relevant governing parameters. Relations for estimating the energy dissipation on boulder block ramps with staggered configuration of the boulders have been proposed in the similitude range of the tested conditions. The derivations made from the detailed analyses permitted formulation of design guidelines and plots that can aid water resources engineers and planners in practical applications of boulder block ramps. The design methodologies have been formulated by also taking the philosophy of relevant studies and findings reported for block ramps and similar stream restoration structures. The element of block ramp application in the field has been demonstrated with a case study highlighting the riparian river conditions and the effectiveness of the design approach.

6.1 CONCLUSIONS DERIVED FROM THE STUDY

The following conclusions have been derived from the analysis of data of the experimental study carried out on block ramps in various configurations. The inferences obtained have been concentrated on block ramps with boulders in staggered configuration.

- In general, it was found that relative energy dissipation (ΔE_r or ΔE_{rB}) increases with the steeper slopes in various conditions of block ramps in the tested conditions $0.07 \leq h_c/H \leq 0.26$. While, there is no significant variation in $\Delta E_{rB}/\Delta E_r$ with slope..

- The Reynolds number was found to range from 2.55×10^4 to 10.68×10^4 with a distinct association for each tested slope with respect to the relative energy dissipation in the tested conditions. The Froude number was found to range from 1.64 to 3.98 and had low correlation with the relative energy dissipation in the tested conditions.
- On the smooth ramp, it was found that relative energy dissipation on the tested ramp slopes: for 1V:5H in the range of 54 to 71 %, for 1V:7H in the range of 30 to 49 % and for 1V:9H in the range of 12 to 35 %. When the relative energy dissipation was evaluated using the Pagliara and Chiavacinni (2006a) equation with the observed dataset, it was inferred that the computed relative energy dissipation was in parity with observed values for 1V:5H sloped ramp. However, the same relation estimates the relative energy dissipation for the other two slopes i.e. 1V:7H and 1V:9H, by more than 10%.
- On the block ramps with base material, intermediate roughness conditions were found to mainly prevail for the tested range of base material with $1.95 \leq h_c/d_{50} \leq 5.81$. The rate of energy dissipation was found to gradually decrease with increase in h_c/H and with descent of the ramp slope. Few indications were found that the block ramp with $S \leq 0.14$ can dissipate more energy than at steeper slopes within $0.10 \leq h_c/H \leq 0.26$.
- No significant effect between the angular and round base material (for the same d_{50} size) was being found ascribing the relative energy dissipation function on block ramps with base material in the tested conditions ($0.07 \leq h_c/H \leq 0.26$).
- For block ramps with base material, the relative energy dissipation ΔE_r on the tested ramp slopes found were: for 1V:5H in the range of 67 to 82 %, for 1V:7H in the range of 61 to 73 % and for 1V:9H in the range of 48 to 63 %. When compared with the smooth ramp for each respective slope, a significant increase in the relative energy dissipation was found with base material. The difference increased as the ramp slope gets flatter ($S \leq 0.20$).
- When the observed relative energy dissipation on block ramps with base material was compared with that evaluated using the Pagliara and Chiavacinni (2006a) relation, an overestimation by more than 5% of the ΔE_r values were noted for $0.07 \leq h_c/H \leq 0.26$.
- The values of the two roughness parameters E and F (functions of arrangement and roughness of boulders), which was postulated by Pagliara and Chiavacinni (2006b) were found to be 0.23 and 11.6 respectively, for boulders in rows arrangement and rounded (smooth) condition in the present study. The new values of these two

parameters can be considered more suitable for larger boulder sizes ($D_B \geq 0.042$ m) from that adopted by the authors in their study.

- It was found that the boulder block ramps with staggered configuration yielded higher energy dissipation than the rows configuration, for same longitudinal spacing of boulders of same size and test conditions ($\Gamma = 0.10 - 0.12$ and $0.07 \leq h_c/H \leq 0.26$). This is in congruence with the findings of Ahmad et al. (2009).
- On the 1V:5H sloped–boulder block ramp, closer spacing with $S_x/D_B \leq 1.5$ and certain non-uniform configurations exhibited higher dissipation of energy than the uniform distribution on the boulder block ramp with staggered configuration.
- For larger boulders with $W/D_B \leq 3.0$ on the 1V:5H ramp slope, it was found that there is negligible effect of the boulder spacing and distribution on the relative energy dissipation ΔE_{rB} as depicted by the 0.10 m diameter boulders in the tested conditions ($0.05 \leq h_c/H \leq 0.12$).
- For the 1V:5H sloped–boulder block ramp, the relative energy dissipation observed was between 73 – 92 % for the range of various boulder concentration using five boulder sizes in the flow parameter range $0.05 \leq h_c/H \leq 0.12$, and it was found that ΔE_{rB} decreases appreciably as the flow parameter h_c/H increases.
- On the 1V:7H sloped–boulder block ramp, intermingling trends of the relative energy dissipation were observed. For the smaller–sized boulders ($D_B \leq 0.055$ m), larger spacing exhibited slightly higher dissipation of energy than that ascribed by the closer spacing ($S_x/D_B \leq 1.5$).
- The non–uniform distribution in the staggered configuration of boulders on the 1V:7H sloped–boulder block ramp exhibited higher dissipation of energy than the uniform distribution especially in the case with bigger boulders for $D_B \geq 0.080$ m.
- For the 1V:7H sloped–boulder block ramp, the relative energy dissipation observed was between 74 – 83 % for a boulder concentration range of $\Gamma = 0.14 - 0.29$ and flow parameter range $0.14 \leq h_c/H \leq 0.29$.
- No significant effect of the boulder spacing or distribution was found for the smaller boulder size tested ($D_B = 0.042$ m and 0.055 m) on the 1V:9H sloped–boulder block ramp. This condition was also found on the 1V:7H sloped–boulder block ramp. Hence it can be affirmed that at slopes $S \leq 0.11$ for $W/D_B \geq 5.5$, the boulder spacing and distribution is not significant in describing the relative energy dissipation within the test conditions.

- The non–uniform (NU–4) configuration exhibited higher dissipation of energy than the other tested configurations in the case of bigger–sized boulders (for D_B = 0.065 m and 0.080 m) on the 1V:9H sloped–boulder block ramp.
- For the 1V:9H sloped–boulder block ramp, the relative energy dissipation observed was in the range of 67 to 77 % for the flow parameter range $0.18 \leq h_c/H \leq 0.26$, and ΔE_{rB} decreases considerably as the flow submergence increases, for the range Γ = 0.19 – 0.29.
- It was found that there was a rise in the relative energy dissipation trend with increase of boulder concentration upto a certain range of Γ beyond which further increase of boulder density led either to decay of the $\Delta E_{rB}/\Delta E_r$ function or it remained constant. This threshold boulder concentration was found to be in the range 0.22 – 0.25 for the tested boulder sizes and configurations ($0.08 \leq \Gamma \leq 0.32$).
- The analogy of flow resistance with the relative energy dissipation on boulder block ramps have been examined in terms of the resistance function $(8/f)^{1/2}$ and it was found that this function varied inversely with the relative energy dissipation function, asserting that higher flow resistance described by the friction factor f, showed increase in the energy dissipation on boulder block ramps.
- A modified relation based on the Sayre and Albertson's (1961) relation has been presented to evaluate the longitudinal and transverse spacing of boulders on block ramps with staggered boulders. The relation Eq (4.7) may be satisfactorily used for block ramp applications for the range Γ = 5 to 35 %.
- A relation (Eq. 4.13) has been formulated for computation of relative energy dissipation on block ramps with staggered configuration of boulders. The relation can be used satisfactorily within ± 5% error limits for the range Γ = 0.17 – 0.30 and $0.05 < h_c/H < 0.29$. The same relation has been also presented in terms of coefficients which are specific for particular boulder ranges as given by Eq. (4.14) to provide more accurate estimation of ΔE_{rB} in practical applications of boulder block ramps.
- Design recommendations and guidelines for practical application of boulder block ramps have been formulated based on the findings of the present study.
- The critical discharge for the stability of the block ramp increases with non-dimensional parameter d^*_{50} while decreases with chute slope. The critical discharge also increases exponentially with the increase in uniformity coefficient of the boulders.

- The data of Robinson et al. (1997) and present study are used to arrive at a specific relationship, i.e. Eq. (4.16) for critical discharge estimation at local failure. The proposed relationship satisfactorily estimates the critical discharge at local failure with 30% error.
- Due to scale effect, aeration in flow was not noticed downstream of the block ramp for all the range of data.

6.2 FUTURE SCOPE OF WORKS

It can be thus accomplished that the present study has delved upon the energy dissipation characteristics on block ramps analysis for different configurations of block ramps under varying flow conditions, and with particular focus on the staggered configuration of boulders. The range of test conditions may be exemplified for wider applicability of the relations and design charts for application of block ramps. The limited flow depths entailed during the experimental study, especially at steep slopes, posed constraints to fathom the highly turbulent flow structure on boulder block ramps. This can be taken up as an important theme to be profoundly explored, and boost the functionality of such viable stream restoration structures. Further, performance of the block ramps in the curved channels may be worth investigated. For the stability of a boulder ramp against the likely scour at its toe, it is required that a detailed study shall be carried out in this respect.

References

1. Aberle, J. (2007). *Hydraulik von Blockrampen. Mitteilungen der Versuchsanstalt für Wasserbau*, Hydrologie und Glaziologie, ETH Zürich, Nr. 201, pp.137–159 (in German).
2. Aberle, J. and Smart, G. M. (2003). "The influence of roughness structure on flow resistance on steep slopes." *Journal of Hydraulic Research, IAHR*, 41(3), pp. 259–269.
3. Abrahams, A. D. and Parsons, A. J. 1990. "Determining the mean depth of overland flow in field studies of flow hydraulics." *Water Resources Research*, 26, 501–503.
4. Abt, S. R., Wittler, R.J., Ruff, J.F., LaGrone, D.L., Khattak, M.S., and Nelson, J.D. (1987). "Development of riprap design criteria by riprap testing in flumes: Phase I." *Laboratory Investigation Report*, NUREG/CR-4651, 2, Colorado State University, Fort Collins, CO 80523, USA.
5. Abt, S. R., Wittier, R. J., Ruff, J. E, and Khattak, M. S. (1988). "Resistance to flow over riprap in steep channels." Water Resour. Bull., 24(6), pp. 1193–1200.
6. Afzalimehr, H. and Anctil, F. (2001). "Friction velocity associated to a non-uniform flow and an intermediate scale roughness." *Journal of Hydraulic Research, IAHR*, 39(2), pp. 181–186.
7. Aguirre-Pe, J. and Fuentes, R. (1990). "Resistance to flow in steep rough streams." *Journal of Hydraulic Engineering, ASCE*, 116(11), pp. 1374–1387.
8. Ahmad, Z. Pentappa, N. M. and Westrich, B. (2009). "Energy dissipation on block ramps with staggered boulders." *Journal of Hydraulic Engineering, ASCE*, 135(6), pp 522–526.
9. Anderson, A. G., Paintal, A. S., and Davenport, J. T. (1970). "Tentative design procedure for riprap lined channels." *NCHRP Report*, 108, Hwy. Res. Board, Nat. Acad. of Sci.-Nat. Acad. of Engrg., Washington, D.C.
10. Baiamonte, G., Giordano, G. and Ferro, V. (1995). "Advances on velocity profile and flow resistance law in gravel bed rivers." *Excerpta*, 9, pp. 41–89.
11. Baiamonte, G. and Ferro, V. (1997). "The influence of roughness geometry and Shield's parameter on flow resistance in gravel-bed channels." *Earth Surface Processes and Landforms*, 22, pp. 759–772.
12. Bathurst, J. C. (1978). "Flow resistance of large-scale roughness." *Journal of Hydraulic Division, Proceedings, ASCE*, 104, HY12, pp 1587–1603.
13. Bathurst, J. C., Li, R. M. and Simons, D. B. (1981). "Resistance equation for large scale roughness." *Journal of Hydraulic Engineering, ASCE*, 107 (12), pp 1593–1613.
14. Bathurst, J. C. (1985). "Flow resistance estimation in mountain rivers." *Journal of Hydraulic Engineering, ASCE*, 111(4), pp. 625–643.
15. Bathurst, J.C. (2002). "At-a-site variation and minimum flow resistance for mountain rivers." *Journal of Hydrology*, 269, Elsevier, pp. 11–26.
16. Bombardelli, F.A., Meireles, I. and Matos, J. (2011). "Laboratory measurements and multi-block numerical simulations of the mean flow and turbulence in the non-aerated

skimming flow region of steep stepped spillways." *Journal of Environmental Fluid Mechanics*, 11(3), pp. 263–288.

17. Canovaro, F. and Solari, L. (2007). "Dissipative analogies between a schematic macro-roughness arrangement and a step-pool morphology." *Earth Surface Processes and Landforms*, 32, pp. 1628–1640.
18. Canovaro, F., Paris, E. and Solari, L. (2007). "Effects of macro-scale bed roughness geometry on flow resistance." *Water Resources Research*, 43, W10414.
19. Carling, P.A. (1991). "An appraisal of the velocity-reversal hypothesis for stable pool-riffle sequences in the River Severn, England." *Earth Processes and Landforms*, 16, pp. 19–31.
20. Chinnarasri, C and Wongwises, S. (2006). "Flow patterns and energy dissipation over various stepped chutes." *Journal of Irrigation and Drainage Engineering, ASCE*, 132(1), pp. 70–76.
21. Christodoulou, G. C. (1993). "Energy dissipation on stepped spillways." *Journal of Hydraulic Engineering, ASCE*, 119(5), pp. 644–650.
22. Chamani, M. R., and Rajaratnam, N. (1999a). "Characteristics of skimming flow over stepped spillways." *Journal of Hydraulic Engineering, ASCE*, 125(4), pp. 361–368.
23. Chamani, M. R., and Rajaratnam, N. (1999b). "Onset of skimming flow on stepped spillways." *Journal of Hydraulic Engineering, ASCE*, 125(9), pp. 969–971.
24. Chanson, H. (1993a). "Self-aerated flows on chutes and spillways." *Journal of Hydraulic Engineering, ASCE*, 119(2), pp. 220–243.
25. Chanson, H. (1993b). "Stepped spillway flows and air entrainment." *Canadian Journal of Civil Engineering*, 20(3), pp. 422–435.
26. Chanson, H. (1994). "Hydraulics of nappe flow regime above stepped chutes and spillways." *Australian Civil Engineering Trans.*, I.E.Aust., CE36 (1), pp 69–76.
27. Chanson, H. (1999). "Energy dissipation and drop structures in ancient times: the Roman dropshafts." *Proceedings, Water 99 Joint Congress*, Brisbane, Australia, 6–8 July, pp. 987–992.
28. Chanson, H. (2002). *The Hydraulics of Stepped Chutes and Spillways*. Taylor and Francis, USA, ISBN-10: 9058093522.
29. Chen, C. L. (1992). "Momentum and energy coefficients based on power-law velocity profile." *Journal of Hydraulic Engineering, ASCE*, 118(11), pp. 1571–1584.
30. Chow, V.T. (1959). *Open Channel Hydraulics*. McGraw-Hill Book Company Inc., USA.
31. Church, M. and Zimmermann, A. (2007). "Form and stability of step-pool channels." *Water Resources Research, AGU*, 43, W03415.
32. Clark, S.P., Tsikata, J.M., and Haresign, M. (2010). "Experimental study of energy loss through submerged trashracks." *Journal of Hydraulic Research, IAHR*, 48(1), pp.113–118.
33. Curran, J. C. and Wilcock, P. R. (2005). "Characteristic dimensions of the step–pool bed configuration: An experimental study." *Water Resources Research*, 41(2), W02030.

34. Dunne, T. and Dietrich, W. E. (1980). "Experimental study of Horton overland flow on tropical hillslopes: II, Hydraulic characteristics and hillslope hydrographs." *Zeitschrift fur Geomorphologie, Supple band,* 35, pp. 60–80.

35. Emmett, W. W. (1970). "The hydraulics of overland flow on hillslopes." *United States Geological Survey, Professional Paper*, 662–A.

36. Erpicum, S., Meile, T., Dewals, B.J., Pirotton, M. and Schleiss, A.J. (2009). "2D Numerical flow modeling in a macro-rough channel." *International Journal for Numerical Methods in Fluids*, 61(11), pp. 1227–1246.

37. Federal Interagency Stream Restoration Working Group. (1998). *Stream Corridor Restoration: Principles, Processes, and Practices. National Engineering Handbook,* Part 653, United States Dept. of Agriculture – Natural Resources Conservation Service, FISRWG (15 Federal agencies of the US Govt.), USA.

38. Ferro, V. (1999). "Friction factor for gravel bed channel with high boulder concentration." *Journal of Hydraulic Engineering, ASCE*, 125(7), pp. 771– 778.

39. Ghare, A.D., Ingle, R.N., Porey, P.D., and Gokhale, S.S. (2010). "Block ramp design for efficient energy dissipation." *Journal of Energy Engineering, ASCE,* 136(1), pp. 01–05.

40. Golubtsov, V.V. (1969). "Hydraulic resistance and formula for computing the average flow velocity of mountain rivers." *Soviet Hydr.*, 5, pp. 500–511.

41. Gordon, N.D., McMahon T.A., and Finlayson, B.L. (2004). *Stream Hydrology: An Introduction for Ecologists*. 2nd ed., John Wiley and Sons Ltd, West Sussex, PO19 8SQ, England.

42. Hartung, F. and Scheuerlein, H. (1967). "Macroturbulent flow in steep open channels with high natural roughness." *Proceedings, XII IAHR Congress*, 1, Sept 11-14, Fort Collins, Colarado, USA , pp 01–08.

43. Herbich, J. B. and Shulits, S. (1964). "Large–scale roughness in open channel flow." *Journal of the Hydraulics Division, ASCE*, 90(6), pp. 203–230.

44. Hunziker, Z. and Partner A.G. (2008). *Blockrampen Normalien.* Manual zur Sanierung von Abstürzen, Projekt Nr.A-300 (in German).

45. Janisch-Breuer, T. (2006). "Aufgelöste Blockrampen im Modellversuch – Untersuchungen an der VAW." *Mitteilungen, 201, Minor, H.E. (ed.), Blockrampen Anforderungen und Bauweisen,* Workshop der Versuchsanstalt für Wasserbau, Hydrologie und Glaziologie (VAW), ETH Zürich, Zürich, 63–79 (in German).

46. Janisch-Breuer, T. and Tamagni, S. (2008). "Physikalische Modellversuche zur Stabilisierung der Flusssohle mittels unstrukturierter Blockrampen." Mitteilungen der Versuchsanstalt für Wasserbau, Hydrologie und Glaziologie (VAW), ETH Zürich, Nr. 208, 965–974 (in German).

47. Jarrett, R. D. (1984). "Hydraulics of high-gradient streams." *Journal of Hydraulic Engineering, ASCE*, 110(11), pp. 1519–1539.

48. Jarrett, R. D. (1988). "Hydrologic and hydraulic research in mountain rivers." *Proceedings, Hydrology of Mountain Areas, Štrbské Pleso Workshop*, Czechoslovakia, IAHS Publication 190, 1990, pp. 107–117.

49. Järvelä, J. (2002). "Determination of flow resistance of vegetated channel banks and flood–plain." *Proceedings, River Flow 2002*, Louvain-La-Neuve (Belgium), September 4 – 6, 1, pp. 311 – 318.

50. Jimenez, J. (2004). "Turbulent flows over rough walls." *Rev. Fluid Mechanics, Annuls,* 36,pp. 173–96.

51. Kavianpour, M.R. and Masoumi, H.R. (2008). "New approach for estimating of energy dissipation over stepped spillways." *International Journal of Civil Engineering*, 6(3), pp. 230 – 237.

52. Keller, E.A. (1970). "Areal sorting of bed-load material: The hypothesis of velocity reversal". *Geological Society of America Bulletin*, 82, pp.753–756.

53. Keller, R.J. and Haupt, L.J. (2000). "The influence of rock ramp fishways on the hydraulic characteristics of weirs". *Proceedings, Third Australian Technical Workshop on Fishways,* (http://www-heb.pac.dfo-mpo.gc.ca/congress/2000/Papers/migrationpdf/keller.pdf).

54. Khatsuria, R.M. (2005). *Hydraulics of Spillways and Energy Dissipators*. Marcel Dekker, 270 Madison Avenue, New York 10016, USA.

55. Kucukali, S. and Cokgor, S. (2008). "Laboratory measurements of 3-D flow patterns and turbulence in straight open channel with rough bed." *Journal of Hydraulic Research, IAHR*, 46(3), pp 415–419.

56. Lawrence, D. S. L. (1997). "Macroscale surface roughness and frictional resistance in overland flow." *Earth Surface Processes and Landforms*, 22, pp. 365–382.

57. Lyn, D. A. (1993). "Turbulence measurements in open-channel flows over artificial bed forms." *Journal of Hydraulic Engineering, ASCE*, 119(3), pp 306–325.

58. Maynord, S. T. 1988. "Stable Riprap Size for Open Channel Flows," Technical Report HL-88-4, US Army Engineer Waterways Experiment Station, Vicksburg, Ms

59. .Mahanta, C., Sarma, A.K. and Sarma, B. (2011). "Water quality degradation in the tributaries of the Brahmaputra-Barak basin and their environmental management strategy." *Proceedings., World Environmental and Water Resources Congress 2011: Bearing Knowledge for Sustainability, ASCE*, doi:10.1061/41173(414)483.

60. Marchand, J. P., Jarrett, R.D. and Jones, L.L. (1984). "Velocity profile, water-surface slope, and bed-material size for selected streams in Colorado." *USGS Open File Report*, pp. 84–733.

61. Maryland Department of the Environment. (1999). *Maryland's Waterway Construction Guidelines*, USA.

62. Matos, J. (2000). "Hydraulic design of stepped spillways over RCC dams." *International Workshop on Hydraulics of Stepped Spillways,* Zürich, Switzerland, H.E. Minor sand W.H. Hager (Eds.), Balkema, pp. 187– 94.

63. Matos, J., Frizell, K. H., Andre, S., and Frizell, K. W. (2002). "On the performance of velocity measurement techniques in air water flows." *Proceedings, Intl. ASCE – Hydraulic Measurements and Experimental Methods Conference,* Estes Park, Colorado, USA.

64. Mohanty, P. K. (1957). "The Dynamics of Turbulent Flow in Steep, Rough, Open channels." *Ph.D. Thesis,* Utah State University, Logan, USA.

65. Morris, H. M. (1955). "A new concept of flow in rough conduits." *Transactions, Hydraulics Division, ASCE*, 120, pp. 373–398.

66. Morris, H. M. (1959). "Design methods for flow in rough conduits." *Journal of the Hydraulics Division, Proceedings, ASCE*, 85(7), pp. 43–62.

67. Morris, H. M. (1968). "Hydraulics of energy dissipation in steep, rough channels." *Bulletin* 19, Research division, Virginia Polytechnic Institute, USA.

68. Nikora, V. I., Goring, D. G., McEwan, I. and Griffiths, G. (2001). "Spatially averaged open channel flow over rough bed." *Journal of Hydraulic Engineering, ASCE*, 127(2), pp.123– 133.

69. Nikora, V., Koll, K., McEwan, I., McLean, S. and Dittrich, A. (2004). "Velocity distribution in the roughness layer of rough-bed flows." *Journal of Hydraulic Engineering, ASCE*, 130(10), pp. 1–7.

70. North Carolina State University Stream Restoration Institute. (2004). *Proceedings, Southeastern Regional Conference on Stream Restoration*, NCSRI, Raleigh, NC 27695-8605, USA (http://www.ncsu.edu/sri/).

71. Oertel, M. (2010). "Simulating cross-bar block ramps with *FLOW-3D*." *Application Note, Flow Science, FLOW-3D* News: Fall 2010. *(*http://www.flow3d.com/resources/*news_10/FLOW-3D-newsletter-simulation-contest-winner-fall-2010.html).*

72. Oertel, M., Peterseim, S., and Schlenkhoff, A. (2011). "Drag coefficients of boulders on a block ramp due to interaction processes." *Journal of Hydraulic Research, IAHR*, 49(3), pp. 372 – 377.

73. Oertel, M. and Schlenkhoff, A. (2012). "Crossbar block ramps: flow regimes, energy dissipation, friction factors, and drag forces." *Journal of Hydraulic Engineering, ASCE*, 138 (5), pp. 440–448.

74. Pagliara, S. and Dazzini, D. (2002). "Hydraulics of block ramp for river restoration." *Proceedings, 2nd International Conference on New Trends in Water and Environmental Engineering for Safety and Life: Eco-compatible Solutions for Aquatic Environments*, Capri, Italy.

75. Pagliara, S. and Pozzolini, S. (2003). "The effects of large boulders on the hydraulics of unsubmerged block ramps." *Proceedings, XXX IAHR International Conference*, Thessaloniki, Greece, pp.199–206.

76. Pagliara, S. and Chiavaccini, P. (2004). "Stability of reinforced block ramp." *Proceedings, River Flow 2004* – Greco, Carravetta, and Della Morte (eds.), Taylor and Francis, London.

77. Pagliara, S. and Chiavaccini, P. (2006a). "Energy dissipation on block ramps." *Journal of Hydraulic Engineering, ASCE*, 132 (1), pp. 41–48.

78. Pagliara, S. and Chiavaccini, P. (2006b). "Energy dissipation on reinforced block ramps." *Journal of Irrigation and Drainage Engineering, ASCE*, 132(3), pp. 293–297.

79. Pagliara, S. and Chiavaccini, P. (2006c). "Flow resistance of rock chutes with protruding boulders." *Journal of Hydraulic Engineering, ASCE*, 132(6), pp. 545–552.

80. Pagliara, S., Das, R. and Palermo, M. (2008a). "Energy dissipation on submerged block ramps." *Journal of Irrigation and Drainage Engineering, ASCE*, 134(4), pp. 527–532.

81. Pagliara, S., Lotti, I. and Palermo, M. (2008b). "Hydraulic jump on rough bed of stream rehabilitation structures." *Journal of Hydro-environment Research, IAHR*, 2(1), pp. 29–38.

82. Pagliara, S., Das, R. and Carnacina, I. (2008c). "Flow resistance in large-scale roughness condition." *Canadian Journal of Civil Engineering*, 35, pp.1285–1293.

83. Pagliara, S. and Palermo, M. (2008d). "Scour downstream of a block ramp in asymmetric stilling basins." *Proceedings, Fourth Intl., Conf., on Scour and Erosion,* November 2008, Tokyo, Japan, pp. 240–245.

84. Pagliara, S., Roshni, T. and Carnacina, I. (2009a). "Aeration and velocity profile over block ramp elements." *Proceedings, 33rd IAHR Congress: Water Engineering for a Sustainable Environment*, pp. 4925– 4932.

85. Pagliara, S., Palermo, M. and Carnacina, L. (2009b). "Scour and hydraulic jump downstream of block ramps in expanding stilling basins." *Journal of Hydraulic Research, IAHR*, 47(4), pp. 503–511.

86. Pagliara, S. and Palermo, M. (2012). "Effect of stilling basin geometry on the dissipative process in presence of block ramps." *Journal of Irrigation and Drainage Engineering, ASCE,* 138(11), pp. 1027–1031.

87. Patel, V. C. (1998). "Perspective: flow at high Reynolds number and over rough surfaces-Achilles heel of CFD." *Journal of Fluids Engineering, ASME,* 120, pp. 434–444.

88. Peruginelli, A. and Pagliara, S. (2000). "Energy dissipation comparison among stepped channel, drop and ramp structures." *Hydraulic of Stepped Spillways*, Minor & Hager (eds), Balkema, Rotterdam, Netherlands, pp. 111–118.

89. Peterka, A.J. (1964). *Hydraulic design of stilling basins and energy dissipaters. Engineering Monograph*, 25, US Bureau of Reclamation: Denver, Colorado, USA.

90. Peterson, F. and Mohanty, P. K. (1960). "Flume studies of flow in steep, rough channels." *Proceedings, Journal of the Hydraulics Division, ASCE*, 86(9), pp. 55–76.

91. Peyras, L., Royet, P., and Degoutte, G. (1992). "Flow and energy dissipation over stepped gabion weirs." *Journal of Hydraulic Engineering, ASCE*, 118(5), pp. 707–717.

92. Pillai, C. R. S. (1979). "Effective depth in channels having bed undulations." *Journal of the Hydraulics Division, ASCE*, 105, No HY1, pp. 67–81.

93. Polatel, C. (2006). "Large-scale roughness effect on free-surface and bulk flow characteristics in open-channel flows." *Ph.D. Thesis*, Dept. of Civil and Environmental Engineering, University of Iowa, USA.

94. Rice, C. E., Kadavy, K. C., and Robinson, K. M. (1998). "Roughness of loose rock riprap on steep slopes." *Journal of Hydraulic Engineering, ASCE*, 124(2), pp. 179–185.

95. Rouse, H. (1965). "Critical analysis of open-channels." *Journal of the Hydraulics Division, ASCE*, 91, HY4, pp. 01–25.

96. Sayre, W. W. and Albertson, M. L. (1961). "Roughness spacing in rigid open channels." *Proceedings, Journal of the Hydraulics Division, ASCE*, 87 (3), pp. 121–150.

97. Scott, L., Hegberg C., and Schlindwein, P.E. (2004). "The morphological influence of isolated rock ramp construction on stream channels." *Proeedings, NCSRI Southeastern*

Regional Conference on Stream Restoration, June 21-24, 2004, North Carolina State University Stream Restoration Institute, Raleigh, NC 27695-8605, USA.

98. Semadeni, N., Lange, D. and Bezzola, G.R. (2004). "Aufgelöste Blockrampen - Fallbeispiel an der Emme." *Lebensraum Fluss, Symposium Wallgau,* Versuchsanstalt für Wasserbau, Technical University of München, Bericht 1, pp. 72–81 (*in German*).

99. Shamloo, H., Rajaratnam, N. and Katopodis, C. (2001). "Hydraulics of simple habitat structures." *Journal of Hydraulic Research, IAHR,* 39(4), pp. 351–366.

100. Shields Jr., F.D., Copeland, R.R., Klingeman, P.C., Doyle M.W., and Simon A. (2003). "Design for stream restoration." *Journal of Hydraulic Engineering, ASCE,* 129 (8), pp. 575–584.

101. Sindelar, C. and Knoblauch, H. (2010). "Design of a meandering ramp located at the River Große Tulln." *Proceedings, River Flow 2010,* Dittrich, Koll and Geisenhainer (*Eds.*), Bundesanstalt für Wasserbau, (ISBN 978-3-939230-00-7), pp. 1239 – 1246.

102. Smart, G. M., M. J. Duncan, and Walsh, J. (2002). "Relatively rough flow resistance equations." *Journal of Hydraulic Engineering, ASCE,* 128(6), pp. 568–578.

103. Soto, A.U., and Madrid–Aris, M. (1994). "Roughness coefficient in mountain rivers."

Hydraulic Engineering 1994, Vol. 1, ASCE, Cotroneo, G. and Rumer, R. (eds), New York, USA, pp. 01–08.

104. Tamagni, S., Weitbrecht, V., and Boes, R. (2011). "Design of unstructured block ramps: A state–of–the–art review." *Proceedings, Intl. Conference on the Status and Future of the World's Large Rivers,* April 11-14, 2011, Vienna, Austria.

105. Tullis, B.P. and Larchar, J. (2011). "Determining air demand for small- to medium-sized dam low-level outlet works." *Journal of Irrigation and Drainage Engineering, ASCE,* 137(12), pp. 793–800.

106. Ugarte, A., and Madrid–Aris, M. (1994). "Roughness coefficient in mountain rivers." *Proceedings, Hydraulic Engineering, ASCE,* Reston, Va., pp. 652–656.

107. United States Army Corps of Engineers. (1983). *Hydraulic Design of Energy Dissipators for Culverts and Channels. HEC–14,* Metric version, Manual, USA.

108. United States Army Corps of Engineers. (1990). *Hydraulic Design of Spillways. Engineer Manual* 1110-2-1603, USA.

109. United States Bureau of Reclamation. (1978). *Hydraulic Design of Stilling Basins and Energy Dissipators. Engineering Monograph,* 25, USA.

110. United States Dept. of Agriculture – Natural Resources Conservation Service. (2005). *Design of Stream Barbs. Technical Note, 23,* Oregon Bulletin OR210-2005-2, Oregon 97232, USA.

111. United States Dept. of Agriculture – Natural Resources Conservation Service. (2007). *Stream Restoration Design. National Engineering Handbook,* Part 654, USDA , USA.

112. United States Environmental Protection Agency. (2000). *Principles for the ecological restoration of aquatic resources. U.S. Environmental Protection Agency Report,* EPA841-F-00-003, Office of Water (4501F), Washington, D.C. (http://www.epa.gov/owow/ wetlands/restore)

113. Vischer, D.L. and Hager, W.H. (1995). *Energy Dissipators. Hydraulic Structures Design Manual,* 9, *IAHR,* Balkema, Rotterdam, Netherlands.

114. Weichert, R. (2006). "Bed morphology and stability of steep open channels." *Ph.D. Thesis, Mitteilungen*, 192, Versuchsanstalt für Wasserbau (VAW), Hydrologie und Glaziologie der Eidgenössischen Technischen Hochschule (ETH), CH–8092, Zürich, Switzerland.

115. Whittaker, J. and Jäggi, M. (1986). *Blockschwellen. Mitteilungen*, 91, Versuchsanstalt für Wasserbau Hydrologie und Glaziologie, ETH, Zürich, Switzerland.

116. White, F. M. (1991). *Viscous Fluid Flow*. 2nd eds., McGraw-Hill, Inc, New York.

117. Wilcox, A.C. (2005). "Interactions between flow hydraulics and channel morphology in step–pool streams." *Ph.D. Thesis*, Colorado State University, Fort Collins, Colorado, USA.

118. Wyrick, J.R. and Pasternack. G.B. (2008). "Modelling energy dissipation and hydraulic jump responses to channel nonuniformity at river steps." *Journal of Geophysical Research, AGU*, 113, F03003.

119. Yen, B.C. (2002). "Open channel flow resistance." *Journal of Hydraulic Engineering, ASCE*, 128 (1), pp. 20 – 39.

120. Abt, S. R. & Johnson, T. L. 1991. Riprap design for overtopping flow. Journal of Hydraulic Engineering 117(8), 959–972.

121. Abt, S. R. Ruff, J. F. Wittler, R. J. & LaGrone, D. L. 1987. Gradation and layer thickness effects on riprap. *Proc., Nat. Conf. on Hydraul. Eng., ASCE, New York*, 564–569.

122. Ahmad, Z. Nadimetla M. Petappa & Bernhard Westrich 2009. Energy dissipation on Block ramps with staggered Boulders. *Journal of Hydraulic Engineering* 135(6), 522-526.

123. Aguirre-Pe Olivero, M.L. & Moncada, A.T. 2003. Particle densimetric number for estimating sediment transport. *Journal of Hydraulic Engineering*, 129(6), 428-437.

124. Ashida, K., & Bayazit, M. 1973. Initiation of motion and roughness of flows in steep channels. *Proc. 15th IAHR Congress, Istanbul, Turkey*, 1, 475-484.

125. Frizell, K. H., and J. F. Ruff. 1995. Embankment overtoppingprotection - Concrete blocks or riprap. In ASCE Proc., *Water Resources Conf.*, 1021-1025, 14-18 August, San Antonio, Tex. New York.

126. Pagliara, S. & Lotti, I. 2007. Local failure of base block ramps. *Proc. 32th IAHR Congress, Madrid, Spain*, 2, 649

127. Isbash, S. 1936. Construction of dams by depositing rock in running water, Communication No. 3, *2nd Congress on Large Dams*. Washington, DC. 123–136.

128. Maynord, S. T. 1991. Flow resistance of riprap. *Journal of Hydraulic Engineering* 117(6), 687–695.

129. Pagliara, S., Carnacina, I., and Roshni, T. 2010. Self-aeration and friction over rock chutes in uniform flow conditions. *Journal of Hydraulic Engineering* 136(11), 959-964.

130. Pagliara, S. & Chiavaccini, P. 2004. Stability of reinforced block ramps. *Proc. River flow International Conference, Balkema, Rotterdam*,1291-1295.

131. Pagliara, S., & Chiavaccini, P. 2007. Failure mechanisms of base and reinforced block ramps. *Journal of Hydraulic Research* 45(3), 407–420.

132. Robinson, K.M. Rice, C.E. & Kadavy, K.C. 1995. Stability of rock chutes. *Proc. ASCE Water Resources Conference, San Antonio, TX*, 1481-1485.

133. Robinson, K.M. Rice, C.E. & Kadavy, K.C. 1997. Design of rock chutes. *Transaction of the ASAE*, 41(3), 621-626.

134. Shvidchenko, A. & Pender, G. 2000. Flume study of the effect of relative depth on the incipient motion of coarse uniform sediments. *Water Resources Research* 36(2), 619–628.

135. Whittaker, J. & Jäggi, M. 1986. *Blockschwellen, Mitteilungen 91, in Versuchsanstalt für Wasserbau Hydrologie und Glaziologie*, ETH, Zurich, Switzerland.